EXPERIMENTS ON ECLOGITES AND PERIDOTITES RELEVANT TO MAGMA GENERATION AND TEMPERATURE DISTRIBUTION IN THE UPPER MANTLE

by Susan Howells

Thesis presented for the Degree of Doctor of Philosophy of the University of Edinburgh in the Faculty of Science.

1976

ABSTRACT

Pyroxene solid solutions crystallized experimentally at high pressure (20-35 kb) and high temperature ($>1400^{\circ}C$) have been analysed using optical and x-ray diffraction techniques. Enstatite solid solution in $CaO-MgO-SiO_2$ clinopyroxenes at high temperatures is less extensive than previously accepted, is greatly reduced by pressure increase between 20 and 30 kb, and is dependent on the extent of forsterite saturation. No evidence was found for an inflection in the clinopyroxene(orthopyroxene) solvus or for a field of two clinopyroxenes in the system $CaO-MgO-SiO_2$ at either 20 or 30 kb, or in the system $CaO-MgO-Al_2O_3-SiO_2$ or a natural system at 30 kb. Previous evidence for a reaction from a calcic clinopyroxene-bearing garnet-lherzolite to a subcalcic clinopyroxene-bearing garnet-lherzolite is inconclusive.

Much lower solubilities of Al_2O_3 in orthopyroxene than hitherto predicted were obtained for orthopyroxenes crystallized in equilibrium with garnet from compositions in the system $MgO-Al_2O_3-SiO_2$, and for orthopyroxenes crystallized in the equilibria clinopyroxene + orthopyroxene + garnet $\pm$ olivine from compositions in both the $CaO-MgO-Al_2O_3-SiO_2$ system and a natural system.

Discrepancies between these and previous results reflect the use of different starting materials. The probable errors in the previous determinations may explain the "kink" in deduced pyroxene geotherms.

Stable equilibrium was not achieved at high temperature in experiments on anhydrous $CaO-MgO-Al_2O_3-SiO_2$ gel charges within the

period of reliability of Pt/Pt13Rh thermocouples.

Experiments carried out in the systems $CaO-MgO-Al_2O_3-SiO_2-Na_2O$ and $CaO-MgO-Al_2O_3-SiO_2-Na_2O-H_2O$ at 25 kb showed that nepheline-normative magmas may be generated by partially melting certain anhydrous clinopyroxene-orthopyroxene-garnet assemblages. Orthopyroxene is in reaction with this liquid. Both nepheline- and quartz-normative liquids may be generated by partially melting H_2O-saturated garnet-lherzolite at 1080°C, 25 kb.

The presence of glass spherules, glass coatings and vapour bubbles in H_2O-bearing experimental run products is not evidence of the presence of a vapour phase at high temperature.

CONTENTS

CHAPTER 1

INTRODUCTION

1.1 Geological background of problems and purpose of study

Kimberlitic fluids are believed to have originated at great depth because they contain the high pressure phases diamond and pyropic garnet. The ultrabasic and basic, often pyrope-bearing nodules found in kimberlite are considered to be fragments of the mantle carried to the earth's surface by the erupting kimberlite fluid. A pressure/temperature plot of the equilibration conditions of the nodules found in a kimberlite pipe would define a mantle geotherm at the time of the kimberlite intrusion.

Experimental work at high pressure in natural and synthetic systems has shown that certain parameters of pyroxene solid solutions are sensitive to changes of pressure and/or temperature. Two of these parameters have been used to deduce equilibration pressures and temperatures of garnet-lherzolites (clinopyroxene + orthopyroxene + garnet + olivine) assemblages which are found as nodules in kimberlite. Temperatures are deduced from the allegedly pressure insensitive Ca/(Ca+Mg) ratio of enstatite-saturated clinopyroxenes using the relationship determined by Davis and Boyd (1966) at 30 kb from experiments in the system $CaO-MgO-SiO_2$. Knowing the temperature of equilibration of a garnet-lherzolite its equilibration pressure is estimated from the Al_2O_3 content of the orthopyroxene, using MacGregor's (1974) experimentally determined grid for the solubility of Al_2O_3 in orthopyroxene as a function of temperature and pressure.

MacGregor's grid is based on experiments on bulk compositions in the system $MgO.SiO_2$-Al_2O_3 which are used in preference to the earlier results of Boyd and England (1964) in the same system.

Equilibration conditions of garnet-lherzolite nodules from many kimberlite pipes have been deduced from these parameters and have been used to derive mantle geotherms, e.g. MacGregor (1975); Boyd (1973, 1974). Such geotherms are necessarily crude because the experimentally determined relationships from which they are derived will be affected by chemical components found in the natural rocks but which were not present in the simple synthetic compositions used in the experiments. Certain evidence suggests that there may be considerable errors in these deduced geotherms:-

(i) Al_2O_3 contents of orthopyroxenes crystallized experimentally in equilibrium with clinopyroxene, garnet and olivine from natural starting materials (Howells, Begg and O'Hara, 1975) are much lower than predicted by MacGregor's (1974) grid for simple synthetic compositions. The experiments suggest that equilibration pressure determinations using MacGregor's grid may be overestimated by up to 16 kb.

(ii) Clinopyroxenes in garnet-lherzolite nodules from any one kimberlite pipe frequently show a bimodal distribution in their Ca/(Ca+Mg) ratio (e.g. Boyd, 1973, 1974). This is reflected in a bimodality of their equilibration temperatures as deduced from the Davis and Boyd (1966) clinopyroxene(orthopyroxene) solvus which shows no inflection in the relevant range of Ca/(Ca+Mg) values. Such a bimodality of equilibration temperatures is enigmatic. Selective sampling of the mantle at certain depths, suggested by Boyd (1974),

is an unlikely explanation since the bimodality occurs for similar ranges of clinopyroxene Ca/(Ca+Mg) ratio in the nodules of more than one kimberlite pipe (e.g. Boyd, 1973, 1974; Johnston, 1973; MacGregor, 1975). The bimodality may, however, reflect the presence in the mantle of two layers of garnet-lherzolite enclosing a layer of a different rock type (Boyd, 1974).

These two observations ((i) and (ii)) may be explained by errors in the investigated relationships between pyroxene solid solutions and equilibration pressures and temperatures, or imprecision in the deduced equilibration conditions resulting from the application of equilibria determined in simple synthetic systems to those observed in natural systems.

Further experimental work, some of which was synchronous with the present study, has been carried out to improve the experimental basis of this method used to assign equilibration pressures and temperatures to garnet-lherzolite nodules. This work has involved the redetermination of the same equilibria studied by Davis and Boyd (1966) at 30 kb (Nehru and Wyllie, 1974; Mori and Green, 1975a,b) and at other pressures (Kushiro, 1969a,b; Warner and Luth, 1974; Mori and Green, 1975a,b; Lindsley and Dixon, 1975). Further work has investigated both clinopyroxene and orthopyroxene solid solutions in more complex synthetic (O'Hara and Yoder, 1967; Boyd, 1970; Green and Ringwood, 1970; Akella and Boyd, 1972, 1973; Akella, 1974a; Wood, 1974; O'Hara, 1975) and natural (MacGregor and Ringwood, 1964; O'Hara and Yoder, 1967; Hensen, 1973; Akella and Boyd, 1974) systems at various pressures and temperatures. The results obtained in some of these experimental studies have been extended to

other pressures, temperatures and more complex chemical systems using thermodynamic expressions of pyroxene solid solutions (Wood and Banno, 1973; Wood, 1974; Saxena and Nehru, 1975; Warner and Luth, 1974).

Results of O'Hara (1975, reproduced in Appendix A.8.1) on a composition in the system $CaO-MgO-Al_2O_3-SiO_2$ indicate the presence, at 32 to at least 45 kb, of a pressure insensitive reaction from a calcic clinopyroxene-bearing garnet-lherzolite stable at low temperature to a sub-calcic clinopyroxene-bearing garnet-lherzolite stable at higher temperatures. Such a reaction would explain the bimodal distribution of compositions of clinopyroxenes in garnet-lherzolite nodules if those containing the more calcic clinopyroxenes crystallized at temperatures below that of the reaction and the nodules containing the more sub-calcic clinopyroxenes crystallized at temperatures higher than that of the reaction. Previous equilibration temperature estimates of the sub-calcic clinopyroxene-bearing garnet-lherzolites (estimated from the Davis and Boyd (1966) clinopyroxene (orthopyroxene) solvus) may therefore be too high relative to the equilibration temperature estimates of the calcic clinopyroxene-bearing garnet-lherzolites.

Where a bimodal distribution of clinopyroxene compositions occurs in the garnet-lherzolite nodules of a kimberlite pipe (e.g. Boyd, 1973, 1974), the geotherm defined by the nodules is kinked, with the upper limb deflected to higher temperatures, at a given pressure, than the extrapolated position of the lower limb. Nodules containing calcic clinopyroxenes define the lower temperature limb of such geotherms; those containing sub-calcic clinopyroxenes define

the upper limb. Boyd (1973) suggested that the high temperatures of the upper limb of these geotherms were caused by shear heating in the mantle, the shearing being the result of plate movements which led to the break-up of Gondwanaland. This interpretation has been criticized by Goetze (1975) and Mercier and Carter (1975). Other interpretations of the kinked geotherms have been proposed by Green and Gueguen (1974) and Parmentier and Turcotte (1974). Mercier and Carter (1975) suggested that the kink in these geotherms may be an artefact of the incorrect assignment of equilibration pressures and temperatures to garnet-lherzolite nodules as a result of ignoring the effect of minor components on the relevant equilibria. An alternative possibility was suggested by O'Hara (1975). If the reaction described by O'Hara (1975) does occur in natural assemblages, and if the equilibration temperatures of sub-calcic clinopyroxene-bearing garnet-lherzolites are consequently overestimates relative to the second group of nodules, a pressure/temperature plot for both groups of nodules would define a kinked geotherm.

Further evidence for such a break of slope in the cpx(opx) solvus is found in the equilibria described by Davis and Boyd (1966) and Kushiro (1969a,b) for compositions in the system $CaO-MgO-SiO_2$ at 30 and 20 kb respectively, and by Munoz and Lindsley (1969) at 20 kb for compositions in the system $CaO-FeO-SiO_2$. The break of slope determined in the system $CaO-MgO-SiO_2$ occurs for a range of enstatite-saturated clinopyroxenes which have lower Ca/(Ca+Mg) ratios than those observed in the natural clinopyroxenes under consideration. For this reason the possibility that the bimodal distribution of natural clinopyroxene compositions reflects an inflected solvus

was rejected by Boyd (1970). It is conceivable, however, that an inflection or reaction might occur in the relevant composition range in more complex chemical systems.

In this study further evidence was sought in the system $CaO-MgO-Al_2O_3-SiO_2$ for the reaction described by O'Hara (1975). The results showed that, even at the high temperatures investigated, the phase assemblages crystallized were a function of the starting material used. The equilibria determined by Davis and Boyd (1966) and MacGregor (1974), which are used as a geothermometer and geobarometer respectively, were therefore redetermined using different types of starting materials. The new results were extended into more complicated synthetic and natural systems, involving equilibria in clinopyroxene + orthopyroxene + garnet $\pm$ olivine assemblages. This work throws doubt on the existing calibration of the Ca/(Ca+Mg) ratio of clinopyroxene as a geothermometer, and the Al_2O_3 content of orthopyroxene as a geobarometer for garnet-lherzolites. The new experiments emphasise the control of starting material on experimental results and the uncertainty in the identification of an equilibrium phase assemblage.

The final part of this thesis investigates methods by which nepheline-normative magmas may be generated at high pressure ($>$ 20 kb). Various methods have previously been suggested on the basis of experimental data from natural and synthetic compositions (O'Hara and Yoder, 1967; Bultitude and Green, 1971; Kushiro, 1968, 1972, 1973; Eggler, 1974; Ito and Kennedy, 1974; Wyllie and Huang, 1975). These studies are limited by problems of working in natural systems, difficulty of liquid analysis, and the dangers in

extrapolation of limited data to more complex equilibria. In order to circumvent these problems and to obtain accurate information on the nature of the partial melting products of the mantle under different conditions, systematically designed and carefully controlled experiments must be undertaken, necessarily in synthetic systems. The results of the present study contribute to this experimental programme.

Kushiro (1972) showed that the presence of both Na_2O and H_2O have a considerable effect on the degree of undersaturation of liquids formed by the partial melting of basic and ultrabasic compositions. Previous studies on the effects of these components have mainly involved the investigation of the movement of the orthopyroxene/olivine liquidus boundary. There is little information on liquid + clinopyroxene + orthopyroxene + garnet $\pm$ olivine equilibria in the systems $CaO-MgO-Al_2O_3-SiO_2-Na_2O$ and $CaO-MgO-Al_2O_3-SiO_2-Na_2O-H_2O$. These equilibria have been investigated in the present study.

1.2 Nomenclature and abbreviations

The components CaO, MgO, Al_2O_3, SiO_2, FeO and TiO_2 are usually abbreviated in the following text, tables and figures as C, M, A, S, F and T respectively.

Abbreviations used for mineral names are as follows:-

cpx - clinopyroxene	opx - orthopyroxene
pyx - pyroxene	ol - olivine
gt - garnet	qz - quartz
amph - amphibole	cord - cordierite

sp - spinel

an - anorthite

prclse - periclase

chlor - chlorite

di_{ss} - diopside solid solution

en_{ss} - enstatite solid solution

In the synthetic system, diopside (CMS_2), enstatite (MS), pyrope (M_3AS_3) and forsterite (M_2S) refer only to the pure chemical end members of clinopyroxene, orthopyroxene, garnet and olivine solid solutions respectively. Di_{ss} and en_{ss} refer to the atmospheric pressure pyroxene solid solutions for which structural states were not determined. Garnet and olivine in a phase assemblage refer only to discrete crystals of these phases. Garnet and olivine in textural intergrowth are identified separately (as G/O).

The cpx(opx) solvus is the sub-solidus boundary between the single phase field of clinopyroxene and the phase field of cpx+opx.

In mineral assemblages and chemical systems, "$\pm$" means "with or without" (e.g. cpx+opx$\pm$gt; $(CS_x+MS_y+A_z)\pm M_2S$).

Additional abbreviations used in the tables are as follows:-

Q - crystals quenched from liquid or vapour

Gl - glass

UG - unrecrystallized gel

Xl - crystal

G/O - garnet/olivine intergrowth texture

rexd. - recrystallized

(cpx) - trace of phase present (here cpx)

?cpx - presence of phase (here cpx) queried

Phases listed in "optical identifications" are believed to be primary, not quenched crystals.

Pressure is expressed in kilobars (kb) and temperature in degrees centigrade (^{o}C). All compositions and mixes are in weight % except where stated otherwise. "Starting material" refers to the

material nature of the charge (e.g. glass or gel), not to its composition. Runs are identified in the form X/Y where X is the charge number and Y is the run number.

1.3 Lay-out of thesis and scope of new experiments

Chapters 2-5 consider the experimental basis of the use of the Ca/(Ca+Mg) ratio of enstatite-saturated clinopyroxene as a geothermometer for garnet-lherzolites. New high temperature ($>1400^{o}C$) sub-solidus experiments in the system C-M-S at 30 and 20 kb and in the system C-M-A-S at 30 kb are described in sections 3.1 and 3.2 and Chapter 4 respectively. New experiments in a natural system at 30 kb are presented in section 5.4. Comparison with previous results are made in the relevant sections and possible explanations for the large discrepancies are discussed.

Chapters 6-8 consider the experimental basis of the use of the Al_2O_3 content of orthopyroxene as a geobarometer for garnet-lherzolites. New experimental determinations of solubility for compositions in the systems M-A-S and C-M-A-S at 27-35 kb, 1450-$1650^{o}C$ are presented in section 7.1 where comparisons are made with previous determinations. Section 8.3.1 presents the results of a new determination of Al_2O_3 solubility in natural orthopyroxene at 30 kb.

Chapter 10 describes melting experiments in the systems C-M-A-S-N and C-M-A-S-N-H at 25 kb, and on two natural eclogites at 20-30 kb. The results of these experiments are relevant to the derivation of nepheline-normative magmas at high pressure.

The main conclusions of this thesis are given in sections 9.1,

9.2 and 10.3.6.

Most of these new experiments were carried out on synthetic charges with compositions in the system C-M-A-S-N-H and its sub-systems. This is because the effect of varying one parameter at a time could be investigated, and because the problems of running iron-bearing charges at high pressure have not yet been solved.

This thesis is based on the results of high pressure experiments carried out in solid media equipment, run products being analysed by optical and x-ray diffraction techniques. Investigation of the clinopyroxene geothermometer problem (Chapters 2-5) depended on precise determinations of clinopyroxene compositions. This was attained by constructing composition determinative curves and grids using $CrK\alpha$ radiation diffraction pattern parameters of clinopyroxene solid solutions (further described in Appendices A.3 and A.5).

CHAPTER 2

THE CLINOPYROXENE GEOTHERMOMETER

2.1 Introduction

Davis and Boyd (1966) showed that the Ca/(Ca+Mg) ratio of clinopyroxene coexisting with orthopyroxene at 30 kb is temperature dependent. This parameter of clinopyroxene solid solutions has subsequently been used as a geothermometer for cpx+opx+gt+ol (garnet-lherzolite) assemblages (e.g. Boyd, 1973). The relationship between temperature and the Ca/(Ca+Mg) value of clinopyroxene was determined experimentally by Davis and Boyd for clinopyroxenes coexisting with orthopyroxene alone, at 30 kb, with compositions in the simple system CMS_2-M_2S_2. Use of this relationship may lead to erroneous estimates of equilibration temperatures of garnet-lherzolites for the following reasons:-

(i) It is assumed that clinopyroxene solid solution towards enstatite is pressure insensitive. This assumption is based on a comparison of the clinopyroxene(orthopyroxene) solvus for bulk compositions in the system CMS_2-M_2S_2 at only two pressures, viz. 1 atmosphere (Boyd and Schairer, 1964) and 30 kb (Davis and Boyd, 1966).

(ii) It is assumed that the Ca/(Ca+Mg) ratio of the clinopyroxene in equilibrium with orthopyroxene, garnet and olivine is not affected by solid solution towards Al_2O_3. Although results at 30 kb, 1200°C (Boyd, 1970) suggest that this assumption is justified, experiments in the same system CS-MS-A at 30 kb, 1600°C (O'Hara and Yoder, 1967) showed that the Ca/(Ca+Mg) ratio of aluminous clino-

pyroxene coexisting with orthopyroxene and garnet is higher than that of the clinopyroxene coexisting with orthopyroxene in the Al_2O_3-free system CMS_2-M_2S_2 (Davis and Boyd, 1966) at the same temperature and pressure.

(iii) It is assumed that the Ca/(Ca+Mg) ratio of the clinopyroxene in the garnet-lherzolite assemblage is independent of the presence of olivine. This assumption may not be justified if at least one of the phases clinopyroxene, orthopyroxene or garnet coexisting with olivine is non-stoichiometric. In the simple system C-M-A-S pyroxenes and garnets are non-stoichiometric if their compositions cannot be expressed by the ideal (Ca+Mg):Si ratio of 1:1. The assemblage cpx+opx+gt would then be univariant at a fixed temperature and pressure, i.e. the compositions of the coexisting phases would vary with variation of the bulk composition. The composition of the clinopyroxene would only have a unique value at a fixed temperature and pressure in the invariant 4-phase assemblage cpx+opx+gt+ol. Similarly, if the pyroxenes crystallized in the system C-M-S are non-stoichiometric, then the Ca/(Ca+Mg) ratio of the clinopyroxene coexisting with orthopyroxene at a fixed temperature and pressure would have a unique value only in the presence of olivine.

There is no evidence of non-stoichiometry in the pyroxenes crystallized by Davis and Boyd (1966) at 30 kb. The compositions of clinopyroxenes crystallized in equilibrium with orthopyroxene from different bulk compositions at any one temperature are the same within the limits of the precision of the determinations.

Non-stoichiometric pyroxenes have however been reported from high pressure experiments on other synthetic compositions, e.g. in

the systems MS-A (Boyd and England, 1960) and CMS_2-M_2S (Kushiro, 1969b; Davis, 1964). Synthetic clinopyroxenes also exhibit non-stoichiometry at low pressure (e.g. Biggar and O'Hara, 1969b; Kushiro and Schairer, 1963).

Boyd and England (1960) cited examples of natural orthopyroxenes, from many petrological environments, in which the ratio of divalent cations to Si^{4+} is either less than or greater than unity. O'Hara and Mercy (1963), however, queried the possibility of olivine contamination as a cause of the apparent SiO_2 deficiency in their analyses of clinopyroxenes and orthopyroxenes from garnet-lherzolites.

To the present author's knowledge there are no examples reported of persistent non-stoichiometry in natural or synthetic garnets in equilibrium with clinopyroxene, orthopyroxene and olivine. Non-stoichiometric SiO_2-rich garnet has however been synthesized from the bulk composition M_3AS_3 (Charlu, Newton and Kleppa, 1975).

(iv) Natural clinopyroxenes show solid solution towards oxides other than CaO, MgO, SiO_2 and Al_2O_3 which is the simplest chemical system from which garnet-lherzolite can crystallize. The minor oxides may have a considerable effect on the extent of enstatite solid solution in clinopyroxenes. In particular it may be noted that:-

(v) The application of the cpx(opx) solvus determined by Davis and Boyd (1966) has so far been restricted to temperatures less than about 1400°C. There is a marked break of slope in this solvus at about 1450°C such that the clinopyroxenes coexisting with orthopyroxene at temperatures greater than 1450°C are very much more subcalcic than those coexisting with orthopyroxene at temperatures less

than 1450°C. It is possible that this break of slope occurs in a more calcic range of clinopyroxene compositions (at lower deduced temperatures using the Davis and Boyd cpx(opx) solvus) in multicomponent systems. A break in the cpx(opx) solvus in a more calcic range of clinopyroxene compositions than that reported by Davis and Boyd might explain the bimodal distribution of Ca/(Ca+Mg) ratios of natural clinopyroxenes in garnet-lherzolite nodules from kimberlite (see section 1.1).

(vi) There are possible sources of error in the experimental and analytical techniques used by Davis and Boyd (1966). Glass and submicroscopic intergrowths of clinoenstatite and diopside solid solutions crystallized from glass were used as starting materials to determine the position of the cpx(opx) solvus at temperatures greater than 1300°C. Glass starting materials frequently crystallize to metastable phase assemblages (e.g. Boyd and England, 1964; O'Hara and Schairer, 1963). The position of the cpx(opx) solvus at 1250°C and lower temperatures was determined by the optical identification of small quantities of acicular crystals as orthopyroxene. Since H_2O had been added to the charges run in this temperature range as a catalyst to promote crystal growth, it is possible that these acicular crystals were orthoamphibole. The optical identification of orthopyroxene was reinforced by x-ray diffraction analysis of the composition of the coexisting clinopyroxene. This used a determinative curve (fig. 3.2) which relates the Ca/(Ca+Mg) ratio of a clinopyroxene with the $^{\circ}2\theta$ value of its 220 reflection determined from the x-ray diffraction trace. The determinative curve was derived from the x-ray parameters of clinopyroxenes crystallized in experiments on

charges of known bulk composition run within the single phase field of clinopyroxene solid solution. This curve, which shows a linear variation of Ca/(Ca+Mg) ratio with the $^{o}2\theta$ value of the 220 reflection from $(CMS_2)_{15}(M_2S_2)_{85}$ to $(CMS_2)_{70}(M_2S_2)_{30}$ (mole %), has an unexplained break of slope at $(CMS_2)_{70}(M_2S_2)_{30}$. From this composition to $(CMS_2)_{100}$ the curve is non-linear. Until the cause of this break of slope has been determined, values of the Ca/(Ca+Mg) ratio of enstatite-saturated clinopyroxene deduced from the curve at temperatures below about 1300°C (Ca/(Ca+Mg) = 0.36) must be regarded as suspect.

There is a slight discrepancy in the position of the cpx(opx) solvus determined by the optical and x-ray methods at temperatures less than 1200°C. The maximum extent of this discrepancy is 4 mole % diopside, equivalent to about 50°C.

2.2 Aim of experimental work

An experimental programme was designed to investigate the extent of these possible sources of error in the use of Davis and Boyd's (1966) cpx(opx) solvus as a geothermometer for garnet-lherzolites. In particular, the effect on clinopyroxene solid solutions of using different types of starting material was considered.

The sources of error discussed in 2.1 were appreciated by several investigators who concurrently undertook similar experimental programmes. The results of these studies (Nehru and Wyllie, 1974; Akella, 1974a; Akella and Boyd, 1974; Warner and Luth, 1974; Mori and Green, 1975a,b; Lindsley and Dixon, 1975) are compared here in the relevant sections.

CHAPTER 3

THE CLINOPYROXENE GEOTHERMOMETER:

CLINOPYROXENE SOLID SOLUTIONS IN THE SYSTEM C-M-S

3.1 Clinopyroxene solid solutions in the system C-M-S at 30 kb

3.1.1 Introduction

Experiments on compositions in the system C-M-S at 30 kb were designed:-

(i) to investigate the effect of starting materials and SiO_2 activity on the Ca/(Ca+Mg) ratio of clinopyroxenes coexisting with orthopyroxene.

(ii) to determine whether the reported single phase field of clinopyroxene solid solution on the join CMS_2-M_2S_2 at 30 kb at temperatures higher than 1450°C (Davis and Boyd, 1966) conceals a field of two clinopyroxenes similar to that reported by Kushiro (1969a) on the same compositional join at 20 kb at temperatures above 1450°C.

The compositions of the charges used in this study are given in Appendix 2 (Table A.2.3).

Experimental details and results are tabulated in Appendix 9 (Tables A.9.1, A.9.2 and A.9.4).

3.1.2 Experimental results: gel charges

Fig. 3.1 compares the results of quenching experiments on partially crystalline gel starting materials with the phase diagram obtained by Davis and Boyd (1966) from similar bulk compositions on the join CMS_2-M_2S_2 at 30 kb.

FIGURE 3.1

The results of quenching experiments at 30 kb on partially crystalline gel charges with compositions on the join CMS_2-MS. These experimental results are compared with the phase diagram (shown by dashed lines) for the join CMS_2-MS at 30 kb obtained by Davis and Boyd (1966).

Open triangles indicate compositions which crystallized cpx alone; filled triangles indicate compositions which crystallized cpx+opx. The composition of the clinopyroxene in a two-phase assemblage is shown by an asterisk. The dotted line represents the approximate temperature for the solidus of the cpx+opx assemblage as determined in this study; the cross enclosed by a circle represents a hyper-solidus run product.

Underlined symbols and symbols with no underline indicate the run products of floating-piston and piston-out experiments respectively; symbols with a dashed underline represent run products obtained in both floating-piston and piston-out experiments.

The line A'-A is the approximate position of the cpx(opx) solvus for the gel of bulk composition $(CMS_2)_{40}(MS)_{60}$.

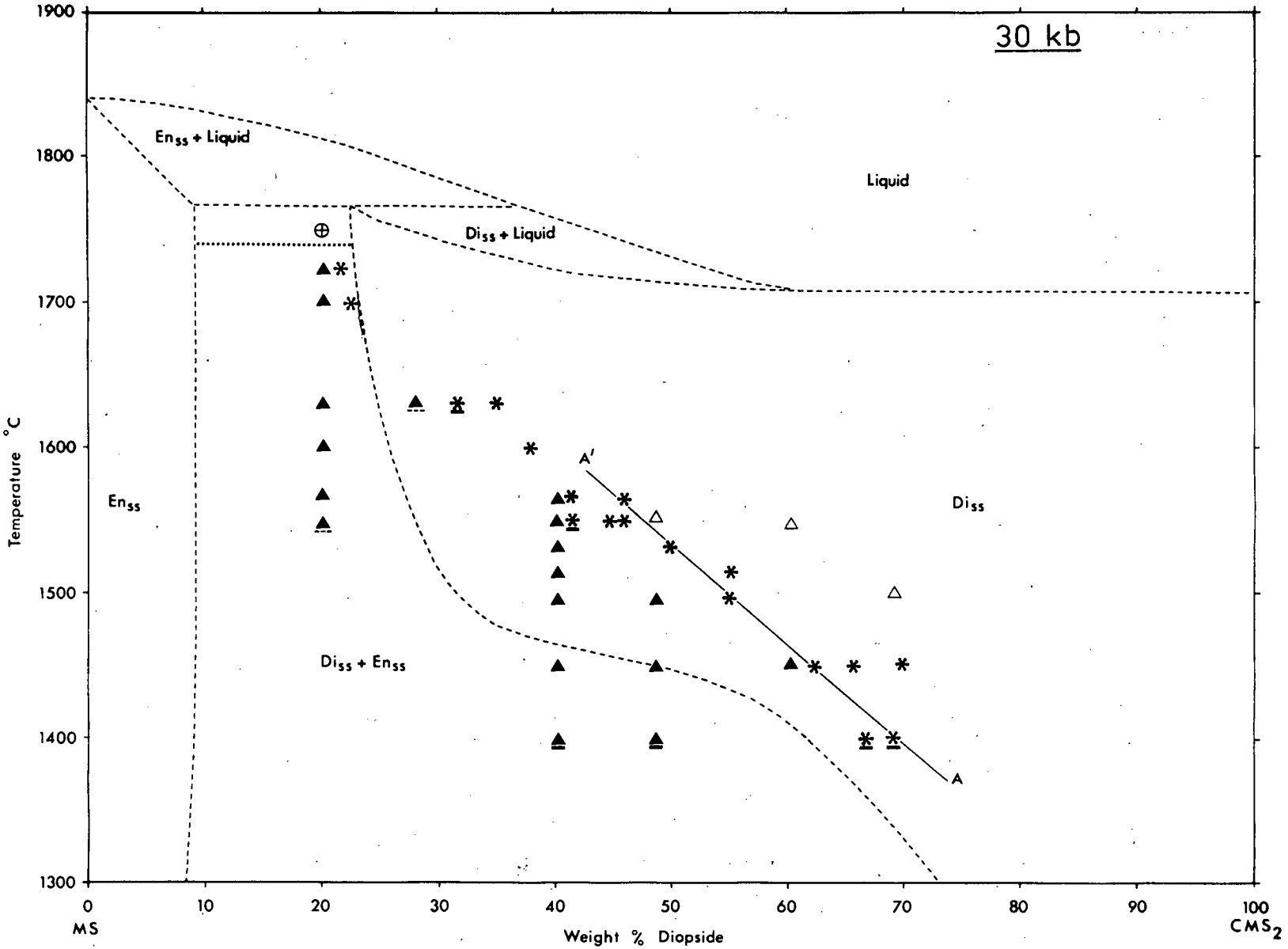
30 kb
Enss + Liquid
Liquid
Diss + Liquid
Enss
Diss
Diss + Enss
A'
A
Temperature °C
1900
1800
1700
1600
1500
1400
1300
0
10
20
30
40
50
60
70
80
90
100
MS
CMS2
Weight % Diopside

The clinopyroxene crystallized in equilibrium with orthopyroxene from gel charges is more calcic than predicted from Davis and Boyd's (1966) diagram in the entire temperature range investigated (1400°C to the solidus at about 1740°C). The sudden inflection in the cpx (opx) solvus at 1450°C towards more magnesian compositions determined by Davis and Boyd could not be reproduced in the experiments on gel charges. These defined a cpx(opx) solvus which showed no break of slope between 1400°C and the solidus.

There was no evidence either optically or using x-ray diffraction techniques of more than one clinopyroxene in run products which crystallized clinopyroxene alone. If a field of two clinopyroxenes is present, the coexisting solid solutions must have compositions which differ by less than 10% diopside. CrKα radiation, used to obtain x-ray diffraction patterns of these run products, is capable of clearly separating the combined ($\bar{1}12$, 002, 221) reflection of two clinopyroxenes which differ in composition by more than 10% diopside.

The compositions of the clinopyroxenes coexisting with orthopyroxene shown in fig. 3.1 were determined from the $^{\circ}2\theta$ value of the 220 reflection of clinopyroxene obtained from the x-ray diffraction pattern of run products. The relation between this parameter and the Ca(Ca+Mg) ratio of clinopyroxenes crystallized along the join CMS_2-M_2S_2 was determined by Davis and Boyd (1966) and reproduced here (see Appendix A.3.4 and fig. 3.2) for clinopyroxenes with compositions in the range $di_{20}en_{80}$ to $di_{69}en_{31}$. The composition of a clinopyroxene lying on the join CMS_2-M_2S_2 can be determined with a precision of $\pm$ 1% diopside (99.7% confidence limits) using this relationship.

FIGURE 3.2

The $^{o}2\theta$ values of the $\bar{2}21$ reflection (top curve) and 220 reflection (bottom curve) of clinopyroxenes with compositions on the join CMS_2-MS.

The encircled asterisks indicate values obtained in this study for clinopyroxenes crystallized at 20-30 kb (details in Appendix table A.3.4). The black dots indicate values obtained by Davis and Boyd (1966).

The continuous line is the best fit of Davis and Boyd's data points for $^{o}2\theta$ 220 cpx and was taken from Davis and Boyd (1966, fig. 2). This continuous line is the determinative curve for clinopyroxene compositions used in the present study and by Davis and Boyd (1966).

The dashed lines are purely eye-guides joining the $^{o}2\theta$ values obtained in the present study.

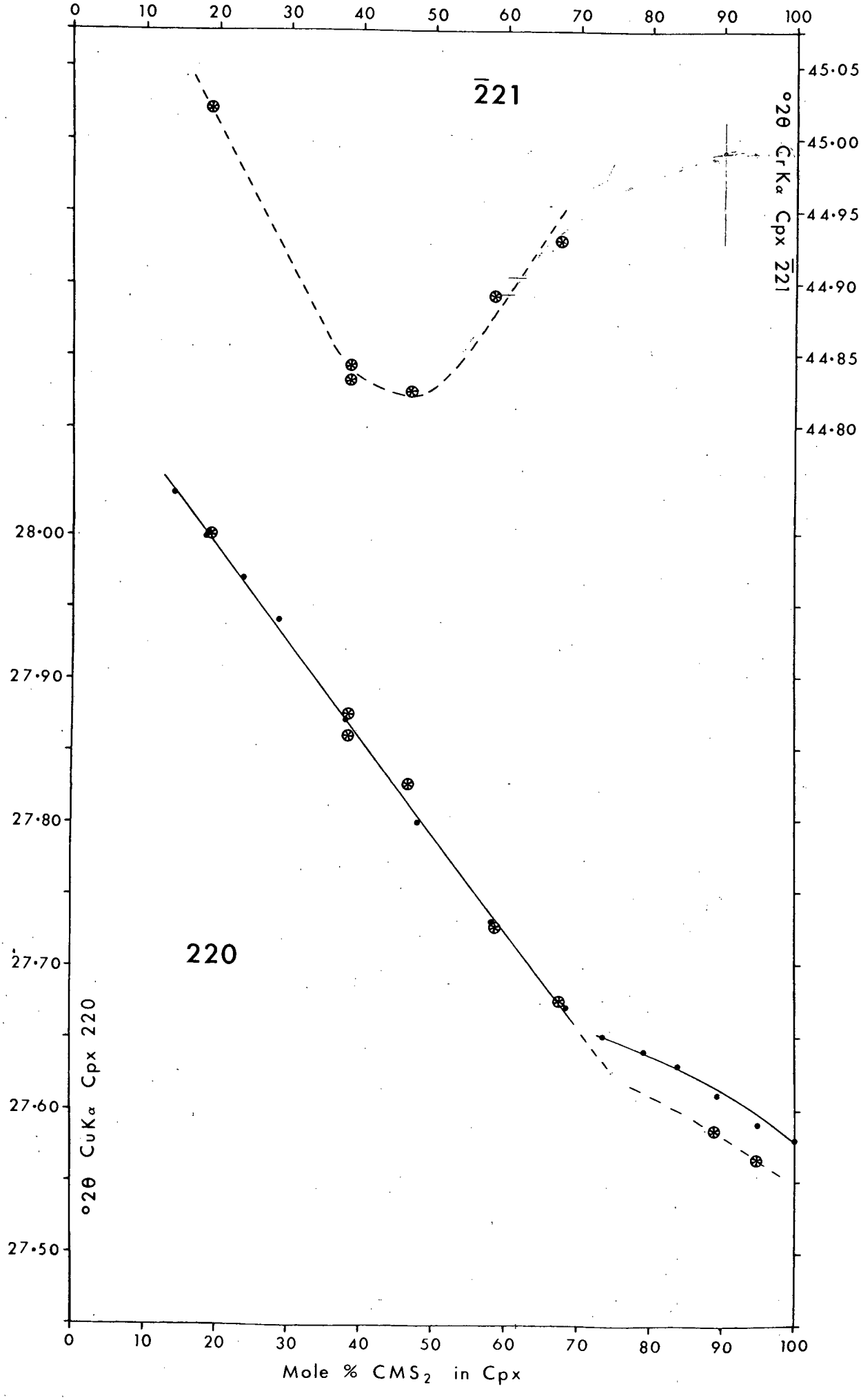
0
10
20
30
40
50
60
70
80
90
100
$\bar{2}21$
°2θ CrKα Cpx $\bar{2}21$
45·05
45·00
44·95
44·90
44·85
44·80
28·00
27·90
27·80
27·70
27·60
27·50
220
°2θ CuKα Cpx 220
Mole % CMS_2 in Cpx

The precision is rather less good for charges containing large amounts of orthopyroxene.

No unique position for the cpx(opx) solvus could be obtained at 30 kb from experiments using compositions on the join CMS_2-M_2S_2. The composition of a clinopyroxene coexisting with orthopyroxene at any one temperature varied with variation of the bulk composition. The more calcic the bulk composition, the smaller was the $^{o}2\theta$ value of the 220 reflection and hence the higher the deduced Ca/(Ca+Mg) ratio of the enstatite-saturated clinopyroxene. For example, at 1450°C bulk compositions $(CMS_2)_{40}(MS)_{60}$ and $(CMS_2)_{60}(MS)_{40}$ crystallized orthopyroxene in equilibrium with clinopyroxenes with apparent compositions $di_{62.3}en_{37.7}$ and $di_{69.6}en_{30.4}$ respectively. Student's t test indicated a difference with a probability of >99.9% for the $^{o}2\theta$ values of the 220 clinopyroxene reflection from which these compositions were deduced.

It is unlikely that this variation of clinopyroxene composition is the result of variation in the rates at which the different bulk compositions attained equilibrium because:-

(i) kinetic studies show that the clinopyroxene crystallized with orthopyroxene from a given bulk composition at any one temperature rapidly attains a stable composition, i.e. the composition does not change with increasing run length. Table 3.1 gives the $^{o}2\theta$ value of the 220 reflection of the clinopyroxenes crystallized with orthopyroxene at 1450°C from bulk composition $(CMS_2)_{40}(MS)_{60}$ (charge E22). The composition of the clinopyroxene changed rapidly for the first 100 minutes, but did not change thereafter, at least in runs of up to 7.5 hours. Since all runs used to determine the 30 kb cpx(opx)

TABLE 3.1

The effect of increasing run duration on the composition of clinopyroxene crystallized with orthopyroxene at 1450°C, 30 kb from bulk composition $(CMS_2)_{40}(MS)_{60}$.

Charge No.	Run Duration (hrs.)	$^{o}2\theta$ CrKα 220 Cpx	Wt.% CMS_2 in Cpx *
E22	(10 secs.)	41.772	56.4
	0.17	41.810	53.0
	0.25	41.809	53.0
	0.50	41.836	50.4
	0.80	41.736	60.3
	1.03	41.828	51.4
	1.70	41.706	63.3
	7.50	41.716	62.3
E22R	0.33	41.688	64.7
	4.08	41.703	63.3

* Clinopyroxene composition deduced from the relationship between the $^{o}2\theta$ value of the clinopyroxene 220 reflection and the Ca/(Ca+Mg) ratio of the clinopyroxene (fig. 3.2).

solvus shown in fig. 3.1 were at higher temperatures than 1450°C, and were longer than 100 minutes in duration, except at temperatures higher than 1600°C where reaction rates are very rapid, the run products are believed to have reached a metastable state, if not stable equilibrium.

(ii) the clinopyroxene composition crystallized with orthopyroxene from a given bulk composition at a given temperature can be reproduced using different types of starting material involving different composition paths towards the (meta)stable assemblage. Table 3.1 gives the results of a kinetic study at 1450°C on partially crystalline gel composition $(CMS_2)_{40}(MS)_{60}$ (charge E22) and on the same composition which had been completely recrystallized at 1307°C, atmospheric pressure to the assemblage cpx $[(CMS_2)_{72.5}(MS)_{27.5}]$ + en_{ss}. The trend towards an unchanging composition for the clinopyroxene crystallized in equilibrium with orthopyroxene from the partially crystalline gel was initially increasing and then decreasing $^{\circ}2\theta$ value of the 220 clinopyroxene reflection; for the totally recrystallized assemblage (charge E22R) the trend was of increasing $^{\circ}2\theta$ value. The final (i.e. unchanging) clinopyroxene compositions crystallized from the different starting materials were the same within 1% diopside (i.e. within the precision limits of the determinations) despite having approached the final assemblages via different clinopyroxene compositions. A similar result was obtained with bulk composition $(CMS_2)_{48.4}(MS)_{51.6}$ using a partially crystalline gel (charge E23) and the atmospheric pressure recrystallized assemblage (charge E23R) cpx $[(CMS_2)_{72.5}(MS)_{27.5}]$ + en_{ss} as starting materials. The clinopyroxenes crystallized with orthopyroxene after more than 4 hours at

1450°C were the same within 1.3% diopside. These results suggest that the assemblages reported are equilibrium assemblages even if they do not represent the most stable equilibrium state.

(iii) the pattern of results in which clinopyroxenes with higher apparent diopside contents crystallized with orthopyroxene at any one temperature from more calcic bulk compositions is reproducible using different types of starting material. The results described in (ii) above show that the enstatite-saturated clinopyroxene crystallized from bulk composition $(CMS_2)_{48.4}(MS)_{51.6}$ is more calcic than the enstatite-saturated clinopyroxene crystallized from bulk composition $(CMS_2)_{40}(MS)_{60}$ whether partially crystalline gels or the atmospheric pressure equilibrium assemblages are used as starting material. Similarly, there is no relation consistent at all temperatures between the composition of the clinopyroxene in equilibrium with orthopyroxene and the use of homogeneous gel as opposed to CMS_2 and MS gel mixes as starting materials. At 1565°C the clinopyroxene crystallized in the two-phase assemblage was more magnesian when the gel mix $(CMS_2)_{20}(MS)_{80}$ was used as starting material than when the homogeneous gel $(CMS_2)_{40}(MS)_{60}$ was used. However, at 1450°C a more magnesian clinopyroxene crystallized with orthopyroxene from the homogeneous gel $(CMS_2)_{40}(MS)_{60}$ than from the gel mix $(CMS_2)_{60}(MS)_{40}$. If the variation of clinopyroxene composition was caused by variation in the rates of attaining equilibrium, then a similar pattern would be expected from the use of the same type of starting material.

A more likely explanation of the variation in composition of enstatite-saturated clinopyroxene with variation of bulk composition at any one temperature is that the cpx+opx assemblages have crystallized

under isobaric and isothermally univariant conditions. This would reflect non-stoichiometric pyroxene solid solutions (see section 2.1) i.e. coexisting orthopyroxenes and clinopyroxenes which cannot be expressed in terms of simple CS-MS substitutions. This possibility was tested at 1550°C and 1565°C in experiments (listed in Appendix table A.9.4) on compositions on the CMS_2-MS join to which sufficient forsterite gel had been added (about 10%) to ensure the crystallization of forsterite-saturated assemblages. If the explanation of the variation of clinopyroxene composition in charges with different bulk composition on the CMS_2-MS join is indeed due to the presence of non-stoichiometric pyroxenes, then clinopyroxenes with a unique composition should crystallize at any one temperature at 30 kb in the isobaric and isothermally invariant equilibrium cpx+opx+ol despite variation of charge bulk composition.

At 1565°C the clinopyroxene crystallized in equilibrium with orthopyroxene from gels of bulk composition $(CMS_2)_{20}(MS)_{80}$ and $(CMS_2)_{40}(MS)_{60}$ were $di_{41.3}$ and $di_{45.9}$ respectively. Student's t test indicated that these determinations are different with a probability of more than 99.9%. When the experiments were repeated with forsterite gel added to each of these same gel charges, the clinopyroxenes ($di_{41.3}$ and $di_{42.8}$) crystallized in equilibrium with orthopyroxene and olivine at 1565°C were similar within the precision limits of the determinations ($<90\%$ probability of being different). One of these clinopyroxenes ($di_{41.3}$) has the same composition as that crystallized in equilibrium with orthopyroxene alone from bulk composition $(CMS_2)_{20}(MS)_{80}$ at 1565°C; the clinopyroxene in the other olivine-bearing assemblage has a composition ($di_{42.8}$) which is not significantly

different (probability of being different $\ll 90\%$) from that of the clinopyroxene crystallized from bulk composition $(CMS_2)_{20}(MS)_{80}$ at $1565^{\circ}C$. The results at $1550^{\circ}C$ show the same pattern.

These experiments indicate that coexisting clinopyroxene and orthopyroxene solid solutions are non-stoichiometric at 30 kb at temperatures higher than $1450^{\circ}C$, and that the compositions of clinopyroxene solid solutions crystallized in equilibrium with orthopyroxene alone are dependent on the bulk composition of the charge.

Fig. 3.3 is a model for coexisting clinopyroxene and orthopyroxene solid solutions in part of the system C-M-S at 30 kb, $1550^{\circ}C$. The form of this model is constrained by the following observations:-

(i) The more calcic the bulk composition, the more calcic is the clinopyroxene crystallized in equilibrium with orthopyroxene.

(ii) The clinopyroxene crystallized in the 3-phase assemblage cpx+opx+ol has a less calcic composition than those crystallized in the absence of olivine.

(iii) The bulk composition $(CMS_2)_{48.4}(MS)_{51.6}$ is slightly richer in diopside than the clinopyroxenes coexisting with orthopyroxene at $1550^{\circ}C$. When about 10% forsterite gel was added to the gel charge of this composition and the mixture was run at $1550^{\circ}C$, the run product contained clinopyroxene and olivine but no orthopyroxene.

These arguments assume that the extent of non-stoichiometry in the clinopyroxenes is small, and that the relation between the $^{\circ}2\theta$ value of the 220 reflection of a clinopyroxene and its Ca/(Ca+Mg) ratio is not significantly different for stoichiometric clinopyroxenes as for clinopyroxenes which show only small degrees of solid solution towards quartz or forsterite. These assumptions have not been investigated but they do not affect the main conclusions of this study.

FIGURE 3.3

A model for phase relations in part of the system C-M-S at 1550°C, 30 kb.

Solid squares indicate bulk compositions which crystallized opx+cpx+ol; solid triangles indicate bulk compositions which crystallized cpx+opx; open squares and open triangles indicate bulk compositions which crystallized the assemblages cpx+ol and cpx respectively. Measured cpx compositions in two or three phase assemblages are shown by asterisks and are joined by tie lines to the estimated compositions of other phases in the assemblage. Clinopyroxene/orthopyroxene tie lines are shown intersecting the CMS_2-MS join.

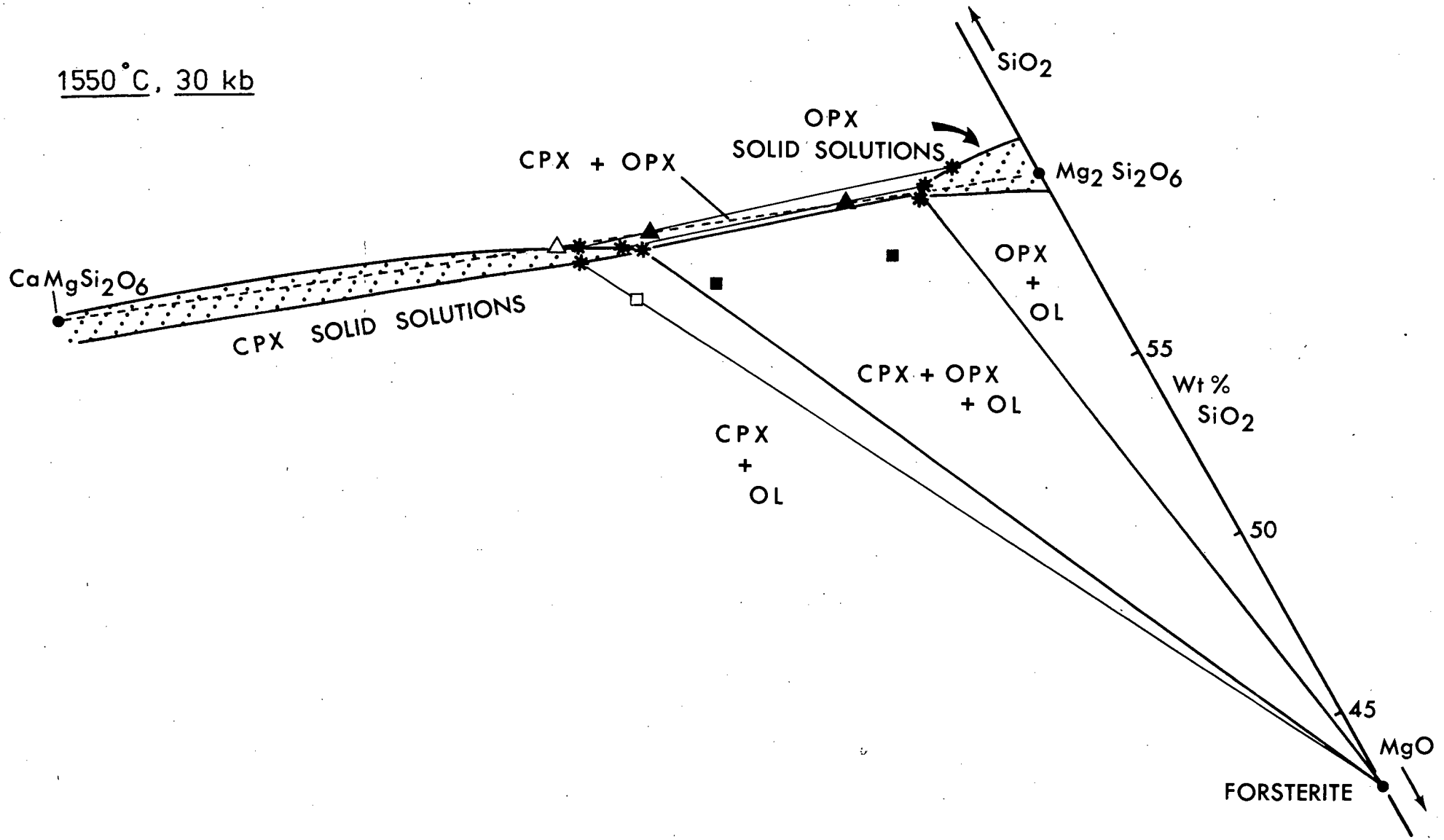
1550°C, 30 kb
SiO2
OPX
SOLID SOLUTIONS
CPX + OPX
Mg2 Si2O6
CaMgSi2O6
CPX SOLID SOLUTIONS
OPX
+
OL
CPX + OPX
+ OL
CPX
+
OL
55
Wt %
SiO2
50
45
MgO
FORSTERITE

3.1.3 Comparison of experimental results with those of Davis and Boyd (1966)

The cpx(opx) solvus determined at 30 kb in this work differs from that obtained by Davis and Boyd (1966) in that it lies closer to pure diopside, it does not show an inflection towards more magnesian compositions at about 1450°C and its position is dependent on SiO_2 activity. Possible explanations for these differences will now be considered.

A. Inter-laboratory differences in the temperature and pressure calibration of the equipment.

Experiments were carried out by Davis and Boyd (1966) using equipment at the Geophysical Laboratory, Washington. Calibration phase field boundaries determined in the Edinburgh laboratory were observed at closely comparable pressure/temperature conditions to those reported for the same equilibria determined using the Washington equipment (see Appendix A.1.2). Differences of pressure and temperature scales cannot therefore account for the observed discrepancies in this C-M-S system.

B. Piston technique.

Most of the new experiments were carried out using the piston-out technique whereas Davis and Boyd (1966) used the floating-piston technique (see Appendix A.1.1). The actual pressures realized using the floating-piston technique are lower than those obtained using the piston-out technique. Fig. 3.1 compares the results of runs carried out in this study using the floating-piston technique with the run results on the same compositions using the piston-out technique. At 1630°C, 1550°C and 1400°C the cpx(opx) solvus using the floating-

piston technique is displaced towards the solvus of Davis and Boyd but is still considerably more calcic than the latter. Differences of piston technique therefore only partly explain the discrepancies under consideration.

C. Run duration.

The duration of these new experiments, which are considered adequate to obtain assemblages which do not change with increasing run duration (see section 3.1.2), are comparable to the duration of the experiments run by Davis and Boyd (1966) and considered by them to be of sufficient length to attain equilibrium.

D. Bulk compositions.

Although the compositions of pyroxenes crystallized in this new study are non-stoichiometric and therefore vary with variation of bulk composition, the bulk compositions used here were similar to those used by Davis and Boyd (1966). The observed discrepancies are not the result of using different bulk compositions.

E. Determination of the position of the cpx(opx) solvus.

The difference in the reported position of this solvus is much too great to be attributed to poor precision in its determination. The x-ray determinative curve used in both studies yields clinopyroxene compositions with a precision of $\pm$ 1-3% diopside in the relevant temperature range. The differences to be explained exceed 20% diopside. Moreover, in the new study large amounts of orthopyroxene, identified optically and by x-ray diffraction techniques, crystallized in equilibrium with clinopyroxene from compositions predicted from the phase diagram of Davis and Boyd (1966) to crystallize clinopyroxene alone at the same temperature.

F. Starting materials.

The starting materials used in these new experiments were homogeneous gels which had been partially crystallized at 900°C, atmospheric pressure; mixtures of these partially crystalline gels; and gels which had been completely recrystallized to $di_{ss}+en_{ss}$ at 1307°C, atmospheric pressure. The starting materials used by Davis and Boyd (1966) at temperatures above 1300°C were glasses and glasses which had been recrystallized at atmospheric pressure. No difference was observed in either study between the results obtained from the different types of starting material.

An attempt was made to repeat Davis and Boyd's (1966) results using glass rather than gel as starting material. The results of runs on a glass (charge E22G) of composition $(CMS_2)_{40}(MS)_{60}$ made by melting and quenching the gel of this composition (see Appendix A.2.1) are illustrated in fig. 3.4. The glass was dried in nitrogen at 1050°C, atmospheric pressure for one hour before running. At 1400°C and 1440°C the run products of floating-piston experiments were orthopyroxene and a clinopyroxene with a composition within 1% diopside of that determined by Davis and Boyd at the same temperature and using the same bulk composition. A second floating-piston run at 1440°C crystallized clinopyroxene alone, conforming with the results of Davis and Boyd which show a marked inflection in the cpx(opx) solvus to more magnesian compositions at a temperature slightly greater than 1440°C. Single phase assemblages of clinopyroxene, whose x-ray diffraction trace reflections showed no signs of splitting, also crystallized from the same glass at 1466°C in a floating-piston run, and at 1522°C in a piston-out experiment in accordance with the

FIGURE 3.4

The results of quenching experiments at 30 kb on glass charges with compositions on the join CMS_2-MS. These experimental results are compared with the phase diagram (shown by dashed lines) for the join CMS_2-MS at 30 kb obtained by Davis and Boyd (1966). A'-A is taken from fig. 3.1.

Open triangles indicate compositions which crystallized cpx alone; filled triangles indicate compositions which crystallized cpx+opx. The composition of the clinopyroxene in a two-phase assemblage is shown by an asterisk.

G and H refer to the phase assemblages crystallized from the glass charges E22G and E22H respectively.

Underlined symbols and symbols with no underline indicate the run products of piston-out and floating-piston runs respectively.

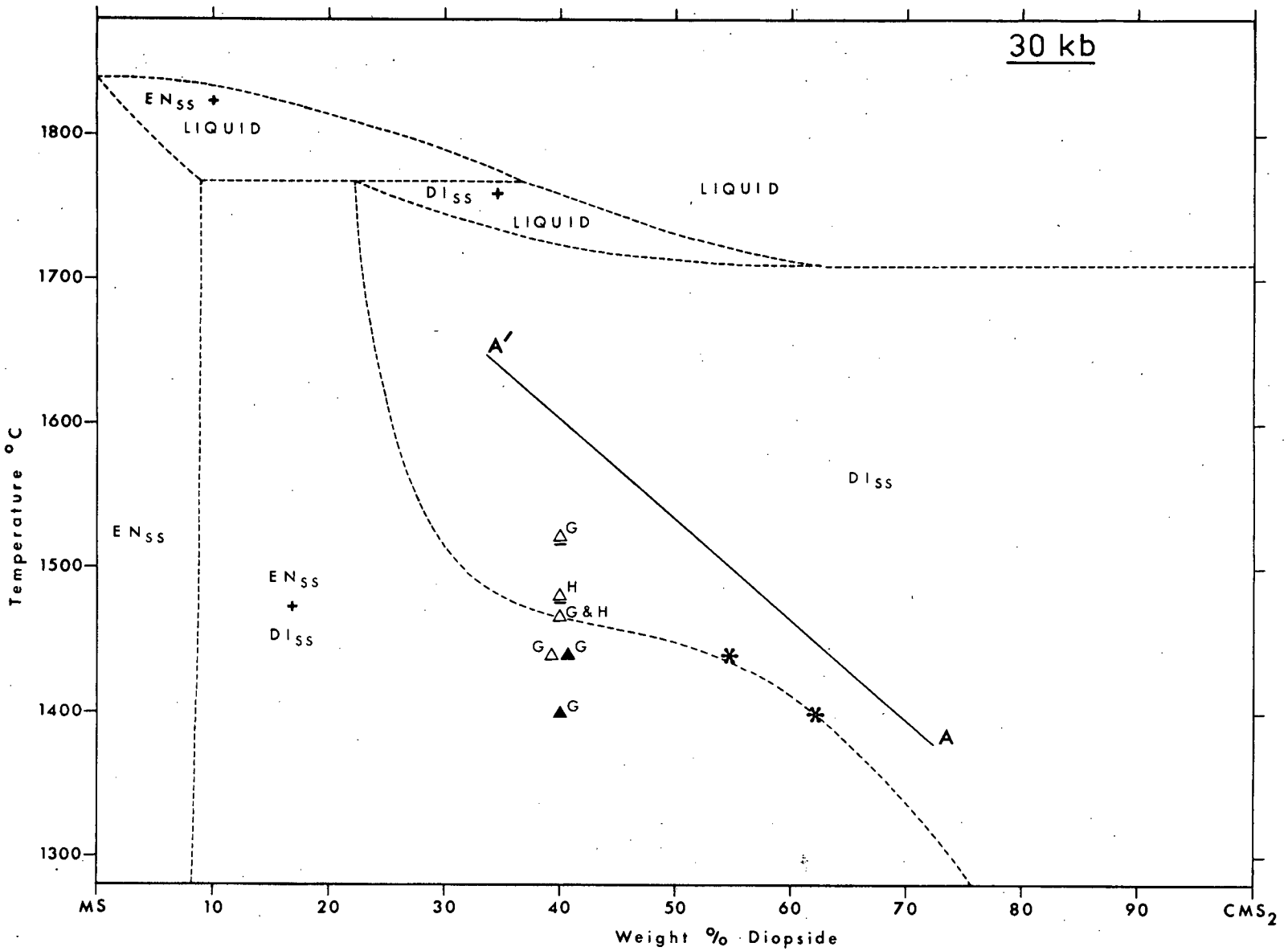
30 kb
EN$_{SS}$ + LIQUID
LIQUID
DI$_{SS}$ + LIQUID
LIQUID
A'
A
DI$_{SS}$
EN$_{SS}$
EN$_{SS}$ + DI$_{SS}$
G
H
G & H
G
G
G
1800
1700
1600
1500
1400
1300
Temperature °C
MS
10
20
30
40
50
60
70
80
90
CMS$_2$
Weight % Diopside

results of Davis and Boyd but contrary to those from gel charges. Similar results were obtained on a glass (charge E22H) with the same bulk composition but prepared by a different method (see Appendix A.2.1).

These experiments show that the discrepancy in the position of the cpx(opx) solvus determined here and by Davis and Boyd (1966) is the result of the difference in the physical state of the starting materials used. However, the run results obtained in this new study using $di_{ss}+en_{ss}$ assemblages (atmospheric pressure recrystallized gels) are also different from those obtained in Davis and Boyd's experiments on the same nominal starting material, viz. $di_{ss}+en_{ss}$ assemblages crystallized at atmospheric pressure. Davis and Boyd's $di_{ss}+en_{ss}$ assemblage starting materials were crystallized from glass not gel charges. If two pyroxenes were still present on reaching run conditions in Davis and Boyd's $di_{ss}+en_{ss}$ assemblage charges (see below), then it seems likely that second-order crystal structures in the phases of the low pressure $di_{ss}+en_{ss}$ assemblages are inherited by the high pressure phases. Such crystal structures, e.g. in terms of Ca-Mg ordering, would be determined by the crystallization history of a starting material.

These results have previously been published in a paper (Howells and O'Hara, 1975) in which the results of the kinetic study at 1450°C (presented in table 3.1) were described, from which it was concluded that the run products from gel charges were a closer approach to equilibrium than those from glass charges. This was based on the trend with increasing run duration of the $^{\circ}2\theta$ value of the 220 reflection of the clinopyroxene crystallized with orthopyroxene from

gel charges (see table 3.1). The $^{o}2\theta$ value initially increased suggesting, from the x-ray determinative curve, movement of the clinopyroxene composition towards enstatite and hence towards the solvus of Davis and Boyd (1966). This trend was reversed in runs longer than 30-60 minutes, with the $^{o}2\theta$ value decreasing towards that of the clinopyroxene indicated for the gel cpx(opx) solvus A'-A (fig. 3.1) at 1450°C. It is now believed that the change in the $^{o}2\theta$ value of the 220 reflection may be caused by the different rates of Ca:(Ca+Mg) and Si:(Ca+Mg) adjustments in the clinopyroxenes. This is suggested by the presence of free silica, and hence of pyroxenes showing considerable non-stoichiometry, in the products of runs of up to one hour in duration. The conclusion, based on the results of this kinetic study, concerning the relative stability of the two solvi is therefore not justified.

An attempt was made to reverse the cpx(opx) solvus A'-A (fig. 3.1) obtained from gel charges in order to determine whether this solvus is a closer approach to equilibrium than that reported by Davis and Boyd (1966). The homogeneous partially crystalline gel of bulk composition $(CMS_2)_{40}(MS)_{60}$ was held at 1620°C for 30 minutes in a piston-out experiment. The crystallization product is predicted from fig. 3.1 to be a single phase assemblage of clinopyroxene. The temperature was reduced to 1500°C under which conditions the charge was held for a further 100 minutes before quenching. The run product (run E22/159) was clinopyroxene alone as predicted by the results of Davis and Boyd but contrary to the results from gel charges shown in fig. 3.1.

The experiment was repeated on the same composition but reducing

the temperature from 1620°C to 1400°C where the charge was held 3 hours before quenching. The run product (run E22/166) was again a single phase assemblage of clinopyroxene, contrary to the results from both glass charges and those shown in fig. 3.1 for gel charges. In both run products (runs E22/159 and E22/166) the clinopyroxene occurred as very large crystals. Evidence from gel starting materials with bulk compositions on the join CMS_2-M_2S_2 shows that at 30 kb at temperatures above 1600°C, runs of only 30 minutes duration are sufficient to grow crystals of more than 40μ in diameter. This compares with a diameter of less than 1μ for partially crystalline gel starting material. The apparent metastable persistence of the single phase clinopyroxene assemblage within the stability field of cpx+opx may be due to the large size of the clinopyroxene crystals, and hence their small surface area and low free energy.

Davis and Boyd (1966) noted that their glass charges initially crystallized entirely to a metastable homogeneous clinopyroxene when held within the stability field of cpx+opx as determined from their run products. This homogeneous clinopyroxene gradually exsolved orthopyroxene, the coexisting clinopyroxene becoming simultaneously more calcic. O'Hara and Schairer (1963) and others have described the metastable persistence of pyroxenes crystallized as flash devitrification products of C-M-A-S glasses taken to high temperatures at various pressures. The main discrepancy between the present study and that of Davis and Boyd (1966) is the crystallization of cpx+opx phase assemblages from gel charges under conditions at which the glass charges used by Davis and Boyd crystallized single phase assemblages of clinopyroxene. This might reflect the metastable persistence of

the clinopyroxenes crystallized initially as devitrification products of the glass charges. Both partially crystalline and totally recrystallized gels used as starting materials in these new experiments contained abundant nuclei of two pyroxenes (di_{ss}+en_{ss}) at the beginning of the high pressure runs. This explanation for the discrepancy is supported by the results of the attempted reversal experiments described above which demonstrate the ease with which metastable clinopyroxenes persist even at these high temperatures and pressures. However, such an effect does not apparently explain the claimed reversal of Davis and Boyd's solvus using cryptoperthitic intergrowths of en_{ss}+di_{ss}, although such a claim cannot be justified without evidence that two pyroxenes were still present on reaching run conditions.

3.1.4 Comparison with other recent determinations at 30 kb

The cpx(opx) solvus for simple C-M-S pyroxenes has also been studied recently at 30 kb by Mori and Green (1975a,b), using glass and mixes of synthetic diopside (CMS_2) and clinoenstatite (MS) as starting materials; and by Nehru and Wyllie (1974) using recrystallized gel charges. In the temperature range for which comparisons can be made, viz. 1400-1700°C, the results of Nehru and Wyllie and of Mori and Green agree with those discussed above for gel charges in that:-

(i) no inflection in the cpx(opx) solvus towards more magnesian compositions occurred in this temperature range.

(ii) the composition of clinopyroxenes coexisting with orthopyroxene are more calcic than predicted from the cpx(opx) solvus of Davis and Boyd (1966). The compositions of the clinopyroxenes crystallized in equilibrium with orthopyroxene from the bulk composition

$(CMS_2)_{50}(MS)_{50}$ (approximate composition in weight %) at 1500°C in the three studies (Nehru and Wyllie, 1974; Mori and Green, 1975a; the present work) all lie within 1% diopside, which is well within the precision limits of the composition determinations.

There is no evidence for non-stoichiometry in the pyroxenes crystallized by Nehru and Wyllie (1974) at least at 1200°C. Non-stoichiometric pyroxenes were reported by Mori and Green (1975b) at 1500°C. Their results show a reduction in the solubility of enstatite in clinopyroxene in the presence of olivine, whereas the results reported above (section 3.1.2) at 1550°C indicate increased enstatite solubility in clinopyroxene in the presence of olivine.

Mori and Green (1975a) report an experiment on a glass charge which crystallized clinopyroxene alone at a temperature at which their other experimental results predicted the crystallization of cpx+opx. Mori and Green conclude that this single phase assemblage of clinopyroxene is metastable. This result corresponds to those described in the present work for C-M-S gel and glass charges.

The cpx(opx) solvus determined by both Nehru and Wyllie (1974) and Mori and Green (1975a) at low temperature (<1300°C) is less dependent on temperature than that reported by Davis and Boyd (1966). If the results of Nehru and Wyllie and of Mori and Green correspond more closely to the cpx(opx) solvus for natural systems, then the Ca/(Ca+Mg) ratio of enstatite-saturated clinopyroxene is not such a sensitive geothermometer as previously believed.

Warner and Luth (1974) have made a prediction of the 30 kb cpx (opx) solvus in the C-M-S system using thermodynamic extrapolations based on their experimental data points at 2, 5 and 10 kb. They

stress that the model they derive consists of functions which are purely mathematical quantities describing their data points and have no thermodynamic significance. The equation derived for the Margules parameter W_{G2} yielded physically improbable results for pyroxene compositions when extrapolations were made to temperatures above and below the range of the experimental data (1100-1300°C). Warner and Luth therefore modified the equation for W_{G2} to one which yielded more likely results outside this restricted temperature range. Although physically possible pyroxene compositions are obtained when both the original and modified equations are used at pressures outside the range of the experimental data, this does not justify such extrapolations.

3.2 Clinopyroxene solid solutions in the system C-M-S at 20 kb

3.2.1 Introduction

Kushiro's (1969a,b) study of phase relations on the join CMS_2-M_2S_2 at 20 kb used the same types of starting material as used by Davis and Boyd (1966) for experiments in the same system at 30 kb. In view of the possible metastability of the run products obtained by Davis and Boyd, it was necessary to make a redetermination of the CMS_2-M_2S_2 phase diagram at 20 kb using different types of starting material, and in particular to investigate the stability of the two clinopyroxene phase field reported by Kushiro (1969a) at temperatures above 1450°C.

A further aim of this study at 20 kb was to determine the effect of pressure on the clinopyroxene(orthopyroxene) solvus.

Compositions of starting materials used are given in Appendix

table A.2.3.

Experimental details and results are tabulated in Appendix tables A.9.3 and A.9.4. Details of two experiments carried out at the Geophysical Laboratory, Washington are given in Appendix table A.9.6.

3.2.2 Experimental results: gel charges

Fig. 3.5 compares the results of quenching experiments on partially crystalline gel starting materials with the phase diagram obtained by Kushiro (1969a) from similar bulk compositions on the join CMS_2-M_2S_2 at 20 kb.

The phase field of two clinopyroxenes determined by Kushiro (1969a) in the temperature range 1450-1650^{o}C could not be identified in the present study in runs in the same temperature range. The two clinopyroxene field is replaced in the new determinations by a single phase field of clinopyroxene at higher temperatures, and a cpx+opx phase field at lower temperatures. If a field of two clinopyroxenes is present, the coexisting solid solutions must have compositions which differ by less than 10% diopside, which is the minimum compositional difference distinguishable with the most favourable analytical techniques available, viz. x-ray diffraction traces using CrKα radiation (see section 3.1.2 and Appendix A.3.3).

The compositions of clinopyroxenes crystallized in the present study were estimated from the x-ray determinative curve, described in section 3.1.2 and Appendix A.3.4, which uses the relationship between the $^{o}2\theta$ value of the 220 reflection of a clinopyroxene solid solution and its Ca/(Ca+Mg) ratio. These compositional determinations showed that the clinopyroxenes coexisting with orthopyroxene in the

FIGURE 3.5

The results of quenching experiments at 20 kb on partially crystalline gel charges with compositions on the join CMS_2-MS. These experimental results are compared with the phase diagram (shown by dashed lines) for the join CMS_2-MS at 20 kb obtained by Kushiro (1969a,b).

Symbols are as in fig. 3.1. An encircled triangle indicates a bulk composition which yielded both primary and quench clinopyroxene. B'-B is the approximate position of the cpx(opx) solvus obtained from experiments on gel charges. A'-A is taken from fig. 3.1.

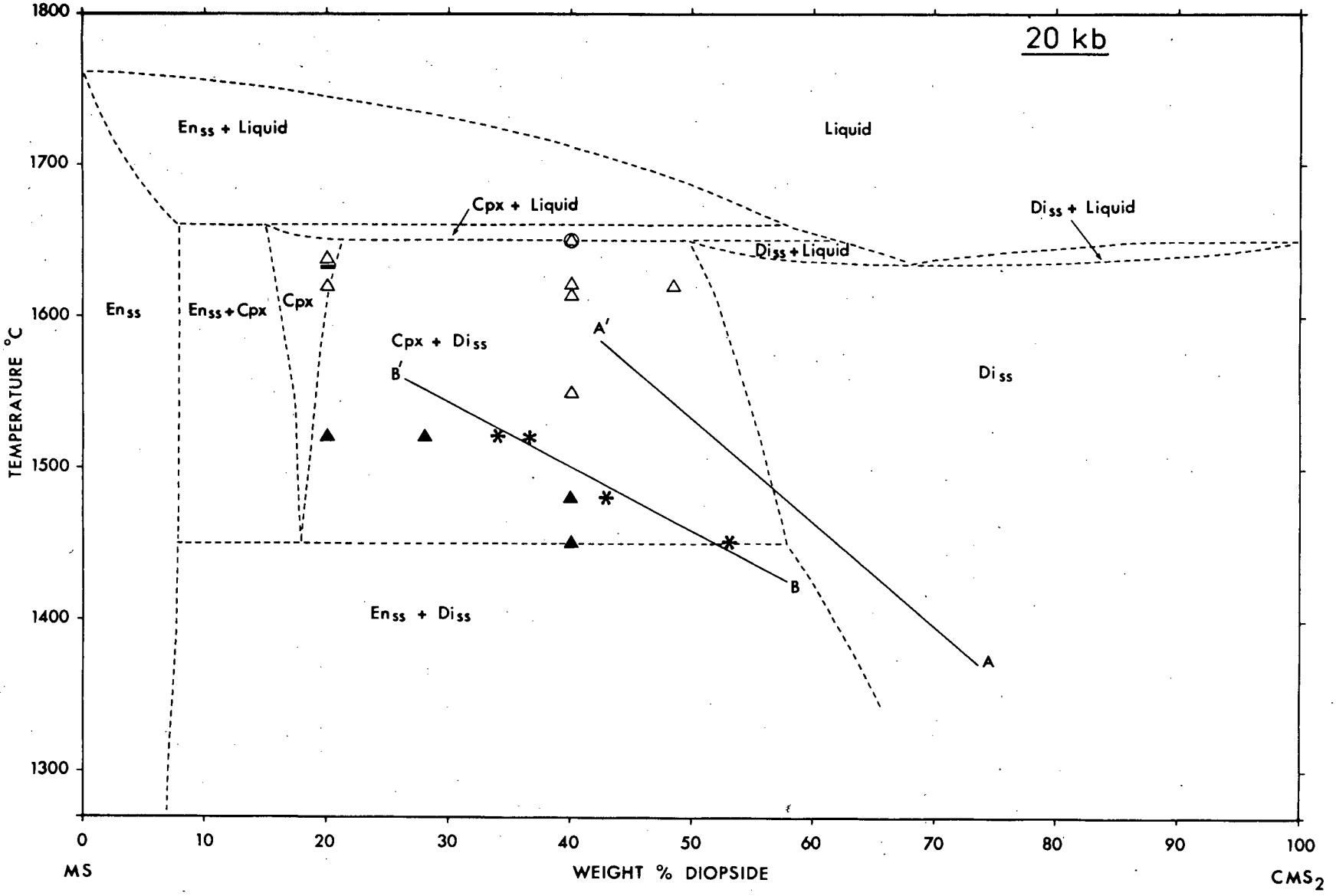
20 kb
Enss + Liquid
Liquid
Cpx + Liquid
Diss + Liquid
Diss + Liquid
Enss
Enss + Cpx
Cpx
Cpx + Diss
A'
B'
Diss
Enss + Diss
B
A
TEMPERATURE °C
1800
1700
1600
1500
1400
1300
0
10
20
30
40
50
60
70
80
90
100
MS
WEIGHT % DIOPSIDE
CMS2

temperature range 1450-1520°C become progressively more magnesian with increasing temperature. There is no evidence for an inflection in the cpx(opx) solvus in this limited temperature range.

Evidence for non-stoichiometric pyroxenes was provided by experiments on two different bulk compositions at 1520°C. At this temperature bulk compositions $(CMS_2)_{20}(MS)_{80}$ and $(CMS_2)_{28}(MS)_{72}$ crystallized orthopyroxene and a clinopyroxene of composition $di_{36.7}$ and $di_{33.7}$ respectively. The composition of the clinopyroxene coexisting in the isobaric and isothermally invariant assemblage cpx+opx+ol was determined at 1520°C in a run on the composition $(CMS_2)_{20}(MS)_{80}$ to which 10% of a partially crystalline forsterite gel was added. The composition of the clinopyroxene was $di_{36.7}$.

The crystallization products of two of these three experiments at 1520°C contained clinopyroxene whose 220 reflection on the x-ray diffraction trace lay very close to a high intensity orthopyroxene reflection which may have interfered with the $^{\circ}2\theta$ value of the clinopyroxene 220 reflection. Further evidence for non-stoichiometry in the pyroxenes crystallized in the system C-M-S at 1520°C, 20 kb was obtained by measuring the $^{\circ}2\theta$ value of the peak, on the x-ray diffraction traces, which represents the combined 310 and $\bar{3}11$ reflections for clinopyroxenes with such magnesian compositions. Student's t tests on the measurements (given in Appendix tables A.9.3 and A.9.4) showed that the clinopyroxenes crystallized in the two olivine-free assemblages were different at the 99.9% probability level. This confirms that the pyroxenes are non-stoichiometric. The clinopyroxene crystallized in the olivine-bearing assemblage had a composition which was much more closely comparable to that

crystallized from bulk composition $(CMS_2)_{20}(MS)_{80}$ than from bulk composition $(CMS_2)_{28}(MS)_{72}$. This is consistent with the results suggested by consideration of the 220 reflection.

3.2.3 Comparison of experimental results with those of Kushiro (1969a,b)

Possible explanations for the differences between these new experimental results and those of Kushiro (1969a,b) will now be considered.

A. Inter-laboratory differences in the pressure and temperature calibration of the equipment.

Kushiro's (1969a,b) experiments were carried out using equipment at the Geophysical Laboratory, Washington. Calibration phase field boundaries determined in the Edinburgh laboratory were observed at closely comparable pressure/temperature conditions to those reported for the same equilibria determined using the Washington equipment (see Appendix A.1.2). Differences of pressure and temperature scale between the two laboratories cannot therefore account for the observed discrepancies in this system.

B. Piston-technique.

The new experiments were carried out using the piston-out technique whereas Kushiro (1969a,b) used the floating-piston technique for his experiments and made a -3% pressure correction to the nominal value. Use of the piston-out rather than the floating-piston technique could lead to different results because of the higher actual pressure realized using the piston-out technique (see Appendix A.1.1), and because of the 5 kb extra pressure on the crystals, albeit for a

few minutes at most, during the piston-out stroke. However, a floating-piston experiment on partially crystalline gel $(CMS_2)_{40}(MS)_{60}$ (charge E22) at 1620°C crystallized to a single clinopyroxene as in a piston-out experiment at 1620°C on the same charge. Composition $(CMS_2)_{40}(MS)_{60}$ lies well inside Kushiro's (1969a) two clinopyroxene phase field. Failure to resolve two clinopyroxenes of the compositions predicted by Kushiro in the x-ray diffraction traces of the run products of this composition is not the result of the predominance of one of the phases.

C. Run duration.

The durations of these new experiments are comparable at similar temperatures to those of experiments on the same compositions at 30 kb in which it was considered that equilibrium had been achieved. Durations of experiments carried out by Kushiro (1969a,b) are similar to those used here at 20 kb.

D. Bulk compositions.

Similar bulk compositions were used by Kushiro (1969a,b) and in these new experiments.

E. Identification of run products.

X-ray diffraction techniques were the principal means of identifying run products in both studies. Two of the criteria used by Kushiro (1969a,b) as evidence for the presence of two clinopyroxenes were splitting of the 220 and 311 reflections of clinopyroxene on the x-ray diffraction powder patterns; and the change in the relative intensity, but not position, of the 311 clinopyroxene reflection with variation in the Ca/(Ca+Mg) ratio of the bulk composition. $CuK\alpha$ radiation was used by Kushiro to obtain his x-ray diffraction traces.

Fig. 3.6 shows the x-ray diffraction patterns using CuKα and CrKα radiation of a mixture of two clinopyroxenes of composition $di_{48.5}en_{51.5}$ and $di_{20}en_{80}$ in the proportion 2:1. This mixture simulates the run product obtained by Kushiro (1969a) from bulk composition $(CMS_2)_{40}(MS)_{60}$ at about 1630°C. The 021 and 220 reflections are clearly separated using CrKα radiation but not using CuKα radiation. Two distinct 311 reflections can be seen on the pattern obtained using CuKα radiation. The $\bar{2}02$ reflection and the multiple peak representing the reflections ($\bar{1}12$, 002 and 221) are clearly separated on both patterns. Fig. 3.7 is the x-ray diffraction pattern obtained using CrKα radiation for the crystallization product of the partially crystalline gel of bulk composition $(CMS_2)_{40}(MS)_{60}$ run in the present study at 1622°C (run E22/60). The pattern is quite different from that predicted (fig. 3.6) by Kushiro. Single peaks occur for the 021, 220 and $\bar{2}02$ reflections and for the combined ($\bar{1}12$, 002 and 221) reflections. Each of these peaks is intermediate in position between the relevant pair illustrated in fig. 3.6. The run product is clearly a single clinopyroxene (or two clinopyroxenes differing in composition by less than 10% diopside) intermediate in composition between the two clinopyroxenes predicted by Kushiro as the crystallization product under these conditions.

F. Starting materials.

The starting materials used by Kushiro (1969a,b) were glass, recrystallized glass and mechanical mixtures of diopside (CMS_2) and clinoenstatite (MS). All three starting materials crystallized the two clinopyroxene phase assemblage under the conditions indicated in fig. 3.5.

FIGURE 3.6

X-ray diffraction powder patterns of a mixture of two clinopyroxenes of composition $di_{48.5}en_{51.5}$ (product of run E23/136) and $di_{20}en_{80}$ (product of run M2I/148) combined in the proportion 2:1. The left hand trace was obtained using CuKα radiation; the right hand trace was obtained using CrKα radiation. This clinopyroxene mixture simulates the run product obtained by Kushiro (1969a,b) from bulk composition $(CMS_2)_{40}(MS)_{60}$ at about 1630°C, 20 kb.

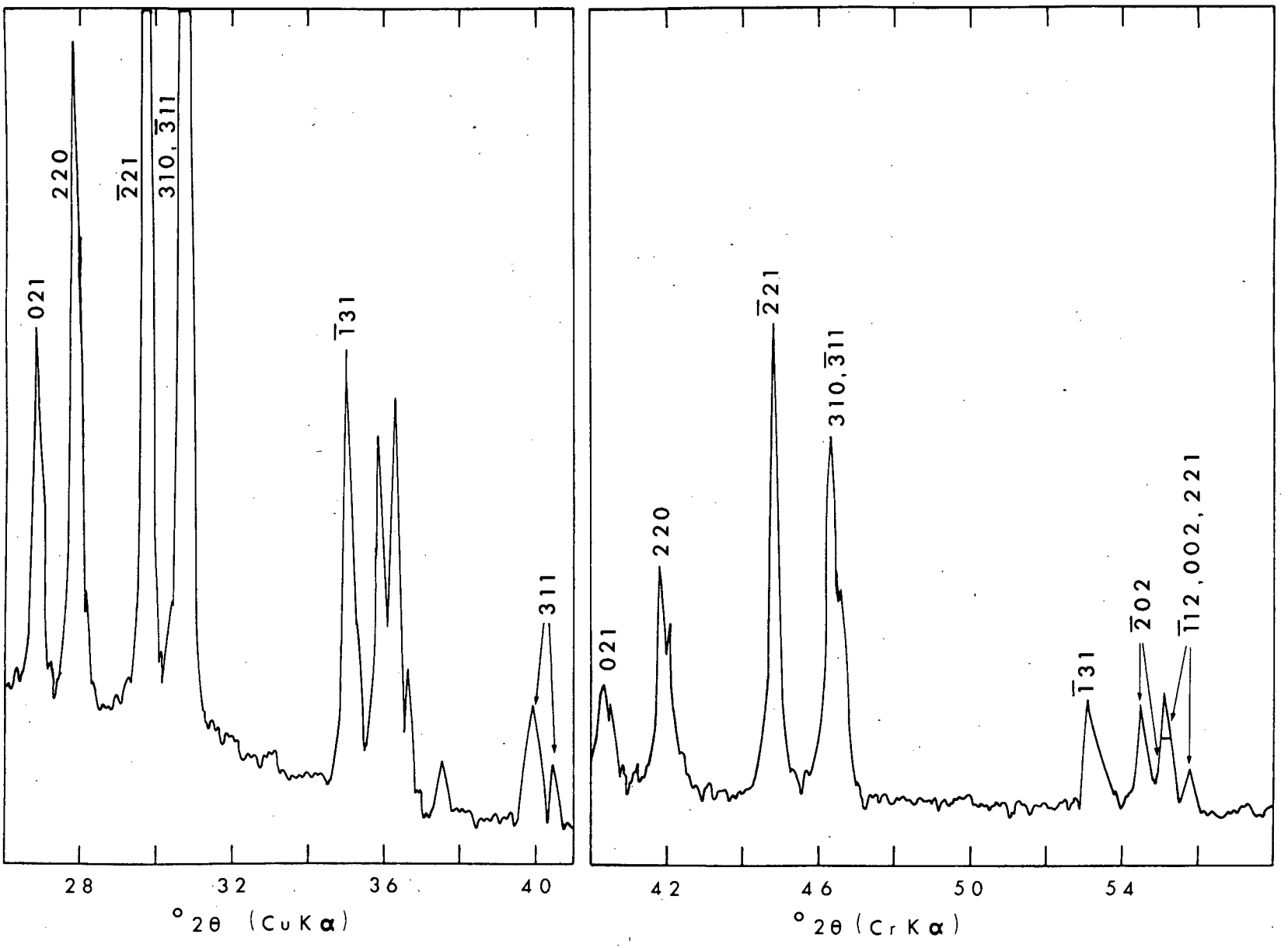
021
220
$\bar{2}21$
310, $\bar{3}11$
$\bar{1}31$
311
28
32
36
40
°2θ (CuKα)
021
220
$\bar{2}21$
310, $\bar{3}11$
$\bar{1}31$
$\bar{2}02$
$\bar{1}12$, 002, 221
42
46
50
54
°2θ (CrKα)

FIGURE 3.7

X-ray diffraction powder pattern, obtained using CrKα radiation, of the crystallization product of the partially crystalline gel of bulk composition $(CMS_2)_{40}(MS)_{60}$ run in the present study at 1622°C, 20 kb.

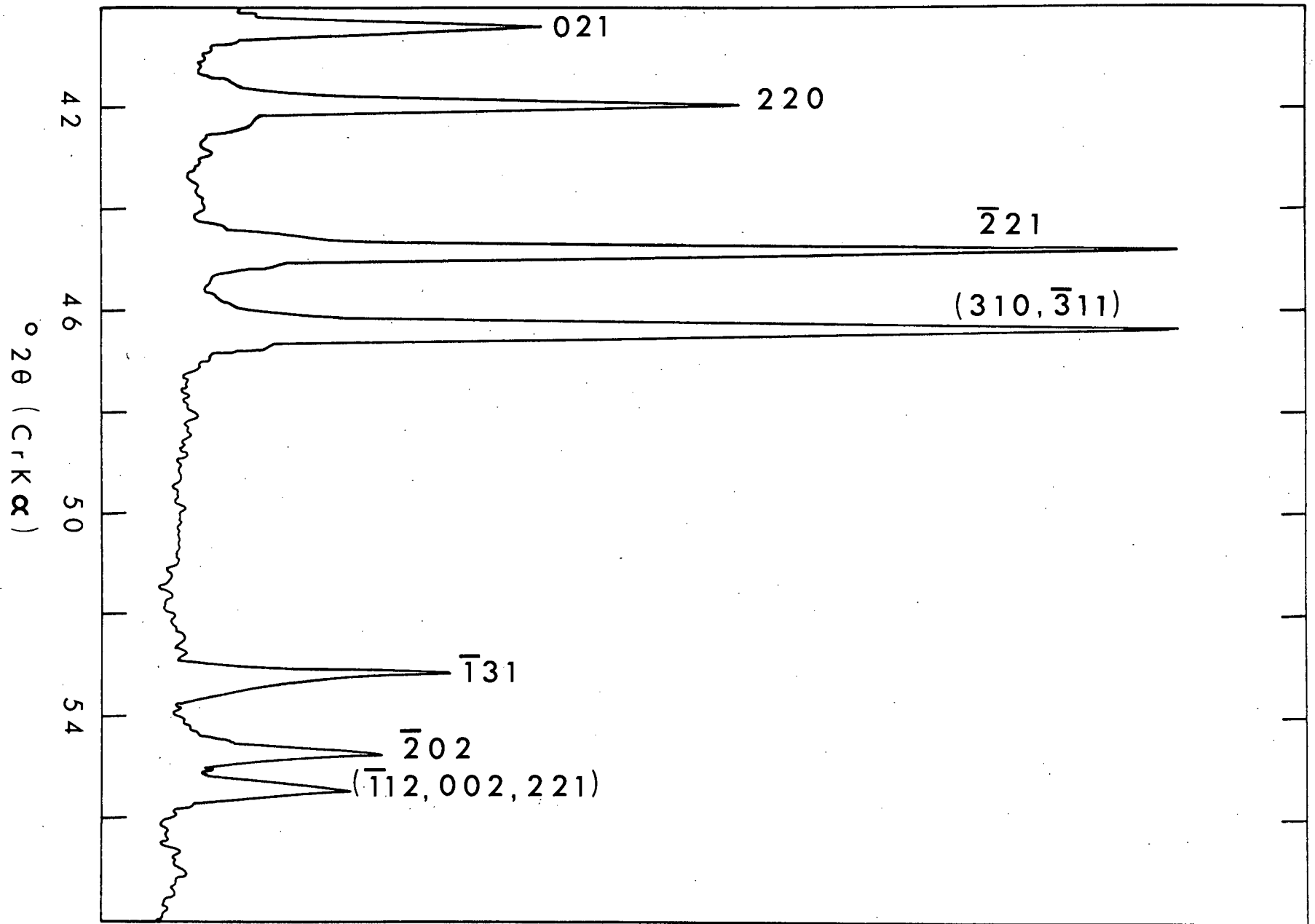
021
220
$\bar{2}21$
(310, $\bar{3}11$)
$\bar{1}31$
$\bar{2}02$
($\bar{1}12$, 002, 221)
42
46
50
54
°2θ (CrKα)

In the new experiments the starting materials used were partially crystalline gels, mechanical mixes of such gels including mixes of CMS_2 and MS end member gels, and two glasses of composition $(CMS_2)_{40}(MS)_{60}$ prepared by two different methods (see Appendix A.2.1) from the homogeneous gel of the same composition. (Fig. 3.5 shows the results of experiments on gel charges only). All starting materials gave consistent results. The bulk composition $(CMS_2)_{40}(MS)_{60}$ crystallized to a single phase assemblage of clinopyroxene at about 1620°C in piston-out experiments whether homogeneous gel, a mix of CMS_2 and MS gels, or glass was used as starting material. The assemblage produced is contrary to the two clinopyroxene assemblage predicted by Kushiro (1969a) under these conditions. Similarly, the glass of bulk composition $(CMS_2)_{40}(MS)_{60}$ crystallized clinopyroxene of composition $di_{45.4}$ at 1475°C in a piston-out experiment. The presence of orthopyroxene could not be confirmed optically or using x-ray diffraction analytical techniques, but it is inferred from the clinopyroxene composition. This clinopyroxene ($di_{45.4}$) lies close in composition to the cpx(opx) solvus B'-B (fig. 3.5) determined from the gel charges but is within the phase field of two clinopyroxenes determined by Kushiro (1969a).

These results do not remove the possibility that differences in the nature of the starting material used have caused the apparent discrepancies under consideration. Crystallization products in this system may be determined by the pre-run thermal treatment of the charge, for example the charge drying procedure, which would affect various parameters of the starting material, such as crystal size and ordering within the crystals.

G. Quenching rates.

The possibility that the field of two clinopyroxenes is a quenching phenomenon was suggested by two observations made by Kushiro (1969a,b).

(i) He was not able to consistently generate the two-clinopyroxene assemblage. Runs at 1600°C on a glass of composition $(CMS_2)_{40}(MS)_{60}$ and a recrystallized glass of composition $(CMS_2)_{35}(MS)_{65}$ both yielded a single clinopyroxene as predicted by the results of runs on gel charges.

(ii) A run on the glass of composition $(CMS_2)_{40}(MS)_{60}$ yielded a single clinopyroxene at 1600°C. This clinopyroxene was ground, reloaded and held at 1620°C for 30 minutes. The x-ray diffraction pattern of the new run product clearly indicated the presence of two clinopyroxenes. Microprobe analysis revealed that two phases, a Ca-rich phase and a Ca-poor phase, were indeed present but that they occurred as intergrowths within individual crystals.

A possible explanation of these phenomena is that the two clinopyroxenes reported by Kushiro (1969a,b) are the breakdown products of a single homogeneous clinopyroxene, the breakdown occurring during the quenching of the experiment.

To test this hypothesis two floating-piston runs at 1620°C on the homogeneous gel $(CMS_2)_{40}(MS)_{60}$ were subjected to a deliberately slow quench. The first (run E22/145) was quenched to room temperature in a single operation in which the temperature was manually reduced at a uniform cooling rate of 80°C/second. In the second experiment (run E22/146) the charge was cooled by the same method and rate of temperature drop to 1300°C where it was held for a further

11 minutes before quenching rapidly to room temperature by the normal method, viz. by switching off the power supply to the equipment. Both run products consisted of a single phase assemblage of clinopyroxene as predicted from the results of runs on gel charges quenched normally from 1620°C.

The glass and homogeneous gel of bulk composition $(CMS_2)_{40}(MS)_{60}$ which were used in these new experiments were run by Dr. B. Harte at 1620°C in the same equipment used by Kushiro (1969a,b). Both run products contained only a single clinopyroxene.

Kushiro (1969b) carried out an experiment, described above, in which a high temperature clinopyroxene broke down to two clinopyroxenes in a second run at 1620°C. This double experiment was repeated in the new run series for a glass with the same composition $(CMS_2)_{40}(MS)_{60}$ as that used by Kushiro. The run product at the end of each stage of the experiment was a single phase assemblage of clinopyroxene.

It is concluded that if the two clinopyroxene phase field is a quenching phenomenon, it could not be reproduced with the starting materials used for these new experiments.

The explanation for the discrepancy between the two sets of results illustrated in fig. 3.5 remains an enigma. The form of the cpx(opx) solvus determined by Kushiro (1969a,b) is similar to that obtained by Davis and Boyd (1966) at 30 kb using similar starting materials. The erratic crystallization of the two clinopyroxene assemblage suggests that the high pressure (meta)stable phase diagram obtained using certain glass starting materials has the shape determined by Davis and Boyd at 30 kb, but that at 20 kb the highly

magnesian clinopyroxenes broke down into two different clinopyroxenes on quenching. The relative stabilities of the inflected form of the cpx(opx) solvus obtained by Davis and Boyd and by Kushiro, and the uninflected solvus determined in the present study are as yet unknown.

The new results discussed in this section and in section 3.1 throw doubt on the stability of the sub-calcic clinopyroxenes crystallized by Kushiro and Yoder (1970) at 2-17.5 kb, from C-M-S compositions using starting materials similar to those used by Kushiro (1969a,b) and Davis and Boyd (1966). Kushiro and Yoder report that the crystallization of this sub-calcic clinopyroxene was erratic and the phase assemblage cpx+opx was obtained as the product of runs on the same composition held at the same conditions as runs in which the sub-calcic clinopyroxene crystallized.

3.2.4 Comparison of experimental results with other recent determinations at 20 kb

The experiments of Lindsley and Dixon (1975) on C-M-S compositions at 20 kb, 1200°C indicate that the compositions of the clinopyroxenes coexisting with orthopyroxene and either olivine or quartz are the same within the precision limits of the determinations. Lindsley and Dixon's results at 20 kb, 900-1200°C agree with the 30 kb results of Nehru and Wyllie (1974) and Mori and Green (1975a) in that their cpx(opx) solvus is much less temperature sensitive at low temperature than reported by Davis and Boyd (1966) or predicted by Warner and Luth (1974) from thermodynamic equations.

3.3 Evidence for a miscibility gap or structural break in C-M-S clinopyroxene solid solutions at high pressure

The possibility of a miscibility gap or structural break in clinopyroxene solid solutions at high pressure was suggested in natural rocks by the bimodal distribution of the Ca/(Ca+Mg) ratio of clinopyroxenes in garnet-lherzolites in kimberlite, and in synthetic systems by the abrupt change in the cpx(opx) solvus determined by Davis and Boyd (1966), Kushiro (1969a,b), Munoz and Lindsley (1969) and O'Hara (1975) (see section 1.1).

The results of Davis and Boyd (1966) and of Kushiro (1969a,b) could not be repeated using different starting materials. Their reported phase assemblages are not considered here to be equilibrium phase assemblages. A small (in terms of range of Ca/(Ca+Mg) ratio) equilibrium phase field of two clinopyroxenes may however have been missed in the new study. The starting materials used by Munoz and Lindsley (1969) were similar to those used by Kushiro (1969a,b) and by Davis and Boyd (1966). The results of Munoz and Lindsley for the system CFS_2-F_2S_2 may also therefore be metastable. Evidence which suggests that O'Hara's (1975) results in the system C-M-A-S are for disequilibrium assemblages is given in section 4.3.

Two observations made in this study of C-M-S clinopyroxenes crystallized from gel charges suggest, however, that these clinopyroxenes show first or second order structural differences:-

(i) Fig. 3.2 shows the clinopyroxene x-ray determinative curve prepared by Davis and Boyd (1966) which relates the $^{o}2\theta$ value of the 220 reflection of a clinopyroxene with its Ca/(Ca+Mg) ratio (see

Appendix A.3.4). The $^{o}2\theta$ 220 values of clinopyroxenes of known composition synthesized from gel charges in the present study (see Appendix table A.3.4) closely bracket the Davis and Boyd curve for clinopyroxenes in the range di_{20} to di_{70} (see fig. 3.2). The $^{o}2\theta$ 220 values for the clinopyroxenes di_{90} and $di_{95.1}$, however, lie well off both Davis and Boyd's curve which is non-linear from di_{70} to di_{100}, and the linear extrapolation of the straight portion of the curve to more calcic clinopyroxenes (fig. 3.2). The non-linear nature of the determinative curve could be caused by the presence in the run products of the synthesis experiments of a phase in addition to clinopyroxene. There was no evidence for this either optically or using x-ray diffraction analysis; it was hoped that the possible presence of small amounts of liquid was removed by repeating the synthesis of the clinopyroxene of intended composition di_{90} at a lower temperature. The composition $(CMS_2)_{90}(MS)_{10}$ was held at 1400°C, which is 300°C below the temperature of the solidus reported by Davis and Boyd (1966). The $^{o}2\theta$ 220 value of the clinopyroxene synthesized was the same as that for the clinopyroxene crystallized from the same bulk composition at 1680°C.

(ii) Fig. 3.2 also shows the $^{o}2\theta$ CrKα values of the $\bar{2}21$ reflection of clinopyroxenes crystallized in the synthesis experiments detailed in Appendix table A.3.4. These values are plotted against clinopyroxene composition. The plot shows a minimum value for $^{o}2\theta$ at the clinopyroxene composition of about $(CMS_2)_{47}$ (mole %) but rises to higher values of $^{o}2\theta$ for more magnesian and more calcic clinopyroxenes. Clinopyroxenes in the range di_{20} to di_{70} only were considered.

These two observations may reflect structural changes in the clinopyroxenes which occurred during quenching. If they in fact reflect first or second order structural differences in the high temperature and high pressure clinopyroxenes crystallized during the experiments, then these differences may control the position of the cpx(opx) solvus. For this reason firm statements cannot yet be made concerning the relative stabilities of the phase assemblages discussed above (sections 3.1.3 and 3.2.3).

A distinction was not made in the present work between clinopyroxenes with the C2/c and $P2_1/c$ structures.

3.4 Effect of pressure on the clinopyroxene(orthopyroxene) solvus in the system C-M-S

Fig. 3.8 compares the position of the cpx(opx) solvus at 30 kb for bulk composition $(CMS_2)_{40}(MS)_{60}$ (solvus A'-A in fig. 3.1) with that obtained at 20 kb (solvus B'-B in fig. 3.5) as a best fit for the limited data points deduced for a wide range of bulk compositions. The compositions of the clinopyroxenes coexisting with both orthopyroxene and olivine at 20 kb, 1520°C, and at 30 kb, 1550 and 1565°C are also shown. (The effect of pressure on the cpx(opx) solvus cannot be obtained with any precision from a comparison of lines A'-A and B'-B in fig. 3.8 because these lines do not represent the isobaric invariant cpx(opx) solvi for olivine-saturated assemblages.)

FIGURE 3.8

The effect of pressure on the cpx(opx) solvus for C-M-S pyroxenes. The figure compares the position of the cpx(opx) solvus determined from experiments on gel charges at 20 kb (line B'-B from fig. 3.5) and at 30 kb (line A'-A) from fig. 3.1). The asterisks indicate the measured compositions of C-M-S clinopyroxenes crystallized at 20 and 30 kb in the assemblage cpx+opx+ol.

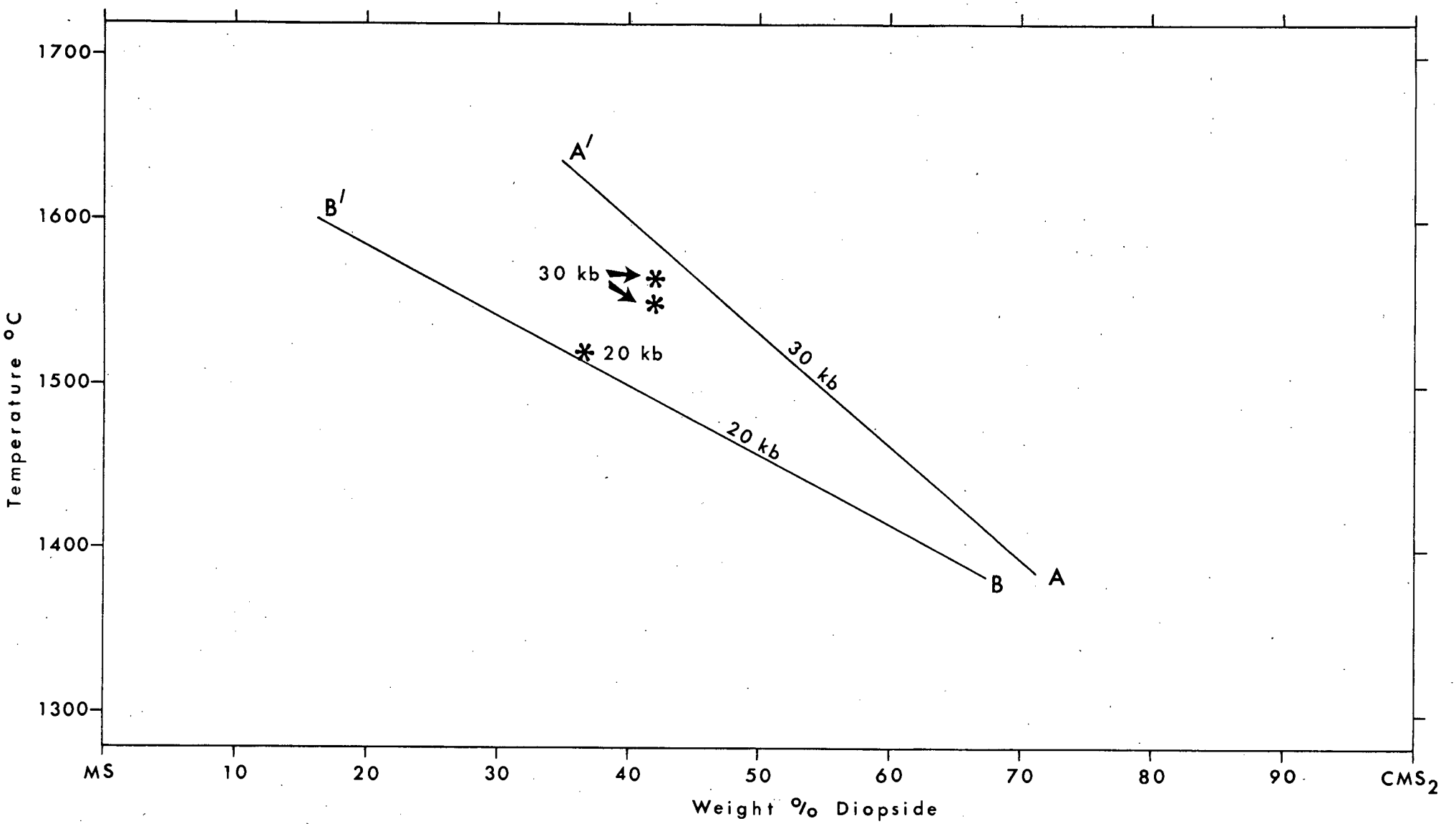
1700
1600
1500
1400
1300
Temperature °C
A'
B'
30 kb
20 kb
30 kb
20 kb
A
B
MS
10
20
30
40
50
60
70
80
90
CMS2
Weight % Diopside

Fig. 3.8 shows that pressure has a large effect on the position of the cpx(opx) solvus, at least at temperatures above 1450°C and in the pressure range 20-30 kb. The extent of this effect in olivine-saturated assemblages at 1535 ±15°C is to increase the diopside content of clinopyroxene by 0.8%/kb. This quantity is approximate because it was deduced by applying the x-ray determinative curve (fig. 3.2) for stoichiometric pyroxenes to non-stoichiometric pyroxenes.

The effect of pressure on the cpx(opx) solvus at temperatures lower than those investigated in the present study is confused because of the range of positions for the solvus determined at any one pressure in different studies (see Mori and Green, 1975a, fig. 2) and by the limited high pressure data, except at 30 kb.

Mori and Green (1975a) showed that increasing pressure reduced the solubility of enstatite in clinopyroxene in equilibrium with orthopyroxene at 1200°C but that at 900°C the pressure effect was trivial. The conclusion concerning the effect of pressure at 900°C must be queried since it is based on only two determinations of clinopyroxene composition, viz. at 10 kb and at 30 kb, one of which was the average result of two experiments which had given different clinopyroxene compositions.

The cpx(opx) solvi determined experimentally by Warner and Luth (1974) at 2, 5 and 10 kb in the temperature range 1100-1300°C showed no consistent pressure effect at all temperatures.

Nehru and Wyllie(1974, p.226) made the suggestion, endorsed here, that "comments about the effect of pressure are premature".

CHAPTER 4

THE CLINOPYROXENE GEOTHERMOMETER:

CLINOPYROXENE SOLID SOLUTIONS IN THE SYSTEM C-M-A-S AT 30 KB

4.1 Introduction

This chapter reports the results of experiments at 30 kb on compositions in the system C-M-A-S. These experiments were designed to:-

(i) determine the Ca/(Ca+Mg) ratio of clinopyroxene in the assemblage cpx+opx+gt±ol at different temperatures.

(ii) obtain further evidence for the coexistence of two clinopyroxenes in the system C-M-A-S at high pressure and temperature as suggested by O'Hara (1975).

Several different starting materials and a large number of closely spaced bulk compositions were used in this study. A comparison of the results obtained from these different charges showed that the latter had failed to crystallize to the stable equilibrium assemblages during the high temperature and high pressure experiments. The evidence for, and causes of this failure to attain stable equilibrium are discussed in this chapter. The implications of these results for the stability of the assemblages reported in previous high pressure studies are also considered.

The compositions of the charges used in this study are given in Appendix table A.2.4.

Experimental details and results for the C-M-A-S charges are presented in Appendix table A.9.5. All runs were carried out

using the piston-out pressure technique.

4.2 A problematic garnet-olivine intergrowth texture

4.2.1 Petrography and composition of the phases in the intergrowth

A textural association of garnet and olivine appeared regularly in the high pressure crystallization products of diopside-rich gels and occasionally in enstatite-rich ones. It was rarely absent from olivine-bearing run products of most partially crystalline gels whose composition contained $\geq 3.0\%$ Al_2O_3 when projected from forsterite onto the plane CS-MS-A. It also occurred to a lesser extent in the run products of many recrystallized gels. (The terms "partially crystalline" and "recrystallized" gel refer to the extent of atmospheric pressure recrystallization of a gel used as a starting material for the high pressure experiments - see Appendix A.2.1)

This texture is an intergrowth of garnet and olivine. It appeared to exhibit a gradation defined by the crystal size of the garnet. At one end of the spectrum large euhedral olivine crystals were shot through with minute crystals, believed to be garnet, which produced a murkiness in the olivine crystals. At the other end of the spectrum much larger anhedral crystals of garnet occurred in clusters or stringers interspersed with and often at least partly surrounded by olivine crystals. The garnet-olivine masses ranged in size from 5-25μ across. The whole textural range was usually seen in each run product and occasionally within a single garnet-olivine mass.

Discrete olivine and garnet crystals, for which a textural

association with the other phase was not identifiable, often occurred along with the intergrowths in the same run product. Discrete garnet crystals were larger (up to 5-10μ) than the largest seen in the garnet-olivine intergrowths and had a subhedral to euhedral shape. (Such garnet is referred to as "euhedral garnet" in the following text.)

The garnet in the intergrowths was only distinguishable by its texture from the euhedral garnet crystals. A few run products contained only traces of euhedral garnet but sufficient garnet in the intergrowths to register on the x-ray diffraction pattern of run products. In these cases even the strongest garnet reflections were too weak to provide an indication of composition for comparison with the composition of euhedral garnet.

Peak splitting on the x-ray diffraction traces, which might have indicated two separate compositions, was not observed for the olivine reflections of run products which contained both discrete olivine crystals and olivine in association with garnet. Table 4.1 compares the $^{o}2\theta$ CrKα values of the 112 reflection (which occurs for pure forsterite at 36.52$^{o}2\theta$ CuKα) of olivines crystallized from various charges. The 112 reflection was chosen because it showed the most variation (see Appendix A.3.5). There is no significant difference in the $^{o}2\theta$ values of the 112 reflection for olivines in two run products (runs AM8/207 and E34F24/219) containing large amounts of garnet-olivine intergrowths and the $^{o}2\theta$ 112 for pure forsterite.

TABLE 4.1

$^{\circ}2\theta$ CrKα values of the 112 reflection of olivines crystallized from different charges at various temperatures at 30 kb (with the exception of pure forsterite which was crystallized at 1 kb)

Run No.	Charge No.	Temp. ($^{\circ}$C)	$^{\circ}2\theta$ CrKα Olivine 112*
-	FR	1000	55.524±0.040*
219	E34F24	1525	55.510±0.032
207	AM8	1500	55.520±0.035
232	FP10	1523	55.544±0.036
224	F10Py	1525	55.552±0.043
199	OHB	1500	55.504±0.042
256	OHBR	1500	55.510±0.026

* Values are quoted with the error $\pm 2\sigma$

4.2.2 High pressure experiments in the system M_2S-M_3AS_3

The garnet-olivine intergrowth texture suggested a solution or exsolution phenomenon in the system garnet-olivine. An attempt was therefore made to homogenize forsterite-rich mixes with compositions in the system M_2S-M_3AS_3 with the aim of:-

(i) determining the extent, if any, of solid solution of M_3AS_3 in forsterite.

(ii) reproducing the garnet-olivine intergrowth texture.

Experiments by Davis (1964) using mixes of pure crystalline M_2S and M_3AS_3 showed no evidence of solid solutions along the join M_2S-M_3AS_3 at 40 kb. Davis failed to homogenize the mixes $(M_2S)_{99}(M_3AS_3)_1$ and $(M_2S)_1(M_3AS_3)_{99}$.

The charges used in these new experiments were:-

F1OPy - a mixture of partially crystalline gels of composition M_2S and M_3AS_3 combined in the ratio $(M_2S)_{90}(M_3AS_3)_{10}$

FP1Θ - a mixture of forsterite (M_2S) crystals and pyrope (M_3AS_3) crystals combined in the ratio $(M_2S)_{90}(M_3AS_3)_{10}$

The experiments described below (and listed in Appendix table A.9.6) were carried out at $1524\pm1^{o}C$, 30 kb using the piston-out technique. These are conditions under which the C-M-A-S gels crystallized the garnet-olivine association or a phase which quenched to produce it. Similar charge-drying techniques and run durations were employed in these runs as in those on the C-M-A-S gels.

The crystallization product of the gel mix (F1OPy) contained very few euhedral garnet crystals. It consisted mainly of large olivine crystals and a small amount of minute anhedral garnet crystals which occurred in and around the former. Olivine, but no

garnet, was identified on the x-ray diffraction pattern.

The x-ray diffraction pattern of charge FP10 showed a fairly strong peak representing the pyrope 420 reflection. It is therefore concluded that the gel mix did not crystallize the maximum 10% of pyrope (M_3AS_3) possible from this bulk composition. This must reflect the solution into forsterite of some or all of the chemical components of pyrope. No phase in addition to garnet and olivine was observed in the run product of charge F10Py. This suggests that some M_3AS_3-M_2S mixes can be homogenized.

The crystallization product of charge FP10 under the same conditions consisted of large euhedral crystals of both olivine and garnet. The garnet appeared from optical examination to constitute a much higher proportion of the run product than of that of the gel mix described above. Garnet in addition to olivine was identified from the x-ray diffraction pattern of run products of charge FP10. Garnet-olivine intergrowths were not observed.

Table 4.1 gives the $^{o}2\theta$ CrKα values for the 112 reflection of olivines crystallized at 1524$\pm$1^{o}C, 30 kb from FP10 and F10Py. These are not significantly different from each other. However, a comparison of this $^{o}2\theta$ value for the olivine in the run product of F10Py with that for pure forsterite indicates a probability of only 5% that the former has the composition of pure forsterite. This probability is much greater for the olivine crystals in the run product of the crystal mix FP10.

It is concluded that Al_2O_3 can be dissolved in forsterite at high temperatures and pressures, but that the amount dissolved depends on the starting material used. This does not mean that

pyrope crystals will dissolve in forsterite under the same conditions. Pyrope nucleation is sluggish (e.g. Boyd and England, 1964) and though it does crystallize from the bulk composition M_3AS_3 under these conditions (Boyd and England, 1962), it may not have had a chance to nucleate in the gel charge F1OPy before the crystallization of an aluminous olivine which may or may not be a stable phase.

The inclusion of minute anhedral garnet crystals in the olivine crystallized from the gel mix is similar to some of the textures of the garnet-olivine intergrowths observed in the C-M-A-S gel run products. However, the proportion of garnet to olivine was usually much greater in the latter than in the former. The garnet-olivine intergrowth texture was not therefore convincingly reproduced.

4.2.3 Possible explanations of the garnet-olivine intergrowth

Possible explanations of the garnet-olivine intergrowth texture are:-

(i) A nucleation effect. The nucleation of olivine may be associated with the nucleation of garnet. The growth of the olivine crystals may then have inhibited the growth and coalescence of small garnet crystals. However, the textural evidence in a run (AM7/206) quenched a few seconds after reaching run conditions shows that this is unlikely. The run product consisted of a fine-grained groundmass containing large olivine crystals with no traces of adjacent crystals or inclusions of garnet. The same charge run for longer at the same temperature (run AM7/205) contained a high proportion of garnet-olivine masses.

(ii) The texture may represent the product of the reaction:

anorthite + forsterite ⟶ garnet

(garnet composition $(C_3AS_3)_{36}(M_3AS_3)_{64}$)

This is one of the numerous reactions which may have occurred in the C-M-A-S charges to convert the low pressure phases (see Appendix A.2.3) to high pressure assemblages. Anorthite and forsterite are both low pressure phases for the diopside-rich compositions under consideration. The garnet-olivine texture may represent the product of this reaction occurring in the presence of excess forsterite. One objection to this interpretation of the garnet-olivine texture is that the texture occurs much more commonly in the run products of partially crystalline gel charges than in those of the recrystallized gel charges in which the anorthite and forsterite are present in much larger quantities and as much bigger crystals.

(iii) The texture may represent the product of the reaction:

orthopyroxene + clinopyroxene + spinel ⟶ garnet + olivine

The phase combination opx+cpx+sp is a possible product or partial product of these charges at intermediate pressures (Herzberg, 1975) and may have formed during the run-up to the higher pressure conditions of the experiment. This interpretation of the garnet-olivine intergrowth texture is rejected as unlikely because spinel characteristically crystallizes in small scattered crystals whereas the garnet-olivine intergrowth occurs in large patches.

(iv) The evidence presented in section 4.2.2 shows that Al_2O_3-bearing olivines can crystallize at high pressures and temperatures. This suggests that the garnet-olivine texture may represent a solution or exsolution phenomenon between garnet and olivine. In particular it may represent: an Al_2O_3-rich phase which is stable

at high pressures and temperatures but which breaks down to olivine + garnet on quenching; a rapidly crystallized metastable Al_2O_3-rich phase which is in process of breakdown to a more stable assemblage; a sluggish process of solution of garnet in olivine to form an Al_2O_3-rich phase. The final hypothesis is unlikely because it fails to explain the textural proximity of the garnet and olivine.

In conclusion, the most plausible interpretation of the garnet-olivine intergrowths is that they represent the breakdown product of an aluminous olivine phase which may or may not have been stable under run conditions.

4.3 The sub-solidus crystallization products of bulk compositions $((CS)_{25.8}(MS)_{66.7}(A)_{7.5})_X(M_2S)_{(100-X)}$: implications for the stability of the proposed garnet-lesotholite facies

4.3.1 Introduction

Experiments on the partially crystalline gel composition $M_{15}C_3AS_{15}$ (O'Hara, 1975; this publication is reproduced in Appendix A.8.1) suggest the presence of a composition gap, at any one pressure, in the cpx(opx) solvus in the system C-M-A-S at high pressures. Because the presence of a break of slope in the cpx(opx) solvus at 20 kb and 30 kb in the system CMS_2-M_2S_2 is a function of starting material (see Chapter 3), it was desirable to reproduce O'Hara's results on composition $M_{15}C_3AS_{15}$ using alternative starting materials.

The starting materials used were four partially crystalline gels:-

OHB - the same material as that used by O'Hara (1975), i.e. $M_{15}C_3AS_{15}$

AM6 - a gel mix whose bulk composition lies in the plane CS-MS-A at the piercing-point in that plane of the line joining M_2S (forsterite) and $M_{15}C_3AS_{15}$

AM7 - $(AM6)_{90.9}(M_2S)_{9.1}$

AM8 - $(AM6)_{76}(M_2S)_{24} \equiv M_{15}C_3AS_{15}$

Portions of AM6, OHB and AM8 were almost completely recrystallized at low pressure (< 1 kb) and so provided three further starting materials, viz. AM6R, OHBR and AM8R respectively.

All experiments were carried out at 30 kb. Details of the experiments are given in table 4.2 and Appendix table A.9.5.

4.3.2 Results of experiments on the partially crystalline gels

No run product contained more than 0.1% unrecrystallized quartz-rich gel starting material.

Experiments on charge OHB in the temperature range 1470-1575°C reproduced the up-temperature "garnet-back" effect in the final three assemblages in the up-temperature phase assemblage sequence cpx+opx+ol+gt, cpx+opx+ol, cpx+opx+ol+gt, cpx+opx+ol reported by O'Hara (1975). However, in the present series of experiments the higher temperature cpx+opx+ol+gt assemblage was observed at a slightly lower temperature (<25°C difference) than reported by O'Hara.*

---

* O'Hara (1975) does not report the up-temperature reappearance of garnet at pressures less than 32 kb. However, re-examination of the optical slides of his run products showed that euhedral garnet was present at 1550°C and 1575°C at 30 kb, but not at 1500, 1525 and 1600°C.

This experiment does not exist.

TABLE 4.2

Run No.	Charge No.	Temp. (°C)	Time (hrs)	Optical Phase Identification*			Garnet on X-Ray Trace
				Gt	G/O	Ol	
216	OHB	1575	1.08	-	-	x	-
192	OHB	1551	2.34	x	-	x	-
202	OHB	1523	3.83	x	-	x	x
199	OHB	1500	4.08	-	?	x	-
215	OHB	1470	3.00	-	?	x	-
207	AM8	1500	2.17	-	x	x	-
205	AM7	1500	4.42	x	x	x	x
204	AM7	1499	2.17	x	x	x	?
194	AM6	1551	2.50	x	x	x	x
195	AM6	1500	4.00	x	x	x	x
256	OHBR	1500	2.70	x	-	x	x
244	AM8R	1525	3.75	x	-	x	x
245	AM8R	1500	3.34	x	-	x	x
251	AM6R	1524	2.00	x	-	x	x

* The phase Gt (euhedral garnet), Ol (discrete olivine crystals) and G/O (garnet-olivine intergrowths) are in addition to clinopyroxene and orthopyroxene which were identified in all phase assemblages.

x indicates the presence of a phase.

Run durations in the present study were comparable to, or longer than, those of O'Hara's (pers. comm.) experiments.

The experiments were repeated using charge AM6 to determine whether the "garnet-absent" temperature interval occurred in the olivine-free system. A small amount of olivine crystallized from this charge at both 1500 and 1551°C. This indicates that at least one of the two pyroxenes or the garnet in the assemblage cpx+opx+ol+gt, which crystallized from AM6 at both temperatures, must contain SiO_2 in excess of that required by the ideal pyroxene and garnet ratio (C+M):S of 1:1.

The garnet-absent product of the run on charge OHB at 1500°C could not be reproduced using charge AM6 in a 1500°C run of comparable duration. Euhedral garnet crystals occurred at both 1500 and 1550°C. AM7 however crystallized only a little euhedral garnet at 1500°C, and AM8, which has the same composition as OHB, crystallized none at all.

Garnet-olivine intergrowths occurred in the run products of AM7 and AM8 at 1500°C and to a lesser extent in that of AM6. The run products of these three charges are much coarser grained than the crystallization products of OHB at comparable temperatures and after comparable run durations. This makes the observation of minute garnet crystals much easier in the run products of AM6, AM7 and AM8. It is possible that small quantities of submicroscopic garnet crystals are present in the run products of OHB at 1470°C and 1500°C. A few olivine crystals in both run products certainly appeared to contain minute inclusions.

The optical evidence for the reappearance of garnet at 1523°C

in the crystallization products of OHB is reinforced by x-ray diffraction analysis. The x-ray diffraction patterns of run products indicate the presence of garnet at 1523°C but not at 1500°C. The absence of garnet from the x-ray diffraction trace of the 1500°C run product is not the result of a bad x-ray trace. This shows that whether or not a small quantity of minute garnet crystals were present at 1500°C, at 1523°C there was a marked increase in the quantity of garnet crystallized.

In summary, the results of runs on partially crystalline gels show that an increase in olivine in the run product is paralleled by a decrease in euhedral garnet in the run product at 1500°C.

Section 4.2.2 described the results of experiments in which aluminous olivine, or some other phase with this composition, crystallized at 1524°C, 30 kb from partially crystalline gel charges with compositions in the system M-A-S. The differences in the crystallization behaviour of the charges AM6, AM7, AM8 and OHB at 1500°C are here interpreted as the result of similar solid solutions of Al_2O_3 in olivine. The evidence for this is:-

A. Experiments in both this calcium-bearing system and in the M-A-S system were carried out under similar pressure and temperature conditions, using the same type of starting material, viz. partially crystalline gels.

B. The occurrence of the garnet-olivine texture in the run products of AM6, AM7 and AM8 at 1500°C. This texture is believed to represent the formation or breakdown of a stable or metastable phase with the composition of an Al_2O_3-bearing olivine (see section 4.2.3). The apparent scarcity of this texture from the run product of charge

OHB at 1500°C may reflect the successful quenching of the aluminous olivine phase despite the fine grain-size of this run product. However, a comparison of the $^{\circ}2\theta$ value of the 112 reflection of the olivine crystallized from OHB at 1500°C with that of pure forsterite (table 4.1) indicates a difference with a probability of only 90%. C. The reduction of the amount of euhedral garnet in the run product with increase of olivine in the run product. This may be explained by the crystallization of aluminous olivine rather than pure forsterite in the assemblage cpx+opx+ol+gt. Fig. 4.1 is a sketch of how the relevant phase diagram might be drawn at 1500°C. It is a projection from CS into the plane M-A-S. The assumptions made are that (i) both pyroxenes contain SiO_2 in excess of that required by their stoichiometric formula and plot on the same point (Px) on the projection; and (ii) aluminous olivine solid solutions lie along the join M_2S-M_3AS_3. Neither assumption affects this argument.

It can be seen from fig. 4.1 that if the olivine coexisting with clinopyroxene, orthopyroxene and garnet shows solid solution towards pyrope, then bulk compositions formed by the progressive addition of pure forsterite (M_2S) to AM6 (which lies in the 4-phase field) will eventually cross the pyroxene-aluminous olivine tie-line, i.e. they will pass from the 4-phase field cpx+opx+ol+gt into the 3-phase field cpx+opx+ol. The relationships of the compositions AM6, AM7, AM8 and OHB to this line are indicated in the diagram.

This explanation for the crystallization behaviour of charges AM6, AM7, AM8 and OHB at 1500°C depends on the assumption that the garnet-olivine masses are breakdown products of the aluminous olivine phase and have not equilibrated with the clinopyroxene, orthopyroxene

FIGURE 4.1

Model of phase relations in the system C-M-A-S at 1500°C, 30 kb to explain the crystallization behaviour of gel charges AM6, AM7, AM8 and OHB.

Phase relations have been projected from CS into the plane M-A-S. Solid squares and solid diamonds indicate bulk compositions which crystallized the phase assemblages cpx+opx+ol and cpx+opx+gt+ol respectively. Asterisks indicate the compositions of the coexisting garnet, olivine and pyroxenes (cpx and opx both project at point Px) in the 4-phase garnet-lherzolite assemblage.

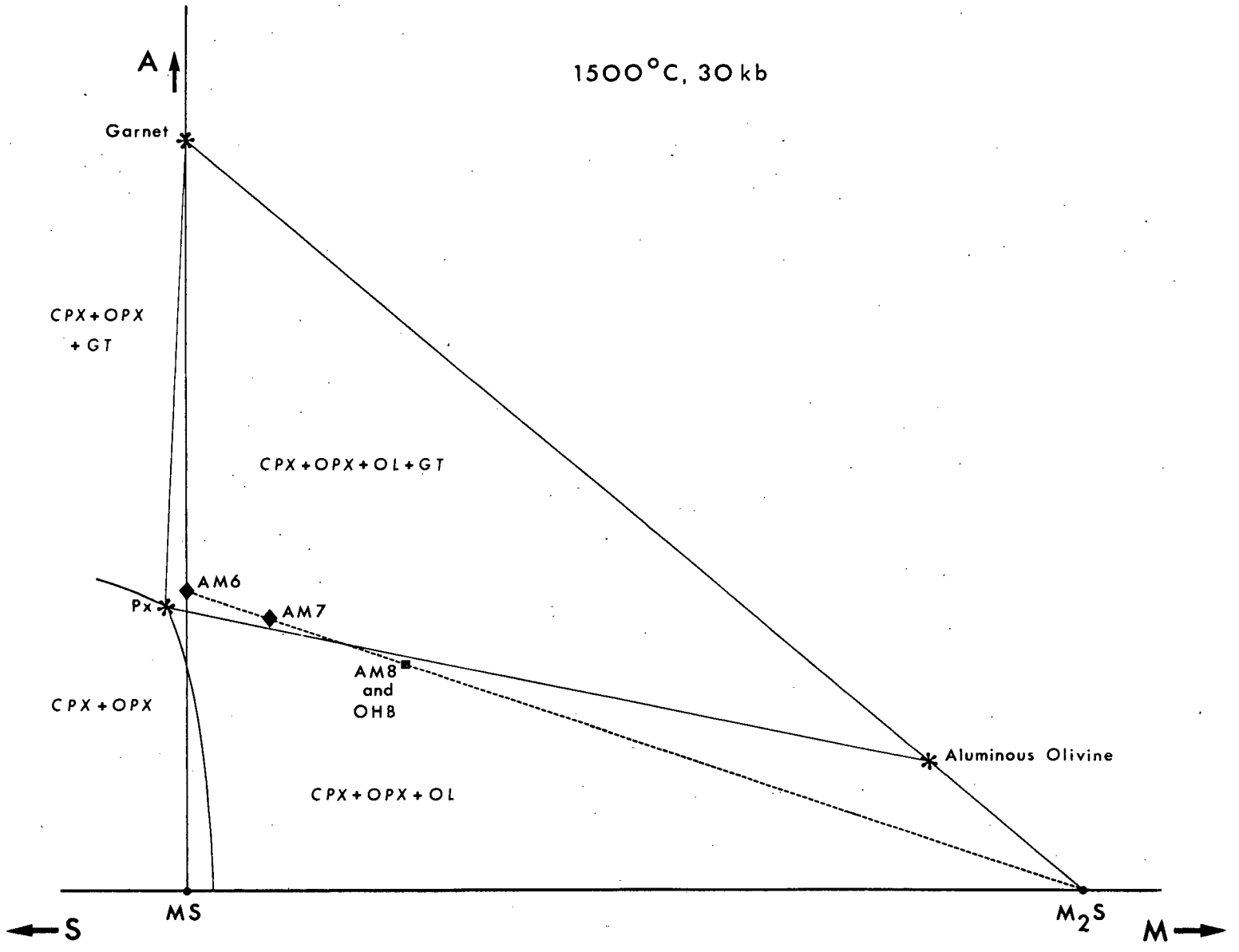
A
1500°C, 30 kb
Garnet
CPX + OPX
+ GT
CPX + OPX + OL + GT
AM6
Px
AM7
AM8
and
OHB
CPX + OPX
Aluminous Olivine
CPX + OPX + OL
MS
M2S
S
M

and euhedral garnet.

D. Comparison of the compositions of the clinopyroxenes crystallized at 1500°C from the different bulk compositions. The total amount of garnet (euhedral and in the intergrowths) crystallized at 1500°C from AM6 is fairly small, but it exceeds the amount crystallized at the same temperature from AM8 and OHB. This is demonstrated by the absence of garnet from the x-ray traces of the run products of AM8 and of OHB but not of AM6 at 1500°C. The larger quantity of total garnet in the run product of AM6 may be the result of the crystallization of a clinopyroxene containing only slightly less Al_2O_3 than the clinopyroxenes crystallized from AM8 and OHB. Such a small compositional difference would not necessarily be detectable with the precision of the x-ray diffraction method of clinopyroxene composition analysis used in this study (see Appendix A.3.4). However, it is worth noting that the Al_2O_3 content of the clinopyroxene crystallized from charge AM6 at 1500°C is not significantly less than that of the clinopyroxenes crystallized from AM8 and OHB at 1500°C (see fig. 4.2). Such an interpretation based on lower Al_2O_3 contents in the clinopyroxenes crystallized from AM6 is not geometrically possible for equilibrium assemblages. It is, however, a possibility that must be considered in view of the evidence for disequilibrium in the run products of C-M-A-S gels which is presented in section 4.4.

Similarly it is possible that variation in the Al_2O_3 content of metastable orthopyroxenes crystallizing from different bulk compositions at 1500°C is the cause of the variation in the amount of garnet in the run products. This interpretation could not be

FIGURE 4.2

Part of the plane CS-MS-A showing the compositions of clinopyroxenes crystallized at various temperatures at 30 kb from partially crystalline and recrystallized gel charges of bulk composition $((CS)_{25.8}(MS)_{66.7}A_{7.5})_X(M_2S)_{(100-X)}$. The clinopyroxenes crystallized in the phase assemblages cpx+opx+ol$\pm$gt$\pm$garnet/olivine intergrowth (see table 4.2). With one exception the clinopyroxenes crystallized after run durations which were comparable at each temperature (see section 4.4.1). The exception is the underlined square which represents the composition of the clinopyroxene crystallized from AM6R at 1524^{o}C in a run of much longer duration. The arrow indicates the direction of change in the composition of the clinopyroxene crystallized from AM6R at 1524^{o}C as the duration of the run increased.

The dashed line links the clinopyroxenes crystallized from charge OHB with increasing temperature.

Clinopyroxene compositions are believed to be precise to within 1% Al_2O_3 and 1% $CaO.SiO_2$.

Charge No.	Temperature (°C)				
	1470	1500	1524	1550	1575
AM6		○		◎	
AM6R			■		
AM8		△			
AM8R		▽	▼		
OHBR		☆			
OHB	◈	◇	◆	◈	◈

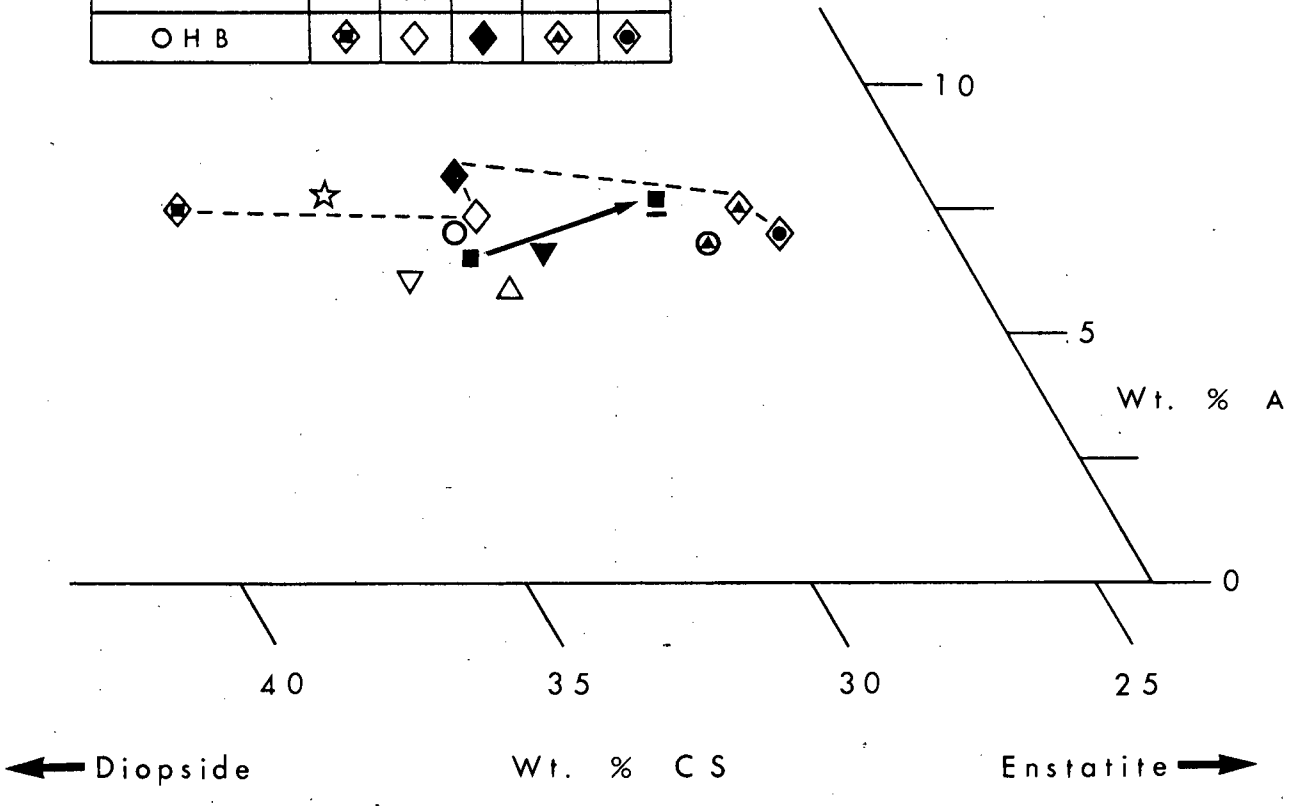

checked because the small quantities of orthopyroxene present in the run products produced peaks of only low intensity on the x-ray diffraction traces. However, evidence presented in Chapter 7 suggests that at these temperatures and pressures, the addition of olivine to a cpx+opx+gt assemblage does not affect the Al_2O_3 content of the orthopyroxene.

Variation of garnet composition has not been considered.

It is concluded that the crystallization of an aluminous olivine is the most likely explanation of the results of the experiments at 1500°C on the partially crystalline gels.

The reappearance of euhedral garnet in the run products of charge OHB at 1523°C is enigmatic. It is accompanied by the crystallization of a clinopyroxene whose composition (see fig. 4.2) contains about 1% more Al_2O_3 than that of the clinopyroxene crystallized from the same charge at 1500°C. This difference is not outside the precision limits of the determinations, but it provides no support for the suggestion (O'Hara, 1975) that the reappearance of garnet is due to the crystallization of a less aluminous clinopyroxene.

There is no evidence from the many runs on enstatite-rich C-M-A-S gels in this temperature range at 30 kb (see Chapter 7) for a sudden up-temperature increase in the quantity of garnet in the run products. A large and sudden change in the composition of garnet coexisting with clinopyroxene, orthopyroxene and olivine is considered unlikely in view of the small variation, especially with respect to the (CS+MS):A ratio, of compositions of garnets crystallized in the C-M-A-S system in previous studies (e.g. Akella, 1974a;

O'Hara and Yoder, 1967; Boyd, 1970).

The most plausible interpretation of the reappearance of garnet in the run products of OHB at 1523°C must be the instability of the aluminous olivine present in the lower temperature assemblages.

4.3.3 Results of experiments on the recrystallized gels

OHB and AM8 were almost completely recrystallized at atmospheric pressure and rerun at 1500°C, 30 kb. Both showed euhedral garnet but no traces of garnet-olivine intergrowths in the run products. Garnet appeared on the x-ray diffraction patterns of the run products of both charges though it had been absent at this temperature when the partially crystalline gels were used as starting materials. Since this absence was not the result of poor patterns producing low peak intensity, it is concluded that much more garnet crystallized from the recrystallized gels than from the partially crystalline gels at 1500°C.

The clinopyroxenes crystallized at 1500°C from both recrystallized gels AM8R and OHBR are more aluminous (fig. 4.2) than the clinopyroxenes crystallized at 1500°C from their partially crystalline counterparts. The extent of these differences is within the precision limits of the determinations, but they suggest that the presence of euhedral garnet in the run product of the recrystallized gels, but not of the partially crystalline gels, is unlikely to be the result of the crystallization of a less aluminous clinopyroxene from the former.

In view of the interpretation of the behaviour of the partially crystalline gels (see section 4.3.2) and the lack of garnet-olivine

intergrowths in the run products of the recrystallized gels, the presence of euhedral garnet in the latter at 1500°C is believed to reflect the crystallization of olivine showing less solid solution towards pyrope than that crystallized in the run products of the partially crystalline gels. However, there is no significant difference in the $^{\circ}2\theta$ values of the 112 reflection of olivines crystallized at 1500°C from OHB and OHBR (see table 4.1).

The olivine crystallized from the recrystallized gels is believed to show some solid solution towards pyrope. The evidence for this is that the amount of euhedral garnet crystallized in the run products of the recrystallized gels is dependent on the amount of olivine in the run product. This is shown by a comparison of the ratio of the intensities of the clinopyroxene $\bar{1}31$ and the garnet 420 reflections (see Appendix A.3.7) on the x-ray diffraction traces of the run products of the two recrystallized gels AM6R and AM8R at 1525°C. The ratios $I\ cpx_{\bar{1}31}/I\ gt_{420}$ were 1.45 and 3.44 respectively. There is, however, no major discrepancy between the values of this intensity ratio for the run products of charge AM8R at 1525 and 1500°C. This indicates that either there is no "garnet-back" reaction of the type observed between 1500 and 1525°C in the run products of the partially crystalline gels, or else that such a reaction does occur for recrystallized gel charges but that there is little difference in the nature of the run products at temperatures above and below the reaction temperature.

4.3.4 Discussion

The results presented above show that the occurrence of a

"garnet-absent" field in the temperature range 1470-1523°C at 30 kb is dependent on the starting material and bulk composition used. The effect is removed when almost completely crystalline gel charges are used or when only a small quantity of olivine is present in the run product. The reaction which led to the reappearance of garnet may also occur for recrystallized gel charges or in the presence of only small quantities of olivine, but it was not observed with the analytical techniques used here.

As yet there is insufficient evidence to determine which starting material gives the more stable result. No low pressure structure has any prima facie case to be preferable to any other. However, there is evidence that both sets of results are metastable. This is presented in section 4.4.

The reaction suggested by O'Hara (1975) involved essentially a change in the composition of the clinopyroxene coexisting with orthopyroxene, olivine and garnet. This change was from a more calcic, more aluminous clinopyroxene at lower temperatures to a subcalcic, less aluminous clinopyroxene at higher temperatures at the same pressure. The evidence for such a reaction was the reappearance of garnet in composition $M_{15}C_3AS_{15}$ (charge OHB) between 1525 and 1550°C at 30-45 kb coinciding with a discontinuity in the plot against temperature of the value of a single parameter of clinopyroxene solid solution determined by x-ray diffraction analysis.

If the reappearance of garnet in the run products of these new experiments (see section 4.3.2) reflects an equilibrium reaction, this reaction is not the same as that suggested by O'Hara (1975). The compositions of the clinopyroxenes crystallized from OHB in the

present study at five temperatures from 1470 to 1575°C are plotted in fig. 4.2. Each point has been fixed by two parameters of clinopyroxene solid solutions and the lower temperature points were checked by a third parameter. Consideration of errors in the determination suggests that the actual compositions lie within 1% Al_2O_3 and 1% CS of these points (see Appendix A.3.4). This precision is verified by consideration of the third parameter.

There is no abrupt change in the composition of the clinopyroxene coinciding with the reappearance of garnet (between 1500 and 1523°C) in the run products of OHB in the present study. In fact the plot suggests that the clinopyroxene at 1523°C is more aluminous than that at 1500°C, in direct opposition to the suggestion of O'Hara (1975).

O'Hara (1975) observed the reappearance of garnet and the abrupt change in clinopyroxene composition at slightly higher temperatures, viz. 1525-1550°C, than that observed here for the reappearance of garnet. In the present study there also appears to be an abrupt change in clinopyroxene composition towards enstatite between 1523 and 1551°C. However this compositional gap is no larger than that between the clinopyroxenes crystallized at 1470 and 1500°C (see fig. 4.2).

Measurements were made by O'Hara (pers. comm.) on the clinopyroxenes crystallized from OHB in these new runs using the same technique and the same parameter (the difference in the $^{\circ}2\theta$ values of the $\bar{2}21$ and 310 reflections) employed in the original experiments carried out by O'Hara (1975). These new measurements produced the pattern of a discontinuity in clinopyroxene composition between

1523 and 1551°C as observed in the original experiments. It is concluded that this discontinuity and probably therefore that described by O'Hara (1975) is independent of the reappearance of garnet in the run products.

It is possible that clinopyroxenes containing less than about 30% CS at alumina contents of about 7.5% have second order structural differences from clinopyroxenes richer in calcium. In that case the use of the x-ray determinative grid for clinopyroxenes (see Appendix A.3.4 and Appendix fig. A.3.1) derived in this study and the x-ray parameter used by O'Hara (1975) would not be a valid method of identifying discontinuities in clinopyroxene compositions. O'Hara did not calibrate his parameter against clinopyroxenes of known bulk composition; the x-ray determinative grid (Appendix fig. A.3.1) was derived using the x-ray parameters of only one clinopyroxene (with 30% CS) containing about 7.5% alumina. This is not however believed to be the explanation of the discontinuity in clinopyroxene compositions because the measured x-ray parameters of a clinopyroxene crystallized with olivine alone at 35 kb, 1625°C from charge OHB are closely comparable to those predicted from the grid. Moreover, the compositions of the clinopyroxenes deduced from the grid to contain more than 30% CS were determined by the use of three x-ray parameters whose values were in agreement with those predicted by the grid when only two parameters are required to uniquely determine a clinopyroxene composition from the grid. This agreement would not be expected if the structure of the clinopyroxenes with 7.5% alumina, CS >30%, differed from that of the clinopyroxene containing 30% CS, 7.5% alumina, used to derive the grid.

The discontinuity in clinopyroxene compositions between 1523 and 1551°C is problematical but may reflect kinetic problems in the high pressure equilibration of the gels. Fig. 4.2 indicates the composition of the clinopyroxene crystallized in the assemblage cpx+opx+gt+ol from charge AM6R at 1525°C after 2 hours and after 7.3 hours. The clinopyroxene crystallized after 7.3 hours was much more subcalcic than the one crystallized after only 2 hours; this subcalcic clinopyroxene has a closely comparable composition to those crystallized at 1550°C after only 2.5 hours. The discontinuity of clinopyroxene compositions reported by O'Hara (1975) may therefore reflect more rapid reaction rates at 1550°C than at lower temperatures.

If there is an equilibrium reaction stabilizing subcalcic cpx+opx+gt+ol (O'Hara's (1975) proposed garnet-lesotholite assemblage) at the expense of the garnet-free assemblage present at lower temperatures, then the results of the present study suggest that it reflects a break in olivine not clinopyroxene solid solutions.

Further investigation of the crystallization behaviour of composition $M_{15}C_3AS_{15}$ is not considered worthwhile until the causes of the disequilibrium in the high pressure run products of C-M-A-S diopside-rich gels (see section 4.4) have been elucidated.

4.4 Disequilibrium in the crystallization products of C-M-A-S gels

4.4.1 Introduction

A series of diopside-rich gels whose compositions can be expressed as $(CS_X+MS_Y+A_Z)\pm M_2S$ were run at 30 kb in the subsolidus

temperature range 1400-1600°C. The aim of the experiments was to determine the composition of the clinopyroxene in the equilibrium assemblage cpx+opx+gt+ol at various temperatures. The starting materials had been either partially or almost completely recrystallized at low pressure ($\leq$1 kb). The experimental results, summarized in figs. 4.3a-e, suggest that the charges did not reach equilibrium within the duration of the experiments. The evidence for this disequilibrium in the run products of the partially crystalline and recrystallized gel charges is given in sections 4.4.2 and 4.4.3 respectively.

Run durations of most of the experiments were comparable at each temperature and were 315-360 minutes at 1450°C; 125-265 minutes at 1500°C; 105-230 minutes at 1525°C; 115-175 minutes at 1550°C; and 30 minutes at 1600°C. At 1500°C and 1525°C, the temperatures at which most of the evidence for non-equilibrated phase assemblages was obtained, charges did not reach equilibrium within the period of reliability of the Pt/Pt13Rh thermocouples used in these experiments.

4.4.2 Evidence for disequilibrium in the run products of partially crystalline gel charges

The occurrence of irregular shaped, quartz-rich masses of unrecrystallized gel starting material in almost all of the high pressure crystallization products of partially crystalline gel charges is evidence for disequilibrium in these run products. The quartz-rich masses, moreover, occurred along with olivine and orthopyroxene in the same assemblage which cannot therefore represent an equilibrium assemblage. The unrecrystallized masses were observed

FIGURE 4.3

The five diagrams 4.3a to 4.3e are isothermal, isobaric (30 kb) projections from M_2S into the plane CS-MS-A showing the results of experiments on gel charges with compositions in the systems C-M-A-S and C-M-S. The experimental results do not represent stable equilibrium conditions.

The symbols explained in fig. 4.3a represent phase assemblages and are plotted at the projected position of the bulk composition of the charge. Critical run products which retained more than a trace of unrecrystallized quartz-rich gel starting material have not been plotted. Phase assemblages containing garnet/olivine intergrowths are included in the figures but are not distinguished. The presence of garnet and/or olivine is only noted where discrete crystals of these phases were observed.

Bulk compositions lying on the M_2S side of the plane CS-MS-A are indicated by the letter F as a left hand superscript to the phase assemblage symbol. All other bulk compositions lie in the plane CS-MS-A.

Asterisks indicate the measured compositions of clinopyroxenes crystallized in the assemblage cpx+opx+ol$\pm$gt. The numeral as a right hand superscript to the clinopyroxene composition is the same as that given as the right hand superscript of the relevant phase assemblage symbol.

An underlined phase assemblage symbol indicates the product of a run on a partially crystalline gel; a phase assemblage symbol with no underline represents the product of a run on a

FIGURE 4.3 (ctd.)

recrystallized gel; run products which crystallized from both partially crystalline and recrystallized gels are shown by a dashed underline.

Crosses on the CS-MS join indicate the composition of a clinopyroxene crystallized with orthopyroxene alone from a C-M-S charge.

The dashed line is the approximate position of the "orthopyroxene-out" boundary (see section 4.4.4).

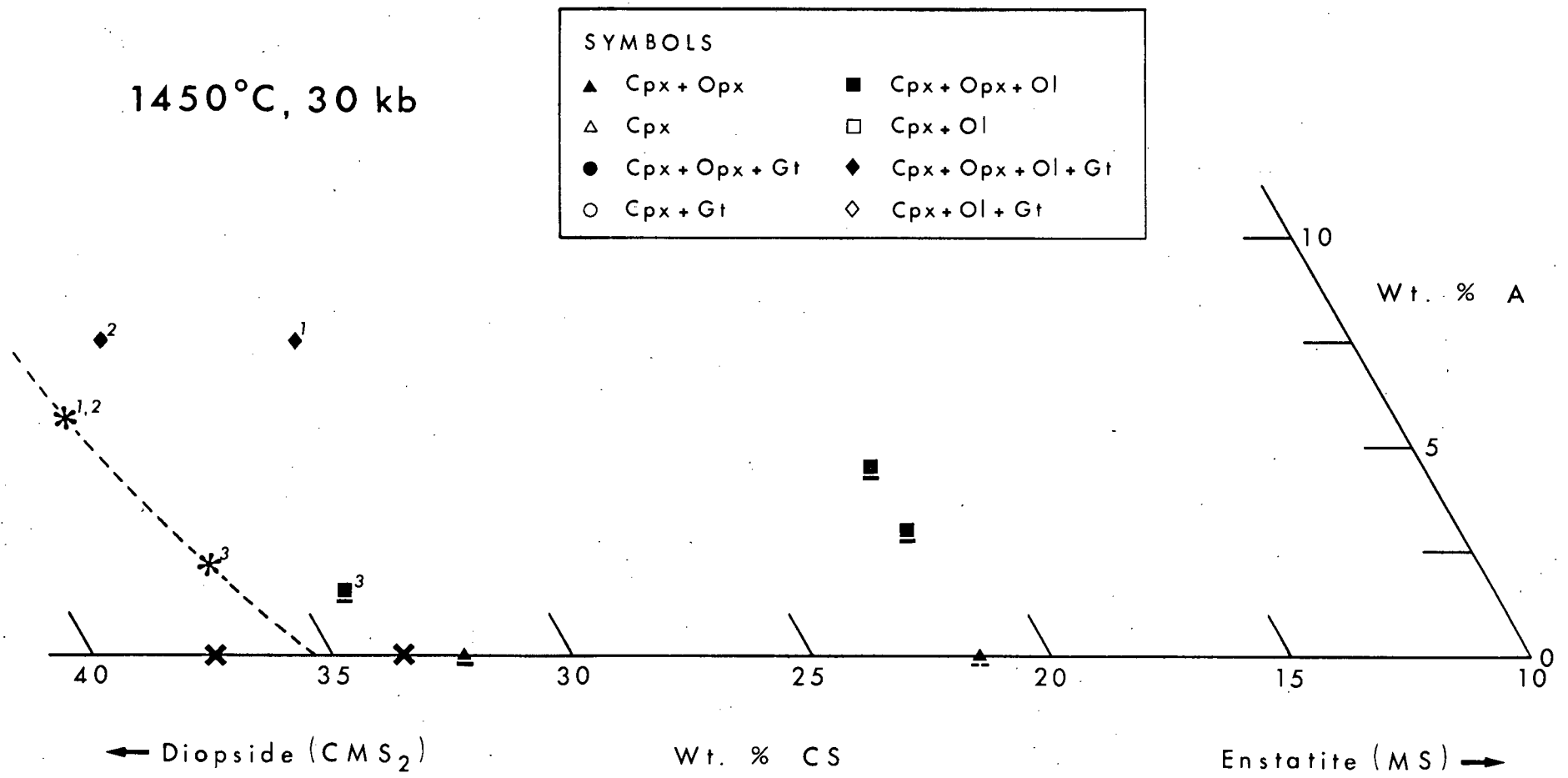
1450°C, 30 kb
SYMBOLS
Cpx + Opx
Cpx
Cpx + Opx + Gt
Cpx + Gt
Cpx + Opx + Ol
Cpx + Ol
Cpx + Opx + Ol + Gt
Cpx + Ol + Gt
1
2
1,2
3
3
10
Wt. % A
5
0
40
35
30
25
20
15
10
Diopside (CMS2)
Wt. % CS
Enstatite (MS)

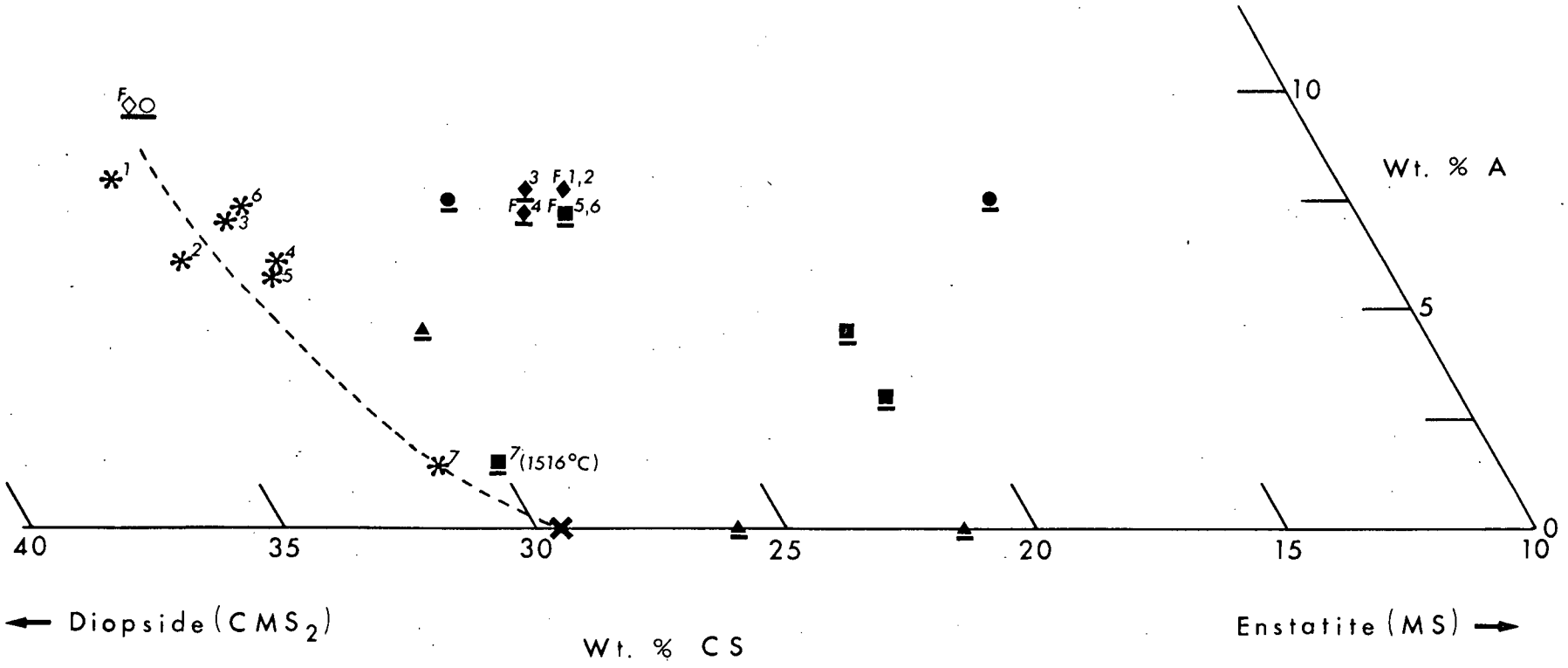
1500°C, 30 kb
F
1
2
3
4
5
6
7
F 1,2
F 3
F 4
F 5,6
7 (1516°C)
10
Wt. % A
5
0
40
35
30
25
20
15
10
Diopside (CMS2)
Wt. % CS
Enstatite (MS)

FIGURE 4.3c

Experimental results at 1524°C, 30 kb.

The composition of the enstatite-saturated C-M-S clinopyroxene was taken from the cpx(opx) solvus A'-A in fig. 3.1.

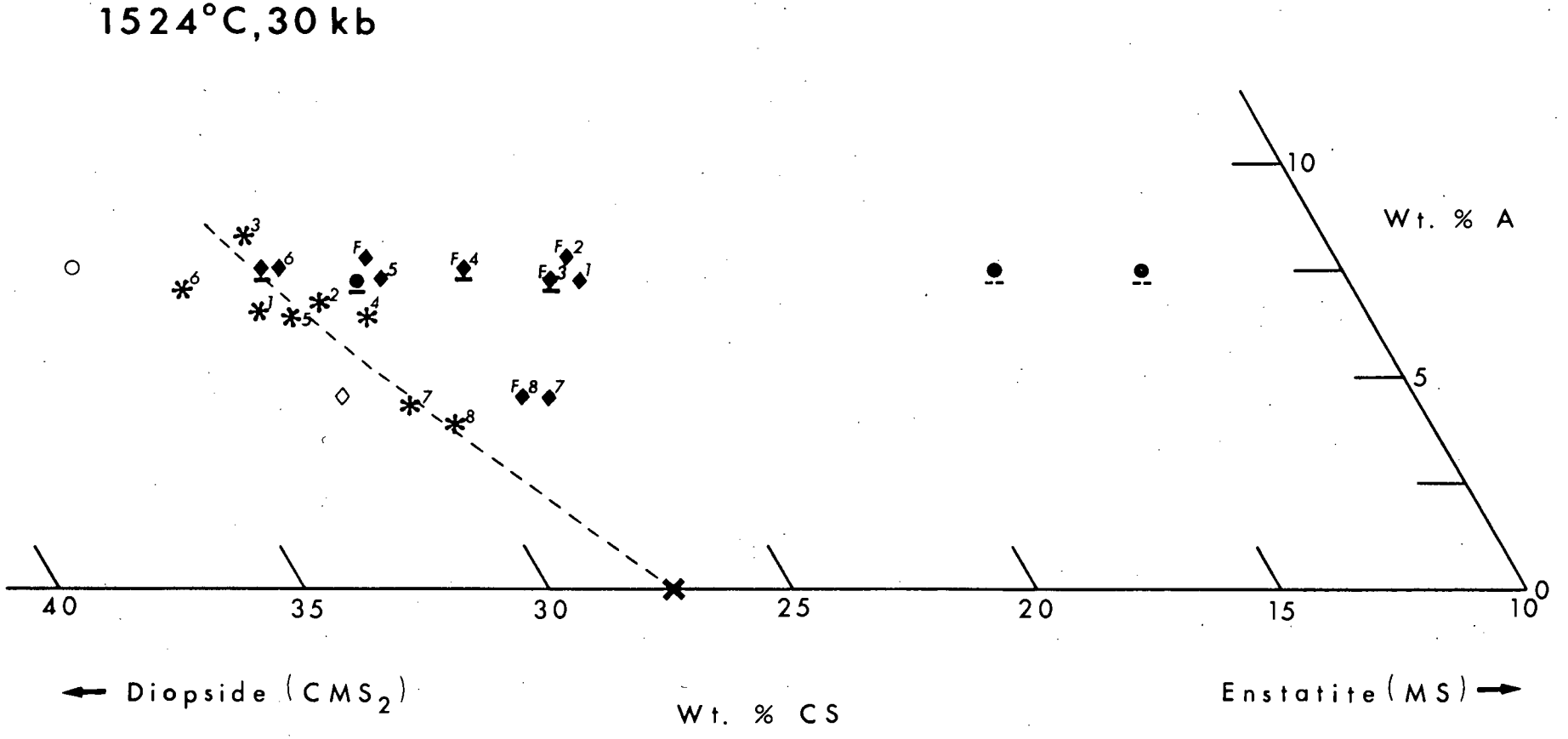
1524°C, 30 kb
10
5
0
Wt. % A
40
35
30
25
20
15
10
Diopside (CMS2)
Wt. % CS
Enstatite (MS)

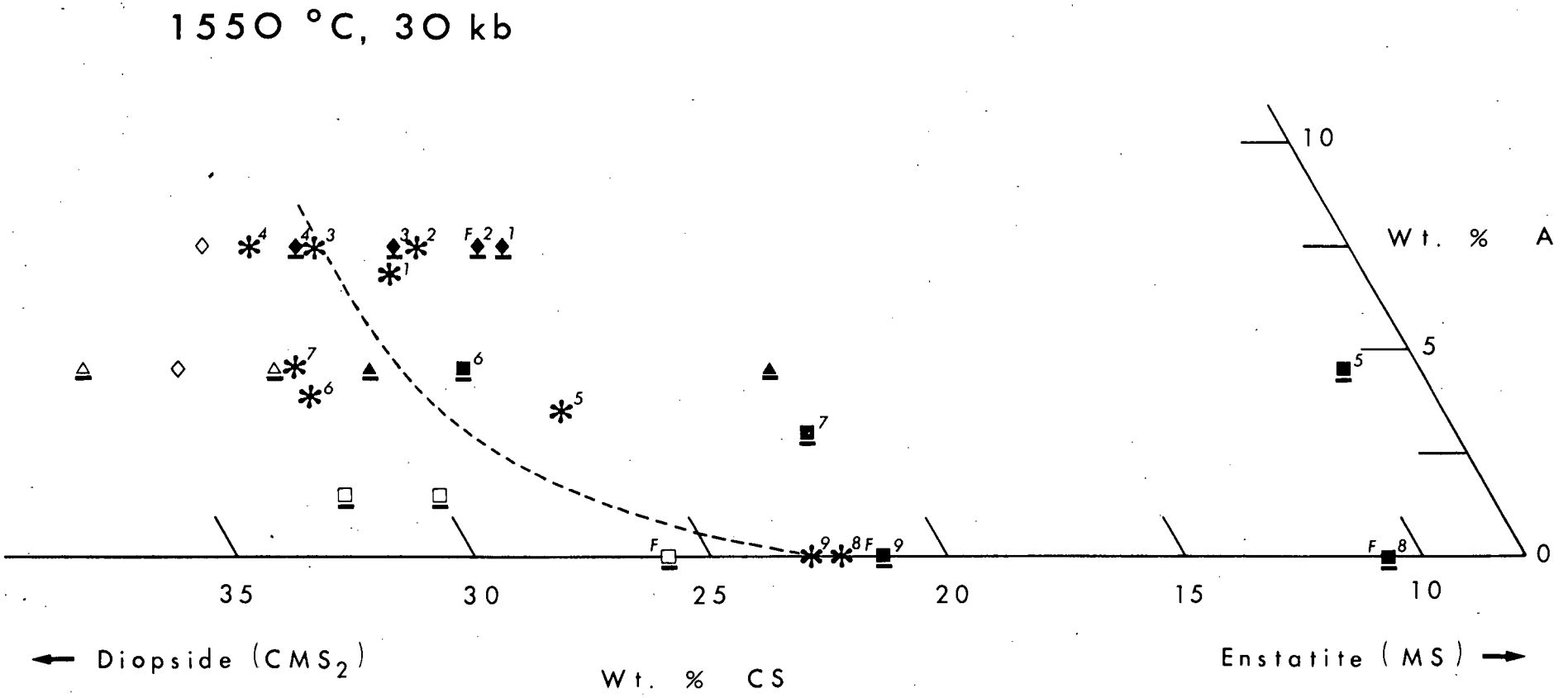
1550 °C, 30 kb
10
Wt. % A
5
0
35
30
25
20
15
10
← Diopside (CMS2)
Wt. % CS
Enstatite (MS) →

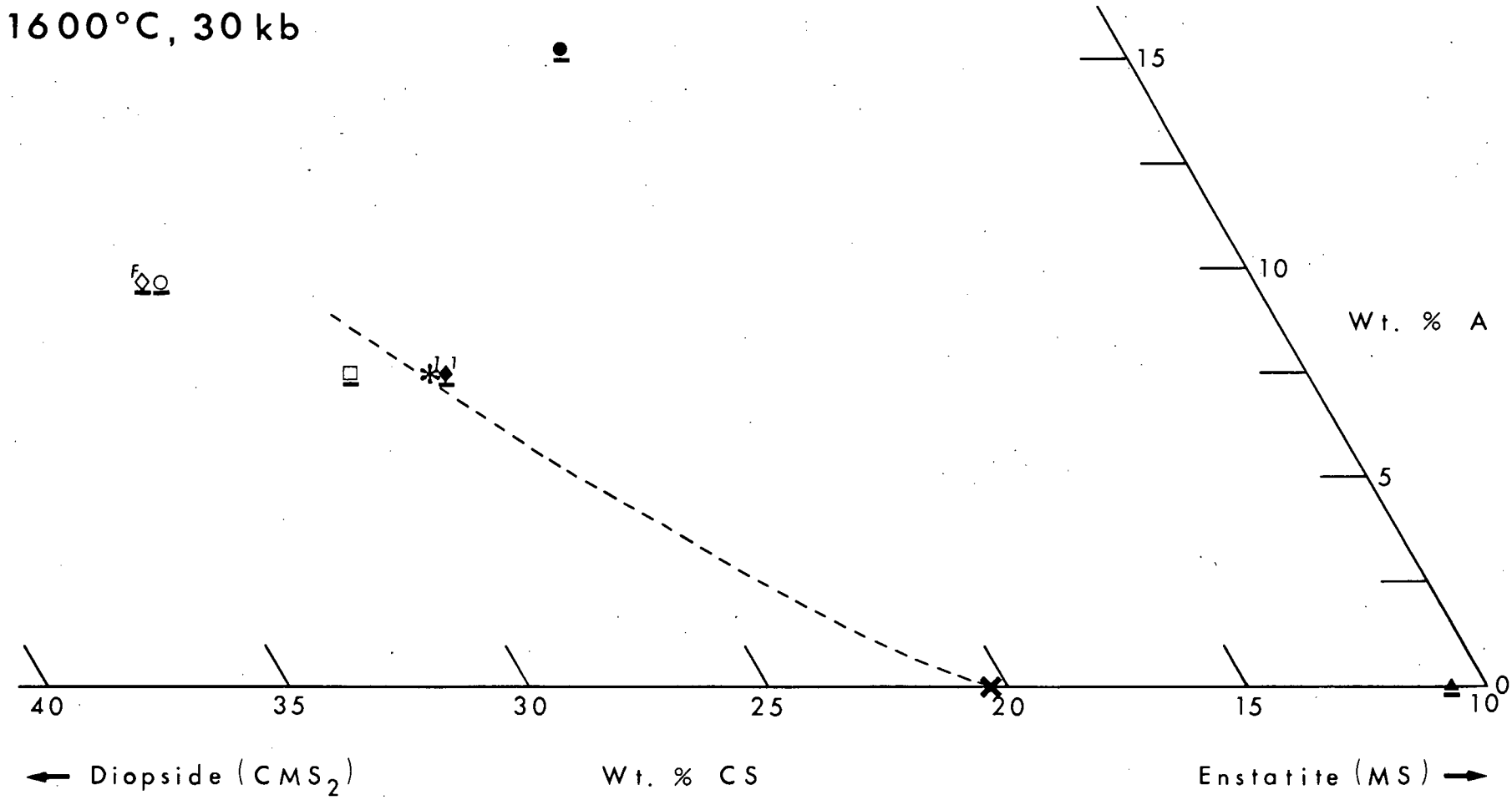
1600°C, 30 kb
15
10
5
0
Wt. % A
40
35
30
25
20
15
10
← Diopside (CMS_2)
Wt. % CS
Enstatite (MS) →

in variable amounts in the entire temperature range investigated but most abundantly in the lowest temperature runs and in runs of short duration. Only occasionally did the quartz occur in sufficient quantity to register on the x-ray diffraction pattern of run products.

Some run products contained only traces of unrecrystallized gel, but these showed additional evidence of a non-equilibrated assemblage. This evidence is the variation in the composition of clinopyroxene crystallized in association with orthopyroxene, olivine and euhedral garnet from different bulk compositions at any one temperature and pressure. In the 4-component system C-M-A-S a 4-phase equilibrium assemblage is invariant at a given temperature and pressure. Isobaric and isothermal variation of clinopyroxene composition is not permissible under equilibrium conditions, and assemblages showing such variation cannot, therefore, have attained stable equilibrium. Garnet-olivine intergrowths (see section 4.2) usually occurred in these assemblages in addition to clinopyroxene, orthopyroxene, olivine and euhedral garnet. If these intergrowths represent an additional phase, or if their constituent phases have compositions which differ from those of the euhedral garnet and olivine in the same run product, then the assemblages contain more than four phases and do not represent equilibrium, except perhaps at one temperature at any given pressure. However, garnet-lherzolite assemblages containing garnet-olivine intergrowths occur over a wide temperature range at 30 kb and crystallize from partially crystalline gels of different composition.

An example of the variation of clinopyroxene composition in

the assemblage cpx+opx+gt+ol ± garnet/olivine intergrowths can be seen in Appendix table A.9.5 for the products of runs at 1550°C. The difference between the two most discrepant clinopyroxene compositions (crystallized from charges OHB and E35 after comparable run durations) is well outside the precision limits of the determinations.

4.4.3 Evidence for disequilibrium in the run products of recrystallized gel charges

The quantity of quartz-rich masses was much reduced on low pressure recrystallization of these charges and very little occurred in the high pressure crystallization products. The garnet-olivine intergrowths crystallized far less frequently and disappeared from the run products of all but the most calcic compositions (Ca/(Ca+Mg) >0.29) at temperatures above 1500°C. However, these recrystallized gels also failed to reach high pressure equilibrium. The evidence for this is:-

(i) variation in the composition of clinopyroxene crystallized in association with orthopyroxene, olivine and euhedral garnet from different bulk compositions at any one temperature at 30 kb. This variation contravenes the phase rule which requires that an equilibrium 4-phase assemblage be isobaric and isothermally invariant in a 4-component system (see section 4.4.2). Appendix table A.9.5 gives the values of three parameters of the clinopyroxenes crystallized with orthopyroxene, garnet and olivine from various bulk compositions at 1524±1°C. The parameters were obtained from the x-ray diffraction patterns of run products and are the same as those used to erect a composition grid of C-M-A-S clinopyroxene compositions

(Appendix fig. A.3.1). Student's t test on the two extreme values of each parameter shows that the probability that they represent the same composition is less than 0.1%. The clinopyroxene compositions were deduced from these parameters using the x-ray determinative grid and are plotted in fig. 4.3c. The maximum difference between the compositions is about 0.038 in terms of Ca/(Ca+Mg) ratio and 3.0% Al_2O_3.

(ii) variation with increased run duration in the composition of clinopyroxene coexisting with orthopyroxene, garnet and olivine. The duration of the runs at 1524°C, discussed above, were between 105 and 230 minutes. Such durations were considered adequate to achieve phase assemblages which would not change within reasonable experimental run lengths. This expectation was based on runs on charge AM7 at 1500°C. The x-ray diffraction parameters of clinopyroxenes crystallized along with orthopyroxene, garnet and olivine after 130 minutes and after 265 minutes were the same within the precision limits of the determination. However, results of runs on the recrystallized gel AM6R at 1525°C show that the composition of the clinopyroxene crystallized in association with orthopyroxene, olivine and garnet after 120 minutes is much more calcic than that crystallized after 440 minutes (see fig. 4.2). This difference is well outside the precision limits of the determinations. Since the Pt/Pt13Rh thermocouples used in these experiments become contaminated after about 250 minutes at this temperature, the longer run on AM6R actually consisted of two runs of roughly equal duration. At the end of the first run the run product was ground, reloaded into a new Pt capsule and dried before rerunning. The grinding at the end of

the first run may have accelerated the change of clinopyroxene composition. Assuming that a change of phase assemblage with increased run duration is a change towards the equilibrium assemblage, experiments on the recrystallized gels were of insufficient duration for equilibrium to have been attained.

4.4.4 Discussion

Reaction rates are often considered rapid enough at these high temperatures (>1450°C) that charges readily crystallize the equilibrium assemblage. The results of runs on C-M-A-S gel charges have shown that stable equilibrium assemblages are frequently not achieved within the period of reliability of the Pt/Pt13Rh thermocouples normally used at these temperatures. The durations of the experiments carried out in this study were similar to those of high pressure runs at comparable temperatures in other studies on synthetic compositions.

The probable absence of change in a phase assemblage (the run products of charge AM7) when the run duration was doubled was not evidence of the attainment of stable equilibrium conditions in the run products of these charges. The disequilibrium was only apparent because:-

(i) the crystallization behaviour of a large number of bulk compositions was studied under comparable conditions. Many experimental studies consider the crystallization behaviour of only one bulk composition (e.g. Akella, 1974a).

(ii) the unrecrystallized quartz-rich gel starting material was optically obvious in the run products of the experiments on the

partially crystalline gel charges. When totally crystalline charges are used as starting material the presence of unreacted material would not necessarily be apparent.

The failure of the run products of charge AM7 to change with increasing run duration suggests that the trend towards stable equilibrium was arrested. There are two likely causes of an arrested path towards equilibrium at these high temperatures. Crystal growth is rapid at high temperatures but must be reduced as crystal size increases and the surface area of the crystals decreases. For crystals above a certain size, diffusion rates may be so slow as to be negligible. This was seen in a run (D90/175, described in Appendix table A.9.6) at 1500°C, 30 kb on a bulk composition on the join CMS_2-M_2S_2. The charge consisted of homogeneous gel $(CMS_2)_{90}(M_2S_2)_{10}$ seeded with a small proportion (about 2%) of large (20-40 μ) euhedral orthopyroxene $[\ (CMS_2)_8(M_2S_2)_{92}\ ]$ crystals. The bulk composition of the charge lies well inside the single phase field of clinopyroxene at this temperature and pressure (see fig. 3.1). However, the orthopyroxene crystals failed to dissolve after 3.5 hours and only one showed any signs of corrosion. The attainment of negligible diffusion rates in coarse-grained material after a certain run duration would affect the nature of the crystalline phases, and not just their texture, only if the equilibrium assemblage had not yet crystallized.

The trend towards equilibrium would also be arrested if it required the nucleation of a phase difficult to nucleate or the solution of a persistent metastable phase. The results of experiments on other compositions in C-M-A-S and its sub-systems show that the

nucleation of garnet can be sluggish (see Chapter 7), and that clinopyroxenes supersaturated in enstatite show little tendency to exsolve orthopyroxene (see section 3.1.3). The garnet-olivine intergrowth texture may also represent a metastable phase.

The large difference in the composition of the clinopyroxene crystallized from AM6R after 120 minutes and in the 2-run experiment after 460 minutes (see section 4.4.3) may be explained in two ways. Warping of crystal structures would have taken place during quenching the first run of the 2-stage experiment and again on re-pressurizing the charge at the beginning of the second part of the experiment. This warping may either have acted as a catalyst and increased reaction rates; or it may have caused actual structural changes in one of the phases, the clinopyroxene solid solution then changing composition in response to the new structure.

It must be noted that the apparent discrepancy in the results of the kinetic studies on charges AM7 and AM6R may, though this is unlikely, reflect the precision of the clinopyroxene composition determinations. The maximum difference in CS content of the clinopyroxenes crystallized from AM7 after 130 minutes and after 265 minutes is 2%. This is equivalent to a rate per minute change which exceeds the minimum per minute rate of change in CS content of the clinopyroxenes crystallized from AM6R.

The high pressure crystallization behaviour of these diopside-rich gels depends on whether they have been completely or only partially crystallized at low pressure (see section 4.3). Different crystal structures may develop at low pressure depending on the thermal treatment of the starting material. These structures may

then be inherited by the high pressure crystalline phases. Such experimentally achieved crystal structures may be different again from those attained in natural systems after extended periods at high temperatures and pressures as in geological situations. Charlu, Newton and Kleppa (1975) have shown that the entropy of pure experimentally synthesized pyrope, calculated using its measured enthalpy of solution, is surprisingly high. They conclude that synthetic pyrope has considerable cationic disorder, and that experimentally determined equilibration conditions of synthetic garnet-bearing assemblages may not be relevant to the situation in nature.

In discussing the evidence for disequilibrium (sections 4.4.2, 4.4.3) it was shown that the clinopyroxenes crystallized in the assemblage cpx+opx+gt+ol at any one temperature and pressure had compositions which varied with variation of the bulk composition of the charge. This observation was considered evidence for non-equilibrated run products since it was assumed that variation of clinopyroxene composition in these assemblages contravened the phase rule. This deduction requires the simplifying assumption that the structures of the clinopyroxenes crystallized in the different run products were identical. If, however, these clinopyroxene crystals had structures which differed at the second order level (e.g. ordering differences), then nominally identical garnet-lherzolite assemblages at a given temperature and pressure would be different phase assemblages all but perhaps one of which would necessarily be metastable equilibrium assemblages.

Evidence for structural differences in C-M-S clinopyroxenes crystallized in the present work was given in section 3.3. Structural differences in the C-M-A-S clinopyroxenes may explain the

extreme deviation of the $^{o}2\theta$ values of certain clinopyroxene reflections on the x-ray diffraction pattern of the run product of charge E18 at 1500°C from the values predicted by the determinative grid (Appendix fig. A.3.1). This grid uses three parameters of the x-ray diffraction pattern of a clinopyroxene whereas only two parameters are required to uniquely determine compositions from this grid. Except for the clinopyroxene crystallized from E18 at 1500°C, the value of the third parameter for all clinopyroxenes crystallized in this work was consistent within the precision limits of the determinations with that indicated by the other two parameters. Using the determinative grid, combinations of two out of the three parameters of the clinopyroxene crystallized from E18 suggest the following compositions:- $(CS)_{27.8}(MS)_{70.4}(A)_{1.8}$; $(CS)_{38.5}(MS)_{52.0}(A)_{9.5}$; $(CS)_{37.5}(MS)_{63.7}(A)_{negative}$. These compositional differences lie well outside the precision limits of the determinations. The inconsistent x-ray parameters may represent a clinopyroxene structure which is different from that of the clinopyroxenes used to erect the determinative grid.

It is necessary to understand the causes of the differences in the run products of the gel charges in order to elucidate the trend towards equilibrium and hence to estimate the nature of the stable equilibrium phase assemblage. The following observations may be critical:-

(i) Partially crystalline gels yielded garnet-olivine intergrowths under conditions at which recrystallized gels of the same bulk composition crystallized euhedral garnet. This may be related to the much coarser crystal size of the run products of partially

crystalline gels than those of recrystallized gels at comparable temperatures and after comparable run durations. This presumably reflects the greater ion mobility in the partially crystalline charges at the beginning of the run. Once such large crystals have formed, however, the resulting low free energy of the crystals would hinder the breakdown of any early-formed metastable phases. Large, and probably aluminous olivine crystals were observed in the run product of the partially crystalline gel AM7 quenched after only a few seconds at 1500°C.

(ii) The clinopyroxenes coexisting with garnet, orthopyroxene and olivine and crystallized from all bulk compositions and all starting materials at temperatures above 1500°C are invariably only slightly less aluminous than the bulk composition of the charge. This is confirmed by the presence of only very small quantities of garnet in the run products. This phenomenon is similar to that observed after comparable run durations in enstatite-rich C-M-A-S gels held under the same pressure and temperature conditions (see Chapter 7). In the enstatite-rich gels the phenomenon appeared to be related to the sluggish crystallization of garnet (e.g. note the run products of charge E41RF2).

(iii) At all run temperatures there is a reasonably constant pattern of increasing enstatite content with decreasing Al_2O_3 content for the clinopyroxene in the assemblage cpx+opx+ol$\pm$gt crystallized after normal run durations. In fig. 4.3 the "orthopyroxene-out" boundary between the assemblages cpx+opx+ol$\pm$gt and cpx+ol$\pm$gt has been drawn at each temperature. Each "orthopyroxene-out" boundary has been projected through the approximate median Ca/(Ca+Mg) value

of clinopyroxenes of similar Al_2O_3-content. The position of the boundary agrees closely with that indicated by the presence or absence of orthopyroxene from a phase assemblage. It does not vary with variation of starting material used, viz. partially crystalline or recrystallized gel, nor with variation in the position of the "garnet-out" boundary between cpx+opx+ol+gt and cpx+opx+ol assemblages. The composition of the clinopyroxene in the garnet-lherzolite assemblage at any one temperature is variable but lies close to the "orthopyroxene-out" boundary for that temperature.

Further detailed experimental information is required in order that estimates may be made of the nature of the stable equilibrium assemblages. The present author believes that this problem should now be tackled by:-

(i) a detailed analysis of the crystal structures of the coexisting phases in run products of experiments carried out under a wide range of experimental conditions. These crystal structures must then be compared with those of naturally occurring minerals.

(ii) detailed kinetic studies of the compositional trend, with increasing run duration, of different phases. X-ray diffraction techniques might not be sufficiently sensitive for this study since they cannot adequately distinguish the details of a compositional spread of a single phase and they do not register the presence of a phase occurring in only minor quantities. The analytical precision required may be achieved by the use of an electron microprobe which can analyse crystals $<5\mu$ across, or by the use of a scanning electron microscope.

(iii) the use of a much wider range of starting materials,

especially those containing phases such as crystalline garnet which nucleate and crystallize only very slowly.

4.5 Lack of evidence for the coexistence of two clinopyroxenes

The results presented in section 4.3 throw doubt on the existence of the reaction reported by O'Hara (1975). Further runs were carried out on both partially crystalline and recrystallized gel charges with the aim of identifying a phase field in which two clinopyroxenes coexist as required by the nature of the reaction (see Appendix A.8.2). Since the gels did not yield stable equilibrium results (see section 4.4) it was appreciated that even if such a field was found it would not necessarily imply the stable coexistence of two clinopyroxenes.

Runs were carried out in the temperature range 1450-1600^{o}C on the series of compositions $(CS_X+MS_Y+A_Z) \pm M_2S$. Exact charge compositions and run temperatures were chosen on the basis of O'Hara's (1975) experimental data and on the positions of the various phase field boundaries which emerged from analysis of the crystallization products of reconnaissance runs. The run products are illustrated in fig. 4.3.

Only one clinopyroxene was identified in all run products. However, since this conclusion is based on the failure to observe peak splitting of clinopyroxene reflections on the x-ray diffraction patterns of run products, a small phase field containing two clinopyroxenes would have been missed if the compositions of the coexisting clinopyroxenes were sufficiently similar to prevent the

resolution of two separate peaks on the x-ray diffraction pattern. Using CrKα radiation and under optimum conditions, i.e. similar quantities of the two clinopyroxenes, reflections with a separation of $0.18^{\circ}2\theta$ can be resolved. This corresponds to a difference in $Ca/(Ca+Mg)$ ratio of 0.082 for two clinopyroxenes when the 220 reflection is considered, provided there is no difference in their Al_2O_3 content. The multiple reflection peak ($\bar{1}12$, 002, 221) is even more sensitive to change in Ca/(Ca+Mg) ratio and two clinopyroxenes with a difference of 0.05 in their Ca/(Ca+Mg) ratio would easily be distinguishable provided there was no difference in their Al_2O_3 content. The isopleths of this multiple reflection and of the 310 peak trend in the same direction on a CS-MS-A section as those of the 220 peak but form a slightly higher angle with the CS-MS join than the latter. If two coexisting clinopyroxenes have the relative compositions suggested by O'Hara (1975), i.e. one is more magnesian and less aluminous than the other, then all three parameters used here might be less sensitive to the presence of two clinopyroxenes than indicated above.

Although no phase field containing two clinopyroxenes was identified in this study, it is emphasized that the run products had not attained stable equilibrium. Moreover, the investigation was limited to experiments at high temperatures, at one pressure and in the simple C-M-A-S system. Phase fields containing two clinopyroxenes and a reaction of the type described by O'Hara (1975) may occur at different pressures, or at lower temperatures, or in the presence of other ions, particularly Fe^{2+}.

4.6 Previous determinations of the compositions of enstatite-saturated clinopyroxenes in the system C-M-A-S

The compositions of enstatite-saturated clinopyroxenes crystallized from bulk compositions in the system CS-MS-A have previously been investigated by O'Hara and Yoder (1967) at 30 kb, 1600°C; Boyd (1970) at 30 kb, 1200°C; and Akella (1974a) in the pressure range 26-44 kb and at temperatures of 1100-1500°C.

None of the previous workers report the presence of olivine, quartz or non-stoichiometric phases as observed in the present experiments but small amounts of non-stoichiometry would not necessarily have been determinable by the analytical techniques used. A phase field containing two clinopyroxenes was not identified in any of the previous studies. All high temperature studies, including the present one, show a consistent result for the effect of Al_2O_3 on the Ca/(Ca+Mg) ratio of enstatite-saturated clinopyroxene: the presence of Al_2O_3 in clinopyroxene increases this ratio. However at low temperatures (c. 1200°C) the results of Boyd (1970) and Akella (1974a) both indicate that Al_2O_3 has little effect on the Ca/(Ca+Mg) ratio of enstatite-saturated clinopyroxenes.

The conclusions of all three previous studies are queried because the assemblages investigated were not olivine-saturated and because of the limited number of independent determinations of the clinopyroxene in the assemblage cpx+opx+gt at any one temperature (see section 4.4.4). Moreover, Boyd (1970) and Akella (1974a) both used unrecrystallized glasses as starting material. The products of high pressure runs on C-M-S compositions using this starting material

may be metastable (see Chapter 3). The possible sources of error in the use of H_2O as a catalyst, as used by Boyd and Akella, are discussed in section 7.1.

CHAPTER 5

THE CLINOPYROXENE GEOTHERMOMETER

ENSTATITE SOLUBILITY IN CLINOPYROXENE IN MULTICOMPONENT SYSTEMS

5.1 Introduction

The solubility of enstatite in clinopyroxene in multicomponent systems has been investigated both experimentally and also using thermodynamic treatments. Experimental programmes have either involved the systematic addition of different oxides to synthetic systems, or the analysis of the compositions of clinopyroxenes crystallized from natural multicomponent systems. These studies are briefly reviewed in this chapter. Results of new experiments on a natural clinopyroxene and orthopyroxene mineral pair are also presented.

5.2 Experimental approach: previous studies on synthetic systems

Section 4.6 showed that current determinations of the effect of Al_2O_3 on the Ca/(Ca+Mg) ratio of enstatite-saturated clinopyroxenes may be in error. All studies however, at least at high temperature, suggest that Al_2O_3 reduces the extent of enstatite solubility in clinopyroxene.

Clinopyroxenes crystallized by Akella (1974a) in the system C-M-A-S-T, and by Akella and Boyd (1972, 1973) in the system C-M-A-S-T-F may be metastable because glasses were used as starting materials (see Chapter 3). Moreover, the crystallization products

of Akella and Boyd's experiments included a small quantity of rutile and ilmenite which would have affected phase relations.

Experiments by Munoz and Lindsley (1969) in the system C-F-S at 20 kb yielded a similar shape for the cpx(opx) solvus as determined by Davis and Boyd (1966) in the system C-M-S at 30 kb but displaced to lower temperatures. The run products obtained by Munoz and Lindsley were crystallized from starting materials similar to those used by Davis and Boyd (1966) and by Kushiro (1969a) and may be metastable (see Chapter 3).

No conclusions can be drawn from these studies until the experiments are repeated using different types of starting material.

5.3 Experimental approach: previous studies on natural systems

Experimental studies of natural iron-poor pyroxenes at high pressure have been made by O'Hara and Yoder (1967) on a natural pyroxene pair, and by Hensen (1973) and Akella and Boyd (1974). Experimental details for the latter two studies are given in Appendix table A.9.15, and the Ca/(Ca+Mg) values of the enstatite-saturated clinopyroxenes are plotted against temperature in fig. 5.1. Fig. 5.1 also shows the most discrepant results from various C-M-S and C-M-A-S synthetic systems. At any one temperature the Ca/(Ca+Mg) ratios of enstatite-saturated clinopyroxenes in the natural and synthetic systems cover a similar range of values. The largest number of analyses for natural systems are at 1100^{o}C and are for the pressure range 23-41 kb (Hensen, 1973; Akella and Boyd, 1974). The clinopyroxenes coexisting with orthopyroxene have Ca/(Ca+Mg) ratios in

FIGURE 5.1

Experimental determinations of the variation of the Ca/(Ca+Mg) ratio of enstatite-saturated clinopyroxene as a function of temperature at high pressure. Determinations are shown at various pressures for both synthetic systems (indicated by dashed lines; open diamonds represent data points) and natural systems (indicated by dotted lines; circles represent data points). The determination of Davis and Boyd (1966), currently used as a geothermometer, is shown as a continuous line. The solid squares plotted on the Davis and Boyd (1966) function represent the compositions of clinopyroxenes in garnet-lherzolite nodules from north Lesotho kimberlite pipes (Nixon and Boyd, 1973a, table 20A).

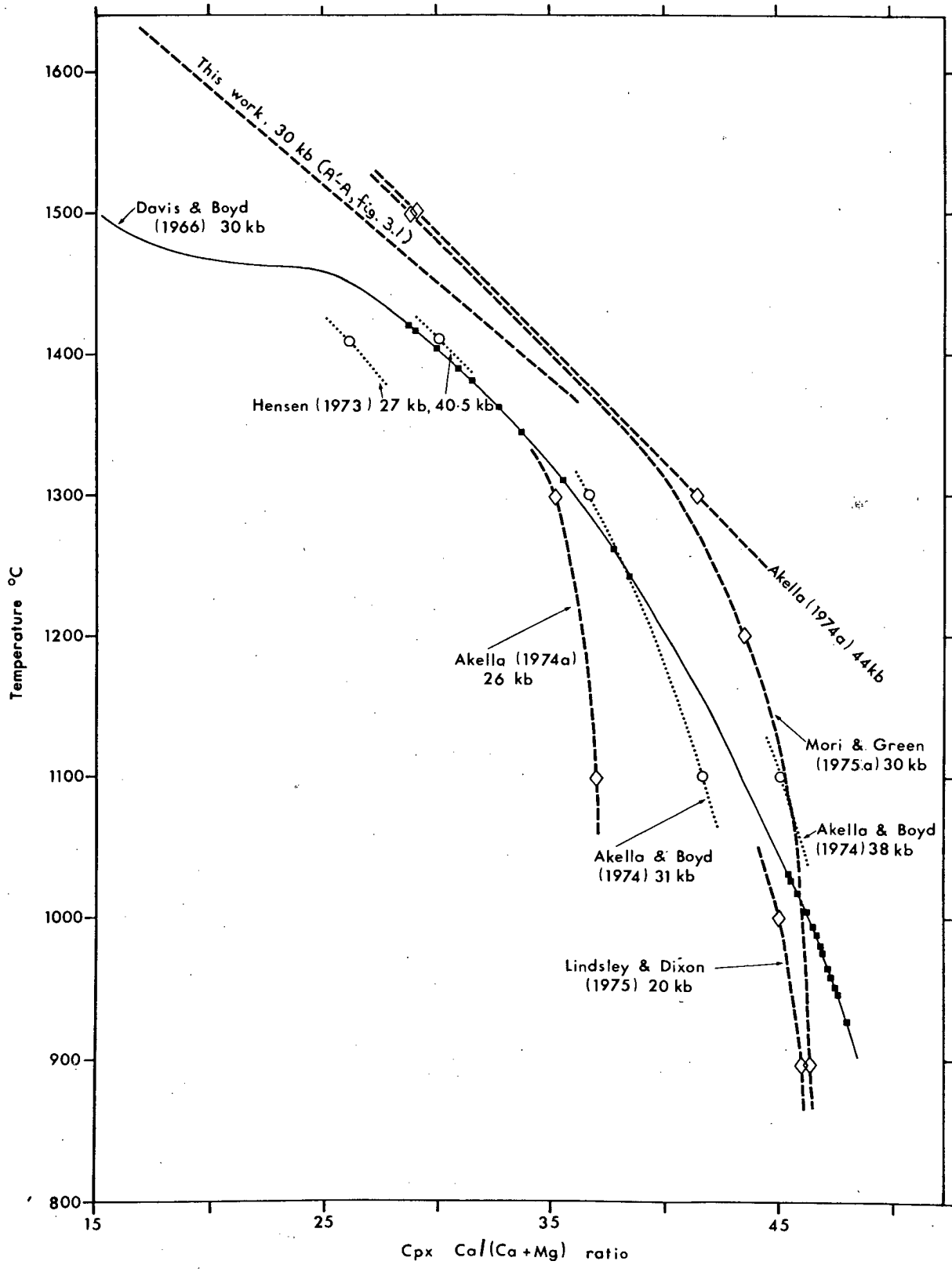
This work, 30 kb (A'-A, fig. 3.1)
Davis & Boyd (1966) 30 kb
Hensen (1973) 27 kb, 40·5 kb
Akella (1974a) 44kb
Akella (1974a) 26 kb
Mori & Green (1975a) 30 kb
Akella & Boyd (1974) 38 kb
Akella & Boyd (1974) 31 kb
Lindsley & Dixon (1975) 20 kb
Temperature °C
1600
1500
1400
1300
1200
1100
1000
900
800
15
25
35
45
Cpx Ca/(Ca+Mg) ratio

the range 0.416 to 0.451 which corresponds with the range covered by the variation in the reported Ca/(Ca+Mg) ratios of enstatite-saturated clinopyroxenes at 30 kb in the system C-M-S (Davis and Boyd, 1966; Nehru and Wyllie, 1974; Mori and Green, 1975a). There are insufficient data to determine whether the range of Ca/(Ca+Mg) values for natural pyroxenes at 1100°C is real and reflects pressure or composition differences, or whether it is the result of experimental and analytical imprecision and errors. It may be noted that both Hensen (1973) and Akella and Boyd (1974) used small quantities of water as a catalyst (see section 7.1 for possible sources of error) and reported sluggish reaction rates and inhomogeneous phases.

Results of experiments in natural systems show that pressure has an effect on the position of the cpx(opx) solvus but that there is no simple pattern which is consistent at all temperatures or even at one temperature in different chemical systems.

No evidence for the presence of a two-clinopyroxene field or for an inflection in the cpx(opx) solvus was reported by O'Hara and Yoder (1967), Akella and Boyd (1974) or Hensen (1973). All three studies were, however, too limited to be conclusive. O'Hara and Yoder's (1967) reconnaissance results on a natural clinopyroxene and orthopyroxene pair from a garnet-lherzolite were therefore extended in the present work and are described in the next section.

5.4 Experimental approach: determination of the clinopyroxene (orthopyroxene) solvus at 30 kb for a natural pyroxene pair

The clinopyroxene and orthopyroxene used in these experiments

were separated from a garnet-lherzolite (A3/10596) nodule from the Wesselton mine, South Africa. The compositions of the two pyroxenes and references to further information on these minerals are given in Appendix table A.4.2 and Appendix A.4 respectively. Details and results of the new experiments are listed in Appendix table A.9.11.

Fig. 5.2 presents the results of quenching experiments at 30 kb on mixes of the A3/10596 clinopyroxene and orthopyroxene. Both the new experiments and those carried out by O'Hara and Yoder (1967) are shown and distinguished from each other. The compositions of the clinopyroxenes crystallized in equilibrium with orthopyroxene were determined from x-ray diffraction determinative curves (see Appendix A.5) and are believed to be precise to within 1.5 or 5% diopside* at the 95.5% confidence level for run products containing very small or very large amounts of orthopyroxene respectively.

The results of O'Hara and Yoder (1967) and the new experiments are in agreement except at 1450°C. The compositions of the clinopyroxenes crystallized at 1450°C in the two studies from different bulk compositions differ by 6% (A3/10596) diopside. This may reflect either non-stoichiometric pyroxenes, evidence for which has not been investigated in this system, or more likely the pressure difference between the two sets of experiments. O'Hara and Yoder (pers. comm.) used the floating-piston technique in their experiments but the piston-out technique was used in the new study.

There is no major inflection in the cpx(opx) solvus in this

---

* Actually the A3/10596 diopside, not CMS_2

FIGURE 5.2

The results of quenching experiments at 30 kb on mixes of the A3/10596 clinopyroxene and orthopyroxene.

Open triangles indicate compositions which crystallized cpx alone; filled triangles indicate compositions which crystallized cpx+opx. The measured composition of a clinopyroxene in a two-phase assemblage is shown by an asterisk.

Underlined symbols represent the products of the runs of O'Hara and Yoder (1967).

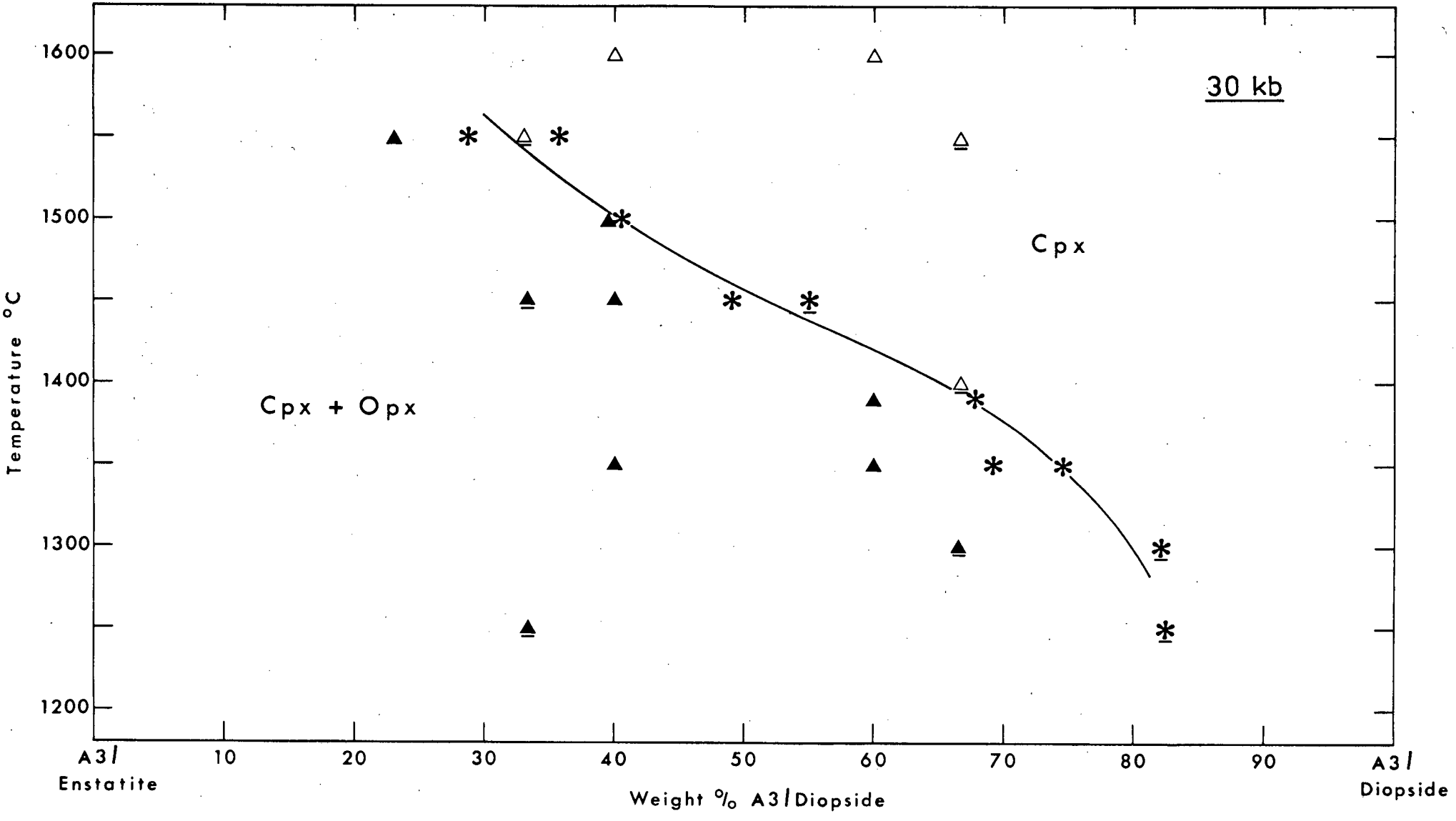
30 kb
Cpx
Cpx + Opx
Temperature °C
1600
1500
1400
1300
1200
A3l
Enstatite
10
20
30
40
50
60
70
80
90
A3l
Diopside
Weight % A3l Diopside

system at 30 kb in the temperature range investigated, viz. 1300-1550°C. The absence of such an inflection is in agreement with the results on synthetic C-M-S gel charges at 30 kb (section 3.1) but contrary to the results of Davis and Boyd (1966). Neither is there any evidence for a field of two clinopyroxenes in the composition and temperature range of Kushiro's (1969a) two clinopyroxene field in the system CMS_2-M_2S_2 at 20 kb. However, the method used in the present study to determine the presence of a two clinopyroxene phase field, viz. the observation of peak splitting on the $\bar{2}02$ and the multiple ($\bar{1}12$, 002 and 221) reflections on the x-ray diffraction patterns obtained using CrKα radiation, is not sufficiently sensitive to distinguish the presence of two clinopyroxenes with a compositional difference of less than 10% (A3/10596) diopside. Both peak positions move by about 0.2°2θ CrKα for an increase of 10% (A3/10596) diopside content.

A meaningful comparison of the extent of solubility of orthopyroxene in clinopyroxene in this system and in the C-M-S system is not possible because it is not known to what extent iron was lost from the natural charges to the Pt capsules during the experiments (see Merrill and Wyllie, 1973).

5.5 Thermodynamic approach

A thermodynamic model of enstatite solubility in clinopyroxene in natural systems has been developed by Wood and Banno (1973) by fitting available experimental data for synthetic and natural systems to a thermodynamic expression. The model is purely empirical and

has "little theoretical justification" (Wood and Banno, 1973, p. 119). Wood and Banno stress that its use may lead to considerable error outside the temperature and compositional space covered by the experiments. The effect of pressure on the solubility of enstatite in clinopyroxene is not considered in the model.

Saxena and Nehru (1975) explored the errors which result from ignoring the effect of non-ideal solid solutions in the thermodynamic models of enstatite solubility in clinopyroxene in multicomponent systems. The size of these errors points to the need to obtain further information on thermodynamic quantities in this system before thermodynamic approaches can be fully developed.

A major limitation of such thermodynamic models is that they are at best only as accurate as the experimental data from which they were derived. The present work has thrown doubt on the stability of some of the experimentally crystallized assemblages used to derive the thermodynamic model of Wood and Banno (1973).

CHAPTER 6

THE ORTHOPYROXENE GEOBAROMETER

6.1 Introduction

Chapters 6-9 consider the experimental basis of the method used to determine the equilibration pressure of garnet-lherzolite assemblages, viz. from the Al_2O_3 content of the orthopyroxene (MacGregor, 1974; Wood and Banno, 1973; Wood, 1974). The application of MacGregor's data for synthetic aluminous orthopyroxenes to natural rocks (see section 1.1) could lead to erroneous pressure determinations for the following reasons:-

(i) Pressure estimates require the independent determination of the equilibration temperature of the garnet-lherzolite assemblages since Al_2O_3 solubility in orthopyroxene is temperature as well as pressure sensitive. Recent experiments (see Chapter 3) suggest that the present method of temperature determination (using the data of Davis and Boyd, 1966) may not be valid.

(ii) Al_2O_3 solubilities determined by MacGregor (1974) are much higher than those in natural orthopyroxenes from garnet-lherzolites (see fig. 9.1). To estimate equilibration pressures of natural assemblages the assumption is made that MacGregor's data can be extrapolated linearly to low temperatures and Al_2O_3 contents. This assumption has not yet been justified.

(iii) Al_2O_3 solubility in orthopyroxene was determined by MacGregor (1974) for orthopyroxenes crystallized in equilibrium with pyrope from bulk compositions in the synthetic system MS-A. In

natural garnet-lherzolites the orthopyroxenes are calcium-bearing and coexist with free clinopyroxene. The application of MacGregor's data to calcium-bearing orthopyroxenes may not be justified according to the results of O'Hara and Yoder (1967), Boyd (1970) and Akella (1974a) for bulk compositions in the plane CS-MS-A. Orthopyroxenes crystallized in equilibrium with clinopyroxene and garnet in these studies showed less solubility towards Al_2O_3 than orthopyroxenes in the calcium-free system investigated by MacGregor. However, these differences may also be explained by the crystallization of non-stoichiometric pyroxene and/or garnet solid solutions (see below) in which case differences in orthopyroxene solid solutions might purely reflect differences of bulk composition in these olivine-free assemblages.

(iv) Al_2O_3 solubilities were determined by MacGregor (1974) in olivine-free assemblages although his data are applied to olivine-bearing rocks. If the pyroxene and/or garnet coexisting in high pressure and temperature assemblages show solid solution along the join M-S then the presence of olivine in an assemblage may affect the Al_2O_3 content of the orthopyroxene. Evidence for the crystallization of non-stoichiometric pyroxenes was given in section 2.1. Further evidence has now been obtained from high pressure experiments on bulk compositions in the system CMS_2-MS (Chapter 3) and in the system C-M-A-S (Chapter 4) though the latter results may not represent stable equilibrium.

(v) MacGregor's (1974) results are for the system MS-A. These results would not be affected by the reaction reported by O'Hara (1975) in the system C-M-A-S (see section 4.3). If this is

an equilibrium reaction at high pressure and temperature it may complicate a pressure/temperature grid of isopleths of Al_2O_3 solubility in multicomponent orthopyroxenes. There is no evidence for this in the limited data of Akella (1974a) for clinopyroxene-bearing but olivine-free synthetic assemblages.

(vi) The solubility of Al_2O_3 in natural orthopyroxenes may be affected by solid solutions towards oxides other than CaO, MgO and SiO_2. This is discussed in Chapter 8.

(vii) MacGregor (1974) used glasses as starting materials for his experiments. These were seeded with pyrope crystals in order to avoid the notorious difficulty of nucleating garnet from glass charges (e.g. Boyd and England, 1964). However, it has not yet been demonstrated that the presence of a small quantity of pyrope seeds will cause the crystallization of the maximum amount of pyrope possible under the given conditions. Failure to nucleate garnet within its stability field would be reflected in the run products of these enstatite-rich bulk compositions as metastable pyroxenes which show higher Al_2O_3 contents than would occur under equilibrium conditions.

(viii) Recent determinations of the entropy of pure synthetic pyrope (Charlu et al., 1975) suggest that synthetic garnets crystallized under laboratory conditions may have considerable cationic disorder. Garnets crystallized under natural conditions may have structures which differ at the second order level from synthetic garnets crystallized in the laboratory. Experimentally determined equilibration conditions of synthetic garnet-bearing assemblages may not therefore be relevant to the situation in nature. Such

structural differences may also occur in the pyroxenes and olivine.

6.2 Aim and scope of experimental work

Experiments were carried out on charges with bulk compositions in the system C-M-A-S (Chapter 7). The aim of the study was to determine whether the results of MacGregor (1974) and Akella (1974a) for the solubility of Al_2O_3 in orthopyroxene could be reproduced:-

a) for different types of starting material.

b) for orthopyroxenes coexisting with garnet, clinopyroxene and olivine.

Experiments were run in the pressure range 27-35 kb to facilitate comparison with results on the coexisting clinopyroxenes (see Chapter 4) and to minimise the breakage of equipment. Al_2O_3 solubilities were determined in the temperature range 1450-1650^{o}C. At these temperatures Al_2O_3 solubilities are higher than those in natural orthopyroxenes from garnet-lherzolites. It was necessary to work in this temperature range to avoid problems of sluggish reaction rates and to make meaningful comparisons with previous studies.

Details of the compositions used are given in Appendix table A.2.4. Experimental details and run products are presented in Appendix tables A.9.7 and A.9.8.

The result of an experimental determination of Al_2O_3 solubility in a natural orthopyroxene is presented in Chapter 8.

CHAPTER 7

THE ORTHOPYROXENE GEOBAROMETER

Al_2O_3 SOLUBILITY IN ORTHOPYROXENE IN THE SYSTEMS M-A-S AND C-M-A-S

7.1 Discrepancies between these and previous results

Figs. 7.1 and 7.2 compare the solubility of Al_2O_3 in orthopyroxene determined in this study with that reported by Akella (1974a) for bulk compositions in the system CS-MS-A, and by MacGregor (1974) and Boyd and England (1964) for bulk compositions in the system MS-A. Fig. 7.1 is a plot of temperature against the Al_2O_3 content of orthopyroxene crystallized from bulk compositions in the system MS-A and C-M-A-S at a nominal pressure of 30 kb. Fig. 7.2 is a plot of temperature against pressure for certain isopleths of Al_2O_3 solubility in orthopyroxene crystallized from bulk compositions in the systems MS-A and CS-MS-A in previous studies and in the system C-M-A-S in this study.

The new determinations of Al_2O_3 solubility in orthopyroxene crystallized with garnet alone from bulk compositions in the system MS-A are much lower than those reported by MacGregor (1974) or by Boyd and England (1964) for a similar piston technique. The solubility of Al_2O_3 in orthopyroxene crystallized in the assemblages opx+cpx+gt and opx+cpx+gt+ol is much lower than reported by Akella (1974a).

The pressure/temperature range of these differences are the equivalent of a pressure uncertainty of $\pm$11 kb or a temperature uncertainty of $\pm$200^{o}C at 1300^{o}C, 30 kb. In terms of geothermal

FIGURE 7.1

The solubility of Al_2O_3 in orthopyroxene as a function of temperature at a nominal pressure of 30 kb: a comparison between results obtained from gel charges in the present work with those obtained from synthetic charges in previous studies.

"Piston-out" and "floating-piston" refer to the pressure technique used. An underlined phase assemblage symbol refers to the result of a floating-piston experiment.

Phase assemblages crystallized in the present study are represented by the following symbols (the symbols are plotted at the Al_2O_3 content of the composition of the charge when projected from M_2S into the plane CS-MS-A):

☆ opx
★ opx+gt
} crystallized from M-A-S compositions

▲ opx+cpx
● opx+cpx+gt
■ opx+cpx+ol
◆ opx+cpx+ol+gt
} crystallized from C-M-A-S compositions

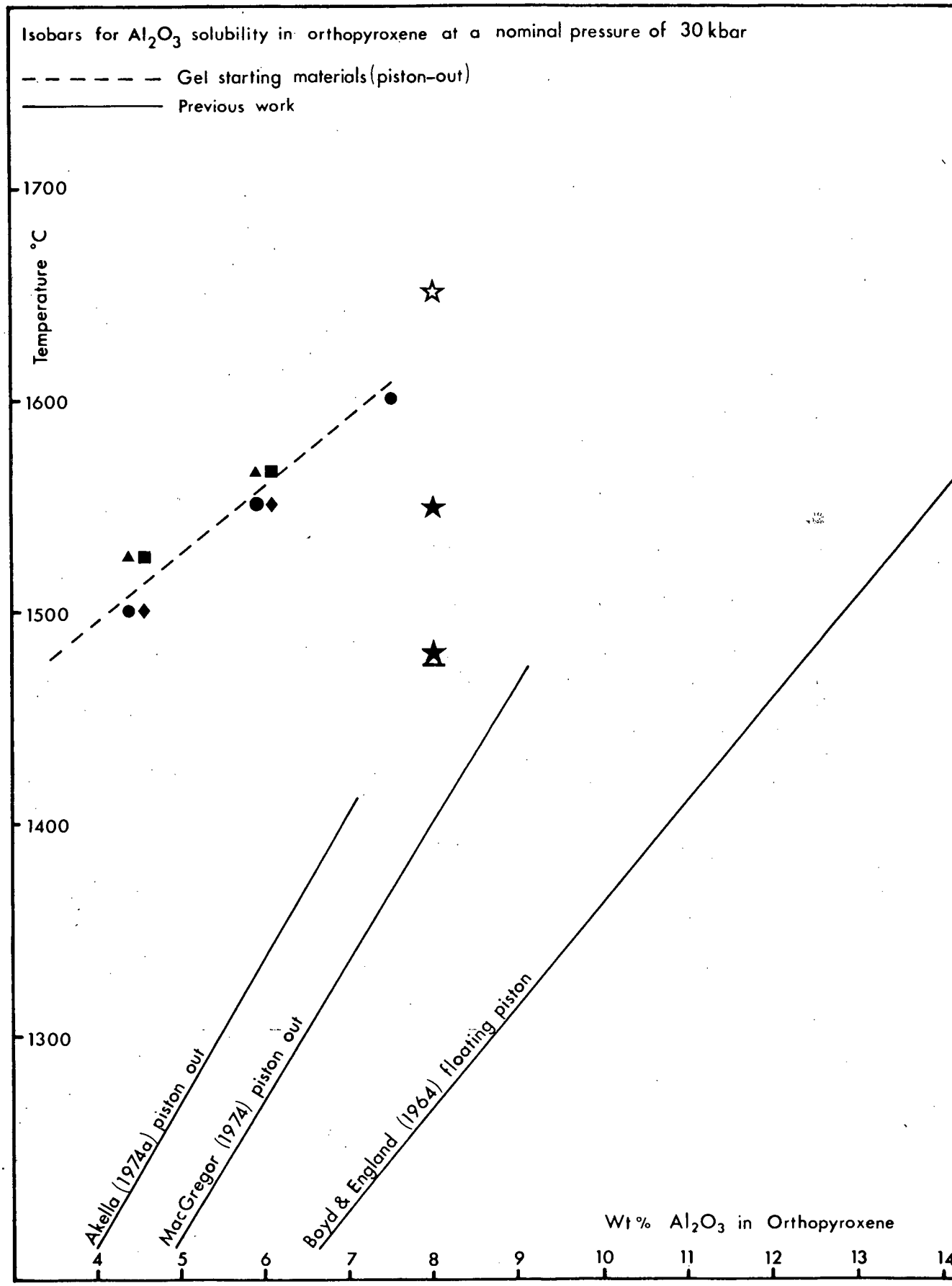
Isobars for Al_2O_3 solubility in orthopyroxene at a nominal pressure of 30 kbar
Gel starting materials (piston-out)
Previous work
Temperature °C
1700
1600
1500
1400
1300
Akella (1974a) piston out
MacGregor (1974) piston out
Boyd & England (1964) floating piston
Wt % Al_2O_3 in Orthopyroxene
4
5
6
7
8
9
10
11
12
13
14

FIGURE 7.2

Variation of the 4.5% and 6% isopleths of Al_2O_3 solubility in orthopyroxene as a function of temperature and pressure. The results obtained in the present work from gel charges with bulk compositions in the system C-M-A-S are compared with those obtained by MacGregor (1974) from bulk compositions in the system MS-A, and by Akella (1974a) from bulk compositions in the system CS-MS-A.

Phase assemblages crystallized in the present study are represented by the symbols described in the figure caption of fig. 7.1. In fig. 7.2 these symbols refer to charges whose compositions, when projected from M_2S into the plane CS-MS-A, contain 6% Al_2O_3. The 4.5% Al_2O_3 isopleth has been drawn parallel to the 6% Al_2O_3 isopleth through the single data point at 30 kb (see fig. 7.1).

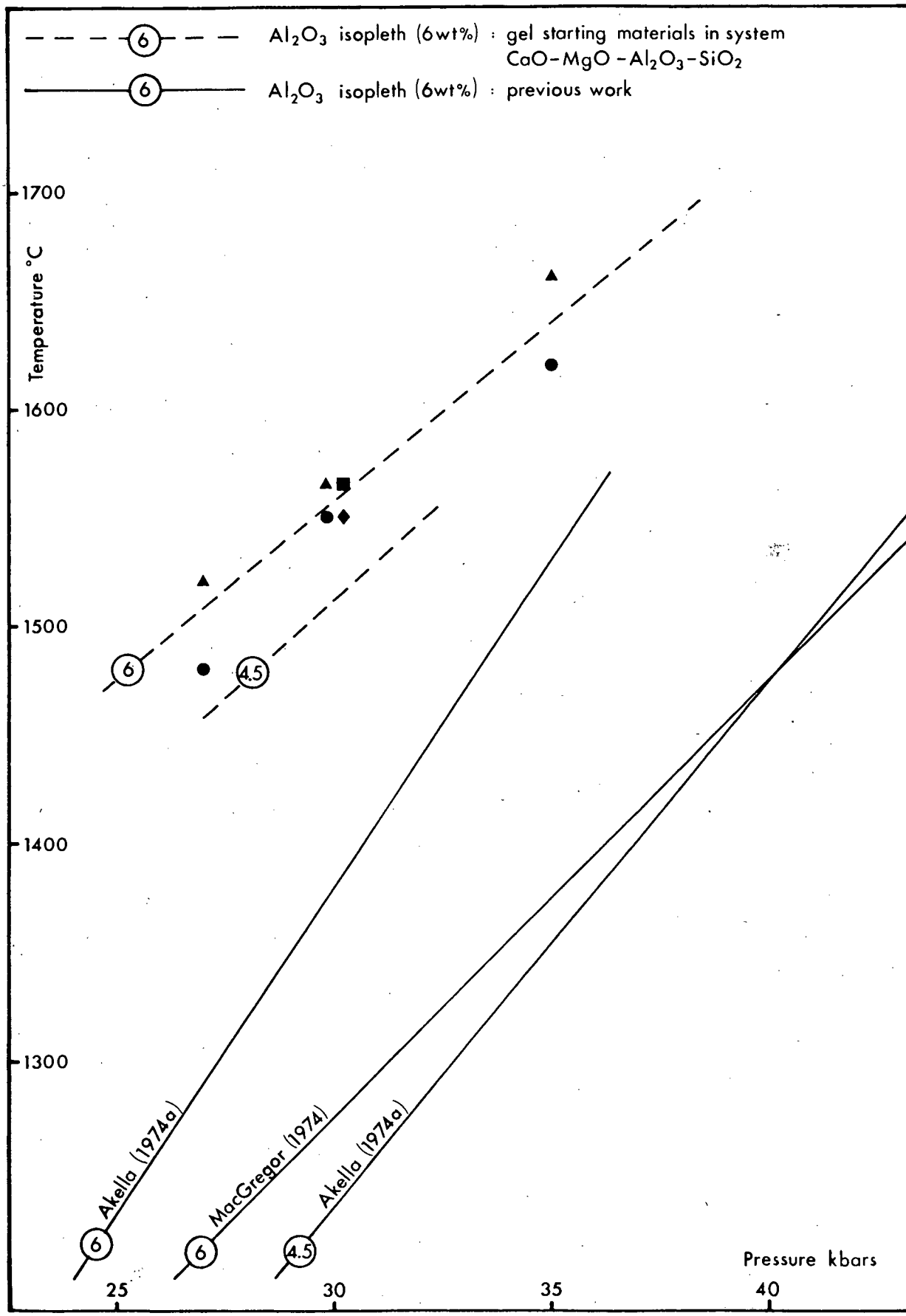
6 Al2O3 isopleth (6wt%) : gel starting materials in system CaO-MgO-Al2O3-SiO2
6 Al2O3 isopleth (6wt%) : previous work
Temperature °C
1700
1600
1500
1400
1300
6
4.5
Akella (1974a)
MacGregor (1974)
Akella (1974a)
6
6
4.5
25
30
35
40
Pressure kbars

gradient these uncertainties amount to about $\pm 6^{\circ}$C/km at a mean gradient of 17°C/km. The use of MacGregor's pressure/temperature grid for Al_2O_3 solubility in orthopyroxene to determine equilibration pressures from the orthopyroxenes crystallized in these experiments would result in pressure errors of up to +19 kb (see Appendix table A.9.7).

Possible explanations for the discrepancies in the reported solubility of Al_2O_3 in orthopyroxene will now be considered. (Details of the experimental techniques used in the previous studies are summarized in Appendix table A.9.15).

A. Inter-laboratory differences in the pressure and temperature calibration of the equipment.

The experiments described by Boyd and England (1964) and Akella (1974a) were carried out using equipment at the Geophysical Laboratory, Washington. Any discrepancies between the results obtained in this and the previous studies do not reflect differences in the calibration of the equipment for the reason discussed in section 3.1.3 and Appendix A.1.2. MacGregor's (1974) charges were run on equipment at the Southwest Center for Advanced Studies; no reference to the calibration of this equipment was stated in MacGregor's publication.

B. Differences of piston technique.

For charges with compositions on the join MS-A, experiments in this study were run using both the piston-out and the floating-piston techniques (Appendix A.1.1). Use of the floating-piston rather than piston-out technique at the same nominal pressure would tend to increase reported Al_2O_3 solubility in orthopyroxene both because of

the lower actual pressures realized using the floating-piston technique, and because the sluggish nucleation of garnet is favoured by the overpressure attained during the piston-out stroke. Solubilities obtained in the new experiments on M-A-S charges whether the floating-piston or piston-out technique was used were lower than those obtained by MacGregor (1974) using the piston-out technique but overpressuring by 3 kb rather than 5 kb, or by Boyd and England (1964) using the floating-piston technique.

Akella's (1974a) piston techniques are equivalent to a piston-out technique at a pressure of 1 kb less than his reported pressures (Akella, 1974b) and his results have been plotted at the lower pressure in figs. 7.1 and 7.2. The new results for compositions in the system C-M-A-S were obtained from piston-out experiments. Although the amount of overpressure used by Akella (1974a) is not stated, the pressure discrepancy between the new results and those of Akella, at a given temperature and Al_2O_3 content of orthopyroxene, is in excess of 5 kb. This pressure difference occurs over a pressure range of at least 8 kb and is much larger than could be expected to result from small discrepancies in overpressure.

The difference between MacGregor's (1974) results and those of Boyd and England (1964) may be entirely explained by the different piston techniques used. Differences of piston technique cannot however account for the discrepancies between these new results and those of Akella (1974a), MacGregor (1974) or Boyd and England (1964).

C. Non-stoichiometric solid solutions.

If garnet and/or pyroxene solid solutions are non-stoichiometric then their compositions in the assemblages opx+gt and

opx+cpx+gt will vary for different compositions. Different bulk compositions will only yield the same orthopyroxene composition at any one temperature and pressure in the invariant assemblages opx+gt+ol (for bulk compositions in the system M-A-S) and opx+cpx+gt+ol (for bulk compositions in the system C-M-A-S).

If the garnet and/or pyroxene solid solutions under consideration are indeed non-stoichiometric, then the results presented in Appendix table A.9.7 and those of Akella (1974a), MacGregor (1974) and Boyd and England (1964) are not strictly comparable because none of the previous workers crystallized forsterite-saturated assemblages. However, the results for gel charges obtained in the present study indicate little difference in the Al_2O_3 contents of orthopyroxenes crystallized in the assemblages opx+cpx+gt and opx+cpx+gt+ol at any one temperature and pressure. Moreover, a large discrepancy in reported Al_2O_3 solubility occurs in the only instance in which a comparison can be made between the run products of a like composition crystallized in this study and in the previous work, viz. for composition $(MS)_{92}(A)_8$ which is closely bracketed by two compositions used by Boyd and England.

It is considered unlikely that non-stoichiometric solid solutions can entirely explain the large and consistent discrepancies illustrated in figs. 7.1 and 7.2.

D. Errors in the different methods used to determine Al_2O_3 solubility in orthopyroxene.

In the present study the run products of the gel starting materials were too small ($<5\mu$) to analyse using the electron microprobe (see Appendix A.3.8). Instead the pattern of Al_2O_3 solubility

in orthopyroxene was obtained indirectly by determining, at any pressure, the minimum temperature at which all the Al_2O_3 in a charge composition would dissolve in orthopyroxene. At lower temperatures, at these pressures, Al_2O_3 in excess of that which can be dissolved in the orthopyroxene crystallizes in the Al_2O_3-rich phase garnet. The Al_2O_3 content of the orthopyroxene in garnet-free assemblages consisting of orthopyroxene alone is the same as the Al_2O_3 content of the bulk composition. The maximum amount of Al_2O_3 that can be dissolved in orthopyroxene at a given temperature and pressure is the Al_2O_3 content of the bulk composition for which the reaction:

$$opx_1 + gt \longrightarrow opx_2$$

goes to completion at this temperature and pressure. The solubility of Al_2O_3 in orthopyroxene was therefore obtained at a given pressure by determining the minimum temperature at which no garnet was observed optically in the run products of a known bulk composition. (X-ray diffraction techniques were not sensitive enough for this problem since they only registered the presence of garnet in concentrations greater than about 2.5%.)

Most of the charges used in this study do not crystallize to orthopyroxene and garnet alone at high pressure. The justification for the use of this method of determining Al_2O_3 contents of orthopyroxene in CaO-bearing charges depends on the very small quantity of clinopyroxene in the run products. Because the amount of clinopyroxene is small, the proportion of total Al_2O_3 in the charge which is dissolved in the clinopyroxene is also small and can be estimated as follows. The maximum possible amount of clinopyroxene crystallized with orthopyroxene and only a trace of garnet from the charges

used here is about 9.3%, viz. for the most calcic bulk composition (charge E41R) at about 1560°C, 30 kb, assuming the least calcic coexisting orthopyroxene (CS c.4.2%, using Davis and Boyd's (1966) data for the cpx(opx) solvus) and the most magnesian clinopyroxene possible (CS c.30%, from the information given for the diopside-rich gels in Chapter 4). The maximum possible Al_2O_3 content of the clinopyroxene in the assemblage cpx+opx+gt at 1560°C, 30 kb is about 7.5% (from the data given in Chapter 4). Under these conditions about 0.7% of the total Al_2O_3 present (6%) in bulk composition E41R will be dissolved in the clinopyroxene.

This argument assumes that the two pyroxenes crystallized from the Al_2O_3-bearing enstatite-rich gels have comparable Al_2O_3 contents and/or Ca/(Ca+Mg) ratios to the pyroxenes crystallized under the same conditions from the Al_2O_3-bearing diopside-rich gels and Davis and Boyd's (1966) Al_2O_3-free glasses. This assumption is supported by the relative intensities of clinopyroxene and orthopyroxene peaks on the x-ray diffraction traces of run products.

For the purposes of this study the Al_2O_3 content of orthopyroxene crystallized with clinopyroxene alone is not significantly less than the Al_2O_3 content of the bulk composition. The Al_2O_3 content of the orthopyroxene in equilibrium with garnet and clinopyroxene is thus the Al_2O_3 content of the bulk composition at the temperature and pressure of the disappearance of garnet from the assemblage opx+cpx+gt.

This method for determining Al_2O_3 solubility in orthopyroxene assumes that no Al_2O_3 is dissolved in any coexisting olivine. Evidence from experiments on diopside-rich gels under these conditions

shows that this is not necessarily true (see section 4.2). This problem has been avoided in the determination of the 6% Al_2O_3 isopleth (fig. 7.2) by considering an assemblage which is only just saturated with forsterite.

Maximum Al_2O_3 contents of orthopyroxene are quoted in this discussion and used in figs. 7.1 and 7.2. Minimum values, which make allowances for Al_2O_3 solubility in clinopyroxene, are given in Appendix table A.9.7.

Boyd and England's (1960) x-ray data for aluminous orthopyroxenes (see Appendix A.3.6) could only be used empirically to check the optical determination of Al_2O_3 solubility in orthopyroxenes crystallized in the present experiments. Boyd and England derived orthopyroxene composition determinative curves which relate the variation of two parameters of the x-ray diffraction patterns of aluminous (M-A-S) orthopyroxenes to the Al_2O_3 content of the orthopyroxenes. The two x-ray parameters indicated different Al_2O_3 contents for any one orthopyroxene crystallized in the present study from the M-A-S gels. In some cases, for example the orthopyroxene crystallized in run EP32/284 (see Appendix table A.9.8), this difference was shown to be significant at the 99.9% probability level using Student's t test. The discrepancy would be explained if the aluminous orthopyroxenes crystallized either by Boyd and England (1960) from glass charges, or in this study, lay off the pure MS-A join. The presence of a phase in addition to garnet and orthopyroxene could not be proved in the run products of the gel charges. Non-stoichiometric M-A-S orthopyroxenes reported by Boyd and England are much more aluminous than those under consideration here. An

alternative explanation for the lack of agreement between the x-ray parameters reported here and by Boyd and England is that the orthopyroxenes crystallized in the two studies may have crystal structures which differ at the second order level.

The x-ray parameters were not suitable for determining Al_2O_3 solubility in the Ca-bearing and possibly non-stoichiometric orthopyroxenes crystallized in the system C-M-A-S.

Appendix table A.9.8 shows that both x-ray parameters varied with increasing temperature at 30 kb for orthopyroxene in equilibrium with garnet crystallized from the M-A-S charge ENA8R; and for orthopyroxene crystallized with garnet, olivine and clinopyroxene from the C-M-A-S charge E4R. This variation is outside limits of reproducibility of the x-ray parameters (see Appendix A.3.6) at the 99.7% probability level in the temperature range 1400–1550°C for charge ENA8R and in the temperature range 1350–1500°C for charge E4R. These temperature ranges are above the minimum temperatures at which total solution of Al_2O_3 in pyroxenes should occur for these compositions at 30 kb according to the results of MacGregor (1974) and Akella (1974a) for the calcium-free and calcium-bearing charges respectively. This variation of the parameters with increasing temperature may be explained by variation of the Al_2O_3 or CaO content or $(CaO+MgO):SiO_2$ ratio of the orthopyroxenes.

Most of the possible errors in the optical method of determining Al_2O_3 solubility in orthopyroxene tend to overestimate the Al_2O_3 solubility and hence decrease the discrepancy between these results and those of Boyd and England (1964), MacGregor (1974) and Akella (1974a).

Possible sources of error are:-

(i) Solubility of Al_2O_3 in clinopyroxene and olivine coexisting with orthopyroxene and garnet.

(ii) Failure to identify small garnet crystals. In some of the run products garnet was scattered through the charge as very small crystals which were only just visible optically at a magnification of x400. Such crystals were identified as garnet because they graded with no change of texture or refractive index into much bigger crystals which were considered to be garnet for the reasons given in Appendix A.3.2. In the critical runs garnet was identified optically as euhedral crystals up to 10 μ across. Submicroscopic garnet crystals may be present at temperatures higher than those at which total solution of garnet in pyroxenes is reported. X-ray diffraction traces and reflection measurements on available run products were not sufficiently sensitive to resolve this possibility.

(iii) Inaccuracies and imprecision in the manufacture of the charges. All starting materials used were gels or treated (e.g. glassed) gels. Any gel whose recovered weight lay outside the limits 9.95-10.03 gms. for an intended 10 gm. sample was discarded (see Appendix A.2.1). The differences between the new results in the C-M-A-S system and those of Akella (1974a) are up to 4% Al_2O_3 which is much greater than the limit of acceptable error for the gel recovery. Certain unlikely combinations of compensating errors could cause the acceptance of a gel with an Al_2O_3 content wildly discrepant from that intended. The coincidence that this happened for all the large number of gels used in this study, and which were manufactured at different times, is very low.

The analytical methods used in the previous studies will now be considered. Boyd and England (1964) also used optical methods, i.e. the presence or absence of garnet, to determine Al_2O_3 solubility in orthopyroxene. They do not report the presence of pinhead garnet crystals. Both Akella (1974a) and MacGregor (1974) determined the Al_2O_3 contents of orthopyroxene directly by electron microprobe analysis. The differences between the new results and those of Akella and MacGregor far exceed their reported imprecision. Neither Akella nor MacGregor report the presence of pinhead garnets in their run products. Failure to recognize such small garnets would lead to an overestimation of Al_2O_3 solubility in orthopyroxene because electron microprobe analysis would include the compositions of any small garnet crystals under the electron beam. This may partly account for the differences between these new results and MacGregor's (1974) high temperature run results, but not for results from the H_2O-bearing charges of Akella (1974a) or MacGregor. Garnet is not expected to remain as very small crystals in the presence of H_2O as a flux (see part E below).

E. The use of H_2O as a flux.

H_2O was used as a flux to promote crystal growth in all experiments run by Akella (1974a) and in the low temperature experiments made by Boyd and England (1964) and MacGregor (1974). With decreasing temperature below about 1350°C run products obtained in the present study contained significant and increasing amounts of unrecrystallized gel starting material, even in runs of up to 17 hours duration, the maximum time for which a Pt/Pt13Rh thermocouple can be used with reliability at these temperatures. Attempts were made to

achieve equilibrium at 30 kb in the temperature range 1100-1200°C in experiments on charge $En_{95}A_5R$ (bulk composition $(MS)_{95}(A)_5$) by adding small amounts of H_2O to the charge. These experiments, described below, suggest possible sources of error in the determination of Al_2O_3 solubility in orthopyroxene as a result of the use of H_2O as a flux.

At 1202°C in the presence of 6.7% H_2O and at 1174°C in the presence of 4% H_2O, the run products of the charge $En_{95}A_5R$ consisted of large orthopyroxene crystals. Very small quantities of glass, vapour beads and olivine occurred in the 1202°C run product. The orthopyroxene crystals returned from both experiments contained sparse quench structures indicating the presence at high temperatures of a liquid which formed crystalline overgrowths on the primary crystals during quenching. Such overgrowths may be indistinguishable optically from the primary crystals. Microprobe analysis of orthopyroxene crystals in such run products may give erroneous values for the solubility of Al_2O_3 in orthopyroxene if the quenched rims were inadvertently analysed as well as, or instead of, the primary crystals.

Both Akella (1974a) and MacGregor (1974) used H_2O as a flux and determined the solubility of Al_2O_3 in orthopyroxene by microprobe analysis of orthopyroxene crystals coexisting with garnet. Neither worker reports textures which indicate the presence of quenched liquid in their run products. O'Hara (pers. comm.) reported that at least one of Akella's (1974a) high temperature run products shows evidence of partial melting. This run was at 31 kb, 1500°C and the orthopyroxene analysis was not included in drawing up

figs. 7.1 and 7.2. Quenched orthopyroxene may, however, have been misidentified as primary orthopyroxene in other run products.

A smaller quantity of H_2O (2.5%) was added to the same charge $En_{95}A_5R$ for a run at 1100°C. The run product consisted of large garnet crystals, packed with inclusions, and a few large orthopyroxene crystals in a very fine-grained matrix of orthopyroxene crystals. This does not necessarily represent an equilibrium assemblage because the large orthopyroxene crystals which grew preferentially may not have the same composition as those in the groundmass. Moreover, the large garnet crystals may have grown poikilitically around, and chemically isolated, incompletely recrystallized starting material. Large metastable crystals may not equilibrate during the duration of these experiments. This run product was not considered suitable for determining the solubility of Al_2O_3 in orthopyroxene since it may not represent an equilibrated assemblage.

The use of H_2O as a flux would also lead to erroneous values for the solubility of Al_2O_3 in orthopyroxene if these high pressure and high temperature orthopyroxenes showed solid solution towards H_2O. Evidence which supports the hypothesis that small amounts of hydroxyl may be dissolved in some pyroxenes was given by Martin and Donnay (1972). The presence or absence of hydroxyl in the hydrothermally synthesized aluminous orthopyroxenes under discussion in this section has not been determined.

The use of H_2O as a flux may explain some of the differences illustrated in figs. 7.1 and 7.2. However, the results of Boyd and England (1964), MacGregor (1974) and the low temperature results of Akella (1974a) all conform to a consistent pattern despite variation

in the amount of H_2O added to the charges. This would not be expected if the presence of H_2O had a large effect on the reported level of Al_2O_3 solubility in orthopyroxene.

F. Variation in type of starting material.

Except for the run on the crystal mix EP32 all the run results of this study shown in figs. 7.1 and 7.2 were obtained from partially crystalline or recrystallized gel starting materials. In the critical runs on partially crystalline gel charges only traces of unrecrystallized quartz-rich gel were observed in the run products. No inconsistency was observed between the results of runs using partially crystalline gels and those of runs using recrystallized gels, nor between the run products of homogeneous gels and the run products of mixes of gels (e.g. the run results of charges AM3 and E41R at 30 kb).

The low solubilities obtained in the experiments on the gel mix ENA8R were reproduced using the garnet-enstatite crystal mix EP32. At 1550°C, 30 kb both starting materials crystallized the assemblage opx+gt. The compositions of the orthopyroxenes crystallized in these two experiments were not significantly different ($<90\%$ probability of being different) as demonstrated by Student's t test comparison of the $^{o}2\theta$ values of the two x-ray diffraction parameters shown by Boyd and England (1960) to be sensitive to changes in the Al_2O_3 content of orthopyroxenes (see Appendix A.3.6).

The low solubilities of Al_2O_3 in orthopyroxenes crystallized in the system C-M-A-S were reproduced at 30 kb using the glass E3H (approximate bulk composition $(CS)_{5.5}(MS)_{90.0}(A)_{4.5}$) as starting material. However, experiments on the glass indicated problems

connected with sluggish crystal growth. Runs at 1350°C (for 9 hours) and 1450°C (for 6.75 hours) contained garnet in accordance with results based on gel charges but contrary to the results of Akella (1974a). In both run products the very small amount of garnet present occurred as minute anhedral crystals. More garnet was observed in the run product of the 1350°C run than in that at 1450°C. The run products of these two runs were mixed and rerun at 1450°C, 30 kb for 6 hours. Garnet was more conspicuous in the new run product than in that of the original run at 1450°C. Two possible explanations of these observations are:-

(i) the presence of sub-microscopic garnet in the run products of the first run at 1450°C. Larger garnet crystals were present in the products of the second run at 1450°C either because larger crystals were already present in the charge from the run product at 1350°C, or because of the extended run duration.

(ii) the failure or reluctance of aluminous orthopyroxenes crystallized initially from glass starting materials to completely break down to garnet plus a less aluminous orthopyroxene (c.f. Boyd and England, 1964, discussed below).

In summary, the low solubilities of Al_2O_3 in orthopyroxene reported in the present work have been reproduced using a variety of starting materials.

Garnet nucleates only with extreme difficulty from glass charges (e.g. Boyd and England, 1959, 1964). MacGregor (1974) seeded his glass charges with pyrope nuclei to avoid this problem. However, it has not yet been demonstrated that metastable aluminous orthopyroxenes crystallized initially from glass charges will necessarily

break down to garnet plus a less aluminous orthopyroxene in the presence of garnet nuclei. Glass starting materials were also used by Akella (1974a).

Experiments by Boyd and England (1964) using mixes of aluminous orthopyroxene and pyrope crystals indicated lower Al_2O_3 solubilities than runs on dry glass charges. The solubilities reported by Boyd and England which have been plotted in fig. 7.1 are their preferred results for the crystal mixes. The assumption that the results from runs on the crystal mixes are a closer approach to equilibrium is based on the crystallization behaviour of the glass starting materials under run conditions. These first crystallized to a homogeneous pyroxene which only gradually exsolved garnet. The crystallization and persistence of metastable pyroxenes from glass starting materials has been noted in other systems (e.g. O'Hara and Schairer, 1963).

These observations of Boyd and England (1964), as well as the sluggish crystallization of garnet from the glass charge used in the present study, suggest that the discrepancy between the new results and those of Akella (1974a) and MacGregor (1974) may be connected with the kinetics of garnet nucleation from different types of starting material. This fails, however, to explain the following two observations:-

(i) the much lower solubility of Al_2O_3 in orthopyroxene crystallized from the garnet-bearing crystal mix EP32 used in this study compared to the solubility reported by Boyd and England (1964) from garnet-bearing crystal mixes. The crystal mix EP32 has the bulk composition $(MS)_{92}(A)_8$ which is predicted to homogenize at a minimum

temperature of 1265°C at 30 kb using the floating-piston technique, according to the results of Boyd and England (1964). However, a temperature of 1550°C, 30 kb using the piston-out technique, was insufficient to completely dissolve the pyrope in the orthopyroxene crystallized from charge EP32. This difference far exceeds the effect of using different piston techniques. Neither can it be explained by non-stoichiometric solid solutions because the composition used, viz. EP32, is closely bracketed by two compositions used by Boyd and England (1964), viz. $(MS)_{90}(A)_{10}$ and $(MS)_{92.5}(A)_{7.5}$. It is unlikely that this discrepancy can be explained by breakdown of pyrope during drying of the charge at atmospheric pressure. A pyrope-enstatite mix dried in nitrogen at 1050°C, atmospheric pressure for one hour showed no signs of breakdown. However the drying procedure used by Boyd and England (1964) is not stated.

(ii) Boyd and England (1964) report that glasses and garnet-bearing crystal mixes yielded results which are within the precision of temperature and pressure measurement when H_2O was added to the charge as a flux. Akella (1974a) used H_2O as a flux at all temperatures; MacGregor (1974) used it only in low temperature experiments. This suggests that garnet nucleation was not a problem in the experiments of either Akella or MacGregor. MacGregor's results for runs on H_2O-bearing charges and those on dry charges are consistent, which implies that he did not encounter the effect described by Boyd and England (1964) for dry glass charges.

These observations suggest that if the discrepancy between the new results and those reported in previous studies is indeed a function of starting material, then it is not connected with problems

of garnet crystallization. The discrepancies may, however, reflect second-order structural differences in the high pressure phases, such structural differences being inherited from the low pressure phases. Second-order structures in the low pressure phases may largely be controlled by the crystallization history of these phases, e.g. the method of manufacturing the glasses which would have devitrified at an early stage in the experiments, and the drying conditions of the charges. The glass E3H used in the new experiments and which reproduced the low Al_2O_3 solubilities obtained with the gel charges, was made by holding a gel at hyper-liquidus temperatures (c.1700°C) for only a few minutes before quenching. The glass E3H may thus have inherited structures from the gel. Similarly, the garnet and orthopyroxene in charge EP32 were both obtained by crystallizing gel charges. On the other hand, the glasses used in the previous studies were manufactured by a different method and would have contained different structures from those in glass E3H.

G. Run durations.

The run durations of these new experiments are comparable to those of MacGregor (1974) at equivalent temperatures. Run lengths were not reported by Boyd and England (1964) or by Akella (1974a). Results of runs on the charge E41RF2 at 1500°C, 30 kb, using the piston-out technique, indicate that the run durations of the new experiments on gel charges were insufficient to nucleate the maximum amount of garnet possible at equilibrium under the given conditions. The run product of this charge after 4 hours was orthopyroxene plus a small amount of garnet, most of which occurred as pinhead crystals scattered through the charge. There were also a few larger euhedral

garnet crystals. The total amount of garnet was less than 2.5% as indicated by its failure to register on an x-ray diffraction trace of the run products. This does not agree with the results of runs on a less aluminous bulk composition (charge E4R) which predicted about 6% free garnet in the run products of E41RF2 at 1500°C. The latter was reloaded and run for a further 4 hours under the same conditions. The new run product contained euhedral garnet in sufficient quantity to appear on the x-ray diffraction trace of run products. The ratio ($Iopx_{131}/Igt_{420}$) of the intensities of the orthopyroxene 131 and garnet 420 reflections (see Appendix A.3.7) for mixes of pure enstatite (MS) and pyrope (M_3AS_3) in the proportion 94:6 and 97:3 are about 2.0 and 3.0 respectively. This intensity ratio for the runs at 1500°C on charge E4R (4 hour duration) and on charge E41RF2 (8 hour duration) was >4.0 and about 0.5 respectively. This shows that the amount of garnet crystallized in the 8 hour run is much more than 6%, i.e. much more than predicted by the run on the less aluminous composition E4R.

These results indicate that the solubility of Al_2O_3 in orthopyroxenes crystallized from gels at a given temperature and pressure may be even lower than indicated in figs. 7.1 and 7.2, and hence may be even further removed from the solubilities observed in previous studies. No kinetic problems were reported by Akella (1974a) or MacGregor (1974), or by Boyd and England (1964) on their crystal mixes. Moreover, the factor hindering the trend towards equilibrium in the run products of the gel charges is the slow crystallization of garnet whereas high Al_2O_3 solubilities were obtained by Boyd and England (1964) by homogenizing garnet-pyroxene mixes. This suggests

that the previous experiments crystallized equilibrium assemblages even if the assemblages are not the most stable ones.

7.2 Discussion

The results discussed in the previous section suggest that neither glass nor gel are satisfactory as dry starting materials for determining Al_2O_3 solubility in orthopyroxene because both may crystallize metastable, highly aluminous orthopyroxenes from which garnet nucleates and grows only slowly. Stable equilibrium may not be achieved within the maximum run durations possible for Pt/Pt13Rh thermocouples.

The most likely explanation for the differences in the reported solubility of Al_2O_3 in orthopyroxene is that there are detailed structural differences between the high pressure garnets and pyroxenes crystallized from the different starting materials. Detailed structural analyses of the pyroxene crystals obtained in the different experiments are required in order to assess this possibility.

A reversal of the new phase field boundaries shown in figs. 7.1 and 7.2 was not attempted in this study because:-

(i) these boundaries are probably not equilibrium boundaries.

(ii) the failure of garnet to crystallize from a single phase assemblage of orthopyroxene is not evidence of the stability of that orthopyroxene single phase assemblage because garnet crystallizes only sluggishly from supersaturated aluminous orthopyroxene.

(iii) it is possible to reverse a metastable phase field boundary (e.g. Richardson, Bell and Gilbert, 1968).

Bearing in mind the possibilities that the assemblages crystallized from the gel charges may not represent stable equilibrium and that any variation of Al_2O_3 solubility in orthopyroxene as determined from the runs on gel charges may reflect different rates of garnet nucleation and crystallization, the results from gel charges show that:-

(i) Al_2O_3 solubility in orthopyroxene is pressure sensitive between 1450 and 1600°C in the pressure range 27-35 kb.

(ii) Al_2O_3 solubility in orthopyroxene coexisting with garnet and clinopyroxene is not affected by the presence of olivine, at least at the pressures and temperatures and for the compositions investigated, at the level of precision of the determinations.

(iii) in the assemblage opx+cpx+gt, results are consistent with previous observations that Al_2O_3 and CaO solubility in orthopyroxene increases with increasing temperature at a fixed pressure, and Al_2O_3 solubility in orthopyroxene decreases with increasing pressure at a fixed temperature. These experiments were too limited and the analytical techniques insufficiently sensitive to determine whether a reaction from a calcic clinopyroxene-bearing to a subcalcic clinopyroxene-bearing garnet-lherzolite occurs within the pressure/temperature range investigated. If such a reaction does occur, it is expected that the variation of orthopyroxene composition as a function of pressure and temperature would be different in the two phase fields.

CHAPTER 8

THE ORTHOPYROXENE GEOBAROMETER: AL_2O_3 SOLUBILITY IN ORTHOPYROXENE IN NATURAL GARNET-LHERZOLITE ASSEMBLAGES

8.1 Introduction

The limitations of the application of MacGregor's (1974) data for synthetic aluminous orthopyroxenes to natural rocks were given in section 6.1 and some of the sources of error were considered in Chapter 7. Two of the remaining sources of error which were not considered in the experimental programme described in Chapter 7 are caused by the paucity of information on:-

(i) orthopyroxenes containing the small amounts ($<2\%$) of Al_2O_3 found in natural garnet-lherzolite assemblages. The lack of this information is due to sluggish reaction rates at the low temperatures at which orthopyroxenes containing such low Al_2O_3 contents are in equilibrium with garnet within the experimentally accessible pressure range.

(ii) the effect of minor elements, other than calcium, on Al_2O_3 solubility in orthopyroxene. Available experimental determinations of orthopyroxene solid solutions crystallized in multi-component synthetic and natural systems are discussed below in sections 8.2 and 8.3.2 respectively. Some new results for a natural assemblage are presented in section 8.3.1.

To circumvent both these limitations in the use of the Al_2O_3 content of orthopyroxene as a geobarometer, thermodynamic models of

Al_2O_3 solubility in orthopyroxene have been developed (Wood and Banno, 1973; Wood, 1974) which extend available experimental data to experimentally unexplored pressure/temperature conditions and to multicomponent systems. The use of such models is considered in section 8.4.

8.2 Experimental approach: previous studies on synthetic systems

Direct determinations of the effect of individual components on the solubility of Al_2O_3 in orthopyroxene have been attempted in various M-A-S-X and M-A-S-C-X systems. Compositions in M-A-S-C were considered in Chapter 7.

Orthopyroxenes crystallized by Akella (1974a) in the system M-A-S-C-T and by Akella and Boyd (1972, 1973) in the system M-A-S-C-T-F may be metastable because glasses were used as starting materials (see Chapters 3 and 7). Moreover, the Al_2O_3 contents of orthopyroxenes crystallized by Akella and Boyd may have been affected by the presence of small quantities of rutile and ilmenite.

Conclusions from the results of Wood (1974) on iron-rich compositions in M-A-S-F and M-A-S-C-F are also unjustified because of probable pyroxene metastability. The starting materials for the experiments were glasses seeded with about 10% each of a synthetic orthopyroxene, containing 12.3% Al_2O_3, and a natural garnet. The Al_2O_3 contents of the high pressure recrystallized orthopyroxene seeds were determined by electron microprobe analysis and reported for orthopyroxenes in equilibrium with garnet. These Al_2O_3 contents are likely to be overestimates of the equilibrium values because the

trend towards equilibrium of the highly aluminous orthopyroxene seeds involves the exsolution of Al_2O_3 as garnet. This is a sluggish process (e.g. Boyd and England, 1964) and would be hindered by the large crystal size (15-20μ) of the orthopyroxene seeds. It is not known to what extent the exsolution process is catalysed by the presence of garnet seeds. Wood's (1974) results are also complicated by the lack of information on the oxidation state of iron in the solid solution. The long run durations given to these iron-rich charges would have resulted in considerable iron-loss to the Ag-Pd capsules (Merrill and Wyllie, 1973). This would have increased the O_2 fugacity of the charge and may have oxidized much of the remaining Fe^{2+} to Fe^{3+}. The presence of iron in two different oxidation states would not be evident from the electron microprobe analysis because SiO_2 was estimated by difference.

8.3 Experimental approach: studies on natural systems

8.3.1 Al_2O_3 solubility in pyroxene in a natural olivine-garnet websterite

Experimental results for the high pressure sub-solidus and hyper-solidus crystallization behaviour of a natural olivine-garnet websterite are reported in Howells, Begg and O'Hara (1975). Certain of these results give an indication of the solubility of Al_2O_3 in a natural orthopyroxene coexisting with clinopyroxene, olivine and garnet. Details of this rock (1031) are given in Appendix A.4 and the compositions of the whole rock and its constituent minerals are presented in Appendix table A.4.1. Results of the relevant

experiments are given in Appendix table A.9.14.

At 1521°C, 30 kb the rock crystallized the assemblage cpx+opx+gt+ol. At 1550°C, 30 kb all Al_2O_3 was dissolved in the pyroxenes and olivine, the run product containing clinopyroxene, orthopyroxene and olivine alone. The rock sample used contained 4.18% Al_2O_3 (5.19% total R_2O_3). In the 1550°C, 30 kb run product most of this Al_2O_3 is expected to be dissolved in the pyroxenes, the small amount of olivine present containing little, if any, Al_2O_3. Assuming roughly comparable Al_2O_3 contents in the two pyroxenes, in accordance with observations on naturally crystallized pyroxene pairs, the Al_2O_3 content of the orthopyroxene in the 1550°C, 30 kb run product is unlikely to exceed 5.5%. This is substantially less than the 11% predicted from MacGregor's (1974) orthopyroxene grid.

A further run was carried out at 1500°C, 30 kb for 127 minutes which is considerably longer than the 20-30 minute duration of the 1521°C and 1550°C experiments described above. The run product contained garnet in agreement with the results of the shorter duration experiments. The presence of garnet in the 1521°C, 30 kb run product, at higher temperatures than predicted by MacGregor (1974), is not therefore the result of kinetic problems.

8.3.2 A review of experimental data for natural systems

Results of experimental studies in natural systems are complicated by problems of garnet nucleation and possible oxidation of the charge.

Fig. 8.1 is a pressure/temperature plot comparing the Al_2O_3 solubility in orthopyroxene determined in various synthetic systems

FIGURE 8.1

A pressure/temperature plot comparing the solubility of Al_2O_3 in orthopyroxene determined in various simple synthetic systems (see figs. 7.1 and 7.2) with results from experiments on natural[1] compositions. The 4.5 and 6% isopleths of Al_2O_3 solubility in orthopyroxene are compared. The results from the simple synthetic compositions are shown by continuous lines.

The results of Akella (1974a) and Akella and Boyd (1974) have been plotted at a pressure of 1 kb less than their reported pressures which were corrected for the effect of friction. Their reported pressures are equivalent to the pressures attained in piston-out experiments at pressures of 1 kb less than their reported pressures (Akella, 1974b).

[1] The composition used by Green and Ringwood (1970) is in fact a synthetically manufactured multicomponent composition which simulates natural compositions.

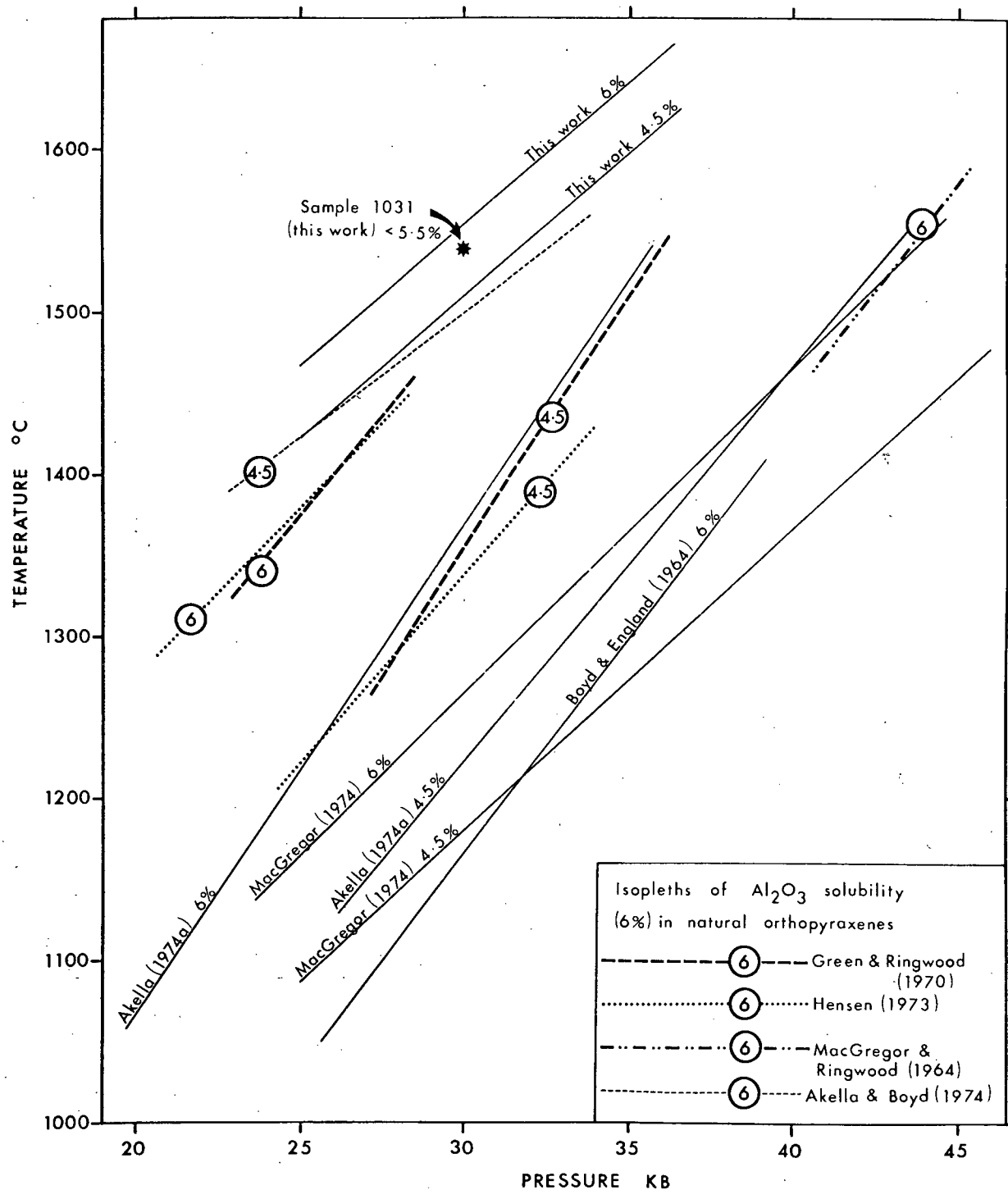
TEMPERATURE °C
1600
1500
1400
1300
1200
1100
1000
20
25
30
35
40
45
PRESSURE KB
This work 6%
This work 4·5%
Sample 1031
(this work) < 5·5%
4·5
6
Akella (1974a) 6%
MacGregor (1974) 6%
Akella (1974a) 4·5%
MacGregor (1974) 4·5%
Boyd & England (1964) 6%
Isopleths of Al_2O_3 solubility
(6%) in natural orthopyraxenes
Green & Ringwood (1970)
Hensen (1973)
MacGregor & Ringwood (1964)
Akella & Boyd (1974)

(described in Chapter 7) with results from experiments on multi-component systems, details of which are given in Appendix table A.9.15. The 4.5 and 6% Al_2O_3 isopleths have been constructed for the different sets of results by assuming linear variation between, and linear extrapolation from limited data points. Results of experiments on the olivine-garnet websterite (see section 8.3.1) and Akella and Boyd's (1974) garnet-lherzolite closely correspond to the results of experiments on calcium-bearing gel charges. Al_2O_3 solubilities determined by Hensen (1973) and Green and Ringwood (1970) are intermediate between the results from gels and those from calcium-bearing glasses (Akella, 1974a). In all four studies on multi-component systems, the equilibria considered are opx+cpx+gt$\pm$ol.

$Mg^{2+}/(Mg^{2+}+Fe^{2+}+Fe^{3+})$ ratios of the pyroxene-rich loaded bulk compositions and of the orthopyroxenes in the run products where this parameter is reported (Hensen, 1973; Akella and Boyd, 1974) all lie in the range c.0.80-0.90. The $Mg^{2+}/(Mg^{2+}+Fe^{2+}+Fe^{3+})$ ratios of the high pressure orthopyroxenes crystallized by Hensen overlap those of orthopyroxenes crystallized by Akella and Boyd at similar pressures and temperatures. The discrepancy in the results plotted in fig. 8.1 for multicomponent cpx+opx+gt$\pm$ol assemblages is therefore not caused by variation in the $Mg^{2+}/(Mg^{2+}+Fe^{2+}+Fe^{3+})$ ratio of the orthopyroxenes.

Fig. 8.1 compares Al_2O_3 contents for orthopyroxenes crystallized in the systems M-A-S and C-M-A-S with Al_2O_3, not total R_2O_3 contents of the multicomponent orthopyroxenes. Cr_2O_3 contents in the multicomponent orthopyroxenes are low where they have been determined. Consideration of the total $(Al_2O_3+Cr_2O_3)$ content rather

than the Al_2O_3 content alone amounts to a pressure difference of less than 2 kb at these high Al_2O_3 solubilities. Similarly, corrections to the R_2O_3 content involving sodium-bearing molecules (e.g. $NaR^{3+}Si_2O_6$) make little difference to the position of the isopleths in fig. 8.1 because of the high $(Al_2O_3+Cr_2O_3)/Na_2O$ ratios of the orthopyroxenes.

Fe_2O_3 contents of these multicomponent orthopyroxenes are unknown because Fe^{3+} and Fe^{2+} are totalled and quoted as FeO in the electron microprobe analyses. The occurrence of Fe^{3+} rather than Fe^{2+} would not be revealed by a lack of site balance in the analyses. Imprecision of probe analysis and possible pyroxene non-stoichiometry would exceed discrepancies of site balance for the low iron contents of these orthopyroxenes, even if all the iron present was trivalent. Information on the O_2 fugacity within a charge for various solid media assemblages is insufficient to determine the oxidation state of the iron in the run products under consideration. Thompson and Kushiro's (1972) results on the O_2 fugacity within graphite capsules are not applicable to the assemblages crystallized by Akella and Boyd (1974), Green and Ringwood (1970) and Hensen (1973) in runs in graphite capsules because of the difference of pressure range, H_2O content of the charges, run durations and the nature of the charge/graphite contact. The O_2 fugacity within the sealed Pt capsules used by Green and Ringwood (1970) and in the experiments reported in section 8.3.1 is also unknown and may be affected by the loss of Fe from the charge to the capsule resulting in O_2 liberation. The results of Green and Ringwood (1970) suggest that this is not a significant effect. Even after 15-40% iron loss from a sub-solidus

garnet-lherzolite assemblage originally containing 0.8% Fe_2O_3 ($FeO+Fe_2O_3$= 9%), the Fe_2O_3 content of the run products did not exceed 1%. Moreover, there was no correlation between the extent of iron loss and the Fe_2O_3 content of the run product. These results cannot, however, be assessed without information on the method used to determine Fe_2O_3 contents.

The presence of Fe^{3+} in the experimentally recrystallized orthopyroxenes may affect their Al_2O_3 contents by increasing their total R_2O_3 contents. However, differences in the Fe^{2+}/Fe^{3+} ratio of the orthopyroxenes is unlikely to explain the apparent discrepancy between the results of Akella and Boyd (1974) and those presented in section 8.3.1 on one hand, and those of Hensen (1973) and Green and Ringwood (1970) on the other. All four sets of experiments gave results which were consistent with the results of other experiments in the set despite variation in those experimental conditions which are likely to considerably affect the O_2 fugacity of the charge, viz. variable duration of runs carried out in Pt capsules; the use of unsealed graphite capsules as container materials for charges containing variable H_2O contents.

A more likely explanation of the discrepancy is that garnet nucleation was less favoured in the experiments of Hensen (1973) and of Green and Ringwood (1970) than in those of Akella and Boyd (1974) and the present study (section 8.3.1) because of the nature of the starting materials used. The charges of Akella and Boyd and charge 1031 (used in the present work) contained garnet, and the trend towards equilibrium was that of solution of Al_2O_3 into orthopyroxene. No garnet was present in the starting materials used by Hensen (1973)

or by Green and Ringwood (1970). The trend towards equilibrium in Hensen's experiments on the Deltex pyroxene pair was the notoriously sluggish exsolution of garnet from highly aluminous pyroxenes. The Al_2O_3 content of the loaded orthopyroxene in the other starting material used by Hensen (viz. the spinel-lherzolite) was not reported.

The results on charge 1031 and those of Akella and Boyd (1974) are therefore believed to be a closer approach to equilibrium than the results reported by Hensen (1973) and by Green and Ringwood (1970). The similarity in the Al_2O_3 contents of orthopyroxenes crystallized from the gel charges (see Chapter 7) and from the natural orthopyroxene, clinopyroxene, garnet and olivine mixes used here (charge 1031) and by Akella and Boyd is not, however, necessarily significant. The orthopyroxenes crystallized from the gel charges, and possibly from the natural minerals, may be metastable or may not have equilibrated. Moreover, Al_2O_3 solubility in natural orthopyroxenes may be affected by components other than CaO, MgO and SiO_2. The results plotted in figs. 7.1 and 7.2 for gel charges cannot directly be used to determine equilibration pressures of natural garnet-lherzolite assemblages.

The 6% Al_2O_3 isopleth for orthopyroxenes crystallized at 1500°C in equilibrium with garnet alone from a natural orthopyroxene (CaO content 0.82%) and garnet (CaO content 5.21%) mix (MacGregor and Ringwood, 1964; see Appendix table A.9.15) is shown in fig. 8.1. The orthopyroxene was not saturated with clinopyroxene. The position of the isopleth is closely comparable to the results of Boyd and England (1964) from runs on compositions in the system MS-A using the same floating-piston technique. The results are not, however,

compatible with the results of Akella and Boyd (1974) and of the present study (charge 1031).

8.4 Thermodynamic models of Al_2O_3 solubility in orthopyroxene in equilibrium with garnet

Thermodynamic models have been developed by Wood and Banno (1973) and Wood (1974) which describe the variation of Al_2O_3 solubility in orthopyroxene in equilibrium with garnet as a function of pressure and temperature in both simple and multicomponent systems. The relation between the compositions of coexisting garnet and orthopyroxene and the pressure and temperature of equilibration is expressed by the equation:-

$$P = 1 + \frac{RT}{\Delta V_r}\left[\ln\left(\frac{\left(X_{Mg}^{M1}\right)_{opx}\left(X_{Mg}^{M2}\right)^2_{opx}\left(X_{Al}^{M1}\right)_{opx}}{\left(X_{Mg_1}^{gt}\right)^3}\right) - \frac{(\Delta H_1^o - T\Delta S^o)}{RT}\right]$$

(equation 8.1)

The form of this equation and an explanation of the symbols used in it are given in Appendix A.6.1.

The values of ΔH_1^o and ΔS^o are unknown and were calculated for these models by fitting equation 8.1 to existing experimental data for which the relation between pressure, temperature and compositions of coexisting phases is known. Once ΔH_1^o and ΔS^o were determined, Al_2O_3 solubility in orthopyroxene was predicted at temperatures and pressures not investigated experimentally and in chemical systems of various degrees of complexity. The validity of these models therefore depends on the accuracy of the experimental

data from which ΔH_1^o and ΔS^o were derived.

The model of Al_2O_3 solubility in orthopyroxene in the simple system MS-A (Wood and Banno, 1973) based on the experimental results of Boyd and England (1964) was modified by Wood (1974) who derived a new model for the same system based on the experimental results of MacGregor (1974). Experiments described in Chapter 7 suggest that neither Boyd and England nor MacGregor necessarily obtained equilibrium results. The thermodynamic models of Wood and Banno and of Wood may not therefore be valid.

The values of ΔH_1^o and ΔS^o derived by Wood (1974) were used to predict Al_2O_3 solubilities in calcium- and iron-bearing orthopyroxenes (Wood, 1974). Al_2O_3 contents calculated for calcium-rich orthopyroxenes correspond closely to new experimental data (Wood, 1974) for compositions in the system CS-FS-MS-A. The agreement is less good for iron-rich orthopyroxenes, an effect which Wood ascribed to non-ideal Fe-Al interactions. The reasonable agreement between Wood's model and his experimental results does not justify the model because the starting materials he used in his experiments may well have crystallized metastable, Al_2O_3-supersaturated orthopyroxenes (see section 8.2) which possibly also occurred in the run products of MacGregor (1974). Moreover, the calculated Al_2O_3 solubilities themselves are based on values for the mole fractions of magnesium, calcium and iron in both garnet and orthopyroxene obtained from the very experimental results with which they are compared.

Fig. 8.2 is an alternative thermodynamic model of the variation of Al_2O_3 solubility in orthopyroxene as a function of temperature and pressure for compositions in the system M-A-S and C-M-A-S. The

FIGURE 8.2

Thermodynamic model of the variation of Al_2O_3 solubility in orthopyroxene as a function of temperature and pressure. The model is based on the results of experiments on gel charges.

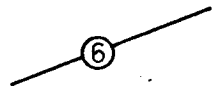

Al_2O_3 solubility (6%) in orthopyroxene crystallized with garnet from M-A-S compositions.

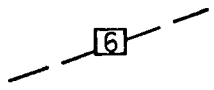

Al_2O_3 solubility (6%) in orthopyroxene crystallized with garnet and clinopyroxene from C-M-A-S compositions.

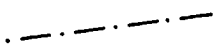

The garnet-peridotite/spinel-peridotite boundary taken from O'Hara *et al.* (1971).

Al_2O_3 content of garnet-saturated orthopyroxene crystallized from M-A-S charges (MacGregor, 1974), and fitted to the thermodynamic model of Wood (1974).

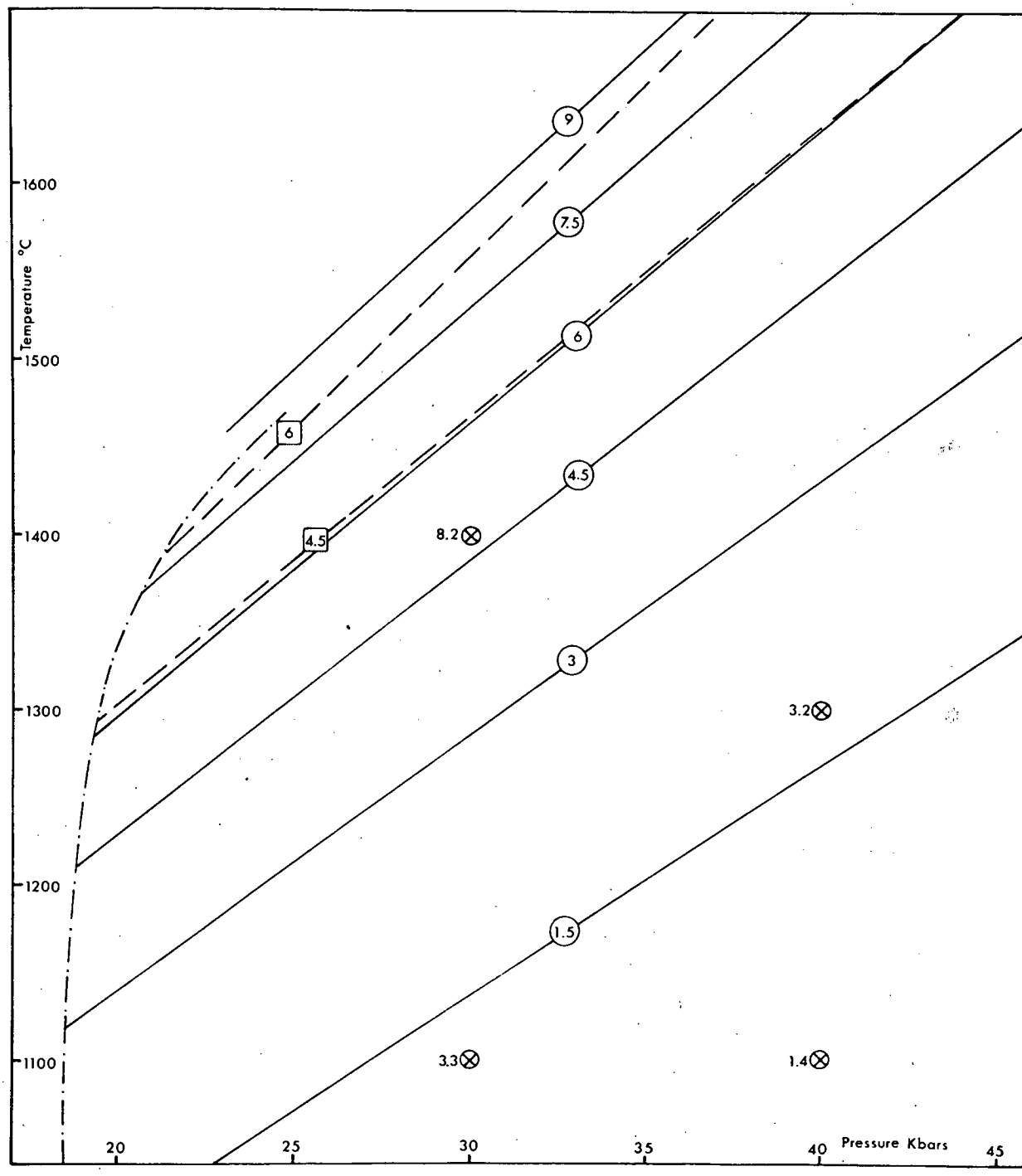
Temperature °C
1600
1500
1400
1300
1200
1100
20
25
30
35
40
45
Pressure Kbars
9
7.5
6
4.5
3
1.5
6
4.5
8.2
3.2
3.3
1.4

model is based on equation 8.1, uses values for ΔH_1^o and ΔS^o derived (see Appendix A.6.2) from the results of experiments on gel charges (see Chapter 7) and makes the same assumptions in the use of equation 8.1 as made by Wood and Banno (1973) and Wood (1974). The values derived for ΔH_1^o and ΔS_o are -14,777 cal mol^{-1} and -7.5 cal K^{-1} mol^{-1} respectively. Fig. 8.2 can be used to obtain approximate equilibration pressures of the assemblages opx+gt (in the system MS-A) and opx+gt+cpx±ol (in the system C-M-A-S) in the pressure and temperature ranges 27-35 kb, 1450–1650°C. Under these conditions the actual pressure of equilibration will not be more than 2.5 kb in excess of the indicated equilibration pressure (see Appendix A.6.2) though it may be many kilobars less than the indicated value if the gels crystallized orthopyroxenes which were considerably oversaturated in Al_2O_3 (but note proviso in Appendix A.6.2).

Isopleths lying outside this pressure/temperature range are shown only to illustrate the size of the discrepancy between this thermodynamic model and that of Wood (1974) at the Al_2O_3 levels found in natural garnet-lherzolites. Such extrapolations to Al_2O_3 isopleths, pressures and temperatures outside the experimental range are worthless, even in the simple MS-A system, because of the assumptions involved. The unlikely assumption is made that ΔV_r does not vary with temperature and pressure. This ensures straight Al_2O_3 isopleths on a pressure/temperature section for orthopyroxenes crystallized in the simple system MS-A because equation 8.1 then becomes an equation of the form:-

$P = mT + c$ (see Appendix A.6.1)

Further currently unjustified assumptions are made when

equation 8.1 is applied to more complicated systems. These are that:-

(i) values of ΔV, ΔH and ΔS derived for the pure MS-A or C-M-A-S systems can be used in equation 8.1 to describe Al_2O_3 solution in much more chemically complicated and possibly structurally different orthopyroxenes.

(ii) Ca^{2+} ions are confined to the M2 site in the orthopyroxene structure. This is a reasonable approximation and probably does not lead to excessive errors.

(iii) in the orthopyroxene crystals "Mg, Fe and Ca are randomly mixed on M2 and Mg, Fe and Al on the M1 position" (Wood and Banno, 1973, p.111). An additional factor was incorporated into equation 8.1 by Wood (1974) to correct for the alleged non-ideal Fe-Al interaction. This was derived empirically by fitting the equation to the experimental data of Wood (1974) and Green and Ringwood (1970) and is therefore queried since both sets of experimental results may be metastable (see sections 8.2 and 8.3.2). The good agreement between Wood's corrected model and the results of Hensen (1973) remarked on by Wood (1974, note in press) would be expected from the close similarity between the results of Hensen and of Green and Ringwood (see fig. 8.1). Hensen, Schmid and Wood (1975) have shown that grossular/pyrope solid solutions are not ideal. Factors allowing for these and other non-ideal garnet and orthopyroxene solid solutions must be incorporated into equation 8.1.

Until more information on the variables in equation 8.1 is available, models based on this equation should only be used in the temperature and pressure range and for similar bulk compositions

as those of the experiments from which ΔH and ΔS values were obtained.

CHAPTER 9

PYROXENE GEOBAROMETRY AND GEOTHERMOMETRY: CONCLUSIONS

9.1 The clinopyroxene geothermometer: conclusions

No evidence was found for an inflection in the cpx(opx) solvus or for a field of two clinopyroxenes at temperatures above 1450°C in the system C-M-S at either 20 kb or 30 kb as required by the results of Kushiro (1969a,b) and Davis and Boyd (1966). The new determinations of the cpx(opx) solvi in the system C-M-S at 20 and 30 kb suggest that enstatite solid solution in simple C-M-S clinopyroxenes at high temperatures is less extensive than previously accepted and is greatly reduced by pressure increase between 20 and 30 kb. The position of the cpx(opx) solvus is, moreover, dependent on SiO_2 activity in the assemblage.

The discrepancy between these new results at 30 kb and those of Davis and Boyd (1966) at the same pressure is a function of the different starting materials used. The two most plausible explanations for this discrepancy are:-

(i) the metastable persistence, within the cpx+opx phase field, of the clinopyroxenes crystallized initially from the glass charges used by Davis and Boyd. This is not a viable explanation if Davis and Boyd's claimed reversal can be justified, i.e. if it can be shown that the two pyroxenes (di_{ss}+en_{ss}) occurring in cryptoperthitic intergrowth in the starting material used for the reversal had not in fact formed a single clinopyroxene phase during the run-up to the

pressure/temperature conditions of the experiment. If the discrepancy between the present work and that of Davis and Boyd is indeed due to the metastable persistence of clinopyroxene crystallized from glass, then the results from gel charges are a closer approach to equilibrium than those of Davis and Boyd. This explanation for the discrepancy may be connected with:-

(ii) the adjustment of clinopyroxene solid solutions to second order structural differences within the crystals produced from different starting materials. These structures would have been different in the clinopyroxenes crystallized from the glasses used by Davis and Boyd from those in the clinopyroxenes crystallized in this study from gel charges. This possibility must be investigated by detailed structural analysis of the clinopyroxenes crystallized at high pressure from both types of starting material.

Determination of the relative stability of these two 30 kb cpx(opx) solvi awaits the further information outlined in (i) and (ii) above, and also a comparison between the structural states of these synthetic clinopyroxenes with those of the natural clinopyroxenes with which they are compared.

Certain evidence, however, suggests that the cpx(opx) solvus determined from experiments on gel charges is a closer approach to equilibrium than that determined by Davis and Boyd (1966). This evidence is:-

(i) The uninflected form of the cpx(opx) solvus determined from gel charges was reproduced in experiments on a natural pyroxene pair (see Chapter 5).

(ii) The uninflected form of the cpx(opx) solvus determined

from gel charges has been reproduced at 30 kb by Nehru and Wyllie (1974) and by Mori and Green (1975a). A large range of starting materials were used in these three studies. Moreover, Mori and Green concluded that a single phase assemblage of clinopyroxene, crystallized from one of their glass charges and which reproduced the results of Davis and Boyd (1966), was metastable relative to the cpx+opx assemblage.

(iii) Davis and Boyd (1966) admitted that the inflection in their cpx(opx) solvus was enigmatic.

(iv) At any one temperature, the smaller extent of solid solution towards enstatite of the clinopyroxenes crystallized from gel charges presumably reflects a more ordered pyroxene structure than that of the more magnesian clinopyroxenes crystallized from glass. With increasing time at high pressures and temperatures more ordered clinopyroxene structures might be expected to develop. Naturally crystallized pyroxenes are thus more likely to have more ordered structures than those crystallized under laboratory conditions. The less magnesian clinopyroxenes crystallized from the gel charges are therefore probably a closer approach to those in the stable equilibrium assemblages than are the clinopyroxenes crystallized from glass charges.

The cpx(opx) solvus determined at 30 kb from gel charges may not, however, be the most stable solvus at this pressure. Evidence was given in sections 3.3 and 4.4.4 that clinopyroxenes crystallized from gels in both the C-M-S and C-M-A-S systems do not have a unique structure, though these structural differences may be a quenching phenomenon.

The most likely explanation of the two clinopyroxene phase field reported by Kushiro (1969a,b) on the CMS_2-M_2S_2 join at 20 kb is that it represents a quenching phenomenon, the two clinopyroxenes being the breakdown product of a single clinopyroxene stable at high temperature. In that case, the phase relations determined by Kushiro at 20 kb are similar to those obtained by Davis and Boyd (1966) on the same join at 30 kb. Kushiro used similar starting materials for his experiments to those used by Davis and Boyd. The explanation for the discrepancy between Kushiro's results and those reported here from experiments on gel charges is probably the same as the explanation for the discrepancy between the new results and those of Davis and Boyd at 30 kb which is discussed above. It may be noted that although Kushiro used mechanical mixtures of clinoenstatite and diopside as starting material for certain experiments, these were not used for experiments run within the field of clinopyroxene plus orthopyroxene as determined from experiments on gel charges.

In agreement with results from C-M-S charges, no evidence was found for a field of two clinopyroxenes or for an inflection in the cpx(opx) solvus at temperatures above 1300°C at 30 kb in a natural system.

No evidence was found in the system C-M-A-S at 30 kb at temperatures above 1450°C either for a two-clinopyroxene-bearing phase field or for the reaction reported by O'Hara (1975) between a garnet-lherzolite containing an aluminous calcic clinopyroxene and one containing a less aluminous sub-calcic clinopyroxene. The evidence

cited by O'Hara for this reaction is not conclusive. There is, however, a reaction involving Al_2O_3 solubility in forsterite in a similar pressure and temperature range.

Non-stoichiometric pyroxenes crystallized in both the C-M-S and C-M-A-S systems at high pressures and temperatures.

C-M-A-S gel starting materials have difficulty in crystallizing stable equilibrium phase assemblages within normal run durations even at high temperatures. Experiments on a large number of closely spaced compositions illustrated the dangers in the use of a limited number of starting bulk compositions.

The Ca/(Ca+Mg) ratio of enstatite-saturated clinopyroxene is a potentially useful geothermometer at high temperatures ($>1300^{o}C$) where it is very temperature sensitive. The position of the cpx(opx) solvus at high temperatures is, however, very dependent on pressure and on clinopyroxene solid solution towards other components, including M_2S, none of which have been thoroughly investigated.

9.2 The orthopyroxene geobarometer: conclusions

The Al_2O_3 contents of orthopyroxenes crystallized in the assemblages opx+gt and opx+cpx+gt$\pm$ol from M-A-S and C-M-A-S bulk compositions using gels as starting materials are lower than those obtained from experiments on glass charges and crystalline phases made from glass charges. The discrepancy is a function of the difference in the crystal structures, at the second order level, of the orthopyroxenes crystallized from the different types of starting material. Although the more stable assemblages cannot yet be identified for

certain, two lines of evidence suggest that the assemblages crystallized in this study from the gel charges are a closer approach to equilibrium than those crystallized from glass charges. The evidence is as follows:-

(i) The lower Al_2O_3 solubilities in the orthopyroxenes crystallized from gel charges closely correspond to the preferred results from experiments in natural systems (Akella and Boyd, 1974; this work, section 8.3.1) though to some extent this close agreement must be fortuitous.

(ii) With increased run duration the gel charges crystallized more garnet, the orthopyroxene crystals becoming simultaneously less aluminous and increasingly discrepant in composition from those crystallized from glass charges in previous studies.

Al_2O_3 solubilities determined using gel charges may themselves be overestimates because of the problem of sluggish garnet crystallization in the geologically short run durations. This sluggish garnet crystallization may be related to changes, with increased run duration, of the detailed crystal structures of the coexisting phases.

The results from gel charges have been used to derive a new thermodynamic model of Al_2O_3 solubility in orthopyroxene. Until more information on thermodynamic quantities and ordering within the crystals is available, the use of such models should be limited to interpolation between existing, experimentally determined data points.

The use of the Al_2O_3 content of orthopyroxene as a geobarometer for garnet-lherzolites depends on the extent to which this parameter

is sensitive to changes of pressure at low Al_2O_3 contents and in natural systems. This has not yet been determined. The present work has shown that current estimates of equilibration pressures based on results of experiments on glass charges, viz. from the pressure/temperature grids and correction factors of MacGregor (1974), Wood and Banno (1973) and Wood (1974), are probably too high.

9.3 Application of experimental determinations of pyroxene solid solutions to estimate equilibration conditions of garnet-lherzolite nodules from kimberlite

Temperatures and pressures of equilibration have been assigned to garnet-lherzolite nodules in kimberlite (e.g. Boyd, 1973) using experimental determinations of pyroxene solid solutions investigated by Davis and Boyd (1966) and MacGregor (1974). A plot of the equilibration pressures and temperatures of such nodules in a single kimberlite pipe defines a mantle geotherm at the time of the kimberlite intrusion. Certain geotherms deduced in this way from garnet-lherzolite nodules in African kimberlite pipes (e.g. Boyd, 1973, 1974) are kinked and indicate an apparent temperature and pressure gap from which no nodules were sampled. The possibility that this temperature/pressure gap reflects an inflection or an abrupt change in the clinopyroxene(orthopyroxene) solvus at high pressure was investigated in the present work. Previous evidence for such an inflection or abrupt change (Davis and Boyd, 1966; Kushiro, 1969a,b; O'Hara, 1975) has not been verified. The present study failed to determine the presence of either a break of slope in the cpx(opx)

solvus, or a large two-clinopyroxene phase field reflecting a miscibility gap or structural break in high pressure clinopyroxenes. An inflection in the cpx(opx) solvus may, however, be present in a compositional range or at temperatures and pressures not investigated in this study.

The two limbs of the kinked Lesotho geotherm (Boyd, 1973) are defined by two compositionally distinct groups of clinopyroxenes, one of which is much more magnesian (in terms of Mg/(Ca+Mg) values) than the other. The two groups of clinopyroxenes are separated by a compositional gap from 0.45 to 0.385 in their Ca/(Ca+Mg) ratios [see fig. 5.1]. The clinopyroxenes crystallized in the present work, both in the synthetic and natural systems, all have Ca/(Ca+Mg) ratios less than 0.38. It is possible that an inflection in the cpx(opx) solvus occurs at both 20 and 30 kb at temperatures lower than those investigated here. No such field has, however, been reported in other recent studies. Where a bimodal distribution of clinopyroxene compositions, in terms of Ca/(Ca+Mg) ratio, occurs in garnet-lherzolite nodules from kimberlite pipes in areas other than northern Lesotho (e.g. Johnston, 1973; Boyd, 1974), the compositional gap covers a similar range of Ca/(Ca+Mg) values as observed in the clinopyroxenes from the Lesotho nodules.

O'Hara (1975) suggested that if an abrupt change in the cpx(opx) solvus does occur, this may explain the unexpected kink in the deduced African geotherms. However, incorrect assignment of pressure and temperature conditions of equilibration to garnet-lherzolite nodules could result in a kinked geotherm without the need to invoke the existence of an inflection or break in the

cpx(opx) solvus. This is demonstrated in Appendix A.7. Sources of error in both the determination of pressure, using MacGregor's (1974) data, and temperature, using the Davis and Boyd (1966) cpx(opx) solvus have emerged from the present study.

The Ca/(Ca+Mg) values of the clinopyroxenes from Lesotho garnet-lherzolite nodules (Nixon and Boyd, 1973a, table 20A) are plotted in fig. 5.1 on the Davis and Boyd (1966) cpx(opx) solvus which was used to determine the equilibration temperatures of the nodules. Alternative positions for this solvus as determined using different starting materials, at different pressures and for different bulk compositions are also shown in fig. 5.1 from which the size of possible temperature errors can be estimated. Although the range of reported Ca/(Ca+Mg) ratios at any one temperature is greater at higher temperatures, temperature errors may be as large at lower temperatures where the solubility of enstatite in clinopyroxene is less sensitive to temperature. There is too much uncertainty as to the position of the cpx(opx) solvus in the simple C-M-S system at 30 kb, let alone the effect of pressure and clinopyroxene solid solution towards components other than MS, to justify the present extensive use of the cpx(opx) solvus as a precise geothermometer for garnet-lherzolites.

New determinations of the solubility of Al_2O_3 in orthopyroxene (see Chapter 7) are lower than those of MacGregor (1974) and suggest that pressure estimates using his solubility determinations will be too high. However, if the isopleths of Al_2O_3 solubility in orthopyroxene are curved on a pressure/temperature section, then pressure estimates using straight-line extrapolations of the new determinations

of solubility are not justified. More data points are needed at low temperatures and for low Al_2O_3 contents.

The Al_2O_3 contents of orthopyroxenes crystallized from C-M-A-S gels (this work, Chapter 7) and from seeded glasses with compositions in the system M-A-S (MacGregor, 1974) are plotted against temperature at various pressures in fig. 9.1. The Al_2O_3 contents of orthopyroxenes from the Lesotho garnet-lherzolite nodules (Nixon and Boyd, 1973a, table 20A) are also plotted in fig. 9.1 against their temperatures of equilibration deduced from the Davis and Boyd (1966) cpx(opx) solvus (see fig. 5.1). Currently available estimates of Al_2O_3 solubility in orthopyroxene are clearly too limited to justify any estimates of the absolute equilibration pressures of such nodules. The Al_2O_3 contents of these natural orthopyroxenes are, moreover, so low that compositional differences in the orthopyroxenes, especially with respect to Al^{3+}:R^{3+} and R^{3+}:Na^{+} ratios, might radically affect their apparent relative pressures of equilibration. Their relative pressures would also be in error if the estimates of relative equilibration temperatures were incorrect.

These sources of error in the assignment of equilibration conditions to garnet-lherzolite nodules may explain the derivation of a geologically unexpected geotherm for northern Lesotho in the Cretaceous. They do not, however, explain the bimodal distribution of clinopyroxene compositions.

Assuming the eventual experimental determination of stable pyroxene solid solutions such as would develop after long periods of time in geological situations, the application to garnet-lherzolites of this knowledge of pyroxene solid solutions, with the aim

FIGURE 9.1

The variation of the solubility of Al_2O_3 in garnet-saturated orthopyroxene as a function of temperature at various pressures.

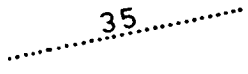

Results obtained from C-M-A-S gel charges (this work, figs. 7.1 and 7.2) at 35 kb; data points indicated by filled triangles.

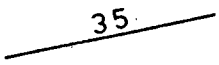

Results obtained by MacGregor (1974) at 35 kb; data points indicated by asterisks.

Open triangles indicate the compositions of orthopyroxenes from garnet-lherzolite nodules plotted at the deduced equilibration temperatures of the nodules (see text).

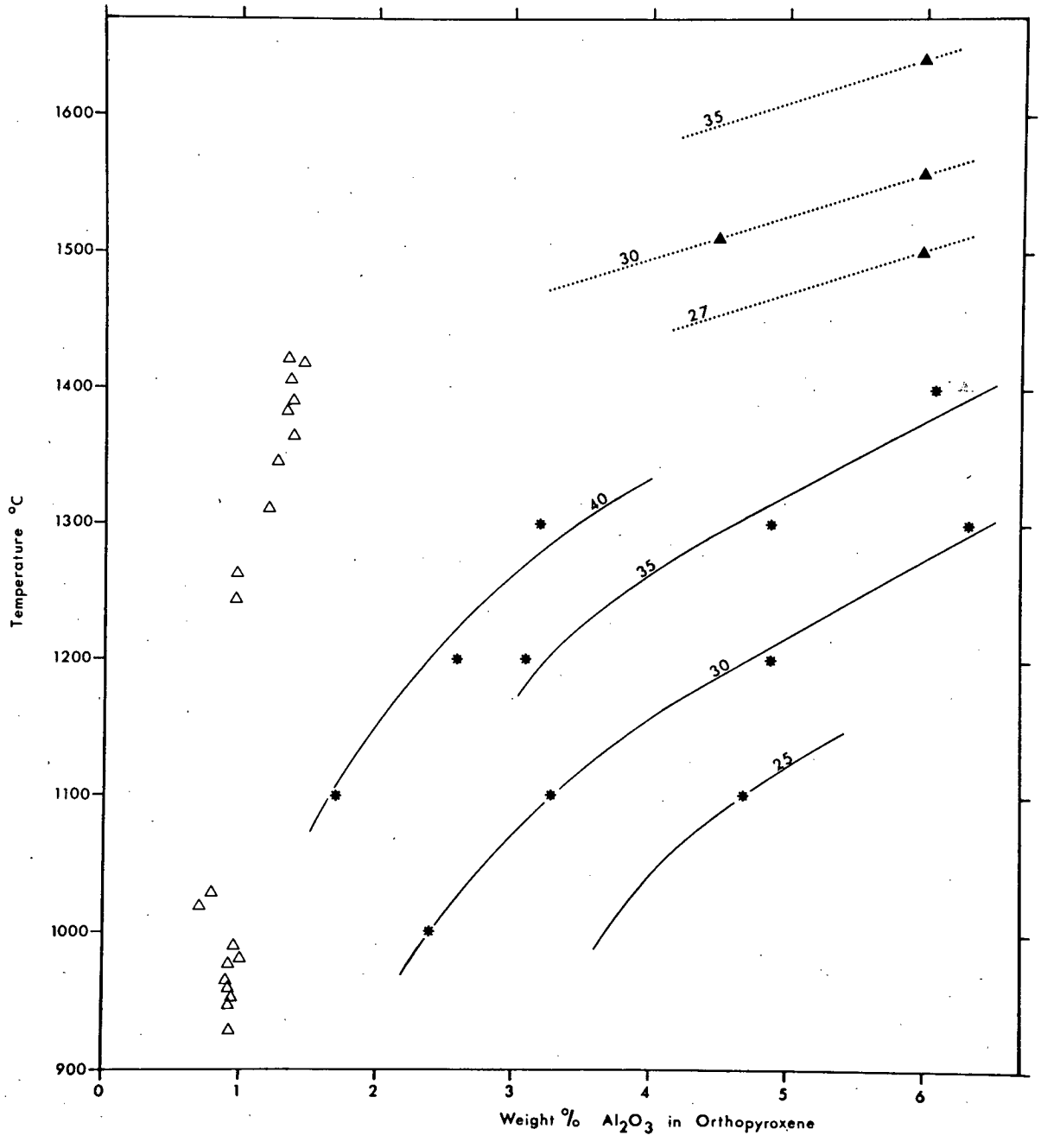
Temperature °C
1600
1500
1400
1300
1200
1100
1000
900
0
1
2
3
4
5
6
Weight % Al_2O_3 in Orthopyroxene
35
30
27
40
35
30
25

of determining pressures and temperatures of equilibration, may not be justified because:-

(i) High pressure experiments are carried out under pressure conditions which are believed to approximate hydrostatic equilibria (e.g. O'Hara, Richardson and Wilson, 1971). A large group of garnet-lherzolites from kimberlite pipes show evidence of shearing stresses (e.g. Boyd, 1973). It is not known to what extent shearing stresses may affect phase equilibria.

(ii) The phases present in a natural garnet-lherzolite may not represent an equilibrated assemblage. The possibility of admixtures of phases from different assemblages under shearing conditions was suggested by Boullier and Nicolas (1973), and evidence for this has recently been found (Gurney, pers. comm.) in natural garnet-lherzolites from South African kimberlite pipes. It is also queried whether garnet-lherzolites which show evidence of only partial textural recrystallization during or after deformation (Boullier and Nicolas, 1973) have necessarily reequilibrated chemically. Boyd (1975) has shown that chemical inhomogeneities do exist between pyroxenes in the groundmass and those occurring as phenocryst phases in some sheared garnet-lherzolites from kimberlite. Minor chemical differences which are, however, outside analytical error, also occur within single phenocrysts.

Finally, it is worth noting that comparisons are often made between experimentally determined pyroxene solid solutions and natural pyroxenes crystallized in a different or unknown phase assemblage. There is no basis for assuming that the pyroxenes will develop similar solid solutions in different assemblages. In particular,

the application of the Davis and Boyd (1966) cpx(opx) solvus, and MacGregor's (1974) aluminous orthopyroxene grid to determine the equilibration conditions of discrete nodules (Nixon and Boyd, 1973b), ilmenite-bearing garnet-lherzolites (Boyd and Nixon, 1973) and chrome-spinel-bearing garnet-lherzolites (MacGregor, 1975) is unjustified.

CHAPTER 10

THE DERIVATION OF NEPHELINE-NORMATIVE MAGMAS AT HIGH PRESSURE

10.1 Review of previous experimental investigations

The occurrence of the high-pressure-phase pyropic garnet in basic and ultrabasic inclusions in certain nephelinitic magmas (e.g. Jackson and Wright, 1970; Best, 1975) suggests a high pressure origin for these magmas. Melting experiments have been designed to determine conditions under which nephelinitic magmas may be generated by the melting and fractionation of mantle materials at high pressure. Much controversy has surrounded the interpretation of the experimental data (see in particular O'Hara, 1968; Kushiro, 1969c; Mysen *et al.*, 1974). Various methods by which nephelinitic magmas may be generated at high pressure (>20 kb) have been suggested on the basis of the experimental data:-

A. Partial melting of a peridotitic mantle.

Experimental data, reviewed by O'Hara (1968), demonstrate that the partial melting product of dry peridotite is nepheline-normative between 10 and 20 kb, but is a hypersthene-normative picrite at higher pressures. Nepheline-normative liquids are only considered to be possible direct partial melting products of dry peridotite at pressures higher than 20 kb in Na_2O-rich (Kushiro, 1968; Bultitude and Green, 1971) or P_2O_5-rich (Kushiro, 1973) compositions. Although Kushiro's (1968, 1974) results in various dry synthetic systems show the progressive expansion of the liquidus field of orthopyroxene at the expense of that of olivine with increasing pressure, liquids

formed by partial melting of dry peridotite at very high pressures are not expected to be nepheline-normative. This is because the liquidus fields of garnet and clinopyroxene expand at the expense of that of orthopyroxene with increasing pressure (O'Hara, 1968).

Experiments in both synthetic (Kushiro, 1972; Modreski and Boettcher, 1973; Eggler, 1975) and natural (e.g. Nicholls and Ringwood, 1973; Boettcher, Mysen and Modreski, 1975) systems have demonstrated the progressive enrichment in SiO_2 of liquids in equilibrium with peridotite as the activity of H_2O in the system increases. The extent of SiO_2 enrichment is, however, under dispute (Mysen et al., 1974). Nepheline-normative magmas may be generated by small degrees of partial melting of hydrous peridotites with low CAS/NAS_4 ratios, but more extensive partial melting would yield hypersthene-normative magmas (Kushiro, 1972).

In a series of publications from Green and co-workers at Canberra (e.g. Bultitude and Green, 1967; Green, 1973), it was demonstrated that orthopyroxene is a liquidus phase for nepheline-normative natural rocks in the presence of small amounts of H_2O but was absent under anhydrous conditions. It was concluded that the primary phase volume of orthopyroxene expands into nepheline-normative compositions in the presence of small quantities of H_2O, and that under these conditions nephelinites could be generated by the partial melting of peridotite. The relation between the low quantities of H_2O used and the degree of H_2O-undersaturation was not stated, making comparisons with other H_2O-bearing systems difficult. The presence of orthopyroxene as a liquidus phase in H_2O-bearing systems but its absence under anhydrous conditions does not

necessarily reflect the expansion of the liquidus field of orthopyroxene into nepheline-normative compositions. This is demonstrated in fig. 10.1 which shows two hypothetical phase diagrams for the melting behaviour of peridotite. In both examples the initial partial melting product of peridotite is less nepheline-normative in the presence of H_2O than under anhydrous conditions. Certain bulk compositions will, however, crystallize orthopyroxene on or near the liquidus under hydrous conditions whereas under anhydrous conditions orthopyroxene will fail to crystallize or will appear at a much greater degree of crystallization. These figures illustrate the dangers of drawing conclusions from experiments on a small number of bulk compositions. The limited experimental results reported by Green and co-workers are not inconsistent with model B in figure 10.1. The evidence adduced for the generation of nephelinites by melting peridotite in the presence of small quantities of H_2O is therefore considered inconclusive.

Recent experiments in natural (Boettcher, Mysen and Modreski, 1975) and synthetic (Eggler, 1974; Wyllie and Huang, 1975) systems have demonstrated that some of the major element features of kimberlites, carbonatites and nephelinites are reproduced by melting products of a CO_2-bearing mantle at high pressure.

The limitations and possible sources of error in the experiments whose results are summarized above are as follows:-

(i) Analysis of liquid compositions. In many of the studies cited above, liquid compositions were obtained by microprobe analysis of quenched glasses, often present in small quantities interstitially and perhaps modified by quench crystallization. The limitations of

FIGURE 10.1

Hypothetical isobaric, isothermal phase relations of the melting of peridotite projected into a simplified chemical system, viz. $(Al_2O_3+CaO+Na_2O)-(MgO+FeO)-SiO_2$. The diagram shows the replacement of a liquidus field of olivine (Model A) or of cpx+gt (Model B) for a nepheline-normative composition (★) under anhydrous conditions with a liquidus or near-liquidus field of orthopyroxene under hydrous conditions. This occurs even though the first liquid (L_H) generated by the partial melting of (amphibole-)garnet-lherzolite under hydrous conditions is less nepheline-normative than that (L) generated under anhydrous conditions. Green and co-workers (e.g. Green, 1973) report orthopyroxene as a liquidus phase of nepheline-normative basic compositions under hydrous but not under anhydrous conditions. However, the number of bulk compositions used are too limited and their reported experimental details insufficient to justify their conclusion that L_H is more nepheline-normative than L. The most complete experimental results are for an olivine-basanite (Green, 1969, 1970) whose crystallization sequence at 27 kb under dry and under hydrous conditions is not inconsistent with that shown in Model B for composition ★. (If the locus of liquid compositions obtained from the anhydrous liquid composition ★ with progressive equilibrium crystallization is as shown by ←← in Model B, then orthopyroxene would not be among the crystallizing phases.)

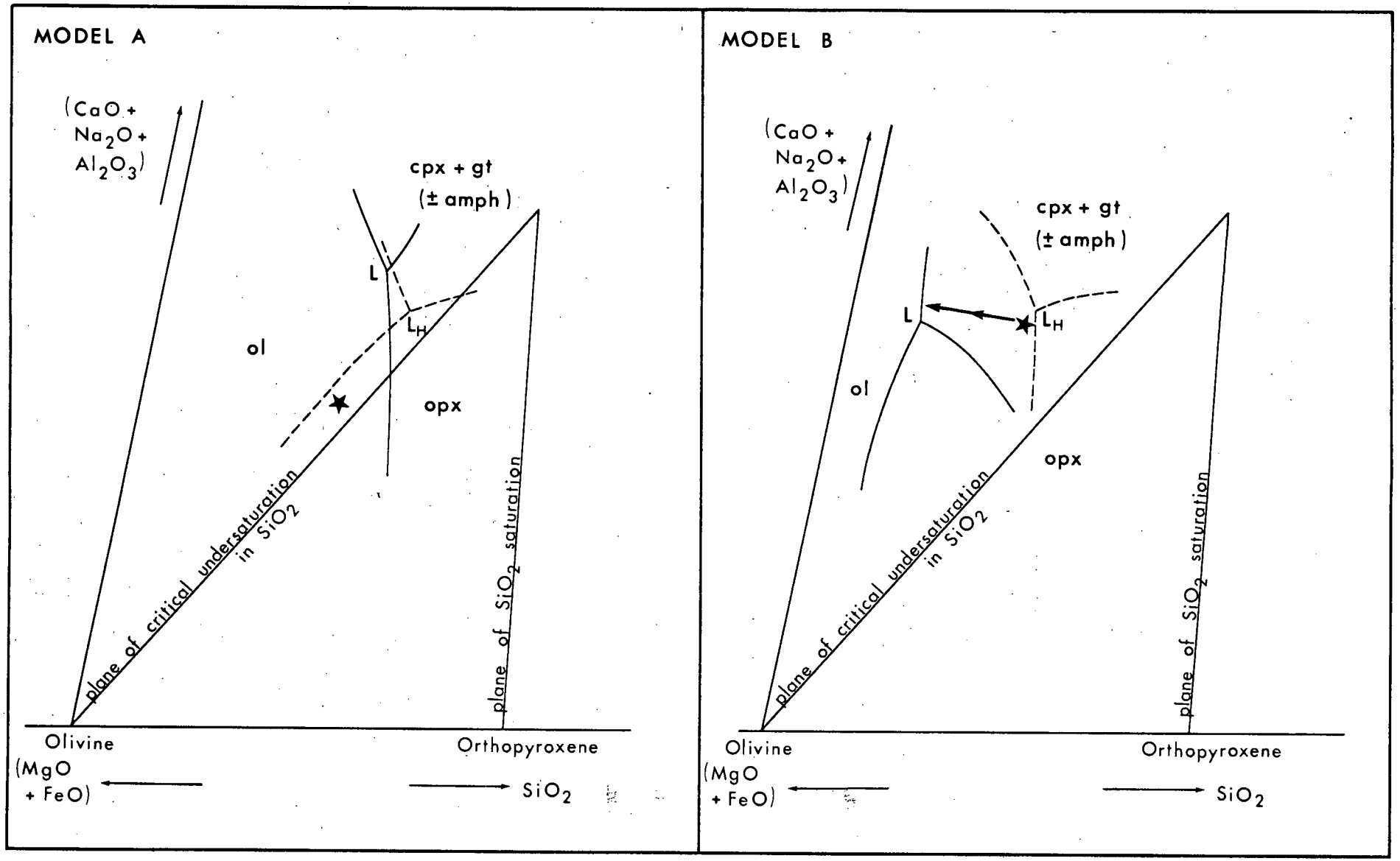
MODEL A
(CaO + Na2O + Al2O3)
cpx + gt
(± amph)
L
LH
ol
opx
plane of critical undersaturation in SiO2
plane of SiO2 saturation
Olivine
(MgO + FeO)
Orthopyroxene
SiO2
MODEL B
(CaO + Na2O + Al2O3)
cpx + gt
(± amph)
L
LH
ol
opx
plane of critical undersaturation in SiO2
plane of SiO2 saturation
Olivine
(MgO + FeO)
Orthopyroxene
SiO2

this method of liquid analysis have been discussed by, for example, Cawthorn et al. (1973) and Wyllie and Nehru (1975).

(ii) Iron loss to sample container material (Wyllie and Nehru, 1975). This is a particularly serious problem in these investigations because it controls the degree of SiO_2-saturation of the bulk composition and also the solidus temperature.

(iii) Choice of starting material. Experimental results, reviewed above, point to the large effect of small quantities of minor oxides, e.g. CO_2, P_2O_5, Na_2O on partial melting liquid compositions. The application to mantle conditions of results from simple synthetic systems has been justifiably criticized. However, the choice of natural compositions to be used in experiments must also be criticized in this context. Conclusions regarding magma genesis based on such experiments frequently reflect preconceived notions as to the genesis of the sample under investigation (see particularly Kushiro, Shimizu, Nakamura and Akimoto (1972) who describe experiments on a spinel-lherzolite which yielded andesitic magmas at 20 kb under hydrous conditions. These experiments are inconclusive as regards the genesis of andesitic magmas if the spinel-lherzolite is a crystal cumulate (O'Hara, 1968) and hence depleted in those very ions, especially Na^+, which greatly affect the degree of undersaturation of partial melts.)

(iv) Choice of equilibria investigated. Most of the studies cited above have not considered the compositions of liquids in equilibrium with more than three phases. Low degrees of partial melting of peridotite containing hydrous minerals, garnet or clinopyroxene may yield liquids of very different compositions from those generated

in the absence of these phases.

The conditions reviewed above under which nepheline-normative liquids are most likely to be generated directly from peridotite at high pressure, viz. low degrees of partial melting of Na_2O and CO_2-rich and H_2O-poor compositions, are considered valid because the effect of these variables has been reproduced in a range of experimental conditions. Detailed knowledge of the melting products of peridotite under different conditions awaits more carefully controlled and systematically designed experiments, necessarily on synthetic systems, such as have been carried out by Kushiro (1968, 1972, 1973, 1974) and Bravo and O'Hara (1975).

Other hypotheses for the derivation of nephelinitic magmas at high pressure are:-

B. Eclogite fractionation of the partial melting product of garnet-lherzolite at high pressure.

If the partial melting product of mantle material lies outside the volume defined by its constituent phases, and on the side of that volume remote from orthopyroxene, then orthopyroxene will not precipitate from such a liquid on fractional crystallization since it is in reaction relation with that liquid. Fractional crystallization of this liquid may yield residual liquids which are critically undersaturated with respect to SiO_2. This would occur even if the partial melting product of the mantle material was hypersthene-normative.

O'Hara and Yoder (1967) report a reaction relation of this type in the system CS-MS-A at 30 kb. Liquidus orthopyroxene is in reaction relation with the hypersthene-normative liquid generated by

the partial melting of dry cpx+opx+gt assemblages. A similar reaction occurred in natural and synthetic ol+cpx+opx+gt assemblages and has been observed in other high pressure experimental studies (reviewed by O'Hara, 1968, p.77).

O'Hara and Yoder (1967) also showed that in C-M-A-S and natural systems, cpx+gt+opx assemblages and adjacent (i.e. Mg-rich) cpx+gt assemblages form a thermal divide at 30 kb, i.e. neither olivine nor quartz occur in the melting interval of any such assemblage. Fractionation of the partial melting product of dry garnet-lherzolite at 30 kb cannot therefore yield residual liquids which lie to the SiO_2-rich side of the plane clinopyroxene-orthopyroxene-garnet. From the frequent occurrence of olivine-free, cpx+gt (i.e. eclogite) assemblages in kimberlite, O'Hara and Yoder (1967) predicted that olivine, in addition to orthopyroxene was in reaction with the liquid formed by melting of garnet-lherzolite at high pressure; garnet and clinopyroxene alone would fractionate from such liquids yielding residual liquids which could only become poorer in SiO_2 with respect to $CaO+Al_2O_3+MgO+FeO+$alkalis and might eventually become critically undersaturated in SiO_2.

Results in the $CaO-MgO-Al_2O_3-SiO_2$ system at other pressures suggest that nephelinites could be derived by such a process at 40 kb (Davis, 1964) but not at 17-26 kb (Kushiro and Yoder, 1974). In the 17-26 kb pressure range olivine is a liquidus phase for compositions in the clinopyroxene-orthopyroxene-garnet plane.

C. Partial melting of an eclogite mantle.

From electron microprobe analyses of the glasses quenched in melting experiments on a natural eclogite, Ito and Kennedy (1974)

concluded that nepheline-normative magmas could be generated at high pressure by low degrees of partial melting of a dry eclogite mantle.

10.2 Aim of experimental work

The purpose of the experiments reported here was to extend the known range of conditions under which nepheline-normative liquids may be derived by high pressure melting and fractionation of basic and ultrabasic compositions.

The main part of this study (section 10.3) considers compositions in the synthetic systems C-M-A-S-N and C-M-A-S-N-H. The compositions of the liquids in the equilibria liquid+cpx+opx+gt±ol were determined at 25 kb. The experiments were designed to:-

(i) test O'Hara and Yoder's (1967) model (discussed in section 10.1) at lower pressures in Na_2O-bearing systems.

(ii) extend Kushiro's (1972) experiments in the system C-M-A-S-N-H and its sub-systems. Most of these were designed to show the changes in position of the olivine/orthopyroxene liquidi boundary for different bulk compositions and at different P_{H_2O}. Kushiro reported little data on the compositions of liquids formed by small degrees of partial melting of garnet-lherzolite.

The new experiments avoid the causes of criticism of much previous work by using iron-free compositions and by determining liquid compositions without the use of electron microprobe analysis. Liquid compositions were determined instead through a knowledge of the bulk compositions and the compositions of the crystallizing phases.

The results of experiments run under anhydrous and hydrous conditions are given in Appendix tables A.9.9 and A.9.10 respectively. The compositions and nature of the charges used are presented in Appendix table A.2.5.

The results of melting experiments on two natural eclogites are presented in section 10.4. These were designed to test whether O'Hara and Yoder's (1967) results for synthetic cpx+gt assemblages could be reproduced in more complicated systems and at different pressures.

10.3 The generation of nepheline-normative liquids in the systems C-M-A-S-N and C-M-A-S-N-H at 25 kb

10.3.1 Introduction

The existence of nepheline-normative liquids in these systems was demonstrated by the observation of orthopyroxene as the only liquidus phase for bulk compositions which lie on the critical plane of SiO_2 undersaturation, or which contained normative nepheline. Since orthopyroxene is extremely rich in normative hypersthene, the liquid generated in equilibrium with orthopyroxene alone from these bulk compositions must be nepheline-normative.

Excluding the presence of H_2O in the hydrous experiments, three bulk compositions were used in this study:-

Z: $(CMS_2)_4(M_3AS_3)_3(NAS_4)_{1.5}$ expressed in molecular proportions. This composition lies on the critical plane of SiO_2 undersaturation.

Z10: composition Z less 10 wt.% MS. This composition contains 4.5% normative nepheline.

Z20: composition Z less 20 wt.% MS. This composition contains 8.1% normative nepheline.

These three compositions are expressed in terms of their constituent oxides and their C.I.P.W. normative minerals in Appendix table A.2.5. In the hydrous experiments capsules were loaded with the anhydrous powder and drops of liquid H_2O.

Homogeneous gels were used as starting materials. In addition, experiments on the homogeneous gel Z (charge Z-HG) were repeated using as starting materials unrecrystallized glass (Z-GL) and a gel mixture (Z-MG) both of which have the same bulk composition as charge Z-HG. Charge Z-MG is a mechanical mixture of homogeneous diopside (CMS_2), pyrope (M_3AS_3) and jadeite (NAS_4) gels. All gel starting materials used in this study had been partially crystallized at 900°C, atmospheric pressure.

10.3.2 Melting experiments on compositions in the system C-M-A-S-N

These experiments showed that the range of liquids generated by melting cpx+opx+gt assemblages in the system C-M-A-S-N at 25 kb include nepheline-normative liquids.

This conclusion is based on the melting behaviour of the gel Z10 illustrated in fig. 10.2. Orthopyroxene is the sole liquidus phase at temperatures between 1524°C and the liquidus at 1532°C. The coexisting liquids in this temperature range must be more nepheline-normative than the bulk composition Z10 i.e. they must contain more than 4.5% normative nepheline. At 1520°C clinopyroxene

FIGURE 10.2

Melting behaviour at 25 kb of three compositions in the system C-M-A-S-N. The right hand side of this figure forms a pseudo-binary section for compositions on the continuation of the join passing through MS (enstatite) and $(CMS_2)_4(M_3AS_3)_3(NAS_4)_{1.5}$ (composition Z). Phase relations for this section were determined using gel as starting material. The melting behaviour of gel composition Z may be compared with that of the same composition but using glass or a gel mixture as starting material, as shown in the first two columns of fig. 10.2.

Explanation of symbols:-

- O liquid
- ▶ orthopyroxene
- ◀ clinopyroxene
- ✱ garnet
- ◊ pyroxene (composition undetermined)

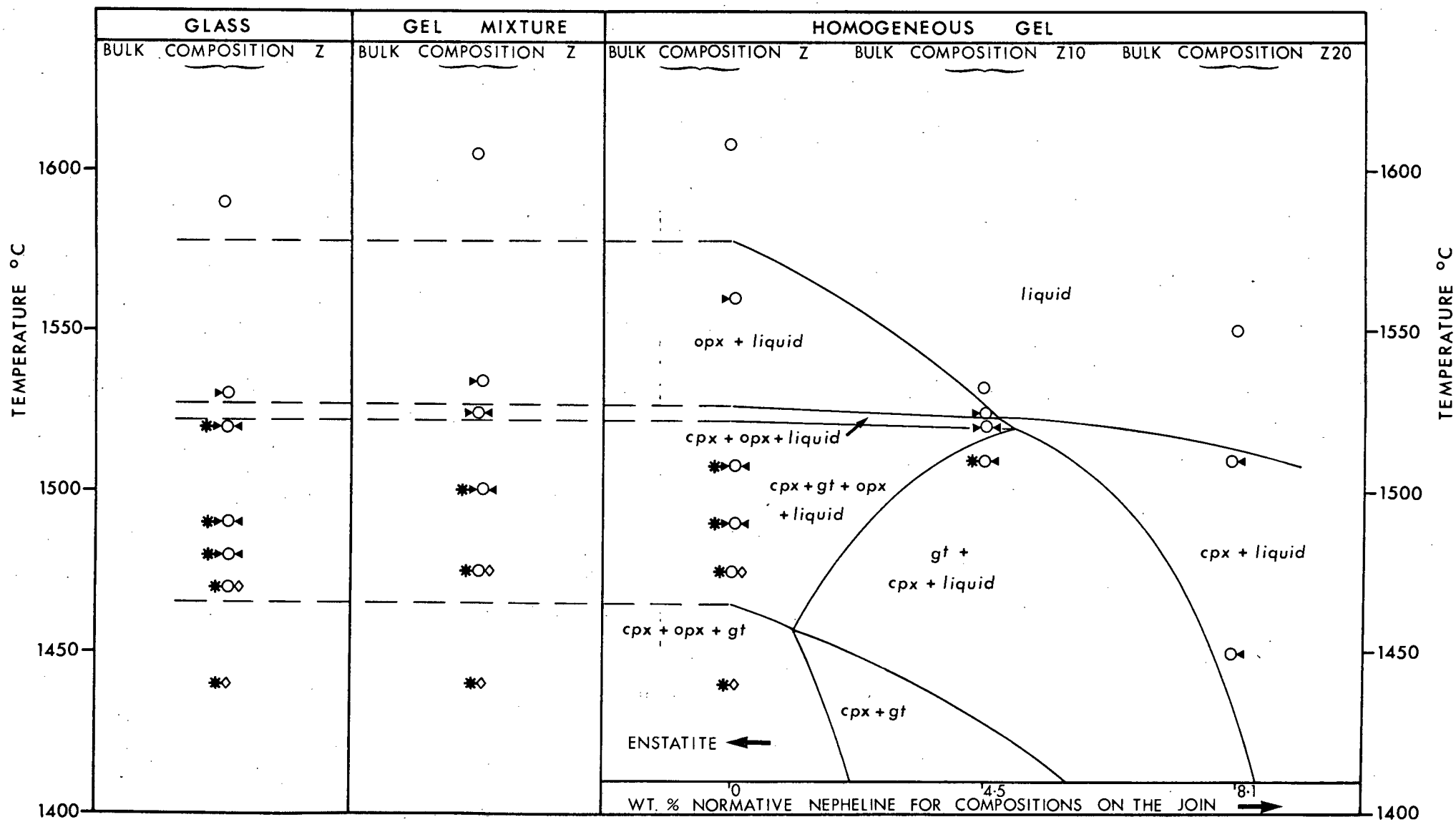
GLASS
GEL MIXTURE
HOMOGENEOUS GEL
BULK COMPOSITION Z
BULK COMPOSITION Z
BULK COMPOSITION Z
BULK COMPOSITION Z10
BULK COMPOSITION Z20
TEMPERATURE °C
1600
1550
1500
1450
1400
liquid
opx + liquid
cpx + opx + liquid
cpx + gt + opx + liquid
gt + cpx + liquid
cpx + liquid
cpx + opx + gt
cpx + gt
ENSTATITE
0
4·5
8·1
WT. % NORMATIVE NEPHELINE FOR COMPOSITIONS ON THE JOIN

and orthopyroxene coexist with liquid. At lower temperatures orthopyroxene is in reaction relation with the liquid and has completely reacted out by 1510°C at which temperature the phase assemblage is cpx+gt+liquid. The presence of a phase field of cpx+opx+gt+liquid was not determined for this composition, i.e. it is not known whether orthopyroxene was totally resorbed in a reaction opx+liquid ⟶ cpx+liquid before the incoming of garnet at slightly lower temperatures. A phase field of cpx+opx+gt+liquid must, however, be encountered in closely comparable compositions in the temperature range 1510-1520°C because of the narrow temperature gap between the phase fields cpx+opx+liquid and cpx+gt+liquid for composition Z10. Moreover, owing to the close proximity of the equilibria encountered by composition Z10 in the temperature range 1510-1524°C to adjacent cpx+opx+gt+liquid assemblages, liquids in the latter assemblages are likely to have compositions similar to those of the liquids formed from the bulk composition Z10 in this temperature range. These liquids are nepheline-normative at temperatures at least as low as 1524°C. Orthopyroxene is predicted to be in reaction relation with these nepheline-normative liquids in such cpx+opx+gt+liquid assemblages.

In the system C-M-A-S-N the equilibrium assemblage cpx+opx+gt+liquid is isobaric divariant. Liquids in this equilibrium at 25 kb will show a range of compositions. The experiments reported here demonstrate that some of these liquids are nepheline-normative.

The melting behaviour of composition Z10 is consistent with the results of experiments on the other two homogeneous gels Z20 and

Z-HG. Experimental results for all three homogeneous gels are illustrated on the right hand side of fig. 10.2 and interpreted there as a temperature/phase relations section for compositions on the join passing through MS (enstatite) and $(CMS_2)_4(M_3AS_3)_3(NAS_4)_{1.5}$ (composition Z) at 25 kb.

A reaction involving consumption of orthopyroxene in the melting history of Z-HG could not be proved. Orthopyroxene coexists with clinopyroxene, garnet and liquid from temperatures of at least 1508°C to 1490°C. At lower temperatures the two pyroxenes could not be distinguished optically, and orthopyroxene was not identified on the x-ray diffraction trace of run products because of the proximity of orthopyroxene and jadeitic clinopyroxene reflections.

The coexistence of clinopyroxene, orthopyroxene, garnet and liquid over a wide temperature range during the melting interval of Z-HG is consistent with the isobaric divariant nature of this assemblage. Orthopyroxene may or may not have been in reaction with liquid in this assemblage over the whole temperature range in which the four phases coexisted.

The melting behaviour of the homogeneous gel Z-HG was reproduced using other types of starting material (see fig. 10.2). The melting relations reported here are not a function of the starting material used as was observed for the sub-solidus behaviour of Na_2O-free compositions (see Chapters 3, 4 and 7).

A very rapid increase of the crystal:liquid ratio when the liquid composition reaches equilibria involving clinopyroxene on reducing the temperature was observed in the melting behaviour of all types of starting material and all bulk compositions.

Neither olivine nor quartz were observed in the melting interval of any of the compositions used in this study. This suggests that magnesium-rich clinopyroxene plus garnet assemblages and the plane clinopyroxene - garnet - orthopyroxene in the system C-M-A-S-N are a thermal divide at 25 kb preventing the generation of quartz-normative liquids by the partial melting of garnet-lherzolite at this pressure. However, the melting data are insufficient to completely rule out this possibility.

10.3.3 Comparison with previous results in C-M-A-S and C-M-A-S-N systems

The reaction between orthopyroxene and nepheline-normative liquids generated by the partial melting of cpx+opx+gt assemblages described above (10.3.2) is similar to that reported in the system C-M-A-S at 30 kb by O'Hara and Yoder (1967) and at 40 kb by Davis (1964). However, in these previous studies on Na_2O-free compositions the liquid coexisting with clinopyroxene, orthopyroxene and garnet and in reaction relation with the orthopyroxene was shown to be hypersthene-normative. Kushiro (1968) reported a reaction relation between orthopyroxene and a nepheline-normative liquid for compositions in the system M-A-N-S at 30 kb. The results of the present experiments on Na_2O-bearing compositions are consistent with these experiments of Kushiro, of O'Hara and Yoder and of Davis which suggest that the degree of SiO_2-undersaturation of the liquid in reaction relationship with orthopyroxene at high pressure is dependent on the NAS_4/CAS ratio of the bulk composition.

Magnesium-rich eclogites and orthopyroxene-- clinopyroxene -

garnet assemblages in the system C-M-A-S constitute a thermal divide at 30 kb (O'Hara and Yoder, 1967) and at 40 kb (Davis, 1964) but not between about 17 and at least 25 kb (Kushiro, 1968). These assemblages are believed to represent a thermal divide in the C-M-A-S-N system studied here at 25 kb. Gt+cpx±opx assemblages apparently constitute a thermal divide at lower pressures in the presence of Na_2O than in the Na_2O-free C-M-A-S system.

Comparison of these new results with previous experiments on compositions in the system CS-MS-A (O'Hara and Yoder, 1967; Davis, 1964; Kushiro, 1968) also shows that nepheline-normative liquids can be generated by melting of Na_2O-bearing cpx+opx+gt assemblages at pressures at which such assemblages in the C-M-A-S system yield hypersthene-normative liquids. The liquid in equilibrium with clinopyroxene, orthopyroxene and garnet in the system C-M-A-S was reported (O'Hara and Yoder, 1967; Davis, 1964) to have a unique composition at any one pressure because the assemblage cpx+opx+gt+liquid was believed to be isobaric invariant with all compositions lying in the plane CS-MS-A. This conclusion may need revision in view of the recently reported (see Chapters 3 and 4) non-stoichiometry of sub-solidus C-M-A-S pyroxenes at high pressure.

The nepheline-normative liquids generated by the initial melting of certain cpx+opx+gt assemblages in the system C-M-A-S-N at 25 kb are predicted to be in reaction relation with orthopyroxene which cannot therefore precipitate from these liquids on fractional crystallization. Only clinopyroxene and/or garnet can fractionate from such liquids since neither olivine nor quartz is believed to be a liquidus phase for these compositions. Compositions of residual liquids of isobaric fractional

crystallization must evolve away from that of the partial melting product. The direction of this change is unknown but, unless there are major effects caused by the crystallization of non-stoichiometric phases, residual liquids will develop progressively lower SiO_2:($CaO+Al_2O_3+Na_2O+MgO$) ratios as fractional crystallization proceeds.

The new results extend those of Kushiro (1968) who showed that the olivine/orthopyroxene phase field boundary lay in hypersthene-normative compositions at both 20 and 30 kb for bulk compositions in the system C-M-A-S, but that its low temperature portion lay in nepheline-normative compositions in the system M-A-S-N at 20 kb, and by extrapolation also at 30 kb.

The present results confirm the wider range of conditions under which nepheline-normative liquids may be generated at high pressure in Na_2O-bearing systems than in Na_2O-free systems as predicted by Kushiro (1968).

10.3.4 Melting experiments on compositions in the system C-M-A-S-N-H

An interpretation of the results of melting experiments on the homogeneous gel Z-HG in the presence of various H_2O contents at 25 kb is given in fig. 10.3. The results show the replacement of orthopyroxene with olivine as the first crystalline phase to appear below the liquidus at water contents greater than about 8%. This effect confirms the results of Kushiro (1972) who demonstrated the expansion of the liquidus field of olivine at the expense of that of orthopyroxene at high P_{H_2O} as opposed to under anhydrous conditions in the systems C-M-S-(H), C-M-A-S-(H) and M-A-S-N-(H) at

FIGURE 10.3

The melting behaviour of gel charge Z-HG (composition $(CMS_2)_4(M_3AS_3)_3(NAS_4)_{1.5}$) at 25 kb in the presence of H_2O.

Phase fields which include vapour have been deduced from the form of the phase diagram; available data points are, however, too limited to determine the precise location of the "vapour-out" boundary.

Symbols underlined represent the run products of experiments using furnace assemblages A or B2; all other experiments were carried out using furnace assemblage B1.

A down-pointing arrow to the right of a run product symbol indicates that crystal settling was observed for all the primary crystalline phases reported.

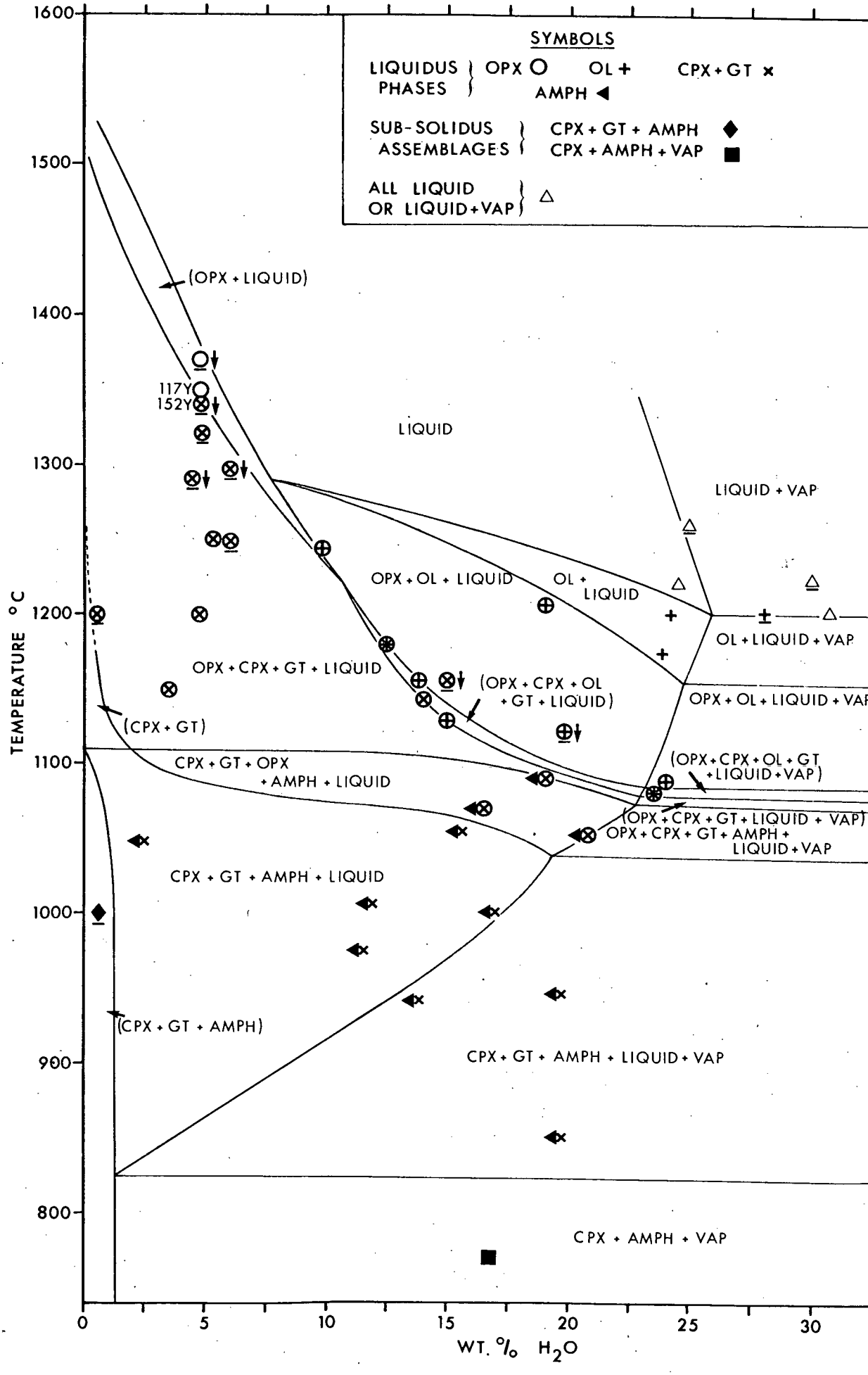
SYMBOLS
LIQUIDUS PHASES
OPX
OL +
AMPH
CPX + GT
SUB-SOLIDUS ASSEMBLAGES
CPX + GT + AMPH
CPX + AMPH + VAP
ALL LIQUID OR LIQUID+VAP
(OPX + LIQUID)
117Y
152Y
LIQUID
LIQUID + VAP
OPX + OL + LIQUID
OL + LIQUID
OL + LIQUID + VAP
OPX + CPX + GT + LIQUID
(OPX + CPX + OL + GT + LIQUID)
OPX + OL + LIQUID + VAP
(CPX + GT)
CPX + GT + OPX + AMPH + LIQUID
(OPX + CPX + OL + GT + LIQUID + VAP)
(OPX + CPX + GT + LIQUID + VAP)
OPX + CPX + GT + AMPH + LIQUID + VAP
CPX + GT + AMPH + LIQUID
(CPX + GT + AMPH)
CPX + GT + AMPH + LIQUID + VAP
CPX + AMPH + VAP
TEMPERATURE °C
1600
1500
1400
1300
1200
1100
1000
900
800
0
5
10
15
20
25
30
WT. % H2O

high pressure. The results do not, however, disprove Green's (1970) contention that the primary phase volume of orthopyroxene expands at the expense of that of clinopyroxene, and possibly of olivine, in the presence of small quantities of water.

At low H_2O contents the small temperature interval, at a given H_2O content, between the phase fields of orthopyroxene plus nepheline-normative liquid and opx+gt+cpx+liquid suggests that the liquid formed by the melting of certain cpx+opx+gt assemblages are nepheline-normative even in the presence of H_2O. However, this conclusion is not completely justified since it is based on results of experiments using two different capsule techniques (see Appendix A.1.1 and fig. 10.3, runs 117Y and 152Y) in which the actual temperature and pressure realized may not be precisely comparable. The temperature gap between the opx+liquid and opx+cpx+gt+liquid phase fields as determined using a uniform capsule technique at about 5% total H_2O content may be as much as $30^{o}C$.

There is insufficient evidence to determine whether the clinopyroxene - orthopyroxene - garnet plane is a thermal divide at low P_{H_2O}.

At H_2O contents in excess of about 14%, the very close proximity of the opx+ol+liquid and the opx+cpx+gt+liquid$\pm$ol phase fields shows that nepheline-normative liquids may be generated in the system C-M-A-S-N-H by small degrees of melting of certain opx+cpx+gt+ol assemblages at high P_{H_2O}. Such liquids must be nepheline-normative since both olivine and the bulk composition lie on the critical plane of SiO_2 undersaturation. Liquids crystallized from this bulk composition in the equilibrium ol+opx+liquid are therefore nepheline-

normative. In summary, fig. 10.3 shows that nepheline-normative liquids are in equilibrium with garnet-lherzolite at 1150°C in the presence of 14% total H_2O, and at 1085°C under vapour-present or near vapour-present conditions.

Olivine is in reaction relationship with the liquid formed in equilibrium with these garnet-lherzolites at 14% total H_2O, and is predicted to be so under vapour-saturated conditions since no olivine crystallized from composition Z at 1050°C. Isobaric fractional crystallization of such nepheline-normative liquids by cpx+gt$\pm$opx precipitation will yield residual liquids with compositions which trend away from that of the initial partial melting product. The direction of this trend is unknown but, unless there are major effects caused by the crystallization of non-stoichiometric phases, residual liquids will develop progressively lower SiO_2:($CaO+Al_2O_3+Na_2O+MgO$) ratios as fractional crystallization proceeds.

Phase field boundaries at lower temperatures in fig. 10.3 are only approximate because of limited run data, the greater imprecision in the measurement of the H_2O content, and the difficulties in distinguishing primary from quench amphibole at the higher temperature limit of its reported stability field. Two features of the low temperature part of this phase diagram are, however, worth comment:-

(i) The stability of amphibole to hyper-solidus conditions. The temperature of the beginning of melting for this composition (charge Z-HG) is consequently dependent on the H_2O-content of the system. The difference in the solidus temperature under vapour-absent and vapour-present conditions is at least 150°C.

(ii) A near-solidus reaction involving consumption of garnet with the production of clinopyroxene and amphibole. A sub-solidus run (run 115Y) which yielded clinopyroxene and amphibole but no garnet was repeated (run 148Y) but seeding the hydrous charge with 1% pyrope crystals. The purpose of this experiment was to determine whether the absence of garnet at this temperature was due to nucleation problems. However, the test was inconclusive since the pyrope seeds neither dissolved nor increased in quantity.

10.3.5 The composition of liquids in equilibrium with garnet-lherzolite in the system C-M-A-S-N-H at high pressure

Phase equilibria in the systems C-M-A-S-N and C-M-A-S-N-H are isobaric invariant only when six or seven phases respectively are involved. The nepheline-normative liquids reported above (see section 10.3.2 and 10.3.4) as the partial melting product of cpx+opx+gt$\pm$ol$\pm$vapour assemblages do not occur in isobaric invariant equilibria. Hence the liquids in the equilibrium assemblages cpx+opx+gt$\pm$ol$\pm$vapour+liquid may not be nepheline-normative at this pressure for other bulk compositions in the C-M-A-S-N or C-M-A-S-N-H systems or at other temperatures.

In the temperature range 1050-1100^{o}C, at 25 kb, Kushiro (1972) reported that bulk compositions in the system C-M-A-S-N-H yielded quartz-normative liquids in equilibrium with H_2O-saturated garnet-lherzolite. These are the same conditions under which the C-M-A-S-N-H composition (charge Z-HG) used in the present study yielded nepheline-normative liquids. On the basis of experiments which indicated the relative positions of the olivine/orthopyroxene

liquidus field boundary in the systems M-A-S-N-H, C-M-S-H and C-M-A-S-H at high pressure, Kushiro (1972) suggested that nepheline-normative liquids could be produced by small degrees of partial melting of peridotites with low CAS/NAS_4 ratios. The present experiments provide confirmation of this prediction. Composition Z can be expressed (in molecular proportions) as $(CMS_2)(MS)_6(CAS)_3(NAS_4)_{1.5}$, giving a CAS/NAS_4 molecular ratio of 2. The composition reported by Kushiro to yield quartz-normative liquids at 25 kb, 1075°C can be expressed (in weight %) as $(MS)_{30}(CMS_2)_{25}(CAS_2)_{32.5}(NAS_6)_{12.5}$. This composition, expressed in terms of S, MS, CMS_2, CAS and NAS_4 has a CAS/NAS_4 molecular ratio of 4.9. The more SiO_2-rich liquid was therefore generated in equilibrium with garnet-lherzolite from the bulk composition with the higher CAS/NAS_4 ratio.

The difference in the liquid composition formed by melting H_2O-saturated garnet-lherzolite as reported by Kushiro (1972) and here under the same conditions can be explained by the difference in the bulk composition since the relevant equilibria are isobaric univariant. However, it is possible that the difference is due to errors or differences in the experimental or analytical techniques used. These will now be considered.

A. Inter-laboratory calibration of equipment used. Kushiro's (1972) experiments were carried out using equipment at the Geophysical Laboratory, Washington which has been calibrated at the same equilibria as those used to calibrate the equipment on which the present experiments were carried out (see Appendix A.1.2).

B. Piston technique. A small pressure difference may exist between

the two sets of results at the same nominal pressure since Kushiro (1972) used the floating-piston technique with a -3% correction for friction (Kushiro, 1969b) whereas the piston-out technique was used in the experiments on Z-HG.

C. Furnace assembly. Kushiro's (1972) experiments and a few of the new experiments were carried out using a single sealed platinum capsule and a furnace assembly similar to that described in Appendix A.1.1. A modified furnace assembly (Appendix A.1.1) was however used for most of the new experiments run under hydrous conditions. Results of experiments using the two different furnace assemblies are distinguished in fig. 10.3. The modified furnace assemblage involves a double capsule consisting of an outer stainless steel cup in which is inserted a small sealed platinum capsule loaded with the starting material. This capsule technique was preferred to the single capsule technique used by Kushiro since it requires less compression of the platinum capsule to fit the assemblage and hence there is less chance of cracking the platinum which results in H_2O escape from the charge.

The new furnace assembly has not yet been calibrated. Although the actual temperature realized in the two assemblages is expected to be comparable, the pressure may not. This source of difference, along with the difference of piston-technique and the imprecision of $\pm 25^{\circ}C$ in Kushiro's (1972) temperature for the relevant equilibria, suggests that the liquids in equilibrium with hydrous garnet-lherzolite in the two sets of experiments were not generated under precisely comparable conditions. Small compositional differences for the Na_2O-, CaO- and Al_2O_3-rich liquids

produced by melting garnet-lherzolite may be expressed as completely different C.I.P.W. normative minerals. Consequently, although the difference in the pressure and temperature conditions for the two sets of experiments is not likely to have been great, it may have been sufficient to explain the difference in the degree of SiO_2-saturation of the liquids generated.

D. Determination of H_2O-saturated conditions. Kushiro (1972) used the criteria of the presence of glass spherules and glass coatings in his quenched run products as evidence of the presence of a vapour phase at high temperature. Such glass spherules and glass coatings represent the silicates dissolved in the vapour phase during run conditions but which are deposited as solid phases on quenching the run. In the hydrous experiments on Z-HG it was found that glass spherules, glass coatings, vapour bubbles in glass and shattered glass were all found in run products which, from the form of the phase diagram (fig. 10.3), could not have had a free vapour phase at high temperature. Glass spherules, for example, occurred in small quantities in the product of a run (152Y) at 1340°C on a bulk composition containing 4.8% H_2O, and in much larger quantities in the product of a run (132Y) on a bulk composition containing 12.5% H_2O held at a temperature (1180°C) at which the form of the phase diagram indicates that at least 25% H_2O is necessary to saturate the liquid. These glass spherules and coatings are believed to represent silicate material quenched from a silicate-bearing vapour which was itself exsolved from the liquid on quenching. It is concluded that the only satisfactory method of determining the presence of a vapour phase at high temperature is by the form of the phase diagram.

Although Kushiro (1972) may not always have attained H_2O-saturated conditions in runs in which this was reported, this is not a significant factor in explaining the difference between the liquid composition generated in his runs and in the present experiments. The H_2O contents of Kushiro's charges for the relevant experiments exceed 20% and are comparable to those at the same temperature in the experiments on Z-HG in which the liquid was H_2O-saturated.

E. H_2O retention. It was reported above that the capsule technique used by Kushiro (1972) is more likely to lead to H_2O loss than that used in most of the new experiments. H_2O loss is a frequent problem in high pressure experiments and difficult to prove except by the consistency of a phase diagram. Kushiro's experiments are not sufficiently numerous to indicate consistency. H_2O loss is, however, expected to result in an almost completely H_2O-free assemblage. Since Kushiro reports the presence of glass spherules in his run products it is probable that H_2O was retained in his experimental charges.

F. Identification of quench crystals. Kushiro (1972) did not report any problems in distinguishing primary crystals from those formed from the liquid on quenching the run. The criterion used to distinguish primary from secondary crystals in the experiments on charge Z-HG, where this was not obvious texturally (see Appendix A.3.2), was crystal settling. Crystals concentrated in the basal portions of the material in a capsule at the end of a melting experiment are believed to have sunk through the liquid during the run and are therefore primary. Runs in which crystal sinking was

observed are distinguished in fig. 10.3. In these runs, all equilibrium crystalline phases reported had sunk to the base of the capsule. The identification of crystal species as primary in other run products in both the C-M-A-S-N and C-M-A-S-N-H systems is justified by the similarity in texture to that of the same crystal species in the run products in which crystal settling was identified. All four crystalline phases under discussion here, viz. olivine, orthopyroxene, clinopyroxene and garnet, have been observed in basal crystal concentrates in which they occurred in the same crystal form as those reported as primary phases in other run products.

No problem was encountered in the distinction between primary and quench crystals of these four phases. All secondary crystals had feathery textures, or formed quench overgrowths on primary crystals which were not necessarily of the same phase. It is therefore considered unlikely that Kushiro (1972) misidentified quench crystals as primary crystals.

The identification of the liquid in equilibrium with olivine, orthopyroxene, clinopyroxene, garnet and vapour as either quartz-normative (Kushiro, 1972) or nepheline-normative (this work) is based on a consideration of the compositions of the coexisting crystalline phases with respect to that of the bulk composition. The latter lies on the plane of SiO_2 saturation in Kushiro's experiments but on the critical plane of SiO_2 undersaturation in the new experiments. Considerations D, E and F above show that the identification of the composition of this liquid is justified since the coexisting phases in the experiments on Z-HG, and probably also in Kushiro's experiments,

are as reported.

The difference of liquid composition is probably therefore due to the difference in the bulk compositions used, but may be the result of small pressure and temperature differences between the two sets of experiments.

10.3.6 Conclusions

Nepheline-normative liquids may be generated by low degrees of melting of certain cpx+opx+gt assemblages in the system C-M-A-S-N at 25 kb. Orthopyroxene is in reaction relation with this liquid. This result has been confirmed with experiments on different types of starting material.

Although the liquidus field of olivine expands at the expense of that of orthopyroxene in the presence of H_2O, certain ol+cpx+opx+gt+vapour assemblages in the system C-M-A-S-N-H at 25 kb yield nepheline-normative liquids with low degrees of partial melting. Both nepheline- and quartz-normative liquids may be generated in equilibrium with H_2O-saturated garnet-lherzolite in the system C-M-A-S-N-H at about 25 kb, 1080°C.

The presence of glass spherules, glass coatings, vapour bubbles and shattered glass in H_2O-bearing experimental charges is not evidence of the presence of a vapour phase at high temperature.

10.4 The melting behaviour of two natural eclogites at high pressure

10.4.1 Introduction

An orthopyroxene-liquid reaction has been reported in

cpx+opx+gt+liquid assemblages in the melting interval of dry synthetic eclogites (i.e. cpx+gt assemblages) in the system C-M-A-S at 30 kb (O'Hara and Yoder, 1967) and 40 kb (Davis, 1964) and in the system C-M-A-S-N at 25 kb (see section 10.3.2). This reaction, together with the observation that the eclogite plane constitutes a thermal divide under the same conditions, led O'Hara and Yoder (1967) to suggest that eclogite fractionation from the high pressure partial melting product of garnet-lherzolite could yield residual liquids which would be critically undersaturated in SiO_2 (see section 10.1).

As further evidence for their hypothesis, O'Hara and Yoder (1967) investigated the melting behaviour at 30 kb of two natural clinopyroxene + garnet mineral pairs from kimberlite. No olivine was observed in the melting interval of either eclogite which is consistent with the conclusion that the eclogite plane is a thermal divide at high pressure. This was confirmed by the lower temperature of the solidus when olivine was added to one of the eclogites. Orthopyroxene was not, however, observed in the melting interval of either eclogite. O'Hara and Yoder noted that this did not preclude the possibility of an orthopyroxene-liquid reaction in the eclogite plane for natural compositions at 30 kb since the garnets and clinopyroxenes in equilibrium with orthopyroxene and liquid at the reaction could have higher $(MgO+FeO):(R_2O_3+CaO+Na_2O)$ ratios than the eclogites used in the experiments. The garnet-clinopyroxene cotectic would therefore be encountered for the eclogites under investigation at temperatures lower than that of the reaction which would not be observed in the melting interval of these rocks.

However, O'Hara and Yoder (1967) reported an opx-liquid reaction

in the melting interval of a mixture of natural olivine and one of the two natural cpx+gt pairs for which the reaction was not observed in the absence of olivine

An orthopyroxene-liquid reaction in natural cpx+opx+gt+liquid assemblages has subsequently been reported by Ito and Kennedy (1968) in the melting interval of an olivine-tholeiite at 40 kb, and by Ito and Kennedy (1974) in the melting interval of an eclogite at 20 and 25 kb. Neither olivine nor quartz were liquidus phases for either rock at these high pressures.

In order to find evidence for this orthopyroxene-liquid reaction in natural compositions over a wider range of conditions, the melting behaviour of two further eclogites has been investigated. The results of experiments in this study are presented in Appendix tables A.9.12 and A.9.13, interpreted in fig. 10.4, and discussed below.

Both eclogites (samples 1044 and 1058) investigated are from African kimberlite pipes (see Appendix A.4). The compositions of the whole rocks and of their constituent minerals are given in Appendix table A.4.1. Experiments were carried out on the dried powdered whole rock.

10.4.2 Interpretation of results

Orthopyroxene does not appear in the melting interval of sample 1044 between 20 and 30 kb, and it only appeared in the melting interval of sample 1058 at the low pressure end of the pressure range investigated (20-30 kb). The absence of orthopyroxene as a liquidus phase of 1058 at higher pressures is consistent with the results in

FIGURE 10.4

Interpretation of the quenched phase assemblages obtained in experiments on the two natural eclogite samples 1044 and 1058.

Black dots represent data points.

lq - liquid

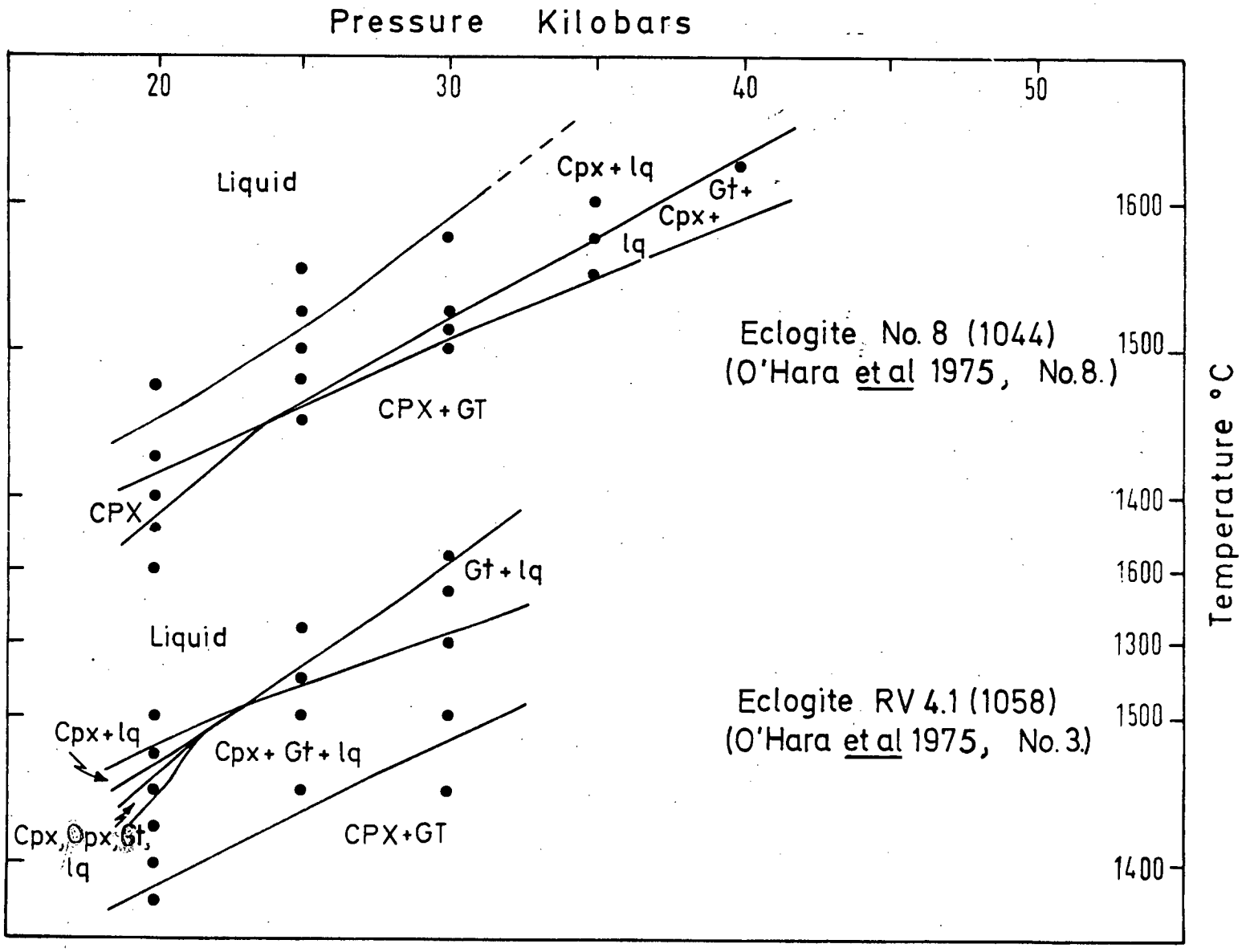
Pressure Kilobars
20
30
40
50
Liquid
Cpx + lq
Gt +
Cpx +
lq
CPX + GT
CPX
Eclogite No. 8 (1044)
(O'Hara et al 1975, No. 8.)
1600
1500
1400
Gt + lq
Liquid
1600
1300
Cpx + lq
Cpx + Gt + lq
Eclogite RV 4.1 (1058)
(O'Hara et al 1975, No. 3.)
1500
Cpx, Opx, Gt, lq
CPX + GT
1400
Temperature °C

the synthetic C-M-A-S system (O'Hara and Yoder, 1967; Davis, 1964) which show a migration of the cpx+opx+gt+liquid isobaric invariant point towards enstatite with increasing pressure. Orthopyroxene was resorbed in the equilibrium opx+cpx+gt+liquid encountered in the melting interval of 1058 at 20 kb. This reaction is similar to that reported in previous studies of natural and synthetic eclogites at high pressure (see sections 10.1 and 10.3.2). The failure of orthopyroxene to appear in the melting interval of 1044, or of 1058 at 25 and 30 kb, does not preclude the possibility of an orthopyroxene-liquid reaction at these pressures for eclogites with higher $(MgO+FeO):(R_2O_3+Na_2O+CaO)$ ratios as explained in section 10.4.1. It is worth noting that this ratio may have been lower in the quenched phase assemblage than in the loaded bulk composition because of rapid Fe-loss from the charge to the platinum capsule at these high temperatures.

Olivine was not observed in the melting interval of either eclogite in the 20-30 kb pressure range. This is consistent with the hypothesis (O'Hara and Yoder, 1967) that the eclogite plane constitutes a thermal divide at high pressure.

The melting behaviour of these two natural eclogites is consistent with O'Hara and Yoder's (1967) suggestion that nepheline-normative magmas may be generated by eclogite fractionation from the partial melting product of anhydrous garnet-lherzolite at high pressure.

APPENDIX A.1

EXPERIMENTAL PROCEDURE

A.1.1 High pressure equipment

Most of the high pressure experiments were run in a single-stage, half-inch diameter piston-in-cylinder solid media pressure equipment similar to that described by Boyd and England (1963). Details of the apparatus used in the Edinburgh laboratory are given in O'Hara et al. (1971). A three-quarter-inch diameter piston-in-cylinder solid media apparatus was used for one experiment to synthesize pyrope crystals.

Two types of furnace assemblage were used:-

A - This is similar to that described by Richardson et al. (1968) without the ceramic disc between the thermocouple tip and the platinum capsule. This assemblage was used for most of the experiments.

B - This is a modification of furnace assemblage A for the purpose of fitting large stainless steel capsules into the half-inch piston-in-cylinder apparatus. It uses the inner parts (ceramic sleeves and spacers and graphite furnace) of assemblage A as used in the three-quarter-inch piston-in-cylinder apparatus, and the outer parts (talc sleeve and lead foil) of assemblage A as used in the half-inch piston-in-cylinder apparatus. The two sections, inner and outer, of the modified furnace assemblage are made to fit by reducing (to 7 mm.)the inner diameter of the boron nitride sleeve of furnace assemblage A as used in the half-inch piston-in-cylinder apparatus. A ceramic disc was used between the thermocouple tip and the

stainless steel capsule. The stainless steel capsule is 5 mm. long, and has an outer diameter of 3.76 mm., an inner diameter of 2.97 mm., and has a tight fitting lid. The sample material was contained in an inner, welded platinum capsule which was placed inside the stainless steel capsule. The inner platinum capsule had the following dimensions: 5-6 mm. long, 1.5 mm. outer diameter, 1 mm. inner diameter. This inner capsule was curved into a horseshoe shape to fit inside the base of the stainless steel cup. The remaining space in the stainless steel cup was filled with crushable Al_2O_3 and Al_2O_3 powder. The stainless steel cup was inverted in the furnace assemblage so that the inner platinum capsule was lying at that end of the steel cup which was closest to the thermocouple tip. This furnace assemblage is referred to as 'B1' in Appendix table A.9.10. In one experiment an uncontorted platinum capsule of the size normally used in the half-inch solid media equipment (viz. 5-6 mm. long, 2 mm. outer diameter, 1.6 mm. inner diameter) was placed in the stainless steel cup and packed around with Al_2O_3 powder. This variation is referred to as furnace assemblage B2 in Appendix table A.9.10.

Furnace assemblage B was used for many of the experiments on hydrous charges. It has the advantage that the platinum capsule containing the charge need only be very slightly bent to fit the stainless steel cup. The chance of developing cracks in the capsule is therefore much less than for the highly compressed platinum capsule used in furnace assemblage A. There is thus a smaller risk of losing volatiles (especially H_2O and Na_2O in the charges used in this study) from the charges contained in furnace assemblage B.

The experiments in which this assemblage was used are distinguished in Appendix table A.9.10; assemblage A was used in all other experiments.

Platinum against platinum 87% rhodium 13% alloy thermocouples were used to simultaneously measure and control furnace temperature.

Details of temperature control are described by O'Hara et al. (1971). A Eurotherm stepless temperature controller was however used instead of the West Viscount controller in most of the experiments. The Eurotherm controller had the following characteristics: proportional term 20-30% (varied to suit individual run conditions); integral time constant 1.5 sec.; derivative time constant 0.3 sec.. The set point of the West Viscount controller can be read to 0.002 mV; the set point of the Eurotherm controller can be read to 0.01 mV, equivalent to 0.7°C. Temperatures were checked using a Pye Precision Decade Potentiometer (serial no. 82064) which can be read to 0.0015 mV, equivalent to 0.1°C. The temperatures quoted in the tables of experimental results are, to the nearest °C, those indicated by the potentiometer just before quenching the run.

The pressure/temperature path to the desired run conditions was achieved in most of the experiments by using the piston-out technique described by Richardson et al. (1968) with an overpressure of 5 kb. Only the experiments in which this piston technique was not used have been distinguished in the tables of run results and in the text. Richardson et al. also describe the piston-in technique (discussed in the text) which yields lower actual pressures than those attained using the piston-out technique. The floating-piston technique was used for some experiments. Here the sample is taken

to run temperature at the desired run pressure. This technique gives actual pressures which are intermediate in value between those attained using the piston-out and the piston-in techniques (Boyd et al., 1967). During all experiments frequent readjustments of pressure were made in order to maintain the sample at the desired conditions. Run pressures quoted in the tables of run results are the pressures recorded just before quenching the run and have not been corrected for frictional effects. The pressure gauge used can be read to the nearest 25 p.s.i., equivalent to 110 bars.

A.1.2 Calibration of high pressure equipment

The following discussion applies to furnace assemblage A (see Appendix A.1.1) which is the standard assemblage used in the Edinburgh laboratory.

No correction has been made for the effects of pressure and temperature gradients on the thermocouple e.m.f. since there is at present too little information to assess the size of these effects. The temperature-sensitive melting curve of diopside has therefore been bracketed at three different pressures and provides calibration points for comparison with other laboratories. Fig. A.1.1 is a plot of the experimental results obtained at Edinburgh which bracket the melting curve of diopside at 10.8 kb (Herzberg, 1975), 22.5 kb (O'Hara et al., 1971) and 25 kb (this work, Appendix table A.9.6). At all three pressures the melting curve of diopside has been bracketed within the brackets obtained by Boyd and England (1963) using equipment at the Geophysical Laboratory, Washington. This shows that there is no major difference between the calibration of

FIGURE A.1.1

The melting interval of diopside (CMS_2) and of pyrope (M_3AS_3) at various pressures, determined at Edinburgh and at the Geophysical Laboratory, Washington.

The melting behaviour of pyrope:-

- Runs carried out at the Geophysical Laboratory (Boyd and England, 1962). Run products are indicated by the labelled phase fields, taken from Boyd and England (1962, fig. 37).

□ quench crystals
■ pyrope (sub-solidus)
} run products of experiments at Edinburgh.

The melting behaviour of diopside:-

○ glass + quench crystals
✱ primary cpx crystals
} run products of experiments at the Geophysical Laboratory (Boyd and England, 1963).

▲ glass + quench crystals
▼ primary cpx crystals
} run products of experiments at Edinburgh (O'Hara et al., 1971; Herzberg, 1975; this work).

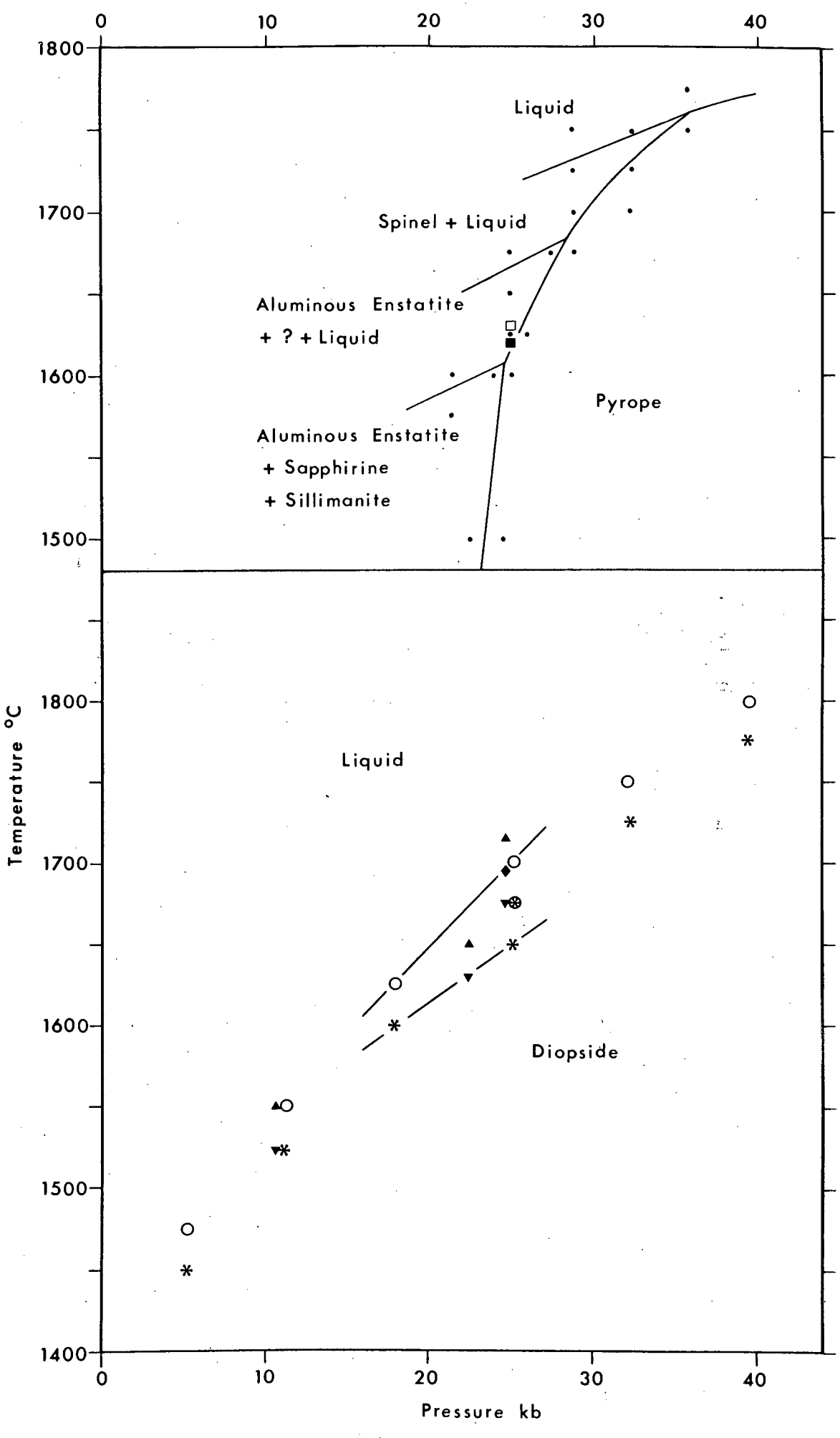
0
10
20
30
40
1800
1700
1600
1500
Liquid
Spinel + Liquid
Aluminous Enstatite
+ ? + Liquid
Pyrope
Aluminous Enstatite
+ Sapphirine
+ Sillimanite
Liquid
Diopside
Temperature °C
1800
1700
1600
1500
1400
0
10
20
30
40
Pressure kb

the temperature scale used by Boyd and England and that used at Edinburgh.

The experimental results of O'Hara et al. (1971) on the pressure sensitive inversions sillimanite $\rightleftharpoons$ kyanite and quartz $\rightleftharpoons$ coesite at 30-35 kb show that the calibration of the pressure scale used in the Edinburgh laboratory is comparable to that of other laboratories. Further evidence for this conclusion was obtained from the result of a new determination of the melting temperature of pyrope at 25 kb. The experimental results are presented in Appendix table A.9.6 and compared in fig. A.1.1 with those of Boyd and England (1962) who determined the solidus temperature of pyrope using equipment at the Geophysical Laboratory, Washington. There is a close similarity between the two sets of results.

Comparisons of the pressure/temperature positions of a phase field boundary determined using the piston-in-cylinder equipment with the same boundary determined from experiments using hydrostatic pressure medium apparatus have been described by Herzberg (1975) at 9 kb, and by O'Hara et al. (1971) at 15-25 kb. These suggest that at temperatures above about 1150°C the actual pressure attained in a piston-out experiment in the piston-in-cylinder apparatus may be less than that attained at the same nominal pressure in the hydrostatic pressure medium apparatus. Below about 1150°C the discrepancy appears to be reversed with the higher actual pressures being attained in the piston-in-cylinder apparatus.

Much of the work presented in this thesis is concerned with the explanation of differences in experimental results obtained in

this study and in studies carried out in other laboratories. It is believed that the discrepancies do not reflect differences in the calibration of the pressure and temperature scales of solid media equipment in the various laboratories involved. The calibration phase-field boundaries (discussed above) determined in the Edinburgh laboratory were observed at closely comparable pressure/temperature conditions to those reported for the same equilibria determined in the other laboratories. To the author's knowledge the following experimental studies which are discussed in the text were carried out at the Geophysical Laboratory, Washington:- Akella (1974a,b); Akella and Boyd (1974); Boyd (1970); Boyd and England (1964); Davis and Boyd (1966); Hensen (1973); Kushiro (1969a, 1969b, 1972); MacGregor and Ringwood (1964); O'Hara and Yoder (1967). The equipment at the Geophysical Laboratory was used to obtain the positions of the diopside (Boyd and England, 1963) and the pyrope (Boyd and England, 1962) melting curves which are compared in fig. A.1.1 with those obtained from experiments carried out at Edinburgh. The close similarity of the calibration of the pressure scales used at the Geophysical Laboratory and at Edinburgh was also shown by a comparison (O'Hara et al., 1971) of the pressure and temperature conditions of the kyanite $\rightleftharpoons$ sillimanite inversion as determined in the two laboratories.

The experiments of Green and Ringwood (1970) were carried out at the A.N.U., Canberra on equipment which has been calibrated at the quartz $\rightleftharpoons$ coesite inversion. The pressure determined for the inversion was not significantly different from that determined by

O'Hara et al. (1971) using the Edinburgh equipment.

Further sources of inaccuracy and imprecision in the recorded run temperature as indicated by the set point on the controller and by the potentiometer are as follows:-

(i) The temperature measured is that of the thermocouple tip. Evidence from experiments on charges which pass through a rapid succession of phase fields within a narrow temperature interval suggest that the temperature interval between the top and base of the capsule does not exceed 5°C.

(ii) The possibility of a temperature fluctuation occurring too rapidly to register on the controller or potentiometer.

(iii) Thermocouple poisoning or rhodium diffusion within the thermocouple. This is believed to occur during long experiments since after a certain run duration the power needed to maintain a constant thermocouple e.m.f. begins to increase. The critical run durations for these thermocouples were about 18 hrs. at 1400°C, 4-5 hrs. at 1500°C, 3-4 hrs. at 1550°C, ½-1 hr. at 1600°C. Experiments carried out in this study were usually limited to shorter durations than these. Run products were discarded if the power necessary to maintain a constant thermocouple e.m.f. increased more than about 1% over the value recorded 10-20 mins. after the start of the experiment.

Bravo (1973) estimated that run temperatures are reproducible to ±10°C.

Furnace assemblage B (described in Appendix A.1.1) has not been calibrated. Actual run temperatures are believed to be very

close to those attained in charges in furnace assemblage A at the same nominal temperature since the sample material lies at a similar distance from the thermocouple tip in both assemblages. This is, however, only true for furnace assemblage B1. In furnace assemblage B2 there may be a considerable temperature gradient within the charge.

A.1.3 Low pressure furnaces

Low pressure furnaces were used to recrystallize the gel charges, and to prepare glass starting materials from the gels by melting and quenching them. The manufacture of two of the glasses (charges E22H and Z-GL) and the recrystallization of most of the gels were carried out at atmospheric pressure in the furnaces described by Biggar and O'Hara (1969c). Some of the gels were recrystallized at 1 kb in internally heated pressure vessels which were described by Ford (1972).

A.1.4 Capsule preparation: anhydrous charges

Water-bearing charges are indicated in the tables of experimental details and results. All other charges were thoroughly dried before running. Synthetic charges were dried in air at 1050°C for 1-2 hrs. Natural compositions were dried in N_2 at 900-950°C for ½-3 hrs. All charges were dried inside crimped platinum capsules which were welded within about 3 mins. of removal from the drying furnace.

The capsules, which contained 0.006-0.010 gms. of material, were compressed to fit the half-inch solid media furnace assemblage

A. The platinum capsule containing the charge, the boron nitride sleeve, ceramic sleeve and spacers and the graphite furnace were all dried in N_2 at 900-950°C for 30 mins. before loading into the high pressure equipment.

A.1.5 Capsule preparation: hydrous charges

Distilled H_2O was introduced into the platinum capsule using a small graduated syringe. The powdered charge was then added and the capsule was crimped and welded. During welding the capsule was kept cool by immersing in H_2O its entire length except the crimped welt. The capsule was reweighed after welding to determine whether any H_2O had been lost by evaporation during the welding procedure. It the difference between the weight of the capsule before and after welding exceeded 1.5% of the weight of the total charge (powder plus H_2O), the capsule was discarded. The actual H_2O loss from an acceptable capsule is much less than this maximum capsule weight difference of 1.5% (of the total charge) since most of the weight loss is the result of platinum volatilization.

The capsule was then compressed or bent to fit the furnace assemblage (A or B). As cracks may have developed in the platinum capsule wall during this process, the contorted capsule was immersed in an oil bath maintained at a temperature in excess of 110°C. If no vapour bubbles were observed rising through the oil from the capsule, and if, after cleaning and drying the capsule, its weight was the same as that recorded after welding, it was concluded that the capsule was watertight at this stage. Only these watertight capsules were used for high pressure experiments.

The reported H_2O content of a charge does not include any H_2O present in the undried powder. The undried gel charges used contained less than 1.0% H_2O.

The small platinum capsules, used for furnace assemblage B1, contained 3.5-4.0 mgms. total charge, i.e. gel plus H_2O. The larger platinum capsules, used for furnace assemblages A and B2, contained 7-10 mgms. total charge. In all critical runs involving equilibria between some or all of the phases clinopyroxene, orthopyroxene, garnet, olivine and liquid, but not amphibole, and in which the H_2O content of the charge was less than 14%, measurements of charge weight and H_2O content were made to the nearest 0.05 mgm. For most of the other experiments charge measurements were made to the nearest 0.1 mgm. In all critical runs the actual H_2O content of the charge is believed to have been within 2.5% of the reported content.

APPENDIX A.2

COMPOSITION AND NATURE OF STARTING MATERIALS: SYNTHETIC CHARGES

A.2.1 Material preparation

Partially crystalline gels, recrystallized gels, gel mixtures and glasses were all used as synthetic starting materials in this study.

Gels were prepared by a method involving the dehydration of a gelatinous mixture of hydroxides. This method was described by Biggar and O'Hara (1969a). Gels were rejected if their weight on recovery was less than 99.5%, or exceeded 100.3% of the intended weight. This method of manufacturing gels is believed to yield samples whose major oxides are within 0.2% (of the total charge) of the proportions intended.

All gels were partially crystallized at 900-1150°C, atmospheric pressure for 8-40 hrs. before use. Certain gels were further recrystallized under low pressure conditions ($\leq$1 kb) to yield a material which contained no, or only very little unrecrystallized gel. Such gels are referred to as "recrystallized gels" in the text. The unqualified term "gel" refers to either recrystallized or only partially crystalline gel. Details of the final thermal treatment (excluding the immediate pre-run drying procedure) of all charges (except the glasses) are given in Appendix tables A.2.1 and A.2.2. Recrystallization at 1 kb was carried out in the presence of small amounts of water.

Further starting materials were prepared by mechanically mixing

TABLE A.2.1

Crystal nuclei present at atmospheric pressure in charges with compositions in the system C-M-A-S and its subsystems

Charge No.	Final Heat Treatment*				Phases Identified (by X-Ray Diffraction)	Phases Predicted from O'Hara (1969, fig.23)	Remarks
	Temp.(°C)	Pressure	Time	H_2O content (%)			
DR	1200	1 atm.	?	-	Cpx	Cpx	Total rexzn.
EN	?	1 atm.	?	-	En_{ss},Ol	En_{ss}	
ENR	1200	1 atm.	28 days	-	En_{ss},Ol	En_{ss}	
F	?	1 atm.	?	-	Ol,?Qz,Prclse	-	
FR	1000	1 kb	4 days	~4	Ol	-	Total rexzn.
PY	?	1 atm.	?	-	Ol,Cord,Sp	Ol,Cord,Sp	
PYR	(see Appendix A.2.1)				Gt	-	Total rexzn.
DP2	900	1 atm.	8 hrs.	-	Cpx,En_{ss},An,Ol	Cpx,En_{ss},An,Ol	
BOH	1150	1 atm.	24 hrs.	-	Cpx,En_{ss},An,Ol	Cpx,En_{ss},An,Ol	
ENA8R	1000	1 kb	28 hrs.	~4.5	En_{ss},Ol,Cord	En_{ss},Ol,Cord	Odd X-R.D. reflection at 50.3° 2θ CrKα
E5	900	1 atm.	24 hrs.	-	En_{ss},Ol,(?An)	En_{ss},Ol,An,Cord	
E6	900	1 atm.	24 hrs.	-	Cpx,En_{ss},Ol	Cpx,En_{ss},An,Ol	
AM1R	1190	1 atm.	33 days	-	Cpx,En_{ss},An,(Ol)	Cpx,En_{ss},An,Ol	
OHB	1150	1 atm.	40 hrs.	-	Cpx,En_{ss},An,Ol	Cpx,En_{ss},An,Ol	
OHBR	1005	1 kb	23 hrs.	3	Cpx,En_{ss},An,Ol	Cpx,En_{ss},An,Ol	
E34	900	1 atm.	24 hrs.	-	?	Cpx,En_{ss},An,Ol	Poor pattern
E36R	1190	1 atm.	33 days	-	Cpx,En_{ss},An,Ol	Cpx,En_{ss},An,Ol	
E38R	1000	1 kb	28 hrs.	3	Cpx,En_{ss},(?An),(?Ol)	Cpx,En_{ss},An,Ol	
E41R	1200	1 atm.	28 days	-	En_{ss},Ol	En_{ss},An,Ol,(Cord)	

TABLE A.2.1 ctd.

Charge No.	Final Heat Treatment*				Phases Identified (by X-Ray Diffraction)	Phases Predicted from O'Hara (1969, fig.23)	Remarks
	Temp.(°C)	Pressure	Time	H_2O content (%)			
$En_{95}A_5R$	1200	1 atm.	28 days	-	En_{ss},Ol	En_{ss},Ol,Cord	
E3R	1200	1 atm.	28 days	-	En_{ss},Ol	(Cpx),En_{ss},An,Ol	
E30R	1000	1 kb	28 hrs.	4.7	Cpx,En_{ss},An,(Ol)	Cpx,En_{ss},An,Ol	
E22	900	1 atm.	24 hrs.	-	Cpx,En_{ss},Ol	Cpx,En_{ss}	
E22R	1307	1 atm.	14 days	-	En_{ss},Cpx($di_{72.5}en_{27.5}$)	Cpx,En_{ss}	Total rexzn.
E23	900	1 atm.	24 hrs.	-	?	Cpx,En_{ss}	Poor pattern
E23R	1307	1 atm.	14 days	-	En_{ss},Cpx($di_{72.5}en_{27.5}$)	Cpx,En_{ss}	Total rexzn.
D90	1300	1 atm.	24 hrs.	-	?	Cpx	Poor pattern
D95	900	1 atm.	3 hrs.	-	Cpx	Cpx	

NOTES Starting materials called "recrystallized gels" in the text have a charge number which ends with an 'R'.

* This refers to the final prolonged heat treatment of the starting material but does not include the drying technique.

Cpx refers to a diopside-rich clinopyroxene.

TABLE A.2.2

Final heat treatment (excluding pre-run drying procedure) of C-M-A-S and C-M-A-S-N gel charges not already presented in Table A.2.1. Starting materials called "recrystallized gel" in the text have a charge number which ends with an "R".

Charge No.	Final Heat Treatment			
	Temp.(°C)	Pressure	Time	H_2O Content (%)
DP1	900	1 atm.	8 hrs.	-
DP3	900	1 atm.	16 hrs.	-
AM2R	1190	1 atm.	33 days	-
AM6R	1190	1 atm.	33 days	-
AM8R	1190	1 atm.	33 days	-
E35	900	1 atm.	24 hrs.	-
E35R	1190	1 atm.	33 days	-
E35F24R	1190	1 atm.	33 days	-
E36	900	1 atm.	24 hrs.	-
E3	900	1 atm.	24 hrs.	-
E4	900	1 atm.	24 hrs.	-
E4R	1200	1 atm.	28 days	-
E10	900	1 atm.	24 hrs.	-
E15	900	1 atm.	24 hrs.	-
E17	900	1 atm.	24 hrs.	-
E27	900	1 atm.	24 hrs.	-
E27R	1190	1 atm.	33 days	-
E28	900	1 atm.	24 hrs.	-
E29	900	1 atm.	24 hrs.	-
E29R	1000	1 kb	28 hrs.	0.8
E31	900	1 atm.	24 hrs.	-
E18	900	1 atm.	24 hrs.	-
E24	900	1 atm.	24 hrs.	-
E25	900	1 atm.	24 hrs.	-
Z-HG	900	1 atm.	?	-
Z10	900	1 atm.	?	-
Z20	900	1 atm.	?	-
JDT	900	1 atm.	?	-

two or three gels using an agate mortar and pestle. Both partially crystalline and recrystallized gels were used as constituents of the mixtures. Some of the mixtures were subsequently recrystallized at low pressure (≤ 1 kb) before use. The term "homogeneous gel" used in the text refers to a single gel charge rather than a gel mixture.

Crystalline garnet was used as a constituent of certain starting materials (viz., charges FP10, EP32, garnet-seeded Z-HG for run 148Y) and in calibration experiments. This crystalline garnet (charge PYR) was pure pyrope (M_3AS_3) and was crystallized from the gel (PY) of bulk composition M_3AS_3 by two high pressure methods:-

(i) The undried gel PY was run in the half-inch piston-in-cylinder apparatus for 1 hr. at 1400°C, 30 kb using a floating-piston pressure technique. The gel was totally converted to pyrope crystals.

(ii) The gel PY was seeded with 3% pyrope seeds (made using method (i) above), dried at 800°C at atmospheric pressure for 20 mins., and run in the three-quarter-inch piston-in-cylinder equipment for 10.5 hrs. at 1250°C, 25 kb, using the floating-piston technique to attain run conditions. Total conversion of the gel PY to pyrope crystals only occurred in the bottom half of the capsule.

All four glasses used in this study (charges E22G, E22H, E3H, Z-GL) were made at atmospheric pressure by completely melting and quenching a gel of the desired composition. Small quantities (about 0.05 gms.) of the gels were melted in platinum capsules. E22G was obtained by holding gel E22 at 1600°C for 1 hr. before quenching in water. Z-GL was made by heating the soda-bearing gel

Z-HG at 1420°C for 1 hr. before quenching in water. The Na_2O content of the quenched glass (analysed by M. Saunders) was 3.41±0.03%. The intended Na_2O content of the gel Z-HG was 3.466% and is the same as the Na_2O content of the glass within the precision limits of gel manufacture and the oxide analysis. Glasses E22H and E3H were made from gels E22 and E3 respectively by melting the gels at about 1700°C in a radio-frequency heater (kindly carried out by Prof. H.B. Bell of the Metallurgy Dept., University of Strathclyde). The gels were held at this temperature for a few minutes before quenching by removal of the capsules from the heater.

Glasses E22G, E22H and Z-GL contained no detectable quench or primary crystals. E3H contained sparse, minute crystals (estimated proportion is less than 1 part in 100,000) which could not be identified.

In certain experiments the run product of a previous experiment was used as the starting material. This was removed from the capsule, finely ground to $<5\mu$ (except for run D90/175 which required large orthopyroxene crystals) under acetone using an agate mortar and pestle, dried by the normal method and rerun.

A.2.2 Charge compositions

The composition and nature of the C-M-S charges are given in Appendix table A.2.3. Details of charges with compositions in the system C-M-A-S and its subsystems, other than C-M-S, are given in Appendix table A.2.4. Fig. A.2.1 is a plot of these compositions projected from forsterite into the plane CS-MS-A.

Compositional details of the C-M-A-S-N charges are presented

TABLE A.2.3

Compositions in the system CMS_2-MS-M_2S

Composition (wt.%)			Charge	Starting Material
CMS_2	MS	M_2S	No.	
8.0	92.0	-	M5	Gel mixture: $(EN)_{80}(E22)_{20}$
20.0	80.0	-	M2I	Gel mixture: $(EN)_{80}(DR)_{20}$
20.0	80.0	-	M2II	Gel mixture: $(EN)_{50}(E22)_{50}$
28.0	72.0	-	M6	Gel mixture: $(EN)_{30}(E22)_{70}$
40.0	60.0	-	E22	Gel
40.0	60.0	-	E22R	Gel E22H rexd. to en_{ss}+cpx($di_{72.5}en_{27.5}$)
40.0	60.0	-	E22G	Unrexd. glass
40.0	60.0	-	E22H	Unrexd. glass
40.0	60.0	-	M1	Gel mixture: $(EN)_{60}(DR)_{40}$
48.4	51.6	-	E23	Gel
48.4	51.6	-	E23R	Gel E23 rexd. to en_{ss}+cpx($di_{72.5}en_{27.5}$)
60.0	40.0	-	M4	Gel mixture: $(EN)_{40}(DR)_{60}$
69.0	31.0	-	M7	Gel mixture: $(E22)_{51.7}(DR)_{48.3}$
90.0	10.0	-	D90*	Gel
95.1	4.9	-	D95*	Gel
100.0	-	-	DR *	Rexd. gel
-	-	100.0	F *	Gel
-	100.0	-	EN *	Gel
18.2	72.7	9.1	M2F10	Gel mixture: $(M2I)_{90.9}(F)_{9.1}$
36.4	54.5	9.1	E22F10	Gel mixture: $(E22)_{90.9}(F)_{9.1}$
43.6	46.4	10.0	E23F10	Gel mixture: $(E23)_{90}(F)_{10}$

* Charge kindly supplied by other students or staff at the Grant Institute of Geology.
Constituents of gel mixtures (referred to by their charge number) are described in the "Charge No." column.

TABLE A.2.4

Bulk compositions in the system C-M-A-S and its subsystems (except C-M-S)

Charge No.	Bulk composition as wt.% oxides				Starting Material	Bulk composition as $(CS)_X(MS)_Y(A)_Z(M_2S)_{OL}$(wt.%)			
	CaO	MgO	Al_2O_3	SiO_2		OL	100X/(X+Y+Z)	100Y/(X+Y+Z)	100Z/(X+Y+Z)
DP2*	10.26	25.49	15.26	48.99	Gel	-	21.26	63.48	15.26
60	-	34.77	13.40	51.83	Gel mix: $(PY)_{53}(EN)_{47}$	-	-	86.60	13.40
DP1*	12.93	24.31	12.66	50.10	Gel	-	26.79	60.55	12.66
BOH*	15.98	22.98	9.68	51.36	Gel	-	33.10	57.22	9.68
AM4	16.02	22.96	9.63	51.39	Gel mix: $(DP1)_{34.88}(DP3)_{65.12}$	-	33.18	57.19	9.63
AM5	14.42	26.39	8.67	50.52	Gel mix: $(AM4)_{90}(F)_{10}$	10.00	33.18	57.19	9.63
DP3*	17.67	22.24	8.01	52.08	Gel	-	36.60	55.39	8.01
ENA8R	-	36.91	8.09	55.00	Gel mix: $(PY)_{32}(EN)_{68}$rexd.	-	-	91.91	8.09
EP32	-	36.91	8.09	55.00	Xl. mix: $(PYR)_{32}(ENR)_{68}$	-	-	91.91	8.09
E5	2.66	34.94	7.50	54.91	Gel	-	5.50	87.00	7.50
E6	4.59	33.33	7.50	54.58	Gel	-	9.50	83.00	7.50
AM1	6.82	31.47	7.50	54.21	Gel mix: $(E6)_{75}(E34)_{25}$	-	14.13	78.37	7.50
AM1R	6.82	31.47	7.50	54.21	Gel mix (AM1)rexd.	-	14.13	78.37	7.50
AM2	8.29	30.24	7.50	53.96	Gel mix: $(E6)_{58.51}(E34)_{41.49}$	-	17.18	75.32	7.50
AM2R	8.29	30.24	7.50	53.96	Gel mix (AM2)rexd.	-	17.18	75.32	7.50
AM6	12.47	26.77	7.50	53.26	Gel mix: $(E6)_{11.7}(E34)_{88.3}$	-	25.84	66.66	7.50
AM6R	12.47	26.77	7.50	53.26	Gel mix (AM6)rexd.	-	25.84	66.66	7.50
AM7	11.34	29.54	6.82	52.29	Gel mix: $(AM6)_{90.9}(F)_{9.1}$	9.09	25.84	66.66	7.50
AM8	9.48	34.10	5.70	50.73	Gel mix: $(AM6)_{76}(F)_{24}$	24.00	25.84	66.66	7.50
AM8R	9.48	34.10	5.70	50.73	Gel mix (AM8)rexd.	24.00	25.84	66.66	7.50

TABLE A.2.4 ctd.

Charge No.	Bulk composition as wt.% oxides				Starting Material	Bulk composition as $(CS)_X(MS)_Y(A)_Z(M_2S)_{OL}$ (wt.%)			
	CaO	MgO	Al_2O_3	SiO_2		OL	100X/(X+Y+Z)	100Y/(X+Y+Z)	100Z/(X+Y+Z)
OHB*	9.47	34.05	5.74	50.74	Gel	23.77	25.74	66.73	7.53
OHBR	9.47	34.05	5.74	50.74	Rexd. gel	23.77	25.74	66.73	7.53
E34	13.52	25.90	7.50	53.08	Gel	-	28.00	64.50	7.50
E34F24	10.90	31.98	6.05	51.07	Gel mix: $(E34)_{80.65}(F)_{19.35}$	19.35	28.00	64.50	7.50
E35	14.48	25.10	7.50	52.92	Gel	-	30.00	62.50	7.50
E35R	14.48	25.10	7.50	52.92	Rexd. gel	-	30.00	62.50	7.50
E35F24R	11.68	31.33	6.05	50.94	Gel mix: $(E35)_{80.65}(F)_{19.35}$ rexd.	19.35	30.00	62.50	7.50
E36	15.45	24.29	7.50	52.76	Gel	-	32.00	60.50	7.50
E36R	15.45	24.29	7.50	52.76	Rexd. gel	-	32.00	60.50	7.50
E38R	17.38	22.69	7.50	52.43	Rexd. gel	-	36.00	56.50	7.50
AM3	2.62	35.57	6.00	55.81	Gel mix: $(E5)_{50}(E3)_{50}$	-	5.43	88.58	6.00
E41R*	3.14	35.14	6.00	55.73	Rexd. gel	-	6.50	87.50	6.00
E41RF2	3.08	35.58	5.88	55.47	Rexd. gel mix: $(E41R)_{98}(FR)_2$	2.00	6.50	87.50	6.00
$En_{95}A_5R$*	-	38.12	5.07	56.81	Rexd. gel	-	-	94.93	5.07
E3	2.59	36.20	4.50	56.71	Gel	-	5.36	90.15	4.50
E3R	2.59	36.20	4.50	56.71	Rexd. gel	-	5.36	90.15	4.50
E3H	2.59	36.20	4.50	56.71	Unrexd. glass	-	5.36	90.15	4.50
E4	2.33	38.31	4.05	55.31	Gel	10.00	5.36	90.15	4.50
E4R	2.33	38.31	4.05	55.31	Rexd. gel	10.00	5.36	90.15	4.50
E10	4.59	34.53	4.50	56.38	Gel	-	9.50	86.00	4.50
E15	10.38	29.72	4.50	55.40	Gel	-	21.50	74.00	4.50
E17	12.55	27.91	4.50	55.04	Gel	-	26.0	69.50	4.50

TABLE A.2.4 ctd.

Charge No.	Bulk composition as wt.% oxides				Starting Material	Bulk composition as $(CS)_X(MS)_Y(A)_Z(M_2S)_{OL}$ (wt.%)			
	CaO	MgO	Al_2O_3	SiO_2		OL	100X/(X+Y+Z)	100Y/(X+Y+Z)	100Z/(X+Y+Z)
E27	13.52	27.11	4.50	54.88	Gel	-	28.00	67.50	4.50
E27R	13.52	27.11	4.50	54.88	Rexd. gel	-	28.00	67.50	4.50
E27RF10	12.20	30.05	4.06	53.69	Rexd. gel mix: $(E27R)_{90.26}(FR)_{9.74}$	9.74	28.00	67.50	4.50
E28	14.48	26.30	4.50	54.72	Gel	-	30.00	65.50	4.50
E29	15.45	25.50	4.50	54.55	Gel	-	32.00	63.50	4.50
E29R	15.45	25.50	4.50	54.55	Rexd. gel	-	32.00	63.50	4.50
E30R	16.41	24.70	4.50	54.39	Rexd. gel	-	34.00	61.50	4.50
E31	17.40	23.89	4.50	54.23	Gel	-	36.00	59.50	4.50
E18	10.38	30.32	3.00	56.30	Gel	-	21.50	75.50	3.00
E24	14.48	27.51	1.50	56.51	Gel	-	30.00	68.50	1.50
E25	16.41	25.90	1.50	56.19	Gel	-	34.00	64.50	1.50
PY*	-	30.00	25.28	44.71	Gel	-	-	74.72	25.28
PYR	-	30.00	25.28	44.71	Gel (PY) rexd. to pyrope crystals	-	-	74.72	25.28
EN*	-	40.16	-	59.84	Gel	-	-	100.00	-
ENR	-	40.16	-	59.84	Rexd. gel	-	-	100.00	-
F*	-	57.30	-	42.70	Gel	100.0	-	-	-
FR	-	57.30	-	42.70	Rexd. gel	100.0	-	-	-
FP10	-	54.57	2.53	42.90	Xl. mix: $(PYR)_{10}(FR)_{90}$	90.00	-	74.72	25.28
F10Py	-	54.57	2.53	42.90	Gel mix: $(PY)_{10}(F)_{90}$	90.00	-	74.72	25.28

* Material kindly donated by staff and other students at the Grant Institute of Geology, Edinburgh.
Rexd. gel refers to a gel recrystallized at low pressure (≤ 1 kb) except for charge PYR which was recrystallized at 25-30 kb.
The constituents of the gel mixes are referred to by their charge number and are described elsewhere in this table.

FIGURE A.2.1

Projection from M_2S into part of the plane CS-MS-A of the bulk compositions of C-M-A-S, C-M-S and M-A-S charges used in this study. All bulk compositions which do not lie in the plane CS-MS-A lie within the tetrahedron CS-MS-A-M_2S and are identified by an asterisk. The charge number of the partially crystalline gel only has been reported in this figure for bulk compositions for which both partially crystalline and recrystallized gels were used as starting materials. Charge numbers of recrystallized gels are those of the partially crystalline gel with the same bulk composition but with an additional final 'R'.

Superimposed on this diagram are the 1 atmosphere sub-solidus phase field boundaries for compositions in the plane CS-MS-A as determined by O'Hara (1969) using recrystallized glass charges (boundaries shown by solid lines) and by Biggar (1969) using gel charges (boundaries shown by dashed lines).

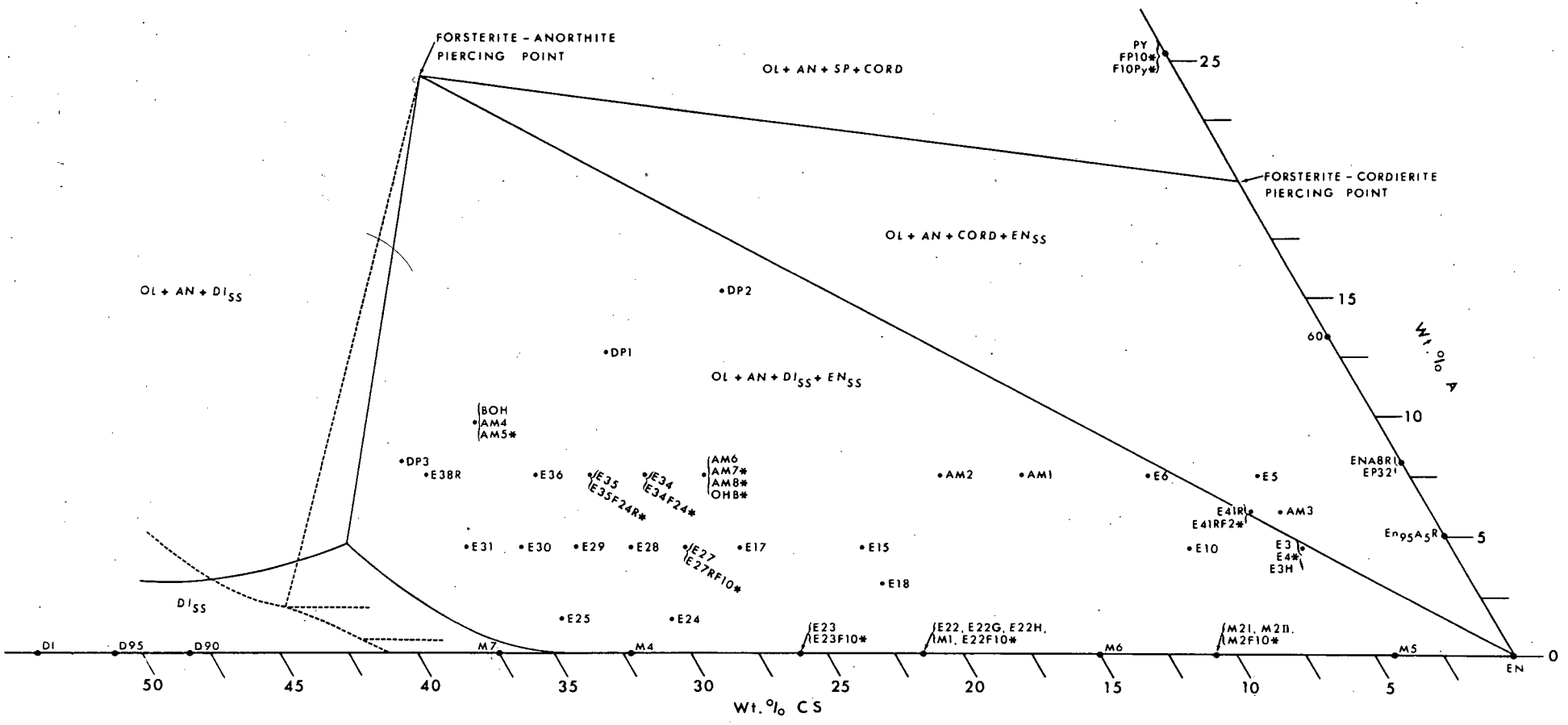
FORSTERITE - ANORTHITE
PIERCING POINT
OL + AN + SP + CORD
PY
FP10*
F10Py*
25
FORSTERITE - CORDIERITE
PIERCING POINT
OL + AN + CORD + EN$_{SS}$
OL + AN + DI$_{SS}$
DP2
15
60
DP1
OL + AN + DI$_{SS}$ + EN$_{SS}$
Wt. % A
BOH
AM4
AM5*
10
DP3
E38R
E36
E35
E35F24R*
E34
E34F24*
AM6
AM7*
AM8*
OHB*
AM2
AM1
E6
E5
ENA8R1
EP32'
E41R
E41RF2*
AM3
En$_{95}$A$_5$R
5
E31
E30
E29
E28
E27
E27RF10*
E17
E15
E10
E3
E4*
E3H
E18
DI$_{SS}$
E25
E24
E23
E23F10*
E22, E22G, E22H,
M1, E22F10*
M21, M2D,
M2F10*
DI
D95
D90
M7
M4
M6
M5
EN
0
50
45
40
35
30
25
20
15
10
5
Wt. % CS

TABLE A.2.5

Details of charges with bulk compositions in the system C-M-A-S-N

Charge No.	Z-HG	Z-GL	Z-MG	Z10	Z20	JDT
Starting Material	Gel	Glass	Gel mixture	Gel	Gel	Gel
Comp. (% oxides)						
C	8.36	↑	↑	9.42	10.29	-
M	19.54	|	|	16.93	14.80	-
A	17.10	as	as	19.27	21.04	25.22
S	51.55			50.47	49.61	49.45
N	3.47	for	for	3.91	4.26	15.33
Comp. (% norm. mins)		Z-HG	Z-HG			
Olivine	31.44	|	|	26.59	22.61	
Hypersthene	0.04	|	|	-	-	
Nepheline	-	|	|	4.51	8.12	
Diopside	8.09	|	|	9.11	9.93	
Anorthite	31.08	|	|	35.03	38.29	
Albite	29.36	↓	↓	24.77	21.05	

All materials were kindly donated by staff at the Grant Institute of Geology, Edinburgh.

The compositions of the materials are expressed as weight % oxides and as weight % C.I.P.W. normative minerals.

in Appendix table A.2.5. The mixed gel Z-MG is a mechanical mixture of the three gels JDT (composition NAS_4), PY (composition M_3AS_3) and DR (composition CMS_2) in the molecular ratio $DR_4PY_3JDT_{1.5}$.

A.2.3 Crystal phases in starting materials

Compositions in the system C-M-A-S and its subsystems

Superimposed on the grid of the projected positions of bulk compositions in fig. A.2.1 are the 1 atmosphere sub-solidus phase field boundaries for compositions in the plane CS-MS-A. The positions of these boundaries were taken from O'Hara (1969) and refer to the compositions in the relevant phase assemblage at a temperature just below the solidus of that particular assemblage. This phase diagram is based on experiments on devitrified glass charges.

The immediate sub-solidus, 1 atmosphere phase assemblage of all the Na_2O-free synthetic bulk compositions used in the present study can be obtained from this phase diagram (fig. A.2.1). All charge compositions which do not lie in the plane CS-MS-A have been projected from forsterite. With the exception of compositions on the join CMS_2-MS, olivine is a 1 atmosphere sub-solidus phase for all charge compositions in the plane CS-MS-A, and for those which have been projected into the plane from forsterite. The sub-solidus phase assemblages for all aluminous bulk compositions used in this study are thus given by the phase assemblages indicated for the projected compositions in the plane CS-MS-A. Compositions on the join CMS_2-MS contain no olivine in their 1 atmosphere sub-solidus assemblages (Boyd and Schairer, 1964); bulk compositions in the system M_2S-MS-CMS_2 lie in the 1 atmosphere sub-solidus phase

fields of olivine plus one or two pyroxenes, at least at 1350°C (Biggar and O'Hara, 1969b, fig. 6).

The phase diagram shown in fig. A.2.1, however, only approximately describes the phases present in the gel charges used in this study because:-

(i) None of the charges had their final heat treatment under precisely the conditions relevant to the phase assemblages shown in fig. A.2.1.

(ii) The phase diagram of O'Hara (1969) shown in fig. A.2.1 is based on experiments on recrystallized glass whereas the starting materials used here were gels. Biggar (1969, fig. 15) has reinvestigated the sub-solidus crystallization products of diopside-rich, Al_2O_3-bearing compositions in the plane CS-MS-A using gels as starting materials. His revised form of the phase diagram is also shown in fig. A.2.1.

(iii) Very few of the starting materials, even the so-called "recrystallized gels", completely recrystallized during their final heat treatment. The crystals in the starting materials may differ from those predicted in fig. A.2.1 both in terms of phases present and in the extent of solid solutions. It has been found that in the early stages of low pressure recrystallization, gels nucleate a large range of crystal species because of their high free energy (Biggar and O'Hara, 1969a). It is therefore expected that a gel charge will have nucleated all the phases indicated in fig. A.2.1 as constituting its equilibrium sub-solidus assemblage, but additional metastable phases may be present. (All recrystallized gel charges in which no unrecrystallized gel was identified optically are

distinguished in Appendix table A.2.1 by the remark "total recrystallization".)

Many of the charges used in the present study were analysed by x-ray diffraction techniques to ascertain how closely their constituent phases agreed with those predicted from fig. A.2.1. The charges chosen for analysis were those most diverse in bulk composition and low pressure pre-run thermal treatment. Phase identification of the charges was carried out using CrKα radiation as described in Appendix A.3.3. Diffraction patterns for most of the charges were obtained for the angular range 14-60°2θ CrKα. The phases identified are reported in Appendix table A.2.1. The low pressure polymorphs of enstatite solid solution (en_{ss}) have not been distinguished.

Although the phase diagram shown in fig. A.2.1 can be used as a guide to the main crystal species present in the gel charges, additional phases, present in too small a proportion to be identified by the analytical techniques used, may also be present. Amorphous SiO_2 is believed to be a constituent of most gels which were not completely recrystallized.

All three soda-free glasses (E3H, E22H, E22G) used in this study devitrified during the pre-run drying technique. The x-ray diffraction pattern of dried charge E22H showed broad, diffuse peaks of clinopyroxene. If orthopyroxene was present it occurred in too small a proportion to register on the poor x-ray diffraction pattern obtained for this charge.

Compositions in the system C-M-A-S-N

The glass Z-GL did not devitrify during the charge drying technique.

The crystal phases identified in the gel starting materials were:-

Z-HG : plagioclase, clinopyroxene, olivine

Z10 : plagioclase, clinopyroxene, olivine, nepheline

Z20 : clinopyroxene, nepheline

JDT : nepheline

These phases were identified by x-ray diffraction analysis using CrKα and CuKα radiation as described in Appendix A.3.3.

A.2.4 Grain size of starting material

One of the features of gel charges is their very small crystal size, and hence large free energy. In this respect they differ markedly from glass charges which normally form large crystals on devitrification (Biggar and O'Hara, 1969a).

The diameter of the largest crystals in these partially crystalline gels rarely exceeded 1μ. The recrystallized gels were a mass of minute crystals with rare patches of unrecrystallized gel. The diameter of the largest crystals in the recrystallized gels varied from $<1\mu$ in the most calcic compositions to 5-8μ in more magnesian compositions though crystals as large as 8μ were very rare.

The devitrification products of the dried glasses consisted of ultra-fine-grained crystals ($< 0.1\mu$).

All charges were finely ground under acetone in an agate mortar to a charge particle size of $< 5\mu$.

APPENDIX A.3

RUN PRODUCT ANALYSIS: SYNTHETIC CHARGES

A.3.1 Introduction

At the end of an experiment the recrystallized charge was removed from the platinum capsule and ground under acetone using an agate mortar and pestle. Some of the powder was reserved for optical analysis; the remainder was ground even finer for analysis by x-ray diffraction techniques. Small chips of the unground recrystallized charge obtained from a few of the runs were retained for electron microprobe analysis.

In certain of the hyper-solidus runs it was necessary to demonstrate that crystal sinking had occurred through the liquid. In such cases the contents of the capsule were divided into top, middle and basal portions before crushing; each portion was analysed separately.

A.3.2 Optical analysis

The ground run product was mounted in an oil of refractive index equal to 1.657 for optical analysis.

The criteria used to distinguish optically between the different primary (as opposed to quench) crystalline phases are listed in Appendix table A.3.1. The mixture of phases referred to as "garnet-olivine intergrowths" is described in the text (section 4.2.1). Sub-solidus runs at temperatures of less than 1450-1525^{o}C usually yielded crystallization products which were too fine-grained to be able to distinguish between clinopyroxene and orthopyroxene.

TABLE A.3.1

Criteria used to identify phases optically

Phase	Refractive Index	Birefringence	Angle of Extinction	Texture
Clinopyroxene	~1.657. Increases with increasing Ca/(Ca+Mg) ratio	Moderate	$>0^{\circ}$	Equidimensional, anhedral crystals
Orthopyroxene	~ 1.657	Low	0°	Euhedral, elongated tabular crystals; but equidimensional anhedral crystals at subsolidus temperatures $<1450\text{-}1525^{\circ}C$.
Olivine	Slightly <1.657	High	0°	Small anhedral crystals to large euhedral tabular crystals
Garnet	>1.657	Isotropic	-	Variable from large dodecahedra to small anhedral crystals barely distinguishable optically ($<0.1\mu$). Large crystals frequently full of inclusions (particularly in the C-M-A-S-N system).
Amphibole	<1.657 (variable)	Moderate to high	$>0^{\circ}$ Variable, usually small	Euhedral elongated crystals

Liquid was identified by the presence in the run product of glass or quench crystals formed from the liquid on quenching the run. At temperatures just above that of the solidus the small amounts of liquid were represented by a thin film of glass around crystal margins. Quench crystals were identifiable as such when they had the following textures:-

(i) feathery sprays of pyroxene containing much interstitial glass.

(ii) clinopyroxene or amphibole overgrowths on orthopyroxene crystals. The overgrowth was distinguishable by the difference in the extinction angle of the quenched crystal compared with that of the enclosed primary crystal.

(iii) orthopyroxene overgrowths on orthopyroxene crystals. These were distinguishable by the presence of sparse quench crystals or more frequent glassy inclusions in the overgrowth; by the presence of a discontinuous thin film of glass around the primary crystal; or by the presence of a very diffuse crystal outline merging into the surrounding feathery quench crystals and glass.

(iv) acicular amphibole crystals frequently enclosing glass spherules or quench crystals. All or part of this texture may be formed from silicate material quenched from the vapour phase rather than from the liquid.

(v) fibrous mats of chlorite in Na_2O-bearing run products containing less than 5% primary crystals.

The presence of a vapour phase in a hydrous charge at high pressure could not be identified by the usual optical criteria as discussed in section 10.3.5. The presence of a vapour phase at

high temperature and pressure could only be determined by the form of the phase diagram.

A.3.3 X-ray diffraction analysis I

A thin layer of the powdered run product was caked onto a glass slide using shellac or acetone.

The products of runs on the Na_2O-bearing charges were analysed with CuKα radiation. Products of runs on the Na_2O-free synthetic compositions were usually analysed with CrKα radiation, but also with CuKα radiation when greater peak intensity was required. The use of CrKα radiation was preferred for the identification and analysis of pyroxenes and olivines synthesized from compositions in the system C-M-A-S and its subsystems because CrKα radiation has a longer wavelength (λ = 2.291 Å) than CuKα radiation (λ = 1.542 Å). The longer wavelength ensures:-

(i) greater precision in the measurement of the d-spacings of reflections.

(ii) greater separation of closely spaced reflections. This was important in the present study in which a search was made for a field of two clinopyroxenes. It was also necessary to use CrKα radiation to separate the major peaks of orthopyroxene from those of the magnesium-rich clinopyroxenes crystallized in many of these experiments. This was difficult using CuKα radiation if one of the two phases was much more abundant than the other.

CuKα radiation was generated at 28 mA and 44 kV in a Philips machine using a nickel filter to remove CuKβ radiation. Radiation from the chromium source was generated at 30 mA and 50 kV in a

Philips machine. The path of the radiation from the chromium source was held under vacuum to reduce the rapid attenuation of this soft radiation. CrKα radiation was used for phase identification, CrKβ radiation having been removed with a vanadium filter. However, the use of the vanadium filter markedly reduces the intensity of reflections on the x-ray diffraction patterns. For the determination of clinopyroxene compositions from the $^{\circ}2\theta$ value of certain reflections, the filter was removed if the intensity of the relevant peaks was too low. The peak positions of the relevant reflections of several run products were measured using both CrKα radiation and unfiltered radiation from a chromium source. The measured $^{\circ}2\theta$ value of any given reflection was the same within the precision limits of the determination whether filtered or unfiltered radiation was used.

Phase identification using CuKα radiation was carried out using a goniometer scanning speed of $2^{\circ}2\theta$/min. and a chart speed of 120 cm./hr. Phase identification with CrKα radiation was carried out using a goniometer scanning speed of $1^{\circ}2\theta$/min. and a chart speed of 60 cm./hr. Crystal phases were identified from the d-spacings of their characteristic hkl reflections listed in Appendix table A.3.2.

The products of runs on Na_2O-bearing charges could not be analysed in detail using x-ray diffraction methods because most of the critical runs were carried out under near-liquidus conditions and the run products contained a high proportion of quench crystals which complicated the analysis of the x-ray diffraction patterns. The x-ray diffraction patterns of such run products were only used to

TABLE A.3.2

List of hkl reflections used to identify phases in run products and starting materials using x-ray diffraction techniques. The hkl reflections of each phase are followed, in brackets, by their d-spacings (in Angstrom units).

Clinopyroxene* (CMS_2) : 220 (3.23); $\bar{2}21$ (2.992); 310 (2.951); $\bar{3}11$ (2.894); **

Orthopyroxene* (MS) : 420 (3.17); 221 (3.15) [Note: these two reflections are separable using CrKα radiation]; 321 (2.936); 610 (2.87); 131 (2.53); 202 (2.49); 521 (2.468)

Olivine* (M_2S) : 130 (2.764); 112, 200 (2.458)

Garnet* (M_3AS_3) : 400 (2.865); 420 (2.562); 642 (1.531)

Clinoamphibole (composition undetermined; d(Å) of major observed reflections given) : 110 (8.4); 310 (3.12)

Chlorite (composition undetermined but similar to that of penninite; d(Å) of major observed reflections given) : 001 (14.2); 003 (4.95); 004 (3.7)

Quartz : 100 (4.26); 101 (3.34)

Phases identified in starting materials only:-

Plagioclase* (CAS_2) : $\bar{1}30$, $\bar{1}\bar{3}1$ (3.78); 130, $\bar{1}\bar{3}2$ (3.62); $\bar{2}20$ (3.26); 040 (3.21); 004 (3.18); $\bar{2}04$ (3.19); 220 (3.12)

Cordierite : 020 (8.52); 110 (8.45); 112 (4.09); 151, 241 (3.04)

TABLE A.3.2 (ctd.)

Nepheline	:	201 (3.83); 210 (3.26); 202 (3.00)
Periclase	:	200 (2.11)
Spinel	:	220 (2.86); 311 (2.44); 400 (2.02); 440 (1.43)

* d-spacings given for the chemical end member (composition given in brackets) of a compositionally variable phase.

** The $^{o}2\theta$ values of the $\bar{1}31$, $\bar{2}02$, 311 and multiple peak ($\bar{1}12$, 002, 221) reflections of the magnesium-rich clinopyroxenes crystallized in this study are shown in figs. 3.6 and 3.7.

confirm the presence of certain phases which had been identified optically. The phases identified from the x-ray diffraction patterns are reported in Appendix tables A.9.9 and A.9.10; these do not necessarily represent primary crystals.

The x-ray diffraction patterns of the sub-solidus run products of the Na_2O-free charges were also used to determine clinopyroxene compositions, the presence of variation in olivine and orthopyroxene solid solutions, and the relative proportions of certain phases in a run product. For these purposes the goniometer scanning speed was reduced to $\frac{1}{4}^{o}2\theta$/min. and the chart speed was 150 mm./hr. For all detailed measurements of peak position and peak height, 6-10 oscillations of the relevant part of the x-ray diffraction pattern were made and the mean of the 6-10 oscillations was obtained. The mean value of the peak position is quoted in the tables of run results, and the scatter of the 6-10 measurements about this mean is expressed as $\pm 2\hat{\sigma}$ (in $^{o}2\theta$). $\hat{\sigma}$ (the best estimate of the standard deviation) is the standard deviation multiplied by $\sqrt{\frac{n}{(n-1)}}$ where n is the number of measurements. The best estimate of the standard deviation was used because the number of measurements made was small. The extent of the scatter is quoted at the 95% probability level.

The position, in $^{o}2\theta$, of a peak was measured at two-thirds of its height from the base of the peak. The peak position was taken to be the median position of the two limbs of the peak at this height. Where the absolute $^{o}2\theta$ value of a reflection was required, the relevant peak was measured against the NaCl 200 (d = 2.821 Å) reflection. Sufficient AnalaR NaCl was ground into the powdered run product to produce a 200 reflection of comparable intensity to that of the

reflection under consideration. With the goniometer scanning speed and chart speed used, $1^{\circ}2\theta$ CrKα covered 10 mm. on the chart, and the position of a peak could be read to the nearest $0.01^{\circ}2\theta$ CrKα .

The intensity of a reflection was taken to be proportional to its peak height which was measured as the height from the background level of the x-ray diffraction pattern to the top of the peak.

Further details of the measurements made are given in the following four sub-sections (A.3.4 to A.3.7).

A.3.4 X-ray diffraction analysis II: determination of clinopyroxene composition

The composition of clinopyroxenes crystallized in the systems C-M-S and C-M-A-S were determined from the position, in terms of $^{\circ}2\theta$, of certain reflections on their x-ray diffraction powder patterns. The variation of the position of these reflections with composition was known by calibrating against the $^{\circ}2\theta$ values obtained from the x-ray diffraction patterns of clinopyroxenes of known composition. The clinopyroxenes used for calibration purposes were synthesized at high temperature and pressure by crystallizing a known bulk composition within the single phase field of clinopyroxene. These calibration clinopyroxenes were synthesized at pressure and temperature conditions similar to those of the investigation experiments in the hope that the detailed structural state, and hence the x-ray diffraction patterns, of the calibration clinopyroxenes was the same as that of the clinopyroxenes of unknown composition with which they were compared.

The parameters used for the clinopyroxene composition

determinations were the absolute $^{o}2\theta$ values of the 220 and $\bar{2}21$ reflections, and the difference in $^{o}2\theta$ between the positions of the 310 and $\bar{3}11$ reflections (referred to as the $310 \wedge \bar{3}11$ parameter). These reflections were chosen because they are of high intensity and because the three parameters are sensitive to changes of clinopyroxene composition in different directions. In addition, the four reflections involved were free from interference by other high intensity peaks in almost all the run products investigated. The $^{o}2\theta$ value of the $310 \wedge \bar{3}11$ parameter decreases as the Mg/(Ca+Mg) ratio of the clinopyroxene increases; the 310 and $\bar{3}11$ reflections are indistinguishable on the x-ray diffraction patterns, obtained using CrKα radiation, for the clinopyroxene of composition $di_{50}en_{50}$ and for Al_2O_3-bearing clinopyroxenes with slightly greater Ca/(Ca+Mg) ratios.

The $^{o}2\theta$ CrKα values of these three parameters were measured as described above (see Appendix A.3.3), and the mean value of 6-10 measurements was obtained. Further series of oscillations were carried out on two of the run products to determine to what extent the mean values of the three parameters were reproducible in other series of oscillations, i.e. to what extent the mean value of 6-10 measurements approached the true $^{o}2\theta$ value of the relevant parameter. Appendix table A.3.3 presents the results of this study.

Two run products were chosen, one (E23/147) containing one phase alone and having a very clear x-ray diffraction trace with sharp, intense clinopyroxene peaks; the other (AM6R/251) containing a large amount of orthopyroxene as well as clinopyroxene and having clinopyroxene peaks which were much less sharp. For each run

TABLE A.3.3

Results of a reproducibility study on pyroxene x-ray diffraction pattern parameters

Run No.	Charge No.	Parameter ($^{o}2\theta$)	$\hat{\sigma}$ of the $^{o}2\theta$ of the parameter for each series of 6-7 oscillations						V($\hat{\sigma}$)	W($2\hat{\sigma}$)	X($3\hat{\sigma}$)	Y(wt.%CS for $3\hat{\sigma}$)	Z(wt.%A for $3\hat{\sigma}$)
			1	2	3	4	5	6					
147	E23	220(cpx)	0.020	0.025	0.017	0.013	0.013	-	0.0026	0.0053	0.0079	0.5	-
251	AM6R	220(cpx)	0.026	0.019	0.017	0.016	0.014	0.018	0.0090	0.0181	0.0272	1.5	<1.0
251	AM6R	$\bar{2}21$(cpx)	0.013	0.011	0.013	0.014	0.015	0.017	0.0081	0.0163	0.0244	3	1.2
251	AM6R	310 ∧ $\bar{3}11$ (cpx)	0.010	0.025	0.016	0.012	0.017	0.015	0.0137	0.0274	0.0411	1	1.5
282	ENA8R	A*(opx)	0.014	0.016	0.018	0.024	0.024	0.015	0.0058	0.0116	0.0173	-	-
		B*(opx)	0.012	0.014	0.017	0.010	0.014	0.008	0.0037	0.0074	0.0111	-	-

Notes 1 * Parameters A and B are described in the footnote to table A.9.8.

2 Columns V, W and X are the values of the best estimate of the standard deviation ($\hat{\sigma}$), $2\hat{\sigma}$ and $3\hat{\sigma}$ respectively of the mean value of the 5-6 mean values whose $\hat{\sigma}$ are given in columns 1-6.
Columns Y and Z list the weight % $CaO.SiO_2$ and the weight % Al_2O_3 respectively which are equivalent to the values of the $3\hat{\sigma}$ (column X) for each of the clinopyroxene parameters of the run products of charges AM6R and E23.
The relationship between $^{o}2\theta$ and $CaO.SiO_2$ and Al_2O_3 components is shown in Appendix fig. A.3.1.

3 The clinopyroxene and orthopyroxene parameters are expressed in $^{o}2\theta$ CrKα and $^{o}2\theta$ CuKα respectively.

product the series of 6-7 oscillations was made five (E23/147) or six (AM6R/251) times, leaving an interval of at least one day between each series of oscillations. The $\hat{\sigma}$ (in $^{o}2\theta$) of each series of 6-7 oscillations is quoted in columns 1-6. Columns V, W and X give the $^{o}2\theta$ values of the $\hat{\sigma}$, $2\hat{\sigma}$ and $3\hat{\sigma}$ respectively of the average of the 5 or 6 mean values. The $\hat{\sigma}$ of the mean values is much smaller for the 220 reflection of the good pattern (E23/147) than for the 220 reflection of the bad pattern (AM6R/251). Columns Y and Z express the standard deviation of the mean values in terms of clinopyroxene composition as indicated by the x-ray diffraction pattern parameter determinative curves and grid discussed below.

Clinopyroxenes in the system C-M-S

The clinopyroxenes crystallized in the equilibria cpx+opx$\pm$ol and cpx+opx+qz in the system C-M-S at 20 and 30 kb exhibit non-stoichiometry, i.e. their ratio of (C+M):S is not 1:1 (see Chapter 3). The compositions of these clinopyroxenes cannot therefore be expressed, as can stoichiometric clinopyroxenes, in terms of two components, viz. CS and MS. The compositions cannot therefore be uniquely determined from knowledge of only one parameter. In this study the compositions of the C-M-S clinopyroxenes have not been uniquely determined because only one parameter has been used to indicate variation of composition. This parameter is the $^{o}2\theta$ value of the 220 reflection. It is expected that the extent of non-stoichiometry in this system is small (e.g. Mori and Green, 1975b) and that the composition of a non-stoichiometric clinopyroxene with a given $^{o}2\theta$ 220 value is not significantly different from the

composition of the stoichiometric clinopyroxene with the same $^{o}2\theta$ 220 value. Variation of the position of the 220 reflection with composition has only been investigated for stoichiometric clinopyroxenes. The $^{o}2\theta$ 220 value of clinopyroxenes crystallized in this study in equilibrium with orthopyroxene were compared with those of the stoichiometric clinopyroxenes. The compositions of enstatite-saturated clinopyroxenes were assumed to be those of the stoichiometric clinopyroxenes with the same $^{o}2\theta$ 220 values. Such compositions are therefore inaccurately expressed in the text and tables as $di_x en_{100-x}$ (or just as di_x). The uncertainty in the compositions of clinopyroxenes as determined from this one parameter does not affect the conclusions of the high pressure experimental study of C-M-S clinopyroxenes (Chapter 3).

The compositions, synthesis conditions and the $^{o}2\theta$ CuKα 220 value (obtained, however, using CrKα radiation) of the clinopyroxenes used for calibrating the composition determinative curve are shown in Appendix table A.3.4. The $^{o}2\theta$ 220 values of all clinopyroxenes richer in magnesium than di_{70} lie within $0.01\,^{o}2\theta$ CuKα, equivalent to 1.5% diopside, of the determinative curve derived by Davis and Boyd (1966) for clinopyroxenes on the join CMS_2-M_2S_2 (fig. 3.2). The difference is within the precision limits of the determinations. The curve of Davis and Boyd is, moreover, a very good fit to the new $^{o}2\theta$ 220 measurements. The Davis and Boyd curve was therefore used in this study to determine the composition of clinopyroxenes which use of the curve indicated to be richer in enstatite than di_{70}.

The results of a reproducibility study on the clinopyroxene 220 reflection were presented in Appendix table A.3.3 and discussed

TABLE A.3.4

X-ray parameters of clinopyroxenes crystallized alone as single phase assemblages in runs on compositions in the system C-M-S

Charge No.	Run No.	Pressure (kb)	Temp. (^{o}C)	Mol.% CMS_2* in Cpx	$^{o}2\theta$ CuKα Cpx 220	$^{o}2\theta$ CrKα Cpx $\bar{2}21$
M2I	148	20	1638	18.82	28.00 ±0.007	45.020±0.028
E22	146	20	1621	38.20	27.875±0.019	-
E22G	84	20	1621	38.20	27.875±0.026	44.843±0.029
M1	62	20	1614	38.20	27.86 ±0.024	44.832±0.032
E23	147	20	1620	46.53	27.825±0.003	44.824±0.022
M4	131	30	1548	58.17	27.73 ±0.017	44.890±0.017
M7	196	30	1500	67.36	27.675±0.017	44.929±0.043
D90	177	30	1680	89.30	27.58 ±0.013	-
D90	200	30	1400	89.30	27.59 ±0.011	-
D95	182	30	1680	94.74	27.57 ±0.013	-
D95	184	30	1600	94.74	27.56 ±0.018	-

* Mol.% CMS_2 refers to the mol.% CMS_2 in the system CMS_2-M_2S_2

above. These suggest that clinopyroxene compositions are reproducible to ±1% diopside at the 99.7% confidence level for clear x-ray diffraction patterns of clinopyroxene-rich assemblages, and reproducible to ±3% diopside at the 99.7% confidence level for poor x-ray diffraction patterns of assemblages containing much orthopyroxene as well as clinopyroxene.

Clinopyroxenes in the system C-M-A-S

Clinopyroxenes with compositions in this system which were crystallized in the present work exhibit non-stoichiometry (see Chapter 4). Three parameters are therefore required to uniquely determine their composition. In erecting and using a composition determinative grid for C-M-A-S clinopyroxenes the degree of non-stoichiometry has been assumed to be small. Clinopyroxene compositions are assumed to lie in the plane CS-MS-A in which case two parameters only are required to uniquely determine clinopyroxene compositions.

The compositions, synthesis conditions and x-ray diffraction parameters of the clinopyroxenes used to calibrate the composition determinative grid are given in Appendix table A.3.5. The clinopyroxenes used were synthesized in phase assemblages which sometimes contained traces of olivine indicating that the synthesized clinopyroxenes were non-stoichiometric since the bulk compositions of the charges lay in the plane CS-MS-A. However, the amount of phases other than clinopyroxene present in these assemblages was very small ($< 0.1\%$) and the degree of non-stoichiometry of the clinopyroxenes was also therefore small.

TABLE A.3.5

X-ray diffraction parameters of clinopyroxenes crystallized alone as single phase assemblages in runs on compositions in the systems C-M-A-S and C-M-S. These parameters were used to draw up the x-ray determinative grid (Appendix fig. A.3.1)

Charge No.	Run No.	Pressure (kb)	Temp. (^{o}C)	Wt.%CS in Cpx	Wt.%Al_2O_3 in Cpx	$^{o}2\theta$ CrKα Cpx 220	$^{o}2\theta$ CrKα Cpx $\bar{2}21$	($^{o}2\theta$ CrKα Cpx 310) - ($^{o}2\theta$ CrKα Cpx $\bar{3}11$)
M7	196	30	1500	37.0	-	41.643 ±0.025	44.929 ±0.043	0.540 ±0.023
M4	131	30	1548	32.2	-	41.729 ±0.025	44.890 ±0.017	0.332 ±0.040
E23	147	20	1620	26.0	-	41.876 ±0.005	44.824 ±0.022	-
E22G	84	20	1621	21.5	-	41.950 ±0.039	44.843 ±0.029	-
E25	47	30	1547	34.0	1.5	41.754 ±0.030	44.949 ±0.035	0.405 ±0.024
E29	52	30	1548	32.0	4.5	41.887 ±0.037	44.998 ±0.024	0.294 ±0.038
E31	49	30	1548	36.0	4.5	41.822 ±0.049	45.034 ±0.030	0.473 ±0.014
E35	103	30	1600	30.0	7.5	41.993 ±0.018	45.062 ±0.030	~0.17

Three parameters of the x-ray diffraction pattern of clinopyroxene were used to erect the composition determinative grid. These were the $^{o}2\theta$ (310 $\wedge \bar{3}11$) value, and the absolute values of the 220 and the $\bar{2}11$ reflections. The composition determinative grid is shown in fig. A.3.1. Unique clinopyroxene compositions can be determined from this grid with the knowledge of only two of the three parameters.

A reproducibility study, described above, of the $^{o}2\theta$ values of these three parameters indicates that the reported composition of a clinopyroxene coexisting with a high proportion of orthopyroxene is reproducible to within 1% Al_2O_3 and 1% CS at the 99.7% confidence level when the $^{o}2\theta$ 220 and (310 $\wedge \bar{3}11$) parameters are used for composition determination. The error resulting from the neglect of non-stoichiometry is not considered significant since the value of the third parameter was almost always consistent, within the precision limits of the determination, with that indicated by the other two parameters using the composition grid.

For clinopyroxene compositions whose 310 and $\bar{3}11$ reflections lie closer than about $0.2^{o}2\theta$ CrKα, measurements of the $^{o}2\theta$ (310 $\wedge \bar{3}11$) parameter are unsatisfactory and only the $^{o}2\theta$ 220 and $\bar{2}21$ parameters could be used for composition determinations.

A.3.5 X-ray diffraction analysis III: determination of olivine composition

Absolute olivine compositions were not determined in this study but it was necessary to know whether olivine crystals synthesized in the various experiments showed any difference in their compositions.

FIGURE A.3.1

Composition determinative grid for clinopyroxenes with compositions in the plane CS-MS-A, using three x-ray diffraction pattern parameters of clinopyroxene solid solutions. The three parameters used are:-

(i) $^{o}2\theta$ CrKα Cpx 220 (shown as continuous lines)

(ii) $^{o}2\theta$ CrKα Cpx $\bar{2}21$ (shown as coarsely dashed lines)

(iii) $^{o}2\theta$ CrKα Cpx $(310 \wedge \bar{3}11)$ (shown as finely dashed lines)

The black dots represent the compositions of clinopyroxenes whose x-ray diffraction parameters were used to erect and calibrate this grid.

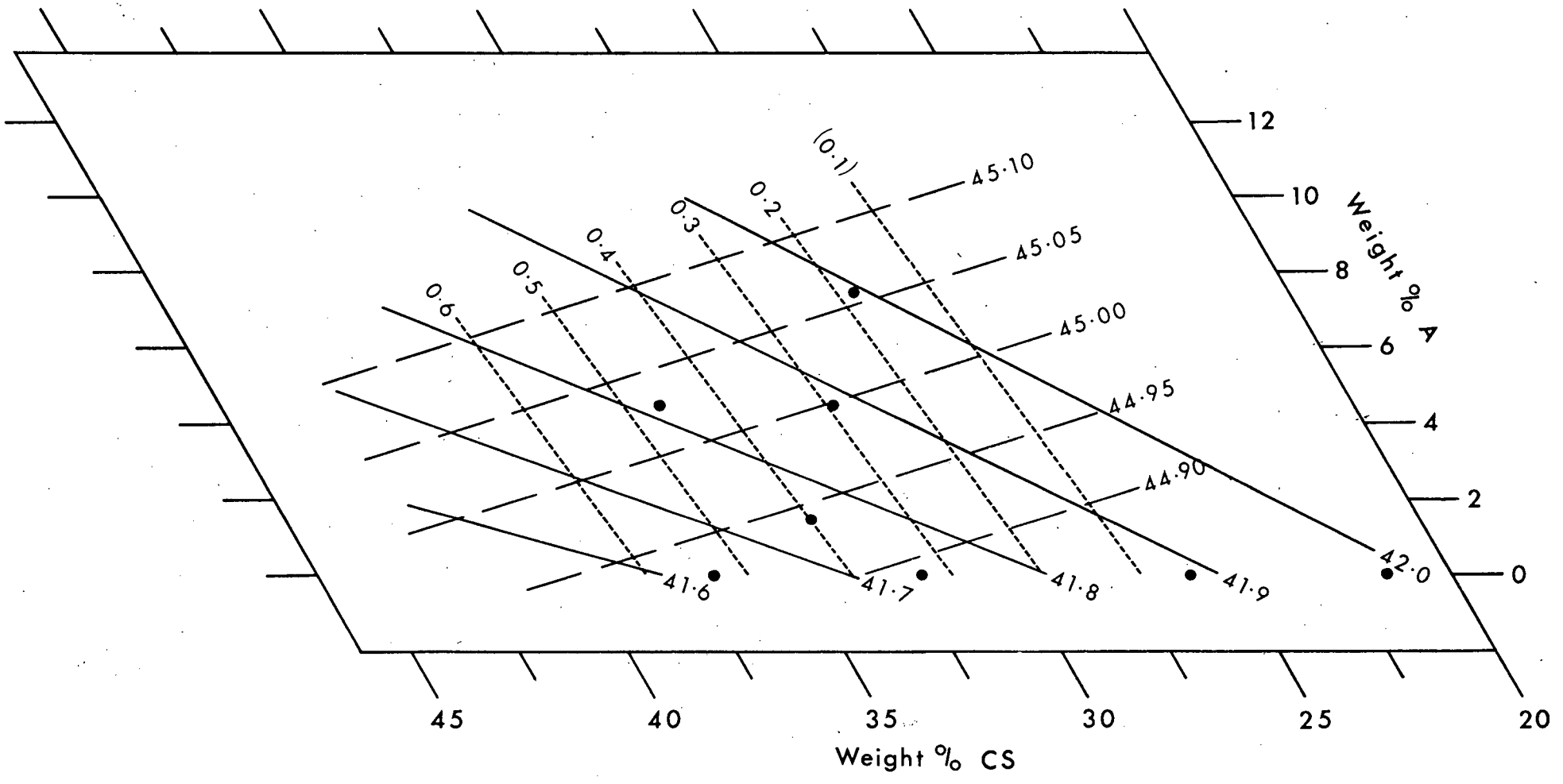
(0·1)
0·2
0·3
0·4
0·5
0·6
45·10
45·05
45·00
44·95
44·90
42·0
41·9
41·8
41·7
41·6
12
10
8
6
4
2
0
Weight % A
45
40
35
30
25
20
Weight % CS

The olivine 112 reflection showed the most variation for different run products and was therefore used for this purpose. The absolute $^{o}2\theta$ value of the 112 olivine reflection was determined using CrKα radiation.

A.3.6 X-ray diffraction analysis IV: determination of orthopyroxene composition

Boyd and England (1960) showed that two parameters of the x-ray diffraction traces of synthetic M-A-S orthopyroxenes were sensitive to changes of Al_2O_3 content. The parameters are:

(i) the difference between the two reflections whose d-spacings for pure orthoenstatite are 2.1143 Å and 2.0970 Å.

(ii) the difference between the two reflections whose d-spacings for pure orthoenstatite are 1.4826 Å and 1.4683 Å.

The $^{o}2\theta$ values of these parameters were measured in the present work, using CuKα radiation, for orthopyroxenes crystallized in the systems M-A-S and C-M-A-S. As a test of the reproducibility of the mean value of 6-10 measurements of the parameters, the series of measurements for run product ENA8R/282 was repeated using new x-ray diffraction patterns obtained on six consecutive days. The results of this reproducibility study, given in Appendix table A.3.3, show that the value of the parameter involving reflections with a d-spacing of about 1.4 Å were reproducible to within $0.017^{o}2\theta$ CuKα at the 99.7% confidence level. The value of the parameter involving the sharper and more intense reflections with a d-spacing of about 2.1 Å are reproducible to within $0.011^{o}2\theta$ CuKα at the 99.7% confidence level.

A.3.7 X-ray diffraction analysis V: determination of the relative abundance of pyroxenes and garnet

As an indication of the relative abundance of clinopyroxene and garnet in the run products of some C-M-A-S gels, measurements were made of the relative intensities of the clinopyroxene $\bar{1}31$ and the garnet 420 reflections which have similar d-spacings. The intensity (I) measurements were made from x-ray diffraction patterns obtained using CrKα radiation. The parameter $Icpx_{\bar{1}31}/Igt_{420}$ was taken to be the peak height of the clinopyroxene $\bar{1}31$ reflection divided by the peak height of the garnet 420 reflection. The value of this parameter for different run products was used only as a measure of the difference in the proportion clinopyroxene : garnet between various run products. A similar use was made of the relative intensity parameter $Iopx_{131}/Igt_{420}$.

A.3.8 Electron microprobe analysis

Attempts made to obtain clinopyroxene compositions directly by the use of the electron microprobe failed because of the very small size of the crystals in the products of even the highest temperature runs which were of interest. The technique of adding small quantities of H_2O to the charge to accelerate crystal growth was considered unsatisfactory for the reasons given in section 7.1.

The assemblages investigated here with the electron microprobe were the products of runs on the C-M-S charges E22 and M2I at 1520°C and 1565°C respectively. Both charges were held at high temperature for 4 hours, which is the maximum duration for reliable performance of Pt/Pt13Rh thermocouples at these temperatures. The crystallization

products of both charges are indicated by fig. 3.1 to be cpx+opx.

The assemblages were analysed with a Cambridge Microscan 5 instrument. The method of analysis and of correction of the raw data was similar to that described by Sweatman and Long (1969). The electron microprobe used is capable of analysing crystals with diameters as small as 5μ. Only the largest clinopyroxene crystals were chosen for analysis. Although these had diameters of 4-5μ, the spread of the analyses, in terms of CS/MS ratio, was large and possibly reflected the interfering effect of adjacent orthopyroxene crystals. Appendix table A.3.6 gives the compositional details of the clinopyroxene analyses with the highest and lowest Ca/(Ca+Mg) ratio for the product of the run on charge E22, and the highest Ca/(Ca+Mg) ratio for the product of the run on charge M2I. The clinopyroxene analysis with the lowest Ca/(Ca+Mg) ratio (for run product of charge E22) was clearly separated by a large compositional gap from the much less variable orthopyroxene analyses.

In view of the probable inclusion of parts of adjacent orthopyroxene crystals in the clinopyroxene analyses, it is reasonable to consider the clinopyroxene analysis with the highest Ca/(Ca+Mg) ratio as the closest approach to the actual composition of the clinopyroxene in an assemblage. Appendix table A.3.6 shows that the most calcic analysis is closely comparable to the composition of the enstatite-saturated clinopyroxene for charge E22 at 1520^{o}C as indicated by fig. 3.1. The most calcic of more than 25 analyses from the run product of M2I at 1565^{o}C is, however, very different from the composition, indicated by x-ray diffraction analysis, of the enstatite-saturated clinopyroxene crystallized from the same

TABLE A.3.6

Microprobe analyses of clinopyroxenes in the run products of C-M-S charges at 30 kb

Charge No.	Temp. (^{o}C)	Clinopyroxene analyses (wt.%)				Wt.% CMS_2 in Cpx	Wt.% CMS_2 in Cpx from fig. 3.1
		C	M	S	Total		
E22	1520	5.04	35.44	59.22	99.70	19	52
E22	1520	13.50	28.65	57.48	99.63	52	52
M2I	1565	14.04	28.79	58.70	101.53	54	41

composition at the same temperature (see fig. 3.1 and Appendix table A.3.6). The electron microprobe analysis indicates a much more calcic composition. The compositional spread obtained by electron microprobe analysis is therefore not only the result of the interfering effect of adjacent orthopyroxene crystals. It may be connected with crystal edge effects. Whatever the cause of the spread, the analyses obtained from the run product of charge M2I show that the procedure of selecting the most extreme electron microprobe analysis, here the composition with the highest Ca/(Ca+Mg) ratio, as being the closest approach to equilibrium is unjustified unless the cause of the analytical spread is known. For this reason Hensen's (1973) preferred analyses of experimentally crystallized natural clinopyroxenes may be in error.

A.3.9 Student's t test

Statistical comparisons between x-ray diffraction pattern parameter measurements were made using Student's t test.

APPENDIX A.4

COMPOSITION AND NATURE OF STARTING MATERIALS: NATURAL CHARGES

Three powdered whole rock samples from African kimberlite pipes were used in this study:-

Vissers 8 (sample number 1044) is an eclogite (gt+cpx assemblage) sample from the Vissers Pipe, Tanzania.

RV 4.1 (sample number 1058) is an eclogite sample from the Roberts Victor Pipe, South Africa.

1031 is an olivine-garnet websterite from Matsoku, Lesotho.

Detailed petrographic studies have not been carried out on any of these samples.

Compositions of the whole rocks and of their constituent phases were reported by O'Hara et al. (1975) and are presented in Appendix table A.4.1.

A study was also made of the sub-solidus behaviour of mixtures of clinopyroxene and orthopyroxene obtained as mineral separates from a garnet-lherzolite nodule (Edinburgh collection A3/10596) from the Wesselton mine, South Africa. This nodule is further described by Holmes (1936) as Wesselton No. 3, and by O'Hara and Yoder (1967). Starting materials for the present study were obtained by remixing the two pyroxenes in different proportions. The compositions of the two pyroxene end members and the bulk compositions of the mixtures are given in Appendix table A.4.2.

All starting materials were ground under acetone using an agate mortar and pestle to a grain diameter of $<8\mu$, although a few

TABLE A.4.1

Chemical analysis (in weight % oxides) of natural rock samples 1058, 1044 and 1031 and their constituent minerals

Sample No.	Mineral or Rock	SiO_2	TiO_2	Al_2O_3	Cr_2O_3	Fe_2O_3	FeO	MnO	NiO	MgO	CaO	Na_2O	K_2O	P_2O_5	H_2O^+
1058	Cpx	55.49	0.35	9.04	0.10	1.33	3.00	0.083	0.040	10.98	13.96	5.19	0.18	0.052	-
"	Gt	41.03	0.27	22.55	0.080	0.50	14.38	0.47	0.008	15.32	5.18	-	-	0.042	-
"	Rock	46.31	0.34	16.67	0.082	1.09	9.58	0.33	0.030	13.75	8.60	2.08	0.35	0.03	0.64
1044	Cpx	51.58	0.49	7.24	0.029	2.71	3.95	0.035	0.024	11.68	19.87	1.98	0.04	0.009	-
"	Gt	39.58	0.24	21.24	0.034	1.04	17.84	0.46	0.004	8.38	11.07	-	-	-	-
"	Rock	45.62	0.72	13.45	0.036	2.99	9.34	0.12	0.015	10.23	15.52	1.14	0.09	0.00	0.64
1031	Cpx	54.66	0.14	2.42	0.80	1.13	2.78	0.11	0.063	16.66	19.50	1.34	0.03	0.013	-
"	Opx	56.85	0.087	0.72	0.15	0.72	6.71	0.15	0.13	33.28	0.85	0.18	0.03	0.019	-
"	Gt	41.89	0.19	22.15	2.00	1.21	9.18	0.22	0.005	18.51	4.94	-	-	0.008	-
"	Rock	51.84	0.12	4.18	0.12	0.89	6.31	0.18	0.12	27.70	6.66	0.62	0.05	0.02	0.77

TABLE A.4.2

Composition	Cpx_{100}	$Cpx_{66.7}Opx_{33.3}$	$Cpx_{60}Opx_{40}$	$Cpx_{40}Opx_{60}$	$Cpx_{33.3}Opx_{66.7}$	$Cpx_{23}Opx_{77}$	Opx_{100}
Charge No. (this work)	A3/Di	*	A3/Di60	A3/Di40	*	A3/Di23	A3/En
Wt.% oxides							
SiO_2	53.90	54.97	55.19	55.83	56.05	56.38	57.12
TiO_2	0.20	0.16	0.15	0.12	0.11	0.10	0.07
Al_2O_3	2.40	2.11	2.05	1.88	1.82	1.73	1.53
Fe_2O_3	1.34	0.91	0.83	0.57	0.49	0.35	0.06
Cr_2O_3	1.55	1.09	1.00	0.72	0.63	0.49	0.17
FeO	1.28	2.52	2.77	3.51	3.76	4.14	5.00
MnO	0.08	0.09	0.09	0.10	0.10	0.10	0.11
NiO	0.05	0.07	0.07	0.08	0.08	0.09	0.10
CoO	tr.	0.001	0.001	0.002	0.002	0.002	0.003
MgO	16.39	23.00	24.32	28.29	29.61	31.66	36.22
CaO	20.57	13.79	12.44	8.37	7.02	4.92	0.24
Na_2O	1.80	1.20	1.08	0.72	0.60	0.41	n.d.
K_2O	0.02	0.01	0.01	0.01	0.01	tr.	n.d.
P_2O_5	0.01	0.01	0.01	0.01	0.01	0.01	0.01
Total	99.59	99.93	100.01	100.21	100.29	100.38	100.63
Fe/(Fe+Mg)	0.078	0.075	0.075	0.074	0.074	0.073	0.073
Ca/(Ca+Mg)	0.474	0.301	0.269	0.175	0.146	0.101	0.005

* Compositions of mixtures used by O'Hara and Yoder (1967)

tr = trace; n.d. = not determined

Compositions are taken from O'Hara and Yoder (1967, Table 4) or calculated from their analyses.

orthopyroxene crystals were longer than this. X-ray diffraction traces of the garnet-bearing assemblages were obtained before and after the pre-run drying procedure. The ratios of clinopyroxene to garnet peak intensities were comparable on the two patterns showing that there had been no significant breakdown of garnet during the drying procedure.

The compositions of these natural starting materials will not be the same as the bulk composition of the run product because of Fe-loss from the charge to the platinum capsules at these elevated temperatures. This problem has been discussed by Merrill and Wyllie (1973) who demonstrated considerable Fe-loss from near-liquidus assemblages. In the present study the durations of runs on natural charges were kept to a minimum to reduce the extent of Fe-loss.

APPENDIX A.5

RUN PRODUCT ANALYSIS:

NATURAL CHARGES

The products of runs on natural charges were analysed by optical and x-ray diffraction methods similar to those described in Appendix A.3 for analysing the run products of synthetic charges. CuKα radiation was used to analyse the run products of samples 1044, 1058 and 1031. Phase identification and clinopyroxene composition determination for the run products of the A3/10596 pyroxene mixes were carried out with radiation from a chromium source using methods similar to those described for the C-M-S and C-M-A-S composition run products (see Appendix A.3).

The compositions of the clinopyroxenes crystallized from the A3/10596 samples were determined from a comparison of the $^{o}2\theta$ values of their 220 reflection on the x-ray diffraction patterns with the value of this parameter for clinopyroxenes of known bulk composition synthesized by homogenizing mixtures of the A3/10596 end member pyroxenes at 1600^{o}C, 30 kb (experimental details in Appendix table A.9.11). The determinative curve showing the relationship between the $^{o}2\theta$ 220 value and clinopyroxene composition is presented in fig. A.5.1 (function A). A similar determinative curve for the peak representing the combined 310 and $\bar{3}11$ reflections is also shown (fig. A.5.1, function B). Function B was used for determining the composition of the clinopyroxene, crystallized at 1550^{o}C, whose $^{o}2\theta$ 220 value may have been affected by the close proximity of the orthopyroxene multiple reflection (420, 221) peak.

FIGURE A.5.1

The variation of the parameters $^{o}2\theta$ 220 cpx and $^{o}2\theta$ 310 cpx (actually the combined 310 and $\bar{3}11$ reflections) with composition for clinopyroxenes synthesized by homogenizing mixes of A3/Diopside and A3/Enstatite obtained from the garnet-lherzolite nodule A3/10596.

Functions A and B are for clinopyroxenes synthesized in the present work (data points shown by encircled asterisks); function C is for clinopyroxenes synthesized by O'Hara and Yoder (1967) (data points shown by black dots).

Measurements for functions A and B were made from x-ray diffraction patterns obtained using CrKα radiation; measurements for function C were made from x-ray diffraction patterns obtained using CuKα radiation.

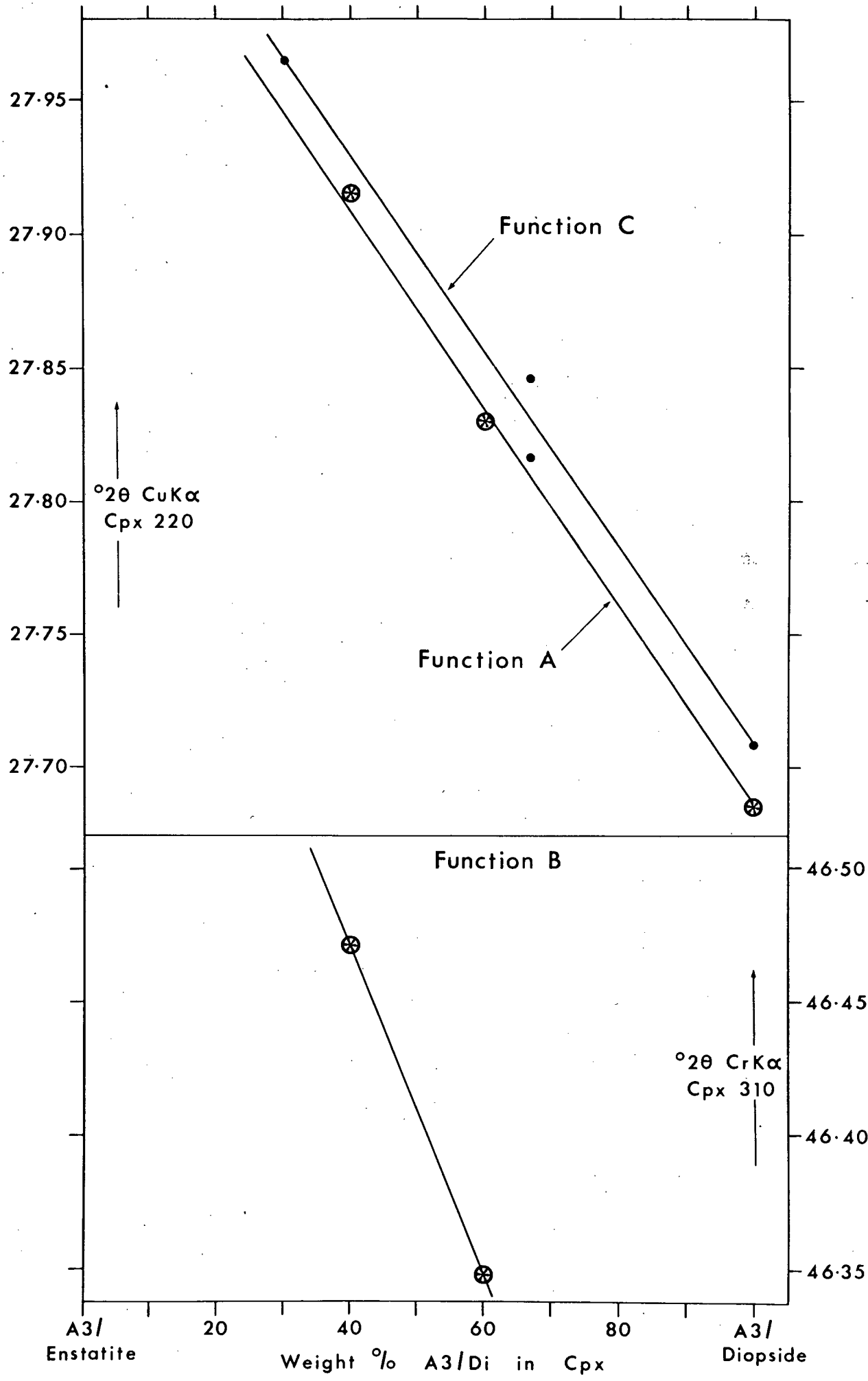
27·95
27·90
27·85
27·80
27·75
27·70
°2θ CuKα
Cpx 220
Function C
Function A
Function B
46·50
46·45
46·40
46·35
°2θ CrKα
Cpx 310
A3/
Enstatite
20
40
60
80
A3/
Diopside
Weight % A3/Di in Cpx

The data of O'Hara and Yoder (1967) which were plotted in fig. 5.2 were taken from their fig. 8. Also shown are the compositions of the clinopyroxenes crystallized in their experiments. These were estimated from the $^{o}2\theta$ values of the 220 clinopyroxene reflections (listed in O'Hara and Yoder (1967, table 8)) using an x-ray determinative curve (fig. A.5.1, function C) similar to that prepared from the new experimental results, but using instead the $^{o}2\theta$ 220 values reported by O'Hara and Yoder (1967, table 8) for clinopyroxenes made by homogenizing A3/10596 clinopyroxene and orthopyroxene mixes. The difference between functions A and C presumably reflects x-ray measuring technique differences since the functions are parallel and show the same discrepancy for the $^{o}2\theta$ 220 values of the unrecrystallized A3/10596 clinopyroxene end member.

The composition determinative functions A, B and C yield only approximate clinopyroxene compositions because a single parameter has been used to measure the variation of complex compositions. $^{o}2\theta$ 220 measurements are believed to be precise to within 0.005 or 0.02$^{o}2\theta$ CrKα (using the results of the reproducibility study, presented in Appendix table A.3.3), equivalent to about 1.5 or 5% diopside* (using the slope of function A), at the 95.5% confidence level for run products containing small or large amounts of orthopyroxene respectively.

---

* Actually the A3/10596 diopside, not CMS_2

APPENDIX A.6

A THERMODYNAMIC MODEL FOR THE SOLUBILITY OF AL_2O_3 IN ORTHOPYROXENE

A.6.1 Form of the thermodynamic equation used to relate compositions of coexisting orthopyroxenes and garnets to equilibration pressures and temperatures

This equation (equation 8.1 in section 8.4), derived by Wood and Banno (1973), is as follows:-

$$P = 1 + \frac{RT}{\Delta V_r}\left[\ln\left(\frac{\left(X_{Mg}^{M1}\right)opx\left(X_{Mg}^{M2}\right)^2 opx\left(X_{Al}^{M1}\right)opx}{\left(X_{Mg_1}^{gt}\right)^3}\right) - \frac{(\Delta G^o)_{1,T}}{RT}\right]$$

(equation A.6.1)

where temperature and pressure are expressed in ^oK and bars respectively; ΔV_r calories is the volume change for the equation; $R = 1.987$ cal K^{-1} mol^{-1}; $(\Delta G^o)_{1,T}$ is the standard free energy change of reaction A.6.1 at 1 bar and T^oK and refers to a standard state of pure phase at 1 bar and T^oK. $(\Delta G^o)_{1,T}$ is obtained from the equation:

$$(\Delta G^o)_{1,T} = \Delta H_1^o - T\Delta S^o$$

where H is expressed in cal mol^{-1} and S is expressed in cal K^{-1} mol^{-1}.

Given the assumption (Wood, 1974) that ΔV_r is constant at constant $\left(X_{Al}^{M1}\right)opx$, then at constant $\left(X_{Al}^{M1}\right)opx$ for compositions in the system M-A-S, equation A.6.1 is the equation for a straight line and may be expressed as:

$$P = \left(\frac{R\ln Z + \Delta S}{\Delta V_r}\right)T - \frac{\Delta H}{\Delta V_r} + 1$$

where $Z = \frac{\left(X_{Mg}^{M1}\right)_{opx}\left(X_{Mg}^{M2}\right)^2_{opx}\left(X_{Al}^{M1}\right)_{opx}}{\left(X_{Mg_1}^{gt}\right)^3}$

ΔS here controls the slope of the isopleths on a pressure/temperature section, and ΔH controls their intercept on the pressure axis and their spacing.

A.6.2 Derivation of the thermodynamic model for Al_2O_3 solubility in orthopyroxene given in fig. 8.2

Values for ΔH_1^o and ΔS^o were obtained by fitting equation A.6.1 to the results of runs at 27, 30 and 35 kb on gel charge AM3 which define the position of the 6% isopleth for Al_2O_3 solubility in orthopyroxene in equilibrium with garnet and clinopyroxene (see fig. 7.2). At all three pressures the mid point of the temperature bracket was taken as the temperature at which the Al_2O_3 content of the orthopyroxene is 6%. The determination of ΔH and ΔS was limited to the results for charge AM3 because of the failure to reach stable equilibrium in experiments on these gel charges. It was considered that the use of results from a single starting material would produce a closer approach to the equilibrium value for ΔS, which controls the slope of the Al_2O_3 isopleths on a pressure/temperature section.

Values of ΔV_r were obtained from Wood (1974).

Ca/(Ca+Mg) ratios of 0.045 and 0.15 for coexisting orthopyroxene and garnet respectively were used for all three data points, and in all calculations to determine the position of the 4.5 and 6% Al_2O_3 isopleths shown in fig. 8.2 for compositions in C-M-A-S.

Three sets of values for ΔH and ΔS were obtained by solving the three pairs of equations derived by substituting information from the three data points for charge AM3 into equation A.6.1. The three values were averaged and the mean ΔH^{o} (-14,777 cal mol^{-1}) and mean ΔS^{o} (-7.5 cal K^{-1} mol^{-1}) values were used in equation A.6.1 to calculate Al_2O_3 solubilities in orthopyroxene in equilibrium with garnet for compositions in the systems C-M-A-S and M-A-S at various pressures and temperatures. The use of the average values for ΔH_1^{o} and ΔS^{o} resulted in a maximum pressure error of 0.3 kb for the data points on the 6% Al_2O_3 isopleth used to derive the ΔH and ΔS values.

The assumptions made in the use of equation A.6.1 to derive values for ΔH_1^{o} and ΔS^{o} and from these to calculate the Al_2O_3 isopleths given in fig. 8.2 are the same assumptions as made in deriving the models of Wood and Banno (1973) and Wood (1974). Some of these assumptions are discussed in section 8.4. In particular, the value of $(\Delta G^{o})_{1,T}$ in equation A.6.1 is actually the value of $(\Delta G^{o})_{P,T}$ where P is the pressure of the experiment used to determine values of ΔH^{o} and ΔS^{o}.

Further sources of error in the calculation of these isopleths are:-

(i) Erroneous values for the Ca/(Ca+Mg) ratios of coexisting orthopyroxenes and garnets in the assemblage opx+cpx+gt. The likely range of values of this ratio for orthopyroxene in the temperature range 1400-1600°C, 25-35 kb is 0.04 to 0.05 (Akella, 1974a). The use of the value 0.04 in equation A.6.1 rather than the chosen value 0.045 results in a pressure difference of only -0.25 kb at 27 kb. The result of errors in the chosen value for the Ca/(Ca+Mg) ratio of

the garnets is more serious. The value chosen is in the middle of the range 0.128 to 0.17 reported by Akella (1974a) for the pressure and temperature ranges 26-44 kb and 1000-1500°C. Use of the most discrepant value, viz. 0.128, in equation A.6.1, rather than the chosen value of 0.15, results in a pressure difference of +5%.

(ii) Errors in the positioning of the 6% isopleth from the experimental results on AM3 because of the size (up to 40°C) of the temperature brackets. The maximum deviation from the preferred position of this isopleth would result in a pressure error of ±1 kb in its position in the 25-35 kb pressure range but this would increase to ±5 kb at 45 kb.

(iii) Complications in the pattern of orthopyroxene solid solutions caused by a possible reaction between calcic clinopyroxene-bearing garnet-lherzolite to subcalcic clinopyroxene-bearing garnet-lherzolite (O'Hara, 1975). No evidence has been found for such a reaction in orthopyroxene-rich compositions and possible complications resulting from such a reaction have not been considered in the derivation of the model presented in fig. 8.2.

In so far as the positions of the isopleths shown in fig. 8.2 have been fitted to the results from gel starting materials and hence are independent of the assumptions used to derive these positions in the immediate pressure and temperature range of the experimental data points (c.25-35 kb, 1450-1650°C), the use of fig. 8.2 as a pressure grid in this limited pressure and temperature range is justified providing that the gels themselves crystallized stable equilibrium assemblages. The errors discussed in (i) and (ii) above suggest that actual pressures of equilibration will not be more than

2.5 kb in excess of the equilibration pressures indicated by fig. 8.2, though they may be many kilobars less than the indicated values if the run products of charge AM3 did not reach stable equilibrium. This conclusion is not justified if there is a major error in the slope of the experimentally determined 6% isopleth caused by major variation in the extent of any Al_2O_3 supersaturation in orthopyroxene between the run products of AM3 at 27, 30 and 35 kb.

APPENDIX A.7

ERRORS IN PYROXENE GEOTHERMOMETRY AND GEOBAROMETRY AS AN EXPLANATION FOR THE KINK IN SOME CONTINENTAL PALAEOGEOTHERMS

A pressure/temperature plot of the equilibration conditions of mantle-derived rocks from a single intrusion would define a mantle geotherm at the time of the intrusion of the rocks (see section 1.1). The problematic kink in some continental palaeogeotherms deduced in this way (e.g. Boyd, 1973) may be purely an artefact of the incorrect assignment of pressures and temperatures of equilibration to garnet-lherzolite nodules equilibrated on an unkinked geotherm.

The method used to determine the equilibration pressure and temperature of a garnet-lherzolite, viz. from the Al_2O_3 content of the orthopyroxene and from the Ca/(Ca+Mg) ratio of the clinopyroxene respectively, is described in section 1.1. The method involves comparing the values of these parameters for natural assemblages with the experimentally determined values for the simple systems MS-A, investigated by MacGregor (1974), and CMS_2-M_2S_2, investigated by Davis and Boyd (1966). The following examples show that if the experimentally determined values are incorrect, then geotherms defined by a plot of incorrectly deduced pressures and temperatures of equilibration may be kinked. In the two models described here the erroneous kinked geotherms are similar in shape to those reported by Boyd (1973, 1974).

The following abbreviations will be used in this discussion:-

RG Real Geotherm

DG Deduced Geotherm

X^R Value of actual isopleths (on a pressure/temperature section) of the parameter used to determine equilibration temperature or equilibration pressure.

X^D Value of experimental (erroneous) isopleths

In the following examples the sets of X^D are hypothetical but are similar in form to those determined by Davis and Boyd (1966) and MacGregor (1974) which were used by Boyd (1973, 1974) to deduce kinked geotherms.

Model A Error in temperature estimate

In this model (fig. A.7.1) temperatures are deduced from the pressure insensitive solvus for the solubility of phase A in phase B. Equilibration pressures are assumed to have been correctly determined independently.

Fig. A.7.1/1 shows the solubility of phase A in phase B as a function of temperature. This has been correctly determined only at low temperatures. A plot (fig. A.7.1/2) of the deduced temperatures and pressures of equilibration of a suite of rocks defines the correct geotherm for temperatures up to that at which the determined and real solvi diverge. At higher temperatures the determined equilibration temperatures are in error and the plot of the DG and RG diverge. The lower temperature correct portion and the higher temperature erroneous portion of the DG form two limbs of a kinked geotherm.

Model B Error in pressure estimate

In this model equilibration pressures are estimated from the

FIGURE A.7.1

Model to demonstrate that a geotherm deduced from estimates of the equilibration conditions of garnet-lherzolite nodules may be kinked if equilibration temperatures have been incorrectly determined.

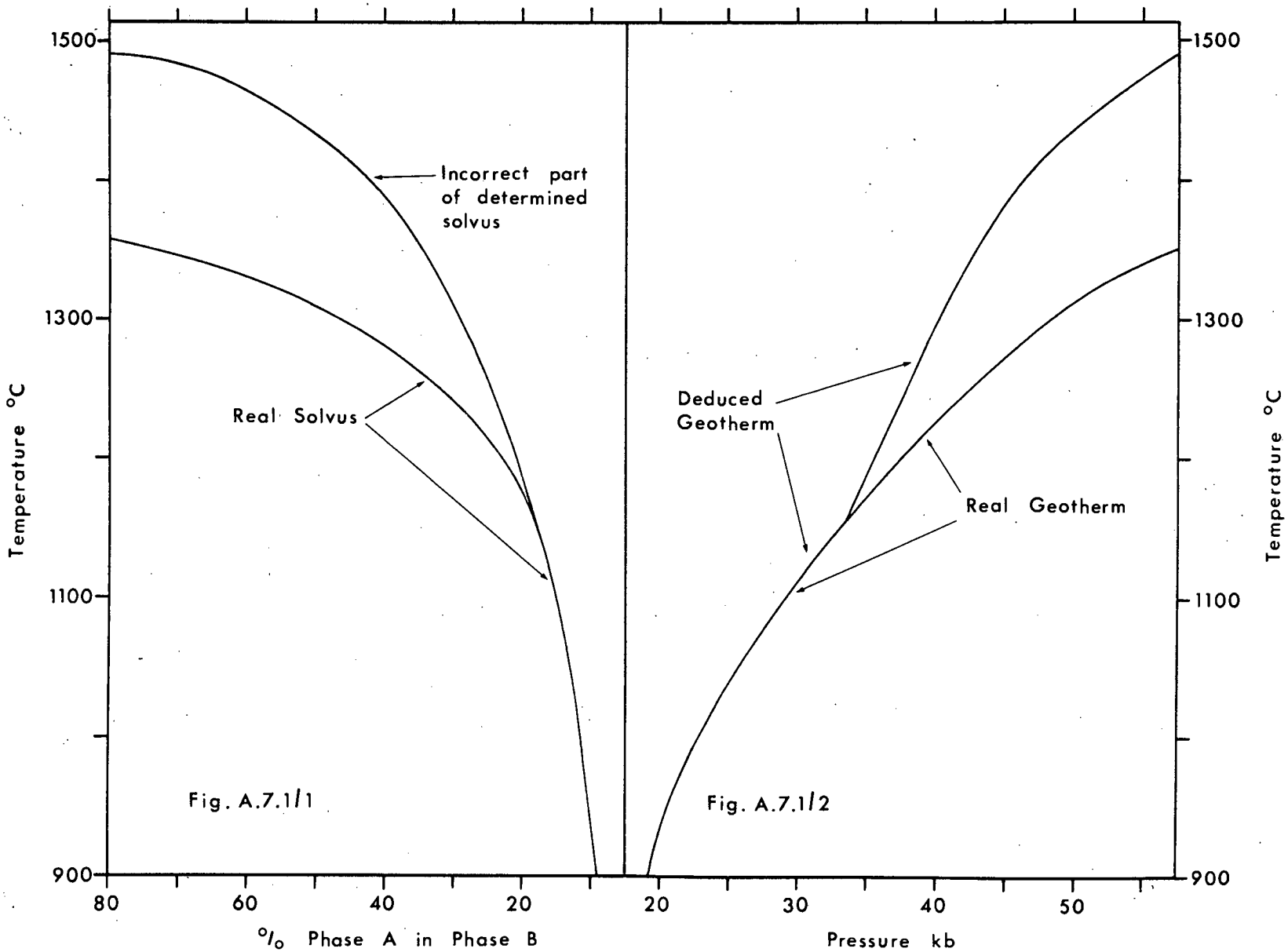
1500
1300
1100
900
Temperature °C
Incorrect part of determined solvus
Real Solvus
80
60
40
20
°/o Phase A in Phase B
Fig. A.7.1/1
Deduced Geotherm
Real Geotherm
20
30
40
50
Pressure kb
Fig. A.7.1/2

solubility of component C in phase P which is a function of both pressure and temperature. Fig. A.7.2/1 is a pressure/temperature plot showing the real geotherm and the real isopleths of component C in phase P. The interaction of X^R and RG is such that a suite of rocks equilibrated at low pressure along the RG show progressively lower contents of component C in phase P with increasing pressure and temperature. At higher pressures and temperatures (temperatures on the RG in excess of about 1200^{o}C) however, phase P shows progressively higher C component contents with increasing pressure and temperature. This phenomenon is similar to that observed for the Al_2O_3 content of orthopyroxene in garnet-lherzolite nodules from Lesotho kimberlite pipes (Boyd, 1973). A kinked geotherm was obtained from a pressure/temperature plot of the equilibration conditions of these nodules.

Fig. A.7.2/2 is a pressure/temperature plot of the erroneous isopleths of component C in phase P. The form of the geotherm has been deduced from the component C content of phase P assuming that the independently determined equilibration temperatures are correct. The deduced geotherm shown in fig. A.7.2/2 is kinked at the temperature at which the C component content of phase P in the nodules is at its minimum value.

FIGURE A.7.2

Model to demonstrate that a geotherm deduced from estimates of the equilibration conditions of garnet-lherzolite nodules may be kinked if equilibration pressures have been incorrectly determined.

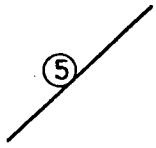

isopleth of the solubility (here 5%) of component C in phase P. Fig. A.7.2/1 shows the real isopleths; fig. A.7.2/2 shows the experimentally determined erroneous isopleths.

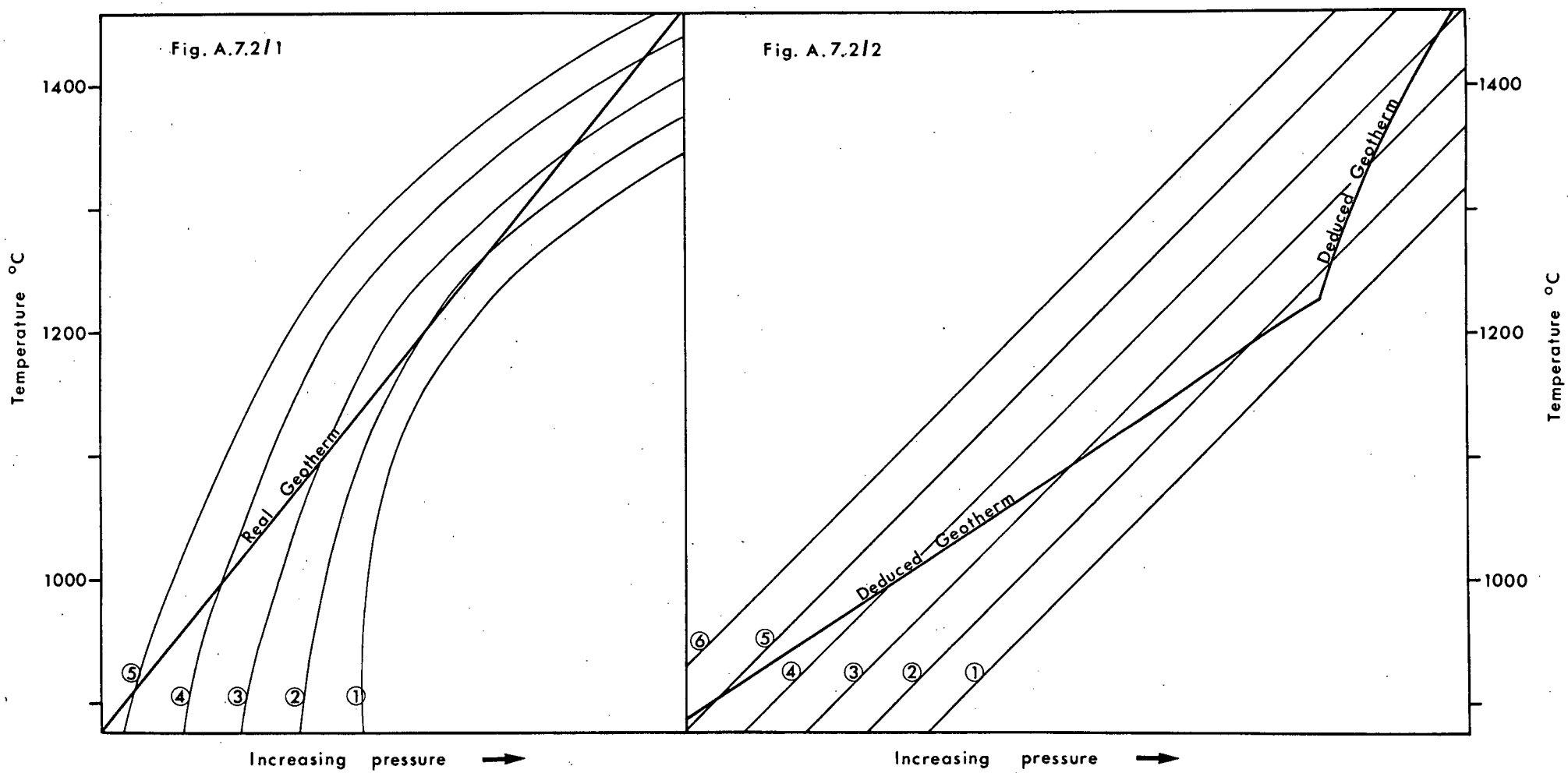
Fig. A.7.2/1
1400
1200
1000
Temperature °C
Real Geotherm
5
4
3
2
1
Increasing pressure
Fig. A.7.2/2
1400
1200
1000
Temperature °C
Deduced Geotherm
Deduced Geotherm
6
5
4
3
2
1
Increasing pressure

APPENDIX A.8

THE PROPOSED (O'HARA, 1975) GARNET-LESOTHOLITE FACIES

A.8.1 Reproduction of abstract "Pyroxene grids, palaeogeotherms and a new mineral facies in the upper mantle" (O'Hara, 1975)

This abstract is reproduced on the following four pages.

The x-ray diffraction parameter plotted in figure 2 of this abstract is $\Delta 2\theta^{\circ}$ CrKα 310-$\bar{2}$21 and not $\Delta 2\theta^{\circ}$ CrKα 310-311 as shown.

PYROXENE GRIDS, PALAEOGEOTHERMS AND A NEW MINERAL FACIES IN THE UPPER MANTLE

M.J.O'Hara (Grant Institute of Geology, Univ. of Edinburgh, Scotland EH9 3JW)

The molar composition $M_{15}C_3AS_{15}$ (M=MgO, C=CaO, A=Al_2O_3, S=SiO_2) can crystallize to forsterite, M_2S plus homogeneous clinopyroxene (Ca/Ca+Mg =0.25, Al_2O_3=7.4wt%) at 30-35kb, c.1600°C by the relation

$$M_{15}C_3AS_{15} \longrightarrow 3M_2S + C_3M_9AS_{12}$$

At lower temperatures enstatite is present, at higher pressures and/or lower temperatures garnet is also present, coexisting with a clinopyroxene of Ca/Ca+Mg $>$ 0.25 and Al_2O_3 content progressively less than 7.4wt% as the amount of garnet crystallized increases. Phases synthesised from this composition (a gel dried and partially recrystallised at atmospheric pressure) in piston-out runs are shown in fig.1, the lower pressure regions being constructed from previously published data, for the same system.

There is a discontinuous change in the type of clinopyroxene present above and below 1550°C as demonstrated by X-ray data in fig. 2, by a reappearance of garnet at 1550-1575°C, 32-35kb (fig.1) and by an abrupt decrease in the strength of enstatite diffraction peaks on the high temperature side of the nearly temperature invariant boundary shown in fig. 1. These changes indicate a reaction:-

$$\text{enstatite}_{ss} + \text{diopside}_{ss} \longrightarrow \text{less aluminous subcalcic clinopyroxene}_{ss} + \text{garnet}$$

which occurs in the presence of forsterite (which may influence stoichiometry and solid solution limites of pyroxenes; see Howells and O'Hara 1975).

In the system CMAS the above reaction is univariant, subdividing from the garnet-lherzolite facies (O'Hara 1967) a higher temperature region characterized by subcalcic rather than diopsidic pyroxene (the difference in Ca/Ca+Mg may be less than 0.05, however). Such a mineral facies has its natural representatives in some of the nodules described from kimberlite diatremes in Lesotho (Nixon and Boyd 1973) hence the suggestion of garnet-lesotholite facies as a name for these conditions and assemblages.

The solubility of enstatite (i.e. the value of Mg/Ca+Mg) in clinopyroxene as a function of temperature is much lower than observed in the alumina-free system CMS by Davis and Boyd (1966), Kushiro (1968), Kushiro and Yoder (1970) or Howells and O'Hara (1975), enstatite remaining in the charges to temperatures 150-100°C above that predicted if Al_2O_3 content of pyroxenes were assumed to have no effect on mutual solubility of the pyroxenes.

The solubility of Al_2O_3 (garnet) in the pyroxene assemblage (chiefly clinopyroxene in this assemblage) is generally less than anticipated from the work of MacGregor (1974) on orthopyroxene (assuming broadly comparable Al_2O_3 contents of coexisting pyroxenes) but the low solubilities are in agreement with results for a natural olivine-garnet websterite from kimberlite (Howells et al. 1975), provided that the clinopyroxenes at c. 1450-1600°C are more aluminous than the coexisting enstatites.

FIGURE I

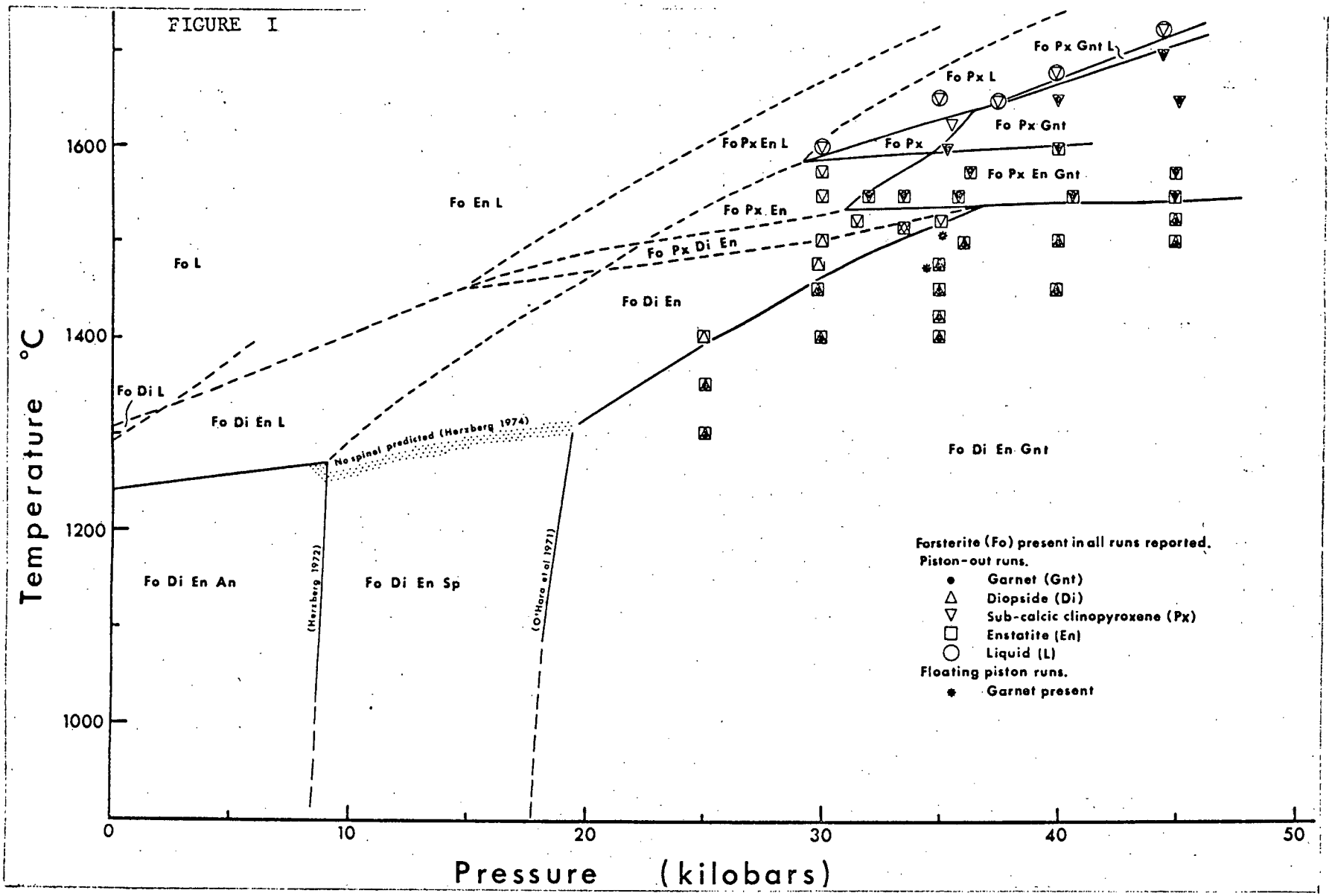
Temperature °C
1600
1400
1200
1000
0
10
20
30
40
50
Pressure (kilobars)
Fo L
Fo En L
Fo Px En L
Fo Px L
Fo Px Gnt L
Fo Px
Fo Px Gnt
Fo Px En
Fo Px En Gnt
Fo Px Di En
Fo Di En
Fo Di L
Fo Di En L
No spinel predicted (Herzberg 1974)
Fo Di En Gnt
Fo Di En An
(Herzberg 1972)
Fo Di En Sp
(O'Hara et al 1971)
Forsterite (Fo) present in all runs reported.
Piston-out runs.
Garnet (Gnt)
Diopside (Di)
Sub-calcic clinopyroxene (Px)
Enstatite (En)
Liquid (L)
Floating piston runs.
Garnet present

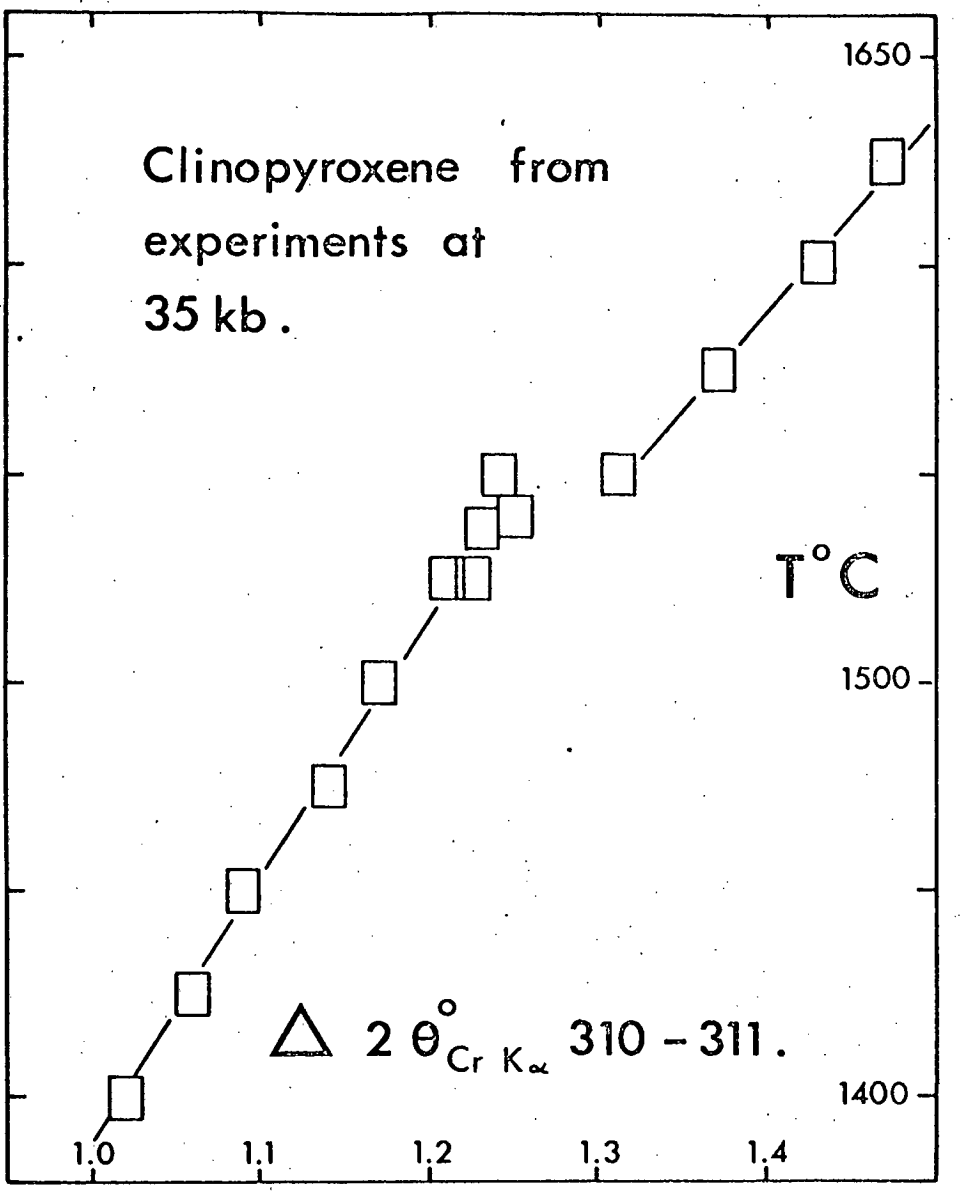

FIGURE 2 Variation of an X-ray parameter, measured by step scanning at 0.02° 2θ intervals, 10 second counts, in clinopyroxenes from charges run at 35-36.5kb (see fig. 1)

The intersection of the garnet-lesotholite facies by natural geotherms, even making allowances for the effect of FeO in lowering the temperature of the reaction to form sub-calcic pyroxene together with the relatively low Al_2O_3 solubility in pyroxene implied by these studies, points to the need to raise the temperatures or lower the pressures at points along previously published palaeogeotherms. Separate from this consideration it is axiomatic that the P,T dependence of Al_2O_3 in enstatite which coexists with diopside will be different from that of enstatite coexisting with subcalcic clinopyroxene, (specifically dT/dP of the Al_2O_3 isopleths should be less in the latter case) and attempts to assign P,T to assemblages using a single set of isopleths will result in a geotherm which is distorted where it crosses the reaction boundary between garnet-lherzolite and garnet-lesotholite facies.

Davis, B.T.C. and Boyd, F.R.,Jr., 1966 The join $Mg_2Si_2O_6$-$CaMgSi_2O_6$ at 30kb pressure and its application to pyroxenes from kimberlite. J. Geophys. Res. 71, 3567-3576.

Herzberg, C.T., 1972 Stability fields of plagioclase- and spinel-lherzolite in Progress in Experimental Petrology. Nat. Env. Res. Council Publ. D. 2, 145-148.

Herzberg, C.T., 1974 Ph.D. Thesis Univ. of Edinburgh.

Howells, S. and O'Hara, M.J., 1975 Palaeogeotherms and the diopside-enstatite solvus. Nature 254, 406-408.

Howells, S., Begg, C. and O'Hara, M.J., 1975 Crystallization of some natural eclogites and garnetiferous ultrabasic rocks at high pressure and temperature. Phys. Chem. Earth 9, 895-902.

Kushiro, I., 1968 Synthesis and stability of iron-free pigeonite in the system $MgSiO_3$-$CaMgSi_2O_6$ at high pressures. Carnegie Instn. Washington Yb. 67, 80-83.

Kushiro, I. and Yoder, H.S.,Jr., 1970 Stability field of iron-free pigeonite in the system $MgSiO_3$-$CaMgSi_2O_6$. Carnegie Instn. Washington Yb. 68, 226-229.

MacGregor, I.D., 1974 The system MgO-Al_2O_3-SiO_2: solubility of Al_2O_3 in enstatite for spinel and garnet-peridotite compositions. Amer. Mineral 59, 110-119.

Nixon, P.H. and Boyd, F.R.,Jr., 1973 Petrogeneses of the granular and sheared ultrabasic nodule suite in kimberlite in Lesotho Kimberlites (ed. P.H. Nixon) Lesotho Nat. Dev. Dorp. Masenu, pp. 48-56.

O'Hara, M.J., 1967 Mineral facies in ultrabasic rocks. In Ultramafic and Related Rocks. ed. P.J. Wyllie, J. Wylie New York, pp. 7-18.

O'Hara, M.J., Richardson, S.W. and Wilson G., 1971 Garnet-peridotite stability and occurrence in crust and mantle. Contr. Min. Petr., 32. 48-68.

A.8.2 Diagrammatic interpretation of phase assemblages reported in Appendix A.8.1

Fig. A.8.1 is a projection from forsterite into the plane CS-MS-A of an interpretation of the phase assemblages described by O'Hara (1975). These phase diagrams are consistent with his interpretation of a reaction from a cpx+opx+gt+ol assemblage containing a calcic, aluminous clinopyroxene (fig. A.8.1/1) to a cpx+opx+gt+ol assemblage containing a less aluminous, subcalcic clinopyroxene (fig. A.8.1/2). At any given pressure the subcalcic cpx-bearing assemblage is stable at higher temperatures. Fig. A.8.1/1 depicts phase relations at temperatures just below that of the reaction; fig. A.8.1/2 depicts phase relations at temperatures just above that of the reaction, at the same pressure as the phase relations in fig. A.8.1/1. The precise compositions of the coexisting phases are not known. Phase fields containing two clinopyroxenes, for which a search was made in this study, are shown in fig. A.8.1.

FIGURE A.8.1

See text for explanation of this model.

✱ - Projection from M_2S into CS-MS-A of the bulk composition $M_{15}C_3AS_{15}$ used by O'Hara (1975).

Fig. A.8.1/1

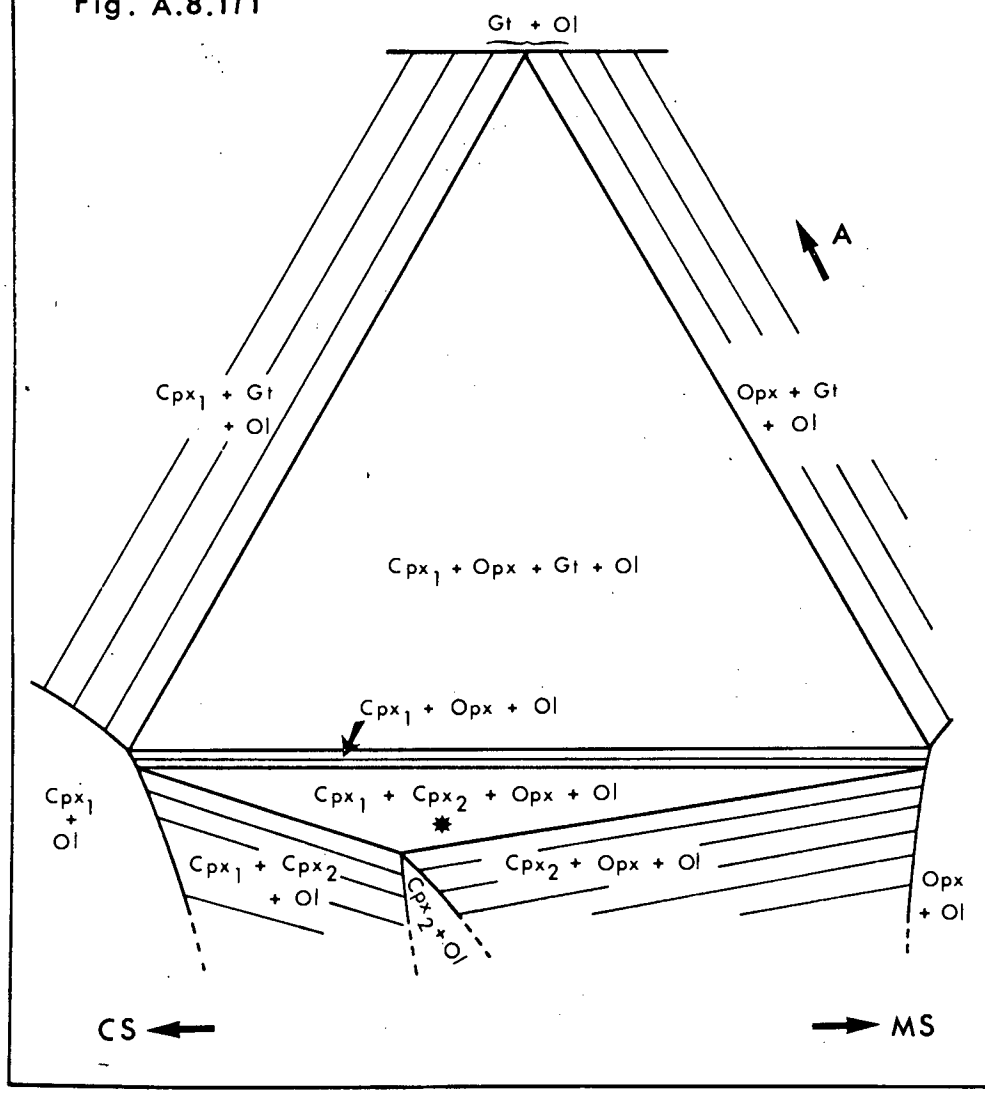

Fig. A.8.1/2

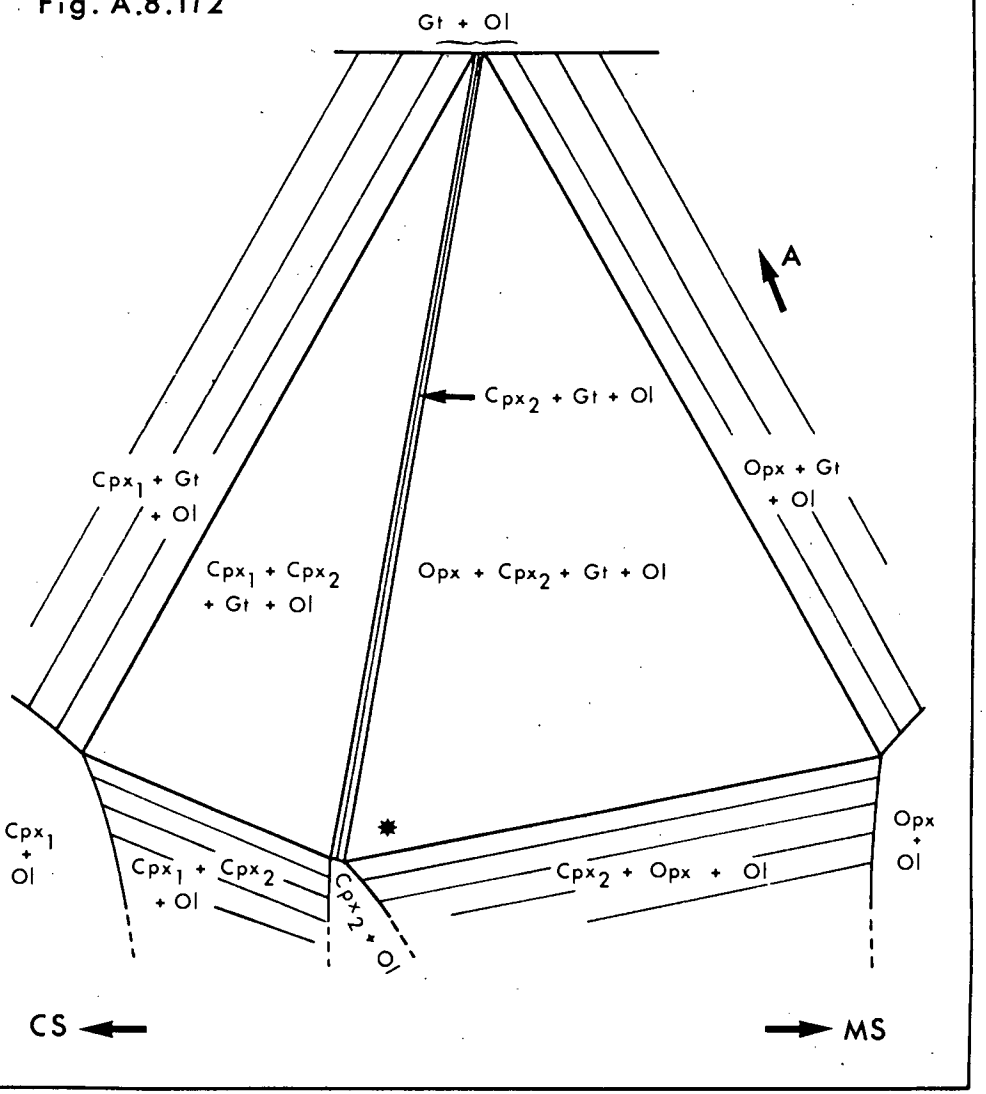

APPENDIX A.9

TABLES OF EXPERIMENTAL DETAILS AND RUN RESULTS

Abbreviations are given in section 1.2.

All experiments were run using the piston-out pressure technique unless otherwise stated.

In this Appendix the number at the top right hand corner of each page is the number of the table given on that page.

TABLE A.9.1

Results of piston-out experiments at 30 kb on compositions on the join CMS_2-MS

Run No.	Charge No.	Wt.% CMS_2 in Charge	Pressure (kb)	Temp. (°C)	Time (hrs)	Phase Identification		$^{\circ}2\theta$ CrKα	Wt.% CMS_2
						Optical	X-Ray Diffraction	Cpx 220	in Cpx
181	M2II	20.0	30.0	1750	0.07	Opx,Gl,Q	Opx,Cpx	-	-
186	M2II		30.0	1723	0.10	Opx,Cpx	Cpx	42.126±0.017	21.8
180	M2II		30.0	1700	0.13	Opx,Cpx	Opx,Cpx	42.116±0.036	22.8
176	M2II		30.0	1630	0.42	Opx,Cpx	Opx,Cpx	-	-
174	M2I		30.0	1600	0.50	Opx,Cpx	Opx,Cpx	41.970±0.068	37.8
163	M2I		30.0	1567	4.08	Opx,Cpx	Opx,Cpx	41.930±0.044	41.3
112	M2I		30.0	1549	3.08	Opx,Cpx	Opx,Cpx	41.898±0.019	44.4
178	M6	28.0	30.0	1630	0.42	Opx,Cpx	Opx,Cpx	42.002±0.014	34.7
159	E22	40.0	30.0	1620 followed by 1500	0.53 followed by 1.67	Cpx	Cpx	41.918±0.051	42.8
166	E22		30.0	1620 followed by 1399	0.50 followed by 3.00	Cpx	Cpx	-	-
113	E22		30.0	1565	3.16	Opx,Cpx	Opx,Cpx	41.878±0.024	45.9
34	E22		30.0	1550	3.50	?Opx,Cpx	Cpx	41.878±0.009	45.9
110	E22		30.0	1532	3.50	Opx,Cpx	Opx,Cpx	41.844±0.021	49.9
36	E22		30.0	1496	4.75	Opx,Cpx	Opx,Cpx	41.786±0.041	54.9
179	E22		30.0	1450	10secs	Pyx,Unrxd.Gel	Opx,Cpx	41.772±0.036	56.4
167	E22		30.0	1448	0.17	Pyx,Unrxd.Gel	Opx,Cpx	41.810±0.033	53.0

TABLE A.9.1 ctd.

Run No.	Charge No.	Wt.% CMS_2 in Charge	Pressure (kb)	Temp. ($^{\circ}C$)	Time (hrs)	Phase Identification		$^{\circ}2\theta$ CrKα	Wt.% CMS_2
						Optical	X-Ray Diffraction	Cpx 220	in Cpx
220	E22	40	30.0	1450	0.25	Pyx,Unrxd.Gel	Opx,Cpx	41.809±0.043	53.0
221	E22		30.0	1451	0.50	Pyx,Unrxd.Gel	Opx,Cpx	41.836±0.025	50.4
213	E22		30.0	1449	0.80	Pyx,Unrxd.Gel	Opx,Cpx	41.736±0.050	60.3
197	E22		30.3	1450	1.03	Pyx	Opx,Cpx	41.828±0.052	51.4
211	E22		30.0	1449	1.70	Pyx	Opx,Cpx	41.706±0.047	63.3
40	E22		30.0	1450	7.50	Pyx	Opx,Cpx	41.716±0.046	62.3
288	E22R	40	30.0	1449	0.33	Pyx	Opx,Cpx	41.688±0.030	64.7
198	E22R		30.0	1450	4.08	Pyx	Opx,Cpx	41.703±0.020	63.3
109	M1	40	30.0	1515	3.70	Opx,Cpx	Opx,Cpx	41.792±0.016	54.9
115	E22G	40	30.0	1522	3.00	Cpx	Cpx	41.906±0.018	43.9
240	E22H	40	30.0	1480	2.03	Cpx	Cpx	41.911±0.027	42.8
22	E23	48.4	30.0	1553	3.80	Cpx	Cpx	41.848±0.046	49.9
25	E23		30.0	1496	4.50	Pyx	Opx,Cpx	41.788±0.044	54.9
233	E23		30.0	1450	6.58	Pyx	Opx,Cpx	41.685±0.035	65.4
225	E23R	48.4	30.0	1450	4.25	Pyx	Opx,Cpx	41.671±0.039	66.7

TABLE A.9.1 ctd.

Run No.	Charge No.	Wt.% CMS_2 in Charge	Pressure (kb)	Temp. ($^{\circ}C$)	Time (hrs)	Phase Identification		$^{\circ}2\theta$ CrKα	Wt.% CMS_2
						Optical	X-Ray Diffraction	Cpx 220	in Cpx
131	M4	60.0	30.0	1548	2.75	Cpx	Cpx	41.729±0.025	60.8
183	M4		30.0	1452	4.25	Opx,Cpx	Opx,Cpx	41.640±0.025	69.6
196	M7	69.0	30.0	1500	3.00	Cpx	Cpx	41.643±0.025	69.0
177	D90	90.0	30.0	1680	0.17	Cpx	Cpx	41.495±0.020	-
200	D90		30.0	1400	6.42	Cpx	Cpx	41.518±0.017	-
182	D95	95.1	30.0	1680	0.17	Cpx	Cpx	41.480±0.019	-
184	D95		30.0	1600	0.50	Cpx	Cpx	41.470±0.027	-

TABLE A.9.2

Results of floating-piston experiments at 30 kb on compositions in the system C-M-S

Run No.	Charge No.	Wt.% CMS_2 in Charge	Pressure (kb)	Temp. (^oC)	Time (hrs)	Phase Identification		$^o2\theta$ CrKα	Wt.% CMS_2
						Optical	X-Ray Diffraction	Cpx 220	in Cpx
143	M5	8.0	30.0	1620	0.50	Opx	Opx	-	-
114	M2I	20.0	30.0	1551	3.17	Opx,Cpx	Opx,Cpx	41.924±0.023	41.3
132	M2I		29.7	1399	9.08	Opx,?Cpx	Opx,Cpx	-	-
173	M6	28.0	30.0	1775	10secs	Opx,Cpx,Q	Cpx	-	-
172	M6		30.0	1630	0.50	Opx,Cpx	Opx,Cpx	42.030±0.033	31.6
149	E22	40.0	30.0	1400	17.00	Opx,Cpx	Opx,Cpx	41.666±0.049	66.7
127	E22G	40.0	30.0	1466	4.70	Cpx	Cpx	41.930±0.052	41.3
128	E22G		30.0	1440	1.17	Pyx	Cpx	41.950±0.024	39.3
129	E22G		30.0	1440	1.50	Pyx	Opx,Cpx	41.798±0.058	54.9
142	E22G		30.0	1400	6.25	Opx,Cpx	Opx,Cpx	41.715±0.036	62.3
273	E22H	40.0	30.0	1467	3.55	Cpx	Cpx	41.942±0.034	39.8
136	E23	48.4	30.0	1600	0.50	Cpx	Cpx	-	-
133	E23		29.8	1400	9.80	?Opx,Cpx	Opx,Cpx	41.644±0.025	69.14

TABLE A.9.3

Results of experiments on compositions on the join CMS_2-M_2S_2 at 20 kb

Run No.	Charge No.	Wt.% CMS_2 in Charge	Pressure (kb)	Temp. (^oC)	Time (hrs)	Phase Identification		$^o2\theta$ CrKα	Wt.% CMS_2	Comments
						Optical	X-Ray Diffraction	Cpx 220	in Cpx	
148	M2I	20.0	20.0*	1638	0.42	Cpx	Cpx	42.148 ±0.010	-	
63	M2I		20.0	1620	0.42	Cpx	Cpx	42.116 ±0.016	22.8	
208	M2II		20.0	1521	1.00	Opx,Cpx	Opx,Cpx	41.975 ±0.045	36.7	$^o2\theta$ CrKα Cpx 310 ∧ $\bar{3}$11 = 46.430±0.0126
191	M6	28.0	20.0	1521	3.00	Opx,Cpx	Cpx	42.014 ±0.028	33.7	$^o2\theta$ CrKα Cpx 310 ∧ $\bar{3}$11 = 46.515±0.038
60	E22	40.0	20.0	1622	0.50	Cpx	Cpx	-	-	
145	E22		20.0*	1620	0.50	Cpx	Cpx	-	-	Slow quench
146	E22		20.0*	1621	0.58	Cpx	Cpx	41.950 ±0.028	-	Slow quench
58	E22		20.0	1550	3.42	Cpx	Cpx	-	-	
134	E22		20.0	1481	5.80	Opx,Cpx	Cpx	41.916 ±0.028	42.8	
141	E22		20.0	1451	7.00	Opx,Cpx	Opx,Cpx	41.810 ±0.071	53.0	
104	M1	40.0	20.0	1650	0.25	Cpx,Q	Cpx	-	-	
62	M1		20.0	1614	0.50	Cpx	Cpx	41.928 ±0.035	41.3	

TABLE A.9.3 ctd.

Run No.	Charge No.	Wt.% CMS_2 in Charge	Pressure (kb)	Temp. (^oC)	Time (hrs)	Phase Identification		$^o2\theta$ CrKα	Wt.% CMS_2	Comments
						Optical	X-Ray Diffraction	Cpx 220	in Cpx	
84	E22G	40.0	20.0	1621	0.50	Cpx	Cpx	41.950 ±0.039	39.3	
237	E22H	40.0	20.0*	1600	0.50	Cpx	-	-	-	
238	Product Run 237	40.0	20.0*	1620	0.50	Cpx	Cpx	-	-	
236	E22H		20.0	1475	1.80	Pyx	Cpx	41.892 ±0.056	45.4	
147	E23	48.4	20.0	1620	0.50	Cpx	Cpx	41.876 ±0.005	-	

* Experiment carried out using the floating-piston technique; piston-out technique used for all other experiments.

TABLE A.9.4

Results of piston-out experiments at all pressures on gel charges with compositions in the system CMS_2-M_2S_2-M_2S

Run No.	Charge No.	Pressure (kb)	Temp. (°C)	Time (hrs)	Phase Identification		$^{\circ}2\theta$ CrKα	Wt.% CMS_2	Remarks
					Optical	X-Ray Diffraction	Cpx 220	in Cpx	
193	M2F10	30.0	1568	2.00	Opx,Cpx,Ol	Opx,Cpx,Ol	41.934±0.030	41.3	
190	M2F10	30.0	1550	3.32	Opx,Cpx,Ol	Opx,Cpx,Ol	41.924±0.033	41.3	
214	M2F10	20.0	1521	1.56	Opx,Cpx,Ol	Opx,Cpx,Ol	41.980±0.023	36.7	$^{\circ}2\theta$ CrKα Cpx 310∧$\bar{3}$11 = 46.455±0.027
212	E22F10	30.0	1564	1.83	Opx,Cpx,Ol	Opx,Cpx,Ol	41.917±0.037	42.8	
209	E22F10	31.0	1550	3.17	Opx,Cpx,Ol	Opx,Cpx,Ol	41.912±0.019	42.8	
188	E23F10	30.0	1550	3.80	Cpx,Ol	Cpx,Ol	41.850±0.030	49.5	

TABLE A.9.5

Results of experiments on diopside-rich C-M-A-S gel charges

Run No.	Charge No.	Temp. (°C)	Pressure (kb)	Time (hrs)	Phase Identification		°2θ CrKα Cpx 220	°2θ CrKα Cpx $\bar{2}21$	°2θ CrKα Cpx(310 ∧ $\bar{3}11$)	Wt%CS in Cpx	Wt%A in Cpx
					Optical	X-Ray Diffraction					
101	DP2	1600	30.0	0.50	Cpx,(Opx),Gt	Cpx,Gt	42.104 ±0.041	45.017 ±0.023	-	25.5	7.2
94	DP2	1523	30.0	3.58	Cpx,Gt	Cpx,(Opx),Gt	42.002 ±0.030	45.041 ±0.026	-	29.2	7.0
83	DP1	1524	30.0	2.87	Cpx,Gt	Cpx,Gt	-	-	-	-	-
105	BOH	1601	30.0	0.55	Cpx,Gt	Cpx	-	-	-	-	-
102	BOH	1500	30.0	4.08	Pyx,Gt	Cpx,Gt	-	-	-	-	-
90	AM4	1500	30.0	4.70	Pyx,Gt	Cpx,Gt	-	-	-	-	-
108	AM5	1600	30.0	0.50	Cpx,Gt,Ol	Cpx,Gt,Ol	-	-	-	-	-
97	AM5	1499	30.0	2.08	Pyx,Gt,Ol	Cpx,Gt,Ol	-	-	-	-	-
76	AM1	1523	30.0	2.92	Cpx,Opx,Gt	Cpx,Opx,Gt	42.078 ±0.027	-	-	-	-
248	AM1R	1525	30.0	2.30	Pyx,Gt	Cpx,Opx,Gt	42.051 ±0.031	-	-	-	-
78	AM2	1523	30.0	2.00	Cpx,Opx,Gt	Cpx,Opx,Gt	42.102 ±0.043	-	-	-	-
80	AM2	1500	30.0	3.80	Cpx,Opx,Gt,(UG)	Cpx,Opx,Gt	42.066 ±0.038	-	-	-	-
252	AM2R	1525	30.0	0.72	Pyx,Gt	Cpx,Opx,(?Gt)	-	-	-	-	-

TABLE A.9.5 ctd.

Run No.	Charge No.	Temp. (°C)	Pressure (kb)	Time (hrs)	Phase Identification		°2θ CrKα Cpx 220	°2θ CrKα Cpx $\bar{2}21$	°2θ CrKα Cpx(310 ∧ $\bar{3}11$)	Wt%CS in Cpx	Wt%A in Cpx
					Optical	X-Ray Diffraction					
194	AM6	1551	30.0	2.50	Cpx,Opx,Gt,(Ol),G/O	Cpx,Opx,Gt	42.014 ±0.012	45.027 ±0.031	-	28.3	6.8
195	AM6	1500	30.0	4.00	Cpx,Opx,Gt,(Ol),G/O	Cpx,Opx,Gt	41.946 ±0.016	45.058 ±0.016	0.321 ±0.028	32.7	7.0
251	AM6R	1524	30.0	2.00	Pyx,Gt,(Ol)	Cpx,Opx,Gt	41.927 ±0.018	45.048 ±0.016	0.326 ±0.027	32.7	6.5
296	AM6R	1525	30.0	3.83	Cpx,Opx,Gt,(Ol)	-	-	-	-	-	-
298	(AM6R-296)	1525	30.0	3.50	Pyx,Gt,(Ol)	Cpx,Opx,Gt	42.026 ±0.056	45.059 ±0.037	-	28.8	7.7
204	AM7	1499	30.0	2.17	Cpx,Opx,Gt,Ol,G/O	Cpx,Opx,?Gt,Ol	41.937 ±0.043	45.035 ±0.020	0.311 ±0.060	32.3	6.4
205	AM7	1500	30.0	4.42	Cpx,Opx,Gt,Ol,G/O	Cpx,Opx,Gt,Ol	41.915 ±0.033	45.026 ±0.013	~0.29	32.0	5.8
206	AM7	1500	30.0	10secs	UG,Ol	Cpx,Ol,Qz	-	-	-	-	-
207	AM8	1500	30.0	2.17	Cpx,Opx,Ol,G/O	Cpx,Opx,Ol	41.918 ±0.022	45.031 ±0.011	0.32 ±0.035	32.3	5.8
244	AM8R	1525	30.0	3.75	Pyx,Gt,Ol	Cpx,Opx,Gt,Ol	41.963 ±0.040	45.045 ±0.013	0.253 ±0.045	31.3	6.7
245	AM8R	1500	30.0	3.34	Pyx,Gt,Ol	Cpx,Opx,Gt,Ol	41.900 ±0.024	45.046 ±0.016	0.383 ±0.033	34.0	6.1

TABLE A.9.5 ctd.

Run No.	Charge No.	Temp. (°C)	Pressure (kb)	Time (hrs)	Phase Identification		°2θ CrKα Cpx 220	°2θ CrKα Cpx $\bar{2}21$	°2θ CrKα Cpx(310∧$\bar{3}$11)	Wt%CS in Cpx	Wt%A in Cpx
					Optical	X-Ray Diffraction					
CB1	OHB	1625	35.0	1.00	Pyx,Ol	Cpx,Ol	42.087 ±0.032	45.023 ±0.015	-	25.8	7.5
216	OHB	1575	30.0	1.08	Pyx,Ol	Cpx,Opx,Ol	42.039 ±0.037	45.023 ±0.011	-	27.0	7.0
192	OHB	1551	30.0	2.34	Pyx,Gt,Ol	Cpx,Opx,Ol	42.035 ±0.026	45.039 ±0.039	-	27.5	7.5
202	OHB	1523	30.0	3.83	Pyx,Gt,Ol	Cpx,Opx,Gt,Ol	41.980 ±0.028	45.086 ±0.016	0.297 ±0.028	32.2	8.2
199	OHB	1500	30.0	4.08	Pyx,Ol,(?G/O)	Cpx,Opx,Ol	41.960 ±0.035	45.070 ±0.023	0.28 ±0.027	32.2	7.3
215	OHB	1470	30.0	3.00	Pyx,Ol,(?G/O)	Cpx,Opx,Ol	41.914 ±0.025	45.086 ±0.015	0.395 ±0.014	37.3	7.5
256	OHBR	1500	30.0	2.70	Pyx,Gt,Ol	Cpx,Opx,Gt,Ol	41.945 ±0.035	45.090 ±0.037	0.353 ±0.021	34.5	7.8
106	E34	1599	30.0	0.50	Cpx,(Opx),Gt,Ol,G/O	Cpx	42.028 ±0.043	45.046 ±0.025	-	28.3	7.5
54	E34	1548	30.0	2.25	Cpx,Opx,Gt,Ol,G/O	Cpx,Opx,Gt	42.000 ±0.042	45.056 ±0.027	-	29.7	7.4
77	E34	1501	30.0	3.58	Cpx,Opx,Gt,G/O	Cpx,Opx	41.929 ±0.031	-	0.320 ±0.020	32.8	6.7
219	E34F24	1525	30.0	2.00	Cpx,Opx,Gt,Ol,G/O	Cpx,Opx,(?Gt),Ol	41.969 ±0.019	45.043 ±0.019	~0.23	30.5	6.3

TABLE A.9.5 ctd.

Run No.	Charge No.	Temp. (°C)	Pressure (kb)	Time (hrs)	Phase Identification		°2θ CrKα Cpx 220	°2θ CrKα Cpx $\bar{2}21$	°2θ CrKα Cpx(310 ∧ $\bar{3}11$)	Wt%CS in Cpx	Wt%A in Cpx
					Optical	X-Ray Diffraction					
103	E35	1600	30.0	0.55	Cpx,(Ol),(G/O)	Cpx	41.993 ±0.018	45.062 ±0.030	~0.17	30.0	7.5
55	E35	1549	30.0	2.17	Cpx,(?Opx),Gt,Ol,G/O	Cpx,Opx,Gt	41.970 ±0.018	45.068 ±0.008	-	31.0	7.5
218	E35	1524	30.0	1.80	Cpx,Opx,Gt,G/O,(UG)	Cpx,Opx,Gt	41.964 ±0.016	45.057 ±0.018	0.281 ±0.019	31.7	7.0
74	E35	1500	30.0	4.80	Pyx,Gt,Ol,G/O,UG	Cpx,Opx,Qz	41.895 ±0.032	-	0.338 ±0.050	33.2	6.0
223	E35	1400	30.0	8.70	Pyx,Gt,Ol,G/O,UG	Cpx,Opx,Ol,Qz	-	-	-	-	-
239	E35R	1525	30.0	2.00	Pyx,Gt,Ol	Cpx,Opx,Gt	41.935 ±0.041	45.037 ±0.063	0.292 ±0.042	32.1	6.3
243	E35F24R	1525	30.0	1.75	Pyx,Gt,Ol	Cpx,Opx,Gt	41.961 ±0.018	-	-	-	-
222	E36	1525	30.0	1.83	Cpx,(Opx),Gt,Ol,G/O	Cpx,Ol	41.887 ±0.014	-	-	-	-
277	E36R	1550	30.0	2.32	Cpx,Gt,Ol,G/O	Cpx,Gt	-	-	-	-	-
241	E36R	1525	30.0	2.08	Cpx,(Opx),Gt,Ol,G/O	Cpx,Gt,Ol	41.923 ±0.027	45.070 ±0.014	0.374 ±0.028	34.0	7.0
247	E36R	1449	30.5	5.25	Pyx,Gt,Ol,G/O	Cpx,Opx	41.818 ±0.023	45.070 ±0.042	0.528 ±0.041	37.7	5.7
276	E38R	1525	30.0	2.70	Pyx,Gt,(G/O)	Cpx,Gt	-	-	-	-	-
271	E38R	1450	30.0	5.75	Pyx,Gt	Cpx,Opx,Gt,Ol	41.816 ±0.013	45.074 ±0.042	0.528 ±0.022	37.8	5.7

TABLE A.9.5 ctd.

Run No.	Charge No.	Temp. (°C)	Pressure (kb)	Time (hrs)	Phase Identification		°2θ CrKα Cpx 220	°2θ CrKα Cpx $\bar{2}21$	°2θ CrKα Cpx(310∧$\bar{3}$11)	Wt%CS in Cpx	Wt%A in Cpx
					Optical	X-Ray Diffraction					
51	E10	1550	30.0	2.00	Cpx,Opx,Ol	Cpx,Opx	41.974 ±0.038	44.932 ±0.029	-	26.3	3.5
26	E15	1548	30.0	3.83	Cpx,Opx	Cpx,Opx	-	-	-	-	-
28	E15	1503	30.0	7.30	Cpx,Opx,Ol,G/O	Poor pattern	-	-	-	-	-
29	E15	1442	30.5	6.00	Cpx,Opx,Ol,G/O,UG	Cpx,Opx,Ol,Qz	-	-	-	-	-
48	E17	1548	30.5	2.75	Pyx,UG	Cpx	-	-	-	-	-
50	E27	1550	30.0	2.20	Cpx,Opx,Ol,G/O	Cpx,Opx	41.933 ±0.030	44.977 ±0.040	-	31.6	3.8
285	E27R	1523	30.0	2.25	Cpx,Opx,Gt,Ol	Cpx,Opx,(?Gt)	41.907 ±0.028	44.980 ±0.040	0.232 ±0.033	30.7	4.3
287	E27RF10	1525	30.0	2.17	Pyx,Gt,Ol	Cpx,Opx,(?Gt),Ol	41.902 ±0.012	44.967 ±0.031	0.200 ±0.012	30.0	3.8
57	E28	1551	30.0	2.00	Cpx,Opx,G/O	Cpx	41.904 ±0.042	44.992 ±0.030	-	-	-
59	E28	1498	30.0	3.17	Cpx,Opx	Cpx,Opx	-	-	-	-	-
52	E29	1548	30.0	2.92	Cpx,(G/O),(UG)	Cpx,(?Gt)	41.887 ±0.037	44.998 ±0.024	0.294 ±0.038	32.0	4.7
286	E29R	1524	30.0	2.70	Pyx,Gt,Ol,G/O	Cpx	41.869 ±0.022	44.990 ±0.041	0.314 ±0.016	32.4	4.1
280	E30R	1549	30.0	2.00	Cpx,Gt,Ol,(UG)	Cpx	-	-	-	-	-

TABLE A.9.5 ctd.

Run No.	Charge No.	Temp. (°C)	Pressure (kb)	Time (hrs)	Phase Identification		°2θ CrKα Cpx 220	°2θ CrKα Cpx $\bar{2}21$	°2θ CrKα Cpx(310 ∧ $\bar{3}11$)	Wt%CS in Cpx	Wt%A in Cpx
					Optical	X-Ray Diffraction					
49	E31	1548	30.0	2.00	Cpx,(G/O)	Cpx	41.822 ±0.049	45.034 ±0.030	0.473 ±0.014	36.0	4.5
41	E18	1550	30.0	3.08	Cpx,Opx,(Ol)	Cpx,Opx	41.900 ±0.021	45.002 ±0.023	-	31.5	4.7
45	E18	1500	30.0	5.50	Cpx,Opx,Ol,G/O	Cpx,Opx	41.884 ±0.059	44.900 ±0.043	0.555 ±0.025	?	?
39	E18	1450	30.0	6.00	Cpx,Opx,Ol,(G/O),UG	Cpx,Opx	-	-	-	-	-
61	E24	1550	30.0	1.92	Cpx,Ol,UG	Cpx,Ol	-	-	-	-	-
75	E24	1516	30.0	3.75	Cpx,Opx,Ol	Cpx	41.814 ±0.047	44.920 ±0.039	-	31.2	1.4
47	E25	1547	30.0	3.00	Cpx,(Ol)	Cpx	41.754 ±0.030	44.949 ±0.035	0.405 ±0.024	34.0	1.5
46	E25	1451	30.0	5.50	Pyx,Ol	Cpx,Opx	41.724 ±0.026	44.976 ±0.022	0.503 ±0.033	36.5	2.1

TABLE A.9.6

Miscellaneous experiments on bulk compositions in sub-systems of the system C-M-A-S

Run No.	Charge No.	Temp. (°C)	Pressure (kb)	Time (hrs)	Phase Identification		Remarks
					Optical	X-Ray Diffraction	
232	FP10	1523	30.0	1.67	Ol,Gt	Ol,Gt	
224	F1OPy	1525	30.0	2.33	Ol,Gt	Ol	
175	D90	1499	30.0	3.50	Cpx,Opx	-	Charge seeded with 2% opx xls. of composition $(CMS_2)_8(MS)_{92}$ (opx xls. from run M5/143)
GLI	E22	1620	20.0*	0.50	Cpx	Cpx	Experiment run at Geophys. Lab.
GLII	E22G	1620	20.0*	0.50	Cpx	Cpx	Experiment run at Geophys. Lab.
12Y	DR	1715	25.0*	0.08	Gl,Q	-	
14Y	DR	1695	25.0*	0.08	Cpx,Gl,Q	-	Primary cpx xls. at base of capsule
13Y	DR	1675	25.1*	0.08	Cpx	-	
20Y	PYR	1630	25.0*	0.17	Opx	Opx	Presence of quench crystals inferred from Boyd and England (1962)
21Y	PYR	1620	25.0*	0.17	Gt	Gt	

* indicates a floating-piston experiment

TABLE A.9.7

The results of experiments on enstatite-rich C-M-A-S charges

Run No.	Charge No.	Starting Material	Pressure (kb)	Temp. (^{o}C)	Time (hrs.)	H_2O Content	Phase Identification		Al_2O_3 content of opx **	Pressure error using MacGregor's (1974) data ***
							Optical	X-Ray Diffraction		
283	ENA8R	Rexd. gel mix	30.0	1650	0.5	-	Opx	Opx	8.0	} +10.5 kb
282	ENA8R		30.0	1550	2.2	-	Opx,Gt	Opx	<8.0	
281	ENA8R		30.0	1400	6.2	-	Opx,Gt	-	<8.0	
290	ENA8R		30.0 (F)	1481	4.0	-	Opx,Gt	-	<8.0	
291	ENA8R		27.0	1480	4.3	-	Opx,Gt	-	<8.0	
284	EP32	Xl. mix: gt+opx	30.0	1550	2.0	-	Opx,Gt	Opx	<8.0	
261	$En_{95}A_5R$	Rexd. gel	30.4	1202	18.0	6.7	Opx,Q,(Gl),(Ol)	-		
268	$En_{95}A_5R$		30.0	1174	17.0	4.0	Opx,Q	-		
257	$En_{95}A_5R$		29.1	1150	17.0	'damp'	?,UG	Opx		
263	$En_{95}A_5R$		29.4	1100	15.5	2.5	Opx,Gt	-	<5.1	
79	E5	Gel	30.0	1599	0.7	-	Pyx,Gt	Opx,Cpx	<7.5 (<7.1)	
68	E5		30.0	1499	4.1	-	Pyx,Gt	Opx,Cpx,Gt	<7.5 (<7.1)	

TABLE A.9.7 ctd.

Run No.	Charge No.	Starting Material	Pressure (kb)	Temp. (°C)	Time (hrs.)	H_2O Content	Phase Identification		Al_2O_3 content of opx **	Pressure error using MacGregor's (1974) data **
							Optical	X-Ray Diffraction		
100	AM3	Gel mix	35.0	1660	0.3	-	Pyx	Opx,Cpx	6.0 (5.6)	+13 kb
98	AM3		35.0	1619	0.4	-	Pyx,Gt	Opx,Cpx*	<6.0 (<5.6)	
96	AM3		35.0	1580	1.5	-	Pyx,Gt	Opx,Cpx	<6.0 (<5.6)	
82	AM3		30.0	1565	2.0	-	Pyx	Opx,Cpx	6.0 (5.6)	+14 kb
91	AM3		30.0	1542	2.6	-	Pyx,Gt	Opx,Cpx*	<6.0 (<5.6)	
81	AM3		30.0	1523	3.8	-	Pyx,Gt	Opx,Cpx,Gt	<6.0 (<5.6)	
86	AM3		27.0	1520	3.5	-	Pyx	Opx	6.0 (5.6)	+14 kb
87	AM3		27.0	1480	5.3	-	Pyx,Gt	Opx,Cpx	<6.0 (<5.6)	
264	E41R	Rexd. gel	30.0	1549	2.5	-	Pyx,(Gt)	Opx,Cpx	<6.0 (<5.3)	
253	E41R		30.0	1534	2.0	-	Pyx,Gt	Opx,Cpx	<6.0 (<5.3)	
272	E3R	Rexd. gel	30.0	1525	2.4	-	Pyx	Opx,Cpx*	4.5 (4.1)	+17.5 kb
269	E3R		30.0	1498	4.4	-	Pyx,Gt	Opx,Cpx*	<4.5 (<4.1)	
65	E3	Gel	30.0	1365	10.2	-	Pyx,Gt,(UG)	Opx,Cpx	<4.5 (<4.1)	
275	E3H	Glass	30.0	1450	6.8	-	Pyx,(Gt)	-	<4.5 (<4.1)	
278	E3H	Glass	30.0	1350	9.0	-	Pyx,(Gt)	-	<4.5 (<4.1)	
279	(E3H/275) +(E3H/278)	Run product mix	30.0	1450	6.0	-	Pyx,Gt	Opx	<4.5 (<4.1)	

TABLE A.9.7 ctd.

Run No.	Charge No.	Starting Material	Pressure (kb)	Temp. (°C)	Time (hrs.)	H_2O Content	Phase Identification		Al_2O_3 content of opx **	Pressure error using MacGregor's (1974) data ***
							Optical	X-Ray Diffraction		
262	E41RF2	Rexd. gel mix	30.0	1565	2.4	-	Pyx,Ol	Opx,Cpx	5.9 (5.2)	} +14 kb
259	E41RF2		30.0	1550	1.5	-	Pyx,Gt,Ol	Opx,Cpx,?Ol	<5.9 (<5.2)	
292	E41RF2		30.0	1500	4.0	-	Pyx,Gt,Ol	-	<5.9 (<5.2)	
294	(E41RF2 /292)	Run product	30.0	1500	4.1	-	Pyx,Gt,Ol	-	<5.9 (<5.2)	
274	E4R	Rexd. gel	30.0	1525	1.9	-	Pyx,Ol,G/O	Opx,Cpx,Ol	4.1 (3.7)	} +19 kb
267	E4R		30.0	1501	4.3	-	Pyx,Gt,Ol	Opx,Cpx,Ol	<4.1 (<3.7)	
266	E4R		30.0	1465	6.0	-	Pyx,Gt,Ol	Opx,Cpx,Ol	<4.1 (<3.7)	
254	E4R		30.0	1350	6.4	-	Pyx,Gt,Ol	Opx,Cpx,Ol	<4.1 (<3.7)	

(F) indicates floating-piston technique; other experiments were carried out using the piston-out technique.

* The occurrence of clinopyroxene could not be conclusively proved but it is assumed to be present because of the relatively large amounts in the run products of composition E41R.

** Maximum Al_2O_3 contents of orthopyroxenes are quoted. The figures in brackets are minimum Al_2O_3 contents (see text).

*** Pressure errors which would result from the determination of equilibration pressures for these assemblages, from MacGregor's (1974) pressure/temperature grid for Al_2O_3 solubility in orthopyroxene. Each pressure error determination uses the equilibration temperature of the assemblage (taken to be the midpoint of the relevant temperature bracket) and the Al_2O_3 content of the orthopyroxene in the assemblage.

TABLE A.9.8

X-ray diffraction parameters of orthopyroxenes crystallized in high pressure experiments described in Table A.9.7

Run No.	Charge No.	Opx X-Ray Diffraction Parameter A* ($^{o}2\theta$ CuKα)	Wt.% Al_2O_3 in Opx from Boyd and England (1960)	Opx X-Ray Diffraction Parameter B* ($^{o}2\theta$ CuKα)	Wt.% Al_2O_3 in Opx from Boyd and England (1960)
283	ENA8R	1.015±0.036	8.3	0.545±0.024	8.6
282	ENA8R	0.998±0.012	8.0	0.544±0.007	8.6
281	ENA8R	0.947±0.033	6.7	0.514±0.022	6.8
291	ENA8R	1.001±0.044	7.8	0.544±0.039	8.6
284	EP32	0.984±0.045	7.5	0.548±0.031	8.8
267	E4R	0.902±0.046	-	0.512±0.048	-
266	E4R	0.871±0.073	-	0.518±0.022	-
254	E4R	0.817±0.070	-	0.478±0.030	-

* Parameter A: the difference (in terms of $^{o}2\theta$ CuKα_1) between the two orthopyroxene reflections whose d-spacings for pure orthoenstatite are 1.4826 and 1.4683 Å.

Parameter B: the difference (in terms of $^{o}2\theta$ CuKα_1) between the two orthopyroxene reflections whose d-spacings for pure orthoenstatite are 2.1143 and 2.0970 Å.

TABLE A.9.9

Results of experiments at 25 kb on anhydrous charges with bulk compositions in the system C-M-A-S-N

Run No.	Charge No.	Temp. (°C)	Time (mins)	Pressure (kb)	Phase Identification	
					Optical	X-Ray Diffraction
33Y	Z-HG	1608	280	25.0	Gl	-
37Y	Z-HG	1560	175	25.0	(Opx),Gl,Q	Cpx,Opx
32Y	Z-HG	1508	335	25.0	Cpx,Opx,Gt,Gl,Q	Cpx,?Opx
69Y	Z-HG	1490	750	25.8	Cpx,Opx,Gt,Gl,Q	Cpx
40Y	Z-HG	1475	930	25.0	Pyx,Gt,Gl,Q	Cpx,Gt
36Y	Z-HG	1440	870	25.5	Pyx,Gt	Cpx,Gt
50Y	Z-MG	1605	105	25.0	Gl	-
53Y	Z-MG	1534	245	25.0	(Opx),Gl,Q	Cpx,Opx
63Y	Z-MG	1524	420	25.0	Cpx,Opx,Gl,Q	Cpx,Opx
49Y	Z-MG	1500	180	25.0	Cpx,Opx,Gt,Gl,Q	Cpx,Gt
47Y	Z-MG	1475	320	25.0	Pyx,Gt,Gl,Q	-
48	Z-MG	1440	240	25.0	Pyx,Gt	-
55Y	Z-GL	1591	70	25.0	Gl	-
61Y	Z-GL	1530	340	25.0	Opx,Gl,Q	Cpx,Opx
56Y	Z-GL	1520	375	25.0	Opx,Cpx,Gt,Gl,Q	Cpx,Opx,Gt
67Y	Z-GL	1490	705	24.7	Opx,Cpx,Gt,Gl,Q	Cpx,Gt

TABLE A.9.9. (ctd.)

Run No.	Charge No.	Temp. (°C)	Time (mins)	Pressure (kb)	Phase Identification	
					Optical	X-Ray Diffraction
70Y	Z-GL	1480	720	25.0	Opx,Cpx,Gt,Gl,Q	Cpx,Gt
59Y	Z-GL	1470	465	25.0	Pyx,Gt,Gl	Cpx,Gt
58Y	Z-GL	1440	720	25.0	Pyx,(Gt)	Cpx,Gt
4X	Z10	1532	100	25.0	Gl	-
8X	Z10	1524	83	25.0	Opx,Gl,Q	-
7X	Z10	1520	85	25.0	Opx,Cpx,Gl,Q	-
5X	Z10	1510	60	25.0	Cpx,Gt,(Gl)	-
1X	Z20	1550	40	25.0	Gl	-
3X	Z20	1510	180	25.0	(Cpx),Gl,Q	-
2X	Z20	1450	240	25.0	Cpx,(Gl)	-

TABLE A.9.10

Results of experiments at 25 kb on the gel Z-HG in the presence of H_2O. (Furnace assemblages A, B1 and B2 are described in Appendix A.1.1)

Run No.	Temp. (°C)	H_2O Content	Time (mins)	Pressure (kb)	Furnace Assembl.	Phase Identification		Remarks
						Optical	X-Ray Diffraction	
153Y	1370	4.8	255	25.0	A	Opx,Gl,Q	-	Xl. settling
117Y	1348	4.8	240	25.0	B1	Opx,Gl,Q	?Cpx,?Opx,Amph	
152Y	1340	4.8	270	25.0	A	Cpx,Opx,Gt,Gl,Q	-	Xl. settling
151Y	1320	4.8	245	25.0	A	Cpx,Opx,Gt,Gl,Q	-	
133Y	1297	6.0	197	25.0	A	Cpx,Opx,Gt,Gl,Q	Cpx,Opx,Gt,Amph	Xl. settling
131Y	1290	4.5	510	25.3	A	Cpx,Opx,Gt,Gl,Q	Cpx,?Opx,Gt,Amph	Xl. settling
84Y	1259	25.0	225	24.3	A	Gl,Q	-	
116Y	1250	5.3	270	25.4	B1	Cpx,Opx,Gt,Gl,Q	Cpx,Opx,Gt,Amph	
122Y	1248	6.0	280	25.0	A	Cpx,Opx,Gt,Gl,Q	Cpx,Opx,Gt	
136Y	1245	9.8	185	25.0	B1	Ol,Opx,Gl,Q	-	
87Y	1223	30.0	265	24.3	A	Gl,Q	-	
142Y	1220	24.5	140	25.0	B1	Gl,Q	-	
106Y	1207	19.0	235	25.0	B1	Ol,Opx,Gl,Q	Amph	
89Y	1201	28.1	240	25.0	A	Ol,Opx,Gl,Q	Amph,Chlor	
123Y	1200	damp	810	25.0	A	Cpx,Opx,Gt,Gl,Q	Cpx,Gt	Charge undried; no H_2O added
141Y	1200	24.2	130	25.0	B1	Ol,Gl,Q	-	
137Y	1200	30.7	425	24.7	B1	Gl,Q	-	
120Y	1199	4.8	215	25.0	B1	Cpx,Opx,Gt,Gl,Q	Cpx,Opx,Gt,Amph	
132Y	1180	12.5	380	25.4	B1	Ol,Cpx,Opx,Gt,Gl,Q	Cpx,Gt,Amph	
139Y	1174	23.8	285	25.0	B1	Ol,Gl,Q	-	

TABLE A.9.10 CTD.

Run No.	Temp. (°C)	H_2O Content	Time (mins)	Pressure (kb)	Furnace Assembl.	Phase Identification		Remarks
						Optical	X-Ray Diffraction	
127Y	1156	13.8	190	25.0	B1	Ol,Opx,Gl,Q	-	
125Y	1156	15.0	210	25.0	B2	Cpx,Opx,Gt,Gl,Q	Cpx,Opx,Gt	Xl. settling
118Y	1149	3.5	240	25.0	B1	Cpx,Opx,Gt,Gl,Q	Cpx,Opx,Gt	
129Y	1144	14.0	205	25.0	B1	Cpx,Opx,Gt,Gl,Q	Cpx,Gt	
146Y	1127	15.0	230	25.0	B1	Ol,Opx,Gl,Q	-	
233Y	1122	19.8	230	25.0	A	Ol,Opx,Gl,Q	-	Xl. settling
114Y	1090	18.8	245	25.0	B1	Cpx,Opx,Gt,Amph,Gl,Q	Cpx,Gt	
149Y	1088	24.0	205	25.0	B1	Ol,Opx,Gl,Q	Ol,Cpx,Amph	
113Y	1081	23.5	240	24.7	B1	Ol,Cpx,Opx,Gt,Gl,Q	Gt,Amph	
111Y	1070	16.3	210	25.0	B1	Cpx,Opx,Gt,Amph,Gl,Q	-	
110Y	1055	15.4	200	25.4	B1	Cpx,Gt,Amph,Gl,Q	Cpx,Gt,Amph	
109Y	1053	20.5	1020	24.1	B1	Cpx,Opx,Gt,Amph,Gl,Q	Cpx,Gt,Amph	
119Y	1048	2.3	220	25.0	B1	Cpx,Gt,Amph,Gl,Q	Cpx,Gt,Amph	
105Y	1006	11.6	290	25.0	B1	Cpx,Gt,Amph,Gl,Q	?Cpx,Gt,Amph	
135Y	1002	damp	1015	24.7	A	Cpx,Gt,Amph	Cpx,?Gt	Charge undried; no H_2O added
103Y	1000	16.8	187	25.0	B1	Cpx,Gt,Amph,Gl,Q	Gt	
107Y	975	11.4	263	25.0	B1	Cpx,Gt,Amph,Gl,Q	-	
104Y	946	19.5	240	25.0	B1	Cpx,Gt,Amph,Gl,Q	Cpx,Gt,Amph	
108Y	941	13.6	745	25.0	B1	Cpx,Gt,Amph,Gl,Q	Gt,Amph	
112Y	850	19.5	1050	25.0	B1	Cpx,Gt,Amph,Gl,Q	Amph	
115Y	770	16.7	1102	25.0	B1	Cpx,Amph	Amph	
148Y	771	15.7	885	25.4	B1	Cpx,Amph	Amph	Charge seeded with gt xls.

TABLE A.9.11

Results of piston-out experiments at 30 kb on mixes of A3/Diopside and A3/Enstatite

Run No.	Charge No.	Temp. (°C)	Time (mins)	Phase Identification		$^{\circ}2\theta$ CuKα	$^{\circ}2\theta$ CrKα	Wt.% A3/Di	Wt.% A3/Di
				Optical	X-Ray Diffraction	Cpx 220 (1)	Cpx 310 (2)	in Cpx from (1)	in Cpx from (2)
152	A3/Di40	1602	5	Cpx	Cpx	27.915±0.018	46.471±0.018	-	-
154	A3/Di60	1600	12	Cpx	Cpx	27.83 ±0.011	46.348±0.020	-	-
228	A3/Di23	1550	15	Cpx,Opx	Cpx,Opx	27.95*±0.025	46.497±0.031	28.7	35.8
150	A3/Di40	1500	30	Cpx,(?Opx)	Cpx,(Opx)	27.91 ±0.020	-	39.7	-
151	A3/Di40	1450	55	Cpx,Opx	Cpx,Opx	27.875±0.021	-	49.0	-
226	A3/Di60	1390	50	Cpx,Opx	Cpx,Opx	27.805±0.030	-	68.0	-
185	A3/Di60	1350	80	Cpx,Opx	Cpx,Opx	27.78 ±0.017	-	74.7	-
187	A3/Di40	1350	83	Cpx,Opx	Cpx,Opx	27.80*±0.034	-	69.3	-

* Not a satisfactory measurement.

$^{\circ}2\theta$ CuKα 220 of A3/Diopside is 27.685±0.030. (A3/Diopside is the unrecrystallized clinopyroxene end member (charge no. A3/Di))

The 310 and $\bar{3}11$ reflections are not distinguishable on the x-ray diffraction patterns, obtained using CrKα radiation, of the clinopyroxenes for which values of the $^{\circ}2\theta$ CrKα 310 parameter (actually the $^{\circ}2\theta$ CrKα 310,311 parameter) are given.

TABLE A.9.12

Results of piston-out experiments on the natural eclogite 1044 from the Vissers Pipe, Tanzania

Pressure (kb)	Temp. (°C)	Time (mins)	Phase Identification	
			Optical	X-Ray Diffraction
20.0	1476	15	Gl,Q	-
20.0	1425	15	Cpx,Gl,Q	Cpx
20.0	1401	15	Cpx	Cpx
20.0	1378	63	Cpx,Gt	Cpx
20.0	1350	60	Cpx,Gt	Cpx
25.0	1556	15	Gl	-
25.0	1528	10	Gl,Q	-
25.0	1502	15	Cpx,Gl,Q	-
25.0	1478	15	Cpx,(Gl),Q	Cpx
25.0	1449	15	Cpx,Gt	Cpx,(Gt)
30.0	1575	15	Cpx,Gl,Q	Cpx
30.0	1527	15	Cpx,Gl,Q	Cpx
30.0	1512	15	Cpx,Gt,Q,Gl	Cpx,Gt
30.0	1500	15	Cpx,Gt	Cpx,Gt
35.0	1601	15	Cpx,Gl,Q	Cpx
35.0	1575	15	Cpx,Gl,Q	Cpx
35.0	1550	15	Cpx,Gt,Gl,Q	Cpx,(Gt)
40.0	1627	15	Cpx,(?Gt),Gl,Q	Cpx

TABLE A.9.13

Results of piston-out experiments on the natural eclogite 1058 from the Robert's Victor Pipe, South Africa

Pressure (kb)	Temp. (^{o}C)	Time (mins)	Phase Identification	
			Optical	X-Ray Diffraction
20.0	1501	16	Gl	-
20.0	1475	15	Cpx,Gl,Q	-
20.0	1455	15	Opx,?Cpx,Gt,Q,Gl	Cpx
20.0	1450	16	Opx,Cpx,Gt,Q,Gl	Cpx,(?Opx),(Gt)
20.0	1424	13	Cpx,Gt,Q,Gl	Cpx,Gt
20.0	1399	15	Cpx,Gt,Q,Gl	Cpx,Gt
20.0	1375	15	Cpx,Gt	Cpx,Gt
25.0	1560	7	Gl	-
25.0	1525	15	Gt,Gl	(Gt)
25.0	1500	15	Cpx,Gt,Gl,(Q)	Cpx,Gt
25.0	1450	15	Cpx,Gt,(Gl),(Q)	Cpx,Gt
30.0	1616	5	Gl	-
30.0	1586	5	Gt,Gl,Q	Gt
30.0	1550	15	Cpx,Gt,Gl,Q	Cpx,Gt
30.0	1500	10	Cpx,Gt,(Q),(Gl)	Cpx,Gt
30.0	1450	15	Cpx,Gt	Cpx,Gt

TABLE A.9.14

Results of experiments on the natural olivine-garnet websterite 1031

Pressure (kb)	Temp. (^{o}C)	Time (mins)	Phase Identification	
			Optical	X-Ray Diffraction
30.0	1570	15	Cpx,Opx,Ol	Cpx,Opx
30.0	1550	20	Cpx,Opx,Ol	Cpx,?Opx (poor pattern)
30.0	1521	30	Cpx,Opx,Gt,Ol	Cpx,Opx,Ol
30.0	1500	127	Cpx,Opx,Gt,Ol	Cpx,Opx,Ol

TABLE A.9.15

Summary of details of experiments in previous studies of the solubility of Al_2O_3 in orthopyroxene at high pressure

Source of work	System containing bulk comps.	Starting materials	Phases in run products	Piston technique	Pressure correction	H_2O as flux	Analytical technique	Remarks
Boyd and England (1964)	MS-A	Glasses; Xl mixes of gt+opx	opx±gt	Fl. Pist.	x	Temp. <1400°C	Optics	
O'Hara and Yoder (1967)	CS-MS-A	Glasses rexd. at atmos. pressure	opx,cpx,gt	Fl. Pist.	x	x	Optics; X-ray diff.*	Data at 1600°C, 30 kb only
Boyd (1970)	CS-MS-A	Glasses	opx+gt±cpx	Fl. Pist.	x	√	Probe	Data at 1200°C, 30 kb only
MacGregor (1974)	MS-A	Glasses seeded with gt	opx+gt	Pist. out	x	Temp. <1300°C	Probe	
Akella (1974a)	CS-MS-A	Glass	opx+cpx+gt	Pist. out or Pist. in	+1 kb / -1 kb	√	Probe	
MacGregor and Ringwood (1964)	Natural	opx+gt	opx±gt	Fl. Pist.	x	x	Optics	
Green and Ringwood (1970)	Synthetic multicmpt.	Glass rexd. at atmos. pressure	opx+cpx+gt+ol	Pist. in	-10%	x	Probe	Pt and graphite capsules
Hensen (1973)	Natural	alum. opx + alum. cpx spinel lherz. →	opx+cpx+gt / opx+cpx+gt+?ol	Pist. in	-10%	(Oxalic acid at 1100°C)	Probe	Graphite capsules; difficulty of attaining equilibrium.
Akella and Boyd (1974)	Natural	opx+cpx+gt+ol	opx+cpx+gt+ol	Pist. out or Pist. in	+1 kb / -1 kb	√	Probe	Graphite capsules; difficulty of attaining equilibrium.

* This x-ray diffraction analysis of a calcium-bearing orthopyroxene uses Boyd and England's (1960) determinative curves for calcium-free orthopyroxenes; O'Hara and Yoder's (1967) analysis is therefore queried (see section 7.1).

ACKNOWLEDGEMENTS

I would like to thank Prof. Sir Frederick Stewart, Prof. G.Y. Craig, and Prof. M.J. O'Hara for placing at my disposal the excellent facilities at the Grant Institute of Geology.

I thank my supervisor, Prof. M.J. O'Hara, for suggesting these topics of study, for much advice and encouragement and for many interesting discussions.

I am very grateful to C. Chaplin and other members of the technical staff for their prompt assistance with technical problems. In particular I would like to thank C. Begg and W. Tullis for bearing with my idiosyncrasies.

Dr. C.E. Ford kindly recrystallized charges in the gas media pressure vessels and I would like to thank both him and Dr. G.M. Biggar for their advice on experimental techniques.

I thank Drs. B. Jefferies and P.G. Hill for tuition on the electron microprobe.

I am very grateful to S. Ballantyne and R. Devine for producing the photographs and to Mrs. P. Scrutton for typing this thesis.

Finally, I gratefully acknowledge the award of a grant from the Natural Environment Research Council and I would like to thank them for suspending the grant for a time during the course of this study.

REFERENCES

Akella, J. (1974a) Solubility of Al_2O_3 in orthopyroxene coexisting with garnet and clinopyroxene for compositions on the diopside-pyrope join in the system $CaSiO_3$-$MgSiO_3$-Al_2O_3. Yb. Carnegie Instn Wash. 73, 273-278.

Akella, J. (1974b) Friction measurement in solid-media, high-pressure apparatus. Yb. Carnegie Instn Wash. 73, 606-609.

Akella, J. and Boyd, F.R. (1972) Partitioning of Ti and Al between pyroxenes, garnets and oxides. Yb. Carnegie Instn Wash. 71, 378-384.

Akella, J. and Boyd, F.R. (1973) Effect of pressure on the composition of coexisting pyroxenes and garnet in the system $CaSiO_3$-$MgSiO_3$-$FeSiO_3$-$CaAlTiO_6$. Yb. Carnegie Instn Wash. 72, 523-526.

Akella, J. and Boyd, F.R. (1974) Petrogenetic grid for garnet peridotites. Yb. Carnegie Instn Wash. 73, 269-273.

Best, M.G. (1975) Amphibole-bearing cumulate inclusions, Grand Canyon, Arizona and their bearing on silica-undersaturated hydrous magmas in the upper mantle. J. Petrology 16, 212-236.

Biggar, G.M. (1969) The isothermal, isobaric, subsolidus diopside solid solution volume in the system CaO-MgO-Al_2O_3-SiO_2. Progress in Experimental Petrology 1, 97-104. Natural Environment Research Council.

Biggar, G.M. and O'Hara, M.J. (1969a) A comparison of gel and glass starting materials for phase equilibrium studies. Mineralog. Mag. 37, 198-205.

Biggar, G.M. and O'Hara, M.J. (1969b) Solid solutions at atmospheric pressure in the system CaO-MgO-SiO_2 with special reference to the instabilities of diopside, åkermanite and monticellite. Progress in Experimental Petrology 1, 86-96. Natural Environment Research Council.

Biggar, G.M. and O'Hara, M.J. (1969c) Temperature control and calibration in quench furnaces and some new temperature measurements in the system CaO-MgO-Al_2O_3-SiO_2. Mineralog. Mag. 37, 1-15.

Boettcher, A.L., Mysen, B.O. and Modreski, P.J. (1975) Melting in the mantle: phase relationships in natural and synthetic peridotite-H_2O and peridotite-H_2O-CO_2 systems at high pressures. Phys. Chem. Earth 9, 855-867.

Boullier, A.-M. and Nicolas, A. (1973) Texture and fabric of peridotite nodules from kimberlite at Mothae, Thaba Putsoa and Kimberley. In Lesotho Kimberlites (ed. P.H. Nixon), pp. 57-66. Lesotho National Development Corporation.

Boyd, F.R. (1970) Garnet peridotites and the system $CaSiO_3$-$MgSiO_3$-Al_2O_3. Mineral. Soc. Amer. Spec. Pap. 3, 63-75.

Boyd, F.R. (1973) A pyroxene geotherm. Geochim. cosmochim. Acta 37, 2533-2546.

Boyd, F.R. (1974) Ultramafic nodules from the Frank Smith kimberlite pipe, South Africa. Yb. Carnegie Instn Wash. 73, 285-294.

Boyd, F.R. (1975) Chemical inhomogeneities in minerals in kimberlite nodules from Lesotho and the Kimberley pipes. Ext. Abstracts, International Conference on Geothermometry and Geobarometry. The Pennsylvania State University.

Boyd, F.R., Bell, P.M., England, J.L. and Gilbert, M.C. (1967) Pressure measurement in single-stage apparatus. Yb. Carnegie Instn Wash. 65, 410-414.

Boyd, F.R. and England, J.L. (1959) Pyrope. Yb. Carnegie Instn Wash. 58, 83-87.

Boyd, F.R. and England, J.L. (1960) Minerals of the mantle. Yb. Carnegie Instn Wash. 59, 47-52.

Boyd, F.R. and England, J.L. (1962) Effect of pressure on the melting of pyrope. Yb. Carnegie Instn Wash. 61, 109-112.

Boyd, F.R. and England, J.L. (1963) Effect of pressure on the melting of diopside, $CaMgSi_2O_6$, and albite, $NaAlSi_3O_8$, in the range up to 50 kilobars. J. geophys. Res. 68, 311-323.

Boyd, F.R. and England, J.L. (1964) The system enstatite-pyrope. Yb. Carnegie Instn Wash. 63, 157-161.

Boyd, F.R. and Nixon, P.H. (1973) Origin of the ilmenite-silicate nodules in kimberlites from Lesotho and South Africa. In Lesotho Kimberlites (ed. P.H. Nixon), pp. 254-268. Lesotho National Development Corporation.

Boyd, F.R. and Schairer, J.F. (1964) The system $MgSiO_3$-$CaMgSi_2O_6$. J. Petrology 5, 275-309.

Bravo, M.S. (1973) Melting of synthetic phlogopite-bearing-spinel- and garnet-lherzolites at high pressures. Ph.D. thesis, Edinburgh University.

Bravo, M.S. and O'Hara, M.J. (1975) Partial melting of phlogopite-bearing synthetic spinel- and garnet-lherzolites. Phys. Chem. Earth 9, 845-854.

Bultitude, R.J. and Green, D.H. (1967) Experimental study at high pressures on the origin of olivine nephelinite and olivine melilite nephelinite magmas. Earth Planet. Sci. Lett. 3, 325-337.

Bultitude, R.J. and Green, D.H. (1971) Experimental study of crystal-liquid relationships at high pressures in olivine nephelinite and basanite compositions. J. Petrology 12, 121-147.

Cawthorn, R.G., Ford, C.E., Biggar, G.M., Bravo, M.S. and Clarke, D.B. (1973) Determination of the liquid composition in experimental samples: discrepancies between microprobe analysis and other methods. Earth Planet. Sci. Lett. 21, 1-5.

Charlu, T.V., Newton, R.C. and Kleppa, O.J. (1975) Enthalpies of formation at 970 K of compounds in the system MgO-Al_2O_3-SiO_2 from high temperature solution calorimetry. Geochim. cosmochim. Acta 39, 1487-1497.

Davis, B.T.C. (1964) The system diopside-forsterite-pyrope at 40 kilobars. Yb. Carnegie Instn Wash. 63, 165-171.

Davis, B.T.C. and Boyd, F.R. (1966) The join $Mg_2Si_2O_6$-$CaMgSi_2O_6$ at 30 kilobars pressure and its application to pyroxenes from kimberlites. J. geophys. Res. 71, 3567-3576.

Eggler, D.H. (1974) Effect of CO_2 on the melting of peridotite. Yb. Carnegie Instn Wash. 73, 215-224.

Eggler, D.H. (1975) CO_2 as a volatile component of the mantle: the system Mg_2SiO_4-SiO_2-H_2O-CO_2. Phys. Chem. Earth 9, 869-881.

Ford, C.E. (1972) Furnace design, temperature distribution, calibration and seal design in internally heated pressure vessels. Progress in Experimental Petrology 2, 89-96. Natural Environment Research Council.

Goetze, C. (1975) Sheared lherzolites: from the point of view of rock mechanics. Geology 3, 172-173.

Green, D.H. (1969) The origin of basaltic and nephelinitic magmas in the earth's mantle. Tectonophysics 7, 409-422.

Green, D.H. (1970) A review of experimental evidence on the origin of basaltic and nephelinitic magmas. Phys. Earth & Planet. Interiors 3, 221-235.

Green, D.H. (1973) Conditions of melting of basanite magma from garnet peridotite. Earth Planet. Sci. Lett. 17, 456-465.

Green, D.H. and Ringwood, A.E. (1970) Mineralogy of peridotitic compositions under upper mantle conditions. Phys. Earth & Planet. Interiors 3, 359-371.

Green II, H.W. and Gueguen, Y. (1974) Origin of kimberlite pipes by diapiric upwelling in the upper mantle. Nature 249, 617-620.

Hensen, B.J. (1973) Pyroxenes and garnets and geothermometers and barometers. Yb. Carnegie Instn Wash. 72, 527-534.

Hensen, B.J., Schmid, R. and Wood, B.J. (1975) Activity-composition relationships for pyrope-grossular garnet. Contrib. Mineral. Petrol. 51, 161-166.

Herzberg, C.T. (1975) Phase assemblages of the system $CaO-Na_2O-MgO-Al_2O_3-SiO_2$ in the plagioclase-lherzolite and spinel-lherzolite mineral facies. Ph.D. thesis, Edinburgh University.

Holmes, A. (1936) A contribution to the petrology of kimberlite and its inclusions. Trans. geol. Soc. S. Afr. 39, 379-428.

Howells, S., Begg, C. and O'Hara, M.J. (1975) Crystallization of some natural eclogites and garnetiferous ultrabasic rocks at high pressure and temperature. Phys. Chem. Earth 9, 895-902.

Howells, S. and O'Hara, M.J. (1975) Palaeogeotherms and the diopside-enstatite solvus. Nature 254, 406-408.

Ito, K. and Kennedy, G.C. (1968) Melting and phase relations in the plane tholeiite-lherzolite-nepheline basanite to 40 kilobars with geological implications. Contrib. Mineral. Petrol. 19, 177-211.

Ito, K. and Kennedy, G.C. (1974) The composition of liquids formed by partial melting of eclogites at high temperatures and pressures. J. Geol. 82, 383-392.

Jackson, E.D. and Wright, T.L. (1970) Xenoliths in the Honolulu Volcanic Series, Hawaii. J. Petrology 11, 405-430.

Johnston, J.L. (1973) Petrology and geochemistry of ultramafic xenoliths from the Jagersfontein Mine, O.F.S., South Africa. Ext. Abstracts, International Conference on Kimberlites, pp. 181-183. University of Cape Town.

Kushiro, I. (1968) Compositions of magmas formed by partial zone melting of the earth's upper mantle. J. geophys. Res. 73, 619-634.

Kushiro, I. (1969a) Synthesis and stability of iron-free pigeonite in the system $MgSiO_3$-$CaMgSi_2O_6$ at high pressures. Yb. Carnegie Instn Wash. 67, 80-83.

Kushiro, I. (1969b) The system forsterite-diopside-silica with and without water at high pressures. Am. J. Sci. (Schairer Vol.) 267A, 269-294.

Kushiro, I. (1969c) Discussion of the paper "The origin of basaltic and nephelinitic magmas in the earth's mantle" by D.H. Green. Tectonophysics 7, 427-436.

Kushiro, I. (1972) Effect of water on the composition of magmas formed at high pressures. J. Petrology 13, 311-334.

Kushiro, I. (1973) Regularities in the shift of liquidus boundaries in silicate systems and their significance in magma genesis. Yb. Carnegie Instn Wash. 72, 497-502.

Kushiro, I. (1974) Pressure effect on the changes of the forsterite-enstatite liquidus boundary with the addition of other cations and the genesis of magmas. Yb. Carnegie Instn Wash. 73, 248-251.

Kushiro, I. and Schairer, J.F. (1963) New data on the system diopside-forsterite-silica. Yb. Carnegie Instn Wash. 62, 95-103.

Kushiro, I., Shimizu, N., Nakamura, Y. and Akimoto, S. (1972) Compositions of coexisting liquid and solid phases formed upon melting of natural garnet and spinel lherzolites at high pressures: a preliminary report. Earth Planet. Sci. Lett. 14, 19-25.

Kushiro, I. and Yoder, H.S., Jr. (1970) Stability field of iron-free pigeonite in the system $MgSiO_3$-$CaMgSi_2O_6$. Yb. Carnegie Instn Wash. 68, 226-229.

Kushiro, I. and Yoder, H.S., Jr. (1974) Formation of eclogite from garnet lherzolite: liquidus relations in a portion of the system $MgSiO_3$-$CaSiO_3$-Al_2O_3 at high pressures. Yb. Carnegie Instn Wash. 73, 266-269.

Lindsley, D.H. and Dixon, S.A. (1975) Coexisting diopside and enstatite at 20 kbar and 900-1200°C. Abstr. with Programs (Geol. Soc. Amer.) 7, 1171.

MacGregor, I.D. (1974) The system MgO-Al_2O_3-SiO_2: solubility of Al_2O_3 in enstatite for spinel and garnet peridotite compositions. Am. Miner. 59, 110-119.

MacGregor, I.D. (1975) Petrologic and thermal structure of the upper mantle beneath South Africa in the Cretaceous. Phys. Chem. Earth 9, 455-466.

MacGregor, I.D. and Ringwood, A.E. (1964) The natural system enstatite-pyrope. Yb. Carnegie Instn Wash. 63, 161-163.

Martin, R.F. and Donnay, G. (1972) Hydroxyl in the mantle. Am. Miner. 57, 554-570.

Mercier, J.-C. and Carter, N.L. (1975) Pyroxene geotherms. J. geophys. Res. 80, 3349-3362.

Merrill, R.B. and Wyllie, P.J. (1973) Absorption of iron by platinum capsules in high pressure rock melting experiments. Am. Miner. 58, 16-20.

Modreski, P.J. and Boettcher, A.L. (1973) Phase relationships of phlogopite in the system K_2O-MgO-CaO-Al_2O_3-SiO_2-H_2O to 35 kilobars: a better model for micas in the interior of the earth. Am. J. Sci. 273, 385-414.

Mori, T. and Green, D.H. (1975a) Pyroxenes in the system $Mg_2Si_2O_6$-$CaMgSi_2O_6$ at high pressure. Earth Planet. Sci. Lett. 26, 277-286.

Mori, T. and Green, D.H. (1975b) Experimental studies of pyroxenes at high pressures. Ext. Abstracts, International Conference on Geothermometry and Geobarometry. The Pennsylvania State University.

Munoz, J.L. and Lindsley, D.H. (1969) Subsolidus relations on the join hedenbergite-ferrosilite at 20 kb. Yb. Carnegie Instn Wash. 67, 88-91.

Mysen, B.O. and Kushiro, I., and Nicholls, I.A. and Ringwood, A.E. (1974) A possible mantle origin for andesitic magmas: discussion of a paper by Nicholls and Ringwood. Earth Planet. Sci. Lett. 21, 221-229.

Nehru, C.E. and Wyllie, P.J. (1974) Electron microprobe measurement of pyroxenes coexisting with H_2O-undersaturated liquid in the join $CaMgSi_2O_6$-$Mg_2Si_2O_6$-H_2O at 30 kilobars, with applications to geothermometry. Contrib. Mineral. Petrol. 48, 221-228.

Nicholls, I.A. and Ringwood, A.E. (1973) Effect of water on olivine stability in tholeiites and the production of silica-saturated magmas in the island arc environment. J. Geol. 81, 285-300.

Nixon, P.H. and Boyd, F.R. (1973a) Petrogenesis of the granular and sheared ultrabasic nodule suite in kimberlites. In Lesotho Kimberlites (ed. P.H. Nixon), pp. 48-56. Lesotho National Development Corporation.

Nixon, P.H. and Boyd, F.R. (1973b) The discrete nodule association in kimberlites from northern Lesotho. In Lesotho Kimberlites (ed. P.H. Nixon), pp. 67-75. Lesotho National Development Corporation.

O'Hara, M.J. (1968) The bearing of phase equilibria studies in synthetic and natural systems on the origin and evolution of basic and ultrabasic rocks. Earth Sci. Rev. 4, 69-133.

O'Hara, M.J. (1969) The atmospheric pressure equilibrium and fractional crystallization of basalt-like mixtures in the $MgSiO_3$-rich part of the plane $CaSiO_3$-$MgSiO_3$-Al_2O_3, and the nature of thermal divides. Progress in Experimental Petrology 1, 129-152. Natural Environment Research Council.

O'Hara, M.J. (1975) Pyroxene grids, palaeogeotherms and a new mineral facies in the upper mantle. Ext. Abstracts, International Conference on Geothermometry and Geobarometry. The Pennsylvania State University.

O'Hara, M.J. and Mercy, E.L.P. (1963) Petrology and petrogenesis of some garnetiferous peridotites. Trans. R. Soc. Edinb. 65, 251-314.

O'Hara, M.J., Richardson, S.W. and Wilson, G. (1971) Garnet-peridotite stability and occurrence in crust and mantle. Contrib. Mineral. Petrol. 32, 48-68.

O'Hara, M.J., Saunders, M.J. and Mercy, E.L.P. (1975) Garnet-peridotite, primary ultrabasic magma and eclogite; interpretation of upper mantle processes in kimberlite. Phys. Chem. Earth 9, 571-604.

O'Hara, M.J. and Schairer, J.F. (1963) The join diopside-pyrope at atmospheric pressure. Yb. Carnegie Instn Wash. 62, 107-115.

O'Hara, M.J. and Yoder, H.S., Jr. (1967) Formation and fractionation of basic magmas at high pressures. Scott. J. Geol. 3, 67-117.

Parmentier, E.M. and Turcotte, D.L. (1974) An explanation of the pyroxene geotherm based on plume convection in the upper mantle. Earth Planet. Sci. Lett. 24, 209-212.

Richardson, S.W., Bell, P.M. and Gilbert, M.C. (1968) Kyanite-sillimanite equilibrium between 700° and 1500°C. Am. J. Sci. 266, 513-541.

Saxena, S.K. and Nehru, C.E. (1975) Enstatite-diopside solvus and geothermometry. Contrib. Mineral. Petrol. 49, 259-267.

Sweatman, T.R. and Long, J.V.P. (1969) Quantitative electron-probe microanalysis of rock-forming minerals. J. Petrology 10, 332-379.

Thompson, R.N. and Kushiro, I. (1972) The oxygen fugacity within graphite capsules in piston-cylinder apparatus at high pressures. Yb. Carnegie Instn Wash. 71, 615-616.

Warner, R.D. and Luth, W.C. (1974) The diopside-orthoenstatite two-phase region in the system $CaMgSi_2O_6$-$Mg_2Si_2O_6$. Am. Miner. 59, 98-109.

Wood, B.J. (1974) The solubility of alumina in orthopyroxene coexisting with garnet. Contrib. Mineral. Petrol. 46, 1-15.

Wood, B.J. and Banno, S. (1973) Garnet-orthopyroxene and orthopyroxene-clinopyroxene relationships in simple and complex systems. Contrib. Mineral. Petrol. 42, 109-124.

Wyllie, P.J. and Huang, W.-L. (1975) Influence of mantle CO_2 in the generation of carbonatites and kimberlites. Nature 257, 297-299.

Wyllie, P.J. and Nehru, C.E. (1975) Compositions of glasses from St. Paul's peridotite partially melted at 20 kilobars. J. Geol. 83, 455-471.

Reprinted from
PHYSICS AND CHEMISTRY OF THE EARTH VOL. 9
Edited by L. H. AHRENS, J. B. DAWSON,
A. R. DUNCAN and A. J. ERLANK
PERGAMON PRESS-OXFORD AND NEW YORK · 1975

58

CRYSTALLIZATION OF SOME NATURAL ECLOGITES AND GARNETIFEROUS ULTRABASIC ROCKS AT HIGH PRESSURE AND TEMPERATURE

By S. HOWELLS, C. BEGG and M. J. O'HARA
Grant Institute of Geology, West Mains Road, Edinburgh EH9 3JW

ABSTRACT

The solidi of two dry bimineralic eclogites (probable high-pressure cumulates) are slightly lower but their quidi are substantially higher in temperature than the solidus of garnet–lherzolite. Olivine does not appear at ne liquidus of either rock and enstatite appears only transiently in the solidus–liquidus interval of one rock at 0 kbar. The two dry eclogites cannot, therefore, represent primary liquids produced from a peridotite source or can they be partially melted to yield peridotite residua. One eclogite shows total solution of garnet in clino-yroxene at the solidus close to 20 kbar, otherwise garnet is retained as a solidus phase in both rocks between 0 and 30 kbar.

A garnet–olivine websterite, thought to have formed originally as an olivine + two aluminous pyroxenes umulate, develops this mineralogy only close to the dry solidus at 30 kbar, 1575°C. Spinel appears at lower ressures, garnet at higher pressures.

An iron- and aluminium-rich garnet–lherzolite, possibly representing a frozen high-pressure primary magma n equilibrium with harzburgite, does not show the required replacement of olivine by orthopyroxene as liquidus hase until pressures in excess of 45 kbar, implying a depth of origin greater than 140 km.

INTRODUCTION

Few experimental data exist for the melting of natural eclogites and pyroxenites from imberlite. The experiments described here were designed to provide constraints on the ermissible conditions and modes of origin of four rocks.

Results of solid media equipment experiments in platinum capsules on dry charges of atural eclogite, garnet–olivine–pyroxenite and an exceptionally iron-rich garnet–lherzolite om kimberlite are presented (Table 1) and results for eclogite summarized in Fig. 1. o minimize the consequences of iron loss to the container most run durations were kept o a minimum (1–15 minutes in presence of liquid; 15 minutes–1 hour in subsolidus). hemical analyses of the four samples investigated appear in O'HARA *et al.* (1973a, b).

TABLE 1. RESULTS OF EXPERIMENTS

Pressure, kbar	Temp., °C	Time, min	Results
1. No. 8 (1044)			
20	1476	15	qu + gl
20	1425	15	cpx + qu + gl
20	1401	15	cpx
20	1378	63	cpx + gr
20	1350	60	cpx + gr
25	1556	15	gl
25	1528	10	qu + gl
25	1502	15	cpx + qu + gl
25	1478	15	cpx + qu + (gl)
25	1449	15	cpx + gr
30	1575	15	cpx + qu + gl
30	1527	15	cpx + qu + gl
30	1512	15	cpx + gr + qu + gl
30	1500	15	cpx + gr
35	1601	15	cpx + qu + gl
35	1575	15	cpx + qu + gl
35	1550	15	cpx + gr + (gl)
40	1627	15	cpx + (?gr) + qu + gl
2. R.V. 41 (1058)			
20	1501	16	gl
20	1475	15	cpx + qu + gl
20	1455	15	opx + ?cpx + gr + qu + gl
20	1450	16	opx + cpx + gr + qu + gl
20	1424	13	cpx + gr + qu + gl
20	1399	15	cpx + gr + qu + gl
20	1375	15	cpx + gr
25	1560	7	gl
25	1525	15	gr + gl
25	1500	15	cpx + gr + gl + (qu)
25	1450	15	cpx + gr + (gl) + (qu)
30	1616	5	gl
30	1586	5	gr + qu + gl
30	1550	15	gr + cpx + qu + gl
30	1500	10	gr + cpx + (qu) + gl
30	1450	15	gr + cpx
3. Matsoku 1031			
20	1688	3	qu + gl
20	1652	10	opx + qu
20	1611	10	opx + fo + qu + (?cpx) + gl
20	1576	15	opx + fo + qu + (?cpx)
20	1515	30	cpx + opx + fo + (gl)
20	1474	20	cpx + opx + fo + (sp)
20	1442	31	cpx + opx + fo + (sp)
20	1401	35	cpx + opx + fo + sp
20	1300	30	cpx + opx + fo + sp + gr
20	1201	120	cpx + opx + fo + sp + gr
20	1200	1080	cpx + opx + fo + sp + gr
25	1742	3	qu
25	1711	3	opx + qu + (gl)
25	1674	15	opx + qu + (?cpx)
25	1625	30	opx + fo + qu + (?cpx) + (gl)
25	1600	15	cpx + opx + fo + (gl)
25	1575	75	cpx + opx + fo + (gl) + qu
25	1525	30	cpx + opx + fo + (sp)

TABLE 1 (*cont.*)

Pressure kbar	Temp., °C	Time, min	Results
25	1500	10	cpx + opx + fo + (sp)
25	1449	15	cpx + opx + fo + sp + gr
25	1399	15	cpx + opx + fo + (sp) + gr
25	1307	30	cpx + opx + fo + sp + gr
30	1596	22	cpx + opx + fo + (gl)
30	1570	15	cpx + opx + fo
30	1550	20	cpx + opx + fo
30	1521	30	cpx + opx + fo + gnt
30	1500	120	cpx + opx + fo + gnt
35	1715	5	opx + qu + (?cpx)
35	1677	15	cpx + opx + (fo) + qu
35	1623	15	cpx + opx + fo + (gl)
35	1600	15	cpx + opx + fo + (gl)
35	1586	15	cpx, opx, fo, gr
35	1570	15	cpx, opx, fo, gr
4. Matsoku 1032			
35	1775	1	(ol), qu, gl
45	1725	10	ol, qu, gl
45	1700	15	opx, ol, qu
45	1675	20	opx, ol, qu
45	1650	30	opx, ol, qu
45	1600	60	opx, ol, qu
45	1550	70	opx, ol, gr, (sp), qu
45	1500	60	opx, ol, gr, cpx

Key to Table 1

( ) = very little.
qu = quenching products (usually cpx, sometimes ol, opx and sp).
? = identification unconfirmed.
gl = glass.
ol = olivine.
opx = orthopyroxene.
cpx = clinopyroxene (calcium-rich).
sp = picotite.
gr = pyralspite.

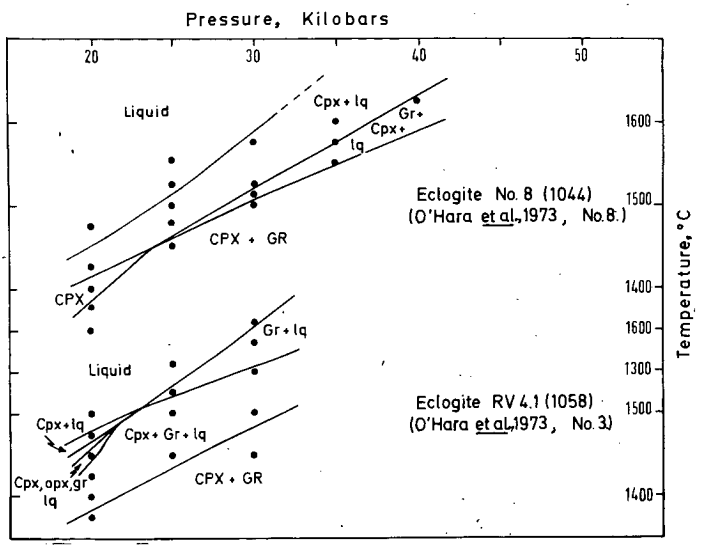

FIG. 1. Interpretation of quenching data for two eclogites.

RESULTS FOR ECLOGITES

We have studied two bimineralic eclogites, which we believe to be high-pressure crys cumulates, with a view to establishing four points:

(i) The maximum possible temperature at which such a rock could have accumulat which is of course its solidus temperature. Accumulation may, however, ha occurred at much lower temperatures from some more complex chemical syste

(ii) The limiting conditions under which such a rock could have precipitated as a gar plus clinopyroxene assemblage (i.e. eclogite), rather than a simple clinopyroxen which later exsolved garnet on cooling. The boundary between these two conditic is given by the "garnet out" boundary in the subsolidus.

(iii) Whether or not olivine appears on the liquidus of these eclogite compositions pressures where eclogite itself is a stable mineral assemblage. If olivine does r appear at the liquidus, the eclogite assemblages are a thermal divide preventi fractionation of primary magma from peridotite source rocks towards quar normative compositions (O'HARA and YODER, 1967).

(iv) If our belief that the two eclogites are cumulates was wrong, these rocks might held to represent frozen liquid compositions. Such liquids might be considered be primary magmas from a peridotite source, in which case olivine and enstat should be simultaneous liquidus phases at the pressure of formation. Determinati of the liquidus relationships provides a test of this proposition.

O'HARA and YODER (1967) reported solidus temperatures at 30 kbar in two natu eclogites and several reconstituted mineral assemblages from kimberlite. Their samp 37079 and TAN 503 resemble sample 1044 (Fig. 1) in being soda-poor and relatively l M(= Mg/Mg + Fe). They yielded a solidus temperature of ca. 1515°C at 30 kbar, simi to that observed in the new experiments. Garnet was present to the solidus, and clir pyroxene was liquidus phase as for 1044, but the new sample displays a higher liquic temperature.

In the new study, garnet does not appear as a liquidus phase below 40 kbar and there an immediately subsolidus field at 20 kbar within which all garnet of the sample has disso ed in the pyroxene.

O'HARA and YODER (1967) also reported a high solidus temperature of ca. 1535°C i kyanite eclogite, TAN 501, at 30 kbar, confirming solution of oriented kyanite intergrov in the clinopyroxene prior to the onset of melting.

Eclogite 1058 from the Roberts Victor mine has high M, combined with high Na/ in the pyroxene; the solidus temperatures are lower than for 1044 (Fig. 1) despite t higher M value. The garnet does not dissolve entirely in the pyroxene under any investigat conditions, and garnet appears as the liquidus phase at and above 25 kbar. Orthopyroxe appears near the liquidus at 20 kbar but reacts out after garnet appears.

No significance can yet be attached to the pressure at which garnet and clinopyroxe are cotectic at the liquidus of the two eclogites; we cannot be sure than the hand specim samples fairly represent the garnet–pyroxene ratio of the source region, nor is there secure basis for assuming that the pressures at which garnet and pyroxene appear sim taneously at the liquidus in these bulk compositions bears any predictable relationship the pressure or temperature at which the original eclogite may have accumulated fr some more complicated magmatic system.

If the eclogites are cumulates, the temperature of the magmas must have been lower th

ıe observed solidus temperatures, i.e. less than 1385 ± 35°C at 20 kbar, or less than 480 ± 30°C at 30 kbar (perhaps very much lower).

Related to this point HARTE and GURNEY (1973) have demonstrated that another eclogite om the Roberts Victor mine preserves exsolution textures indicating previous crystallizaon at temperatures between 1400°C and 1200°C in the pressure range between 38 kbar ıd 25 kbar (respectively), thus demonstrating that the pressure and temperature range of ır experiments is relevant to the natural conditions of formation of eclogite in kimberlite.

Also, it is seen from Table 1 that the kinetics of reaction are such that, in the absence of ivine and orthopyroxene, all the garnet originally present in No. 8 (1044) was dissolved to the pyroxene within 15 minutes at 20 kbar, 1400°C, creating a clinopyroxene containing ver 13% Al_2O_3.

Bimineralogic eclogite is most unlikely to represent the total crystallization product of high pressure liquid because of the special restricted nature of bulk compositions which evelop bimineralic assemblages on solidification (O'HARA and YODER, 1967). Moreover, ıe liquidus temperatures are higher than the solidus temperature of garnet–lherzolite.

If, despite this, the bimineralic eclogites were frozen primary magmas, they would have eveloped in equilibrium with both olivine and enstatite, and should precipitate these ıases for a temperature interval at the liquidus. This is not observed to occur.

Olivine does not appear in the liquidus/solidus interval of these or other investigated imineralic eclogites. The partial melting of dry eclogite cannot, therefore, yield peridotite r garnetiferous peridotite residua in the pressure range investigated (20–40 kbar) and is ven less likely to do so at higher pressures due to the contraction of the primary liquidus ıase volume of olivine (O'HARA, 1968). At lower pressures the eclogite mineralogy is not able to the solidus, olivine may appear in the melting interval joined perhaps by orthoyroxene, but spinel–lherzolites rather than garnet–lherzolites would be the residual eridotite assemblage developed (O'HARA *et al.*, 1971). While such peridotites might crystallize to garnet–lherzolite on cooling in the subsolidus, the simplest interpretation f the experimental data suggests that this could not have happened at less than 15 kbar O'HARA *et al.*, 1971). Models which call for bimineralic eclogite upper mantle to yield ırnet–lherzolite residua on partial melting therefore presuppose restriction of the process) ca. 45–60 km depth (15–20 kbar pressure) and selective sampling by diatremes of wall ocks from those depths (because peridotites greatly exceed eclogites in abundance among ıe nodules in kimberlite).

KUSHIRO (1973) has presented microprobe analyses of liquids produced in equilibrium ith garnet-peridotites. If crystallized at high pressures, these compositions would solidify quartz-eclogites, hence Kushiro's results imply that the eclogite assemblages are *not* a ermal divide at high pressure contrary to the work presented here.

The compositions found by KUSHIRO (1973) are more siliceous than those indicated by xperimental data for synthetic systems and natural basalt compositions (O'HARA 1968).

The previous expectations concerning normative olivine contents of liquids in equilium with peridotite are based upon phase equilibria in basaltic, rather than peridotitic ompositions, and are unaffected by the type of quenching problem discussed below.

When liquid forms only a small proportion of a charge, there is a risk that its composition ay be severely altered during quenching by the additional precipitation of an inconspiuous amount of, e.g. olivine, on the outside of existing olivine crystals, particularly in ater-bearing charges (CAWTHORN *et al.*, 1973). One test which may be applied is to ompare the distribution coefficients for iron and magnesium between olivine and liquid

in the different charges, with that observed at equilibrium in experiments where the amoi of liquid is large and the quenching effect correspondingly small. In relation to an equ brium K_D of 0.335, the runs reported by KUSHIRO (1973) for a granular garnet–lherzo mineral assemblage ranged from 0.39 (20 kbar, 1490°C) through 0.35 to 0.22 (10 kb 1350°C).

The high value in the 20-kbar run cannot readily be explained. The low value in 10-kbar run, and the still lower values obtained in all three experiments on the shea garnet–lherzolite (0.20, 0.17, 0.20, respectively, at 20 kbar, 1475°C; 15 kbar, 1450°C a 10 kbar, 1375°C) are explicable either if substantial amounts (4–5%) of Fe_2O_3 are pres in the liquids (nearly half the total iron present) or if the analysed liquid composition l lost a significant amount of further olivine during the quenching process. Exclusion charges with visible quench crystals from the analyses does not preclude the danger quenching products being present (CAWTHORN *et al.*, 1973). If the only quench ph was olivine, and the quenching olivine is assumed to have the same composition as primary olivine, a calculation indicating the order of size of the effect may be made. For most extreme case, the 15-kbar run on the sheared garnet–lherzolite, approximately 3 olivine would have to be added to the liquid to produce a reasonable distribution coeffici (i.e. assuming 20% apparent melting in this charge, 6.5% of crystals present would h to be quench olivine). Addition of this olivine would change the CIPW norm of the liqu contributing ca. 15% olivine to the norm of the pre-quenching liquid.

Having regard to all these factors, we do not feel that the derivation of quartz–thole as a primary magma from the sheared garnet–lherzolites in the absence of water is an exp mentally established process, even in the 10–20-kbar range. We prefer our own results, a those of O'HARA and YODER (1967), HARTE and GURNEY (1973) in more favourable co positions which indicate that the olivine–liquidus does not penetrate the biminera eclogite composition range.

RESULTS FOR GARNET-OLIVINE-WEBSTERITE AND GARNET-LHERZOLITE

Olivine–garnet websterite 1031 has been suggested (O'HARA *et al.*, 1973a) as a possi cumulate originally consisting of minor olivine, aluminous diopside and enstatite. The sm amount of garnet is considered to have exsolved during subsequent cooling and recryst lization. This sample develops the predicted olivine + enstatite + diopside mine assemblage in the solidus only at high temperature and at a pressure close to 30 kb (Fig. 2). Spinel (picotite) appears in the subsolidus at 20 and 25 kbar at temperatures betwe 1250° and 1550°C, olivine being present in all cases and garnet in some cases. This spine appearing because these conditions lie within or to the low-pressure side of the transiti zone between the spinel- and garnet–lherzolite facies in this composition. At 35 kbar gar is stable to the solidus. The experimental data, therefore, indicate that if this rock is correc interpreted as an olivine–websterite cumulus, it must have precipitated from a virtua dry magma at ca. 1575°C, 30 kbar. (The presence of significant water in the system wo lower the solidus temperature, and altogether eliminate the conditions under which neitl garnet, nor spinel, nor liquid is present in this composition.) The large liquidus–solid interval, and early orthopyroxene crystallization are consistent with the proposed cumu origin.

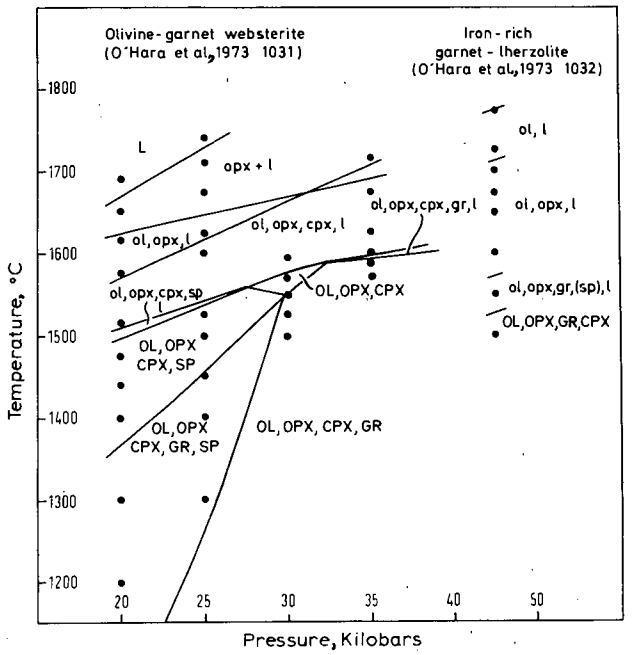

FIG. 2. Interpretation of quenching data for olivine–garnet–websterite and iron-rich garnet–lherzolite.

The bulk rock sample on which the experiments were performed contains 4.2% Al_2O_3 nd when garnet disappears, at ca. 30 kbar, 1550°C, it consists of a small amount of olivine nd a mixture of two pyroxenes. On the assumption that the two pyroxenes contain about ne same amount of Al_2O_3, we anticipate that they will neither contain much more than 5% Al_2O_3, which is substantially less than indicated either by the clinopyroxene grid O'HARA, 1967) or the orthopyroxene grid (MACGREGOR, unpublished). Suspecting the eaction kinetics (despite the evidence of successful solution of over 13% Al_2O_3 in pyroxene om 1044, in 15 minutes) a 1500°C experiment at 30 kbar was performed, holding it for hours instead of the 15–30 minutes of the previous experiments at 1570–1520°C. This we nderstand to be longer than the experiments used to establish the enstatite grid in this egion of the diagram, and garnet was retained.

The very fertile-looking iron-rich and calcium- and aluminium-rich garnet–lherzolite 032 (O'HARA *et al.*, 1973a) might represent a very high-pressure primary magma. If so, here will exist some pressure at which olivine is replaced by orthopyroxene as liquidus hase. Both garnet and diopside might be close to saturation at the liquidus at the same ressure. At 45 kbar olivine is still the liquidus phase, persisting to temperatures greater han 1750°C. Orthopyroxene is present from ca. 1715°C, garnet appears at 1575°C and the olidus lies close to 1525°C. If this rock is to represent a primary liquid in equilibrium with arzburgite or garnet–harzburgite the pressure of its derivation must be greater than 5 kbar.

Whether or not this sample represents a liquid, its major element composition is similar o that of known ultrabasic liquids, and the results must be applicable to such rocks.

REFERENCES

CAWTHORN, R. G., FORD, C. E., BIGGAR, G. M., BRAVO, M. S. and CLARKE, D. B. (1973) Determination of liquid composition in experimental samples: discrepancies between microprobe analysis and other meth *Earth Planet. Sci. Letters* **21**, 1–5.

HARTE, B. and GURNEY, J. J. (1973) Evolution of clinopyroxene and garnet in an eclogite nodule from the Robe Victor kimberlite pipe. *Extended Abstracts, Int. Conf. Kimberlites*, pp. 159–62, Univ. of Capetown.

KUSHIRO, I. (1973) Partial melting of garnet–lherzolites from kimberlite at high pressures. In: *Lesotho Kimber* (editor P. H. NIXON), pp. 294–9, Lesotho Nat. Development Corp., 350 pp.

O'HARA, M. J. (1967) Mineral parageneses in ultrabasic rocks. In: *Ultramafic and Related Rocks* (editor P. J. W LIE), pp. 393–403.

O'HARA, M. J. (1968) The bearing of phase equilibria studies in synthetic and natural systems on the origin evolution of basic and ultrabasic rocks. *Earth Sci. Rev.* **4**, 69–133.

O'HARA, M. J., RICHARDSON, S. W. and WILSON, G. (1971) Garnet–peridotite stability and occurrence in c and mantle. *Contr. Mineral. Petrol.* **32**, 48–68.

O'HARA, M. J., SAUNDERS, M. J. and MERCY, E. L. P. (1973a) Chemistry and assigned origin of some ultram nodules from kimberlite. *Extended Abstracts, Int. Conf. Kimberlites*, pp. 259–62, Univ. of Capetown.

O'HARA, M. J., SAUNDERS, M. J. and MERCY, E. L. P. (1973b) Chemistry of some eclogite nodules from kimber eclogite fractionation. *Extended Abstracts, Int. Conf. Kimberlites*, pp. 263–6, Univ. of Capetown.

O'HARA, M. J. and YODER, H. S., Jr. (1967) Formation and fractionation of basic magmas at high pressures. *Sc J. Geol.* **3**, 67–117.

(Reprinted from Nature, Vol. 254, No. 5499, pp. 406–408, April 3, 1975)

Palaeogeotherms and the diopside–enstatite solvus

THE precise composition of the solid solutions that develop between diopside and enstatite has provided a basis for estimates of the temperature of equilibration of mineral assemblages from peridotites. We report here results of a reinvestigation of these relationships, which demonstrate that the range of solid solutions formed at high temperatures is less than previously believed, and that it is dependent on both pressure and silica activity. The stable existence of an iron-free pigeonite has not been confirmed.

Garnet–lherzolite xenoliths in kimberlite are widely accepted as xenoliths of the upper mantle. They contain olivine, garnet and enstatite coexisting with a clinopyroxene. They can be divided into two groups; in one the clinopyroxene is calcic and in the other it is subcalcic. The distribution of analyses of the clinopyroxenes is bimodal[1].

Temperatures and pressures of equilibration of the mineral assemblages in individual nodules from the xenoliths have been estimated[2]. The palaeogeotherms which existed in the upper mantle immediately before incorporation and transport of the xenoliths by kimberlite eruptions have been derived from data from large numbers of individual xenoliths[2]. These geotherms show an abrupt rise in the rate of increase of temperature with depth, coincident with the change in clinopyroxene composition from calcic to subcalcic diopside.

The temperature estimates were based on a comparison of the Ca/Ca+Mg ratio of the diopside coexisting with enstatite in the natural rocks, with the Ca/Ca+Mg ratio of diopside coexisting with enstatite in the system $CaMgSi_2O_6$–$Mg_2Si_2O_6$, as determined by experiments at 30 kbar (ref. 3). The procedure assumed this relationship to be independent of pressure. The results on the synthetic system indicate that enstatite is in equilibrium with a single clinopyroxene phase over the whole temperature range investigated and that the composition of that diopside solid solution changes continuously with temperature. The rate of change of the diopside composition did not, however, vary regularly, and reached a maximum at temperatures close to 1,450 °C (ref. 3). A study[4] of the same system at 20 kbar reported an abrupt change of the clinopyroxene coexisting with enstatite at this same temperature, from a calcic diopside at lower temperatures to a pigeonite at higher temperatures. Above 1,450 °C a further solvus was reported between the pigeonite and a more calcic diopside. The composition–temperature field occupied by a single clinopyroxene solid solution in the results reported[3] at 30 kbar is thus occupied by three fields, of clinopyroxene A (diopside), clinopyroxene B (pigeonite) and clinopyroxene A plus clinopyroxene B in the results reported[4] at 20 kbar.

The possibility that the abrupt change from diopside to pigeonite in equilibrium with enstatite might have a bearing on the abrupt change from calcic to subcalcic diopside in the xenoliths from kimberlite, and on the change in slope of the inferred palaeogeotherms, prompted this reinvestigation of the clinopyroxene limb of the solvus at 20 and 30 kbar; the results show that pigeonite is not an equilibrium product in this system at those pressures. The position of the equilibrium diopside limb of the solvus at high temperatures is very different from that observed by Davis and Boyd[3]. Coexisting diopside and enstatite solid solutions do not have the same Si/Ca+Mg ratio, that is, the join $CaMgSi_2O_6$–$Mg_2Si_2O_6$ cuts across the tie lines linking coexisting diopside and enstatite solid solutions which depart, in opposite senses, from the ideal 1:1 ratio of Si/Ca+Mg. The position of the diopside limb is, moreoever, pressure dependent.

The discrepancies between these and previous results are predominantly a function of the nature of the starting material. Results obtained from glass starting materials yield metastable products. When very fine-grained crystallised gels are used as starting material they react readily and completely to yield the equilibrium products.

A high pressure piston-cylinder apparatus (see ref. 5) was used in these experiments. Temperatures were measured using Pt/Pt 13 rhodium thermocouples with no correction for pressure effects. The starting materials were finely ground gels which had been recrystallised at 900 °C. Runs were made both on homogeneous gels ($Di_{40}En_{60}$, $Di_{50}En_{50}$) and on mechanical mixtures of pure diopside and enstatite gels (bulk compositions: $Di_{20}En_{80}$, $En_{28}En_{72}$, $Di_{40}En_{60}$, $Di_{60}En_{40}$, $Di_{69}En_{31}$). All com-

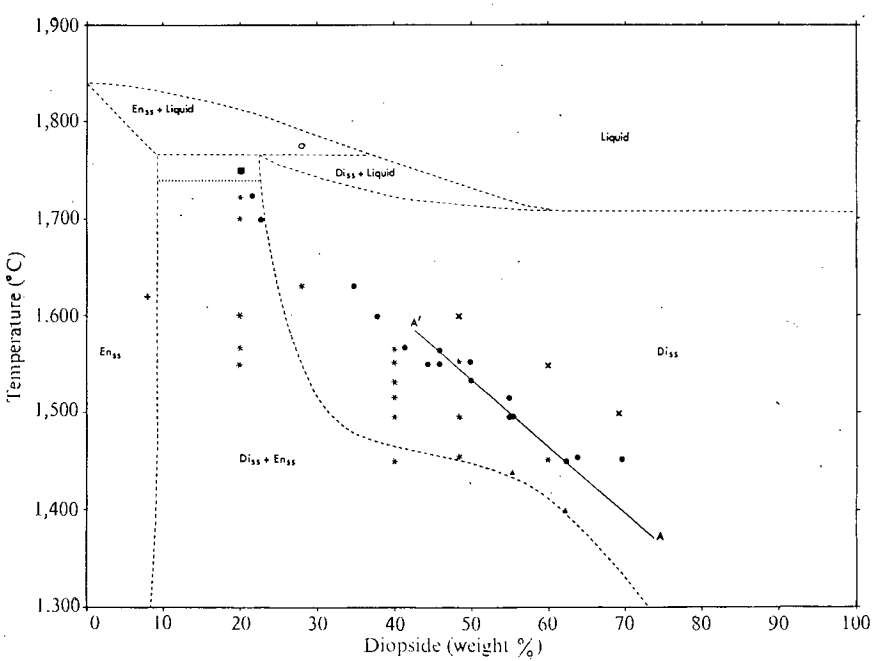

Fig. 1 Results obtained at 30 kbar from compositions lying along the diopside–enstatite join, shown in relation to the interpretation by Davis and Boyd[3] (– – – –). A–A′ = The diopside limb of the diopside–enstatite solvus obtained from runs on the gel composition $Di_{40}En_{60}$ weight %. Results from gel starting materials: ★, bulk composition and temperature of runs which crystallised to a solid solution of diopside plus enstatite; ●, composition of diopside in equilibrium with enstatite, from X-ray measurements; ×, homogeneous diopside solid solution obtained; +, enstatite solid solution obtained; ■, enstatite solid solution plus liquid; ○, liquid; ▲, composition of diopside solid solutions coexisting with enstatite solid solution crystallised from the glass of bulk composition $Di_{40}En_{60}$ weight %; · · · · ·, solidus in present work. SS, solid solution (in all figures).

positions are quoted in weight %. A glass of composition $Di_{40}En_{60}$ was also used for more direct comparison with the earlier works[3,4] which had used glass starting materials. All charges were dried at 1,050 °C for 1 h and sealed in platinum capsules. Runs were initially taken to 5 kbar above the desired pressure, the excess pressure being bled off when the required temperature was reached. In the temperature ranges 1,450–1,500 °C, 1,500–1,565 °C and above 1,600 °C, the durations of the runs were at least 4 h, 2 h and 0.5 h, respectively, except where stated. At 1,450 °C no change in the clinopyroxene composition occurred when experiments were run for longer

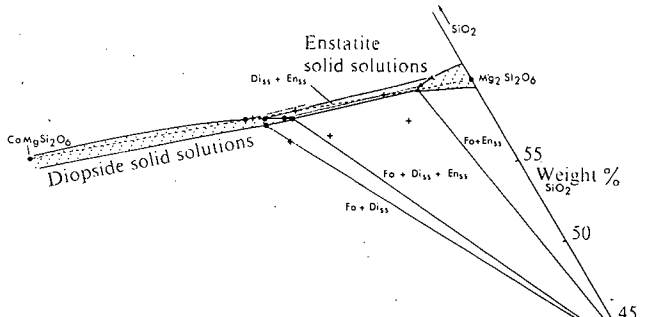

Fig. 2 Part of the system $MgO–SiO_2–CaO$(weight %) at 30 kbar and 1,550 °C, showing bulk compositions of charges (+), and measured clinopyroxene compositions (●), in relation to inferred variation of SiO_2 in the diopside solid solution field (the extent of which along the join $CaMgSi_2O_6–Mg_2SiO_4$ is taken from refs 6 and 7). Tie lines to inferred enstatite compositions (▲) are shown intersecting the $CaMgSi_2O_6–Mg_2Si_2O_6$ join.

than 1.5 h, and it was therefore assumed that equilibrium had been attained in all experiments used for drawing up the diopside solvus.

Products were identified by optical and X-ray diffraction methods. Attempts made to analyse clinopyroxenes using the electron microprobe failed because of the small grain size (< 5 μm) of the crystals; it was not possible to focus the electron beam on a unique grain, and interference from adjacent crystals produced a wide range of clinopyroxene compositions (for example, Ca/Ca+Mg = 0.10–0.25 in one of the coarser grained charges). The X-ray diffraction technique used chromium radiation in an evacuated chamber. Compositions of clinopyroxenes were estimated from the relationship reported by Davis and Boyd[3] which our study verified as valid between and 69 weight % diopside. Clinopyroxene compositions cou be obtained with a precision of ±1% diopside (99.7% co fidence limits). The precision is rather less good for charg containing large amounts of enstatite. This technique is capab of resolving two clinopyroxenes differing by as little as weight % of diopside. Clinopyroxenes which crystallised equilibrium with enstatite at 30 kbar from the starting compositio $Di_{40}En_{60}$ lay along the curve A–A′ (Fig. 1) irrespective whether or not the homogeneous gel or the mixed diopside enstatite gel was used. Clinopyroxenes which crystallised fro starting compositions $Di_{20}En_{80}$ and $Di_{28}En_{72}$ lay away from th curve by up to 4 weight % diopside towards enstatite; clinopy oxenes from starting compositions $Di_{50}En_{50}$ and $Di_{60}En_{40}$ lay u to 7 weight % diopside away from curve A–A[1] towards pu diopside. When 10 weight % of forsterite was added to eac of the gels $Di_{20}En_{80}$ and $Di_{40}En_{60}$ at 1,550 °C and 1,565 °C constant clinopyroxene compositions of $Di_{41.5}En_{58.5}$ an $Di_{42}En_{58}$, respectively, were generated from both composition This indicates that in detail the parageneses have the form shown in Fig. 2.

Experiments using glass of composition $Di_{40}En_{60}$ as startin material yielded homogeneous clinopyroxene above 1,440 °C as required by Davis and Boyd's[3] phase diagram which wa obtained from runs on glass charges. At 1,440 °C and 1,400 °C this starting material crystallised to enstatite and clinopyroxene which lay exactly on the diopside limb of Davis and Boyd's solvus.

Runs on the homogeneous gel $Di_{40}En_{60}$ at 1,450 °C yielde enstatite and a clinopyroxene Di_{56} after 10 s and a progressivel more magnesian clinopyroxene (up to Di_{50}) in longer runs c up to 30 min. This trend towards the solvus found by Davi and Boyd[3] was reversed in longer runs, as the clinopyroxen changed towards the solvus A–A′ (Di_{60} after 50 min; Di_6 after 90 min), indicating the latter to represent the close approach to equilibrium. The effects may indicate that th exchange of Ca and Mg between the two pyroxenes proceed more rapidly than the adjustments in silica content implie in Fig. 2.

Figure 3 shows the results at 20 kbar from composition lying on the diopside–enstatite join in relation to phas boundaries obtained[4] using glass charges. We found tha enstatite coexists with a diopside lying close to the curv B–B′ (Fig. 3). The boundary B–B′ at 20 kbar is significantl displaced towards En relative to A–A′ at 30 kbar, but th pressure effect is for charges which were not saturated wit forsterite. The pressure effect is, however, also significant i forsterite saturated charges. Forsterite (10 weight %) wa

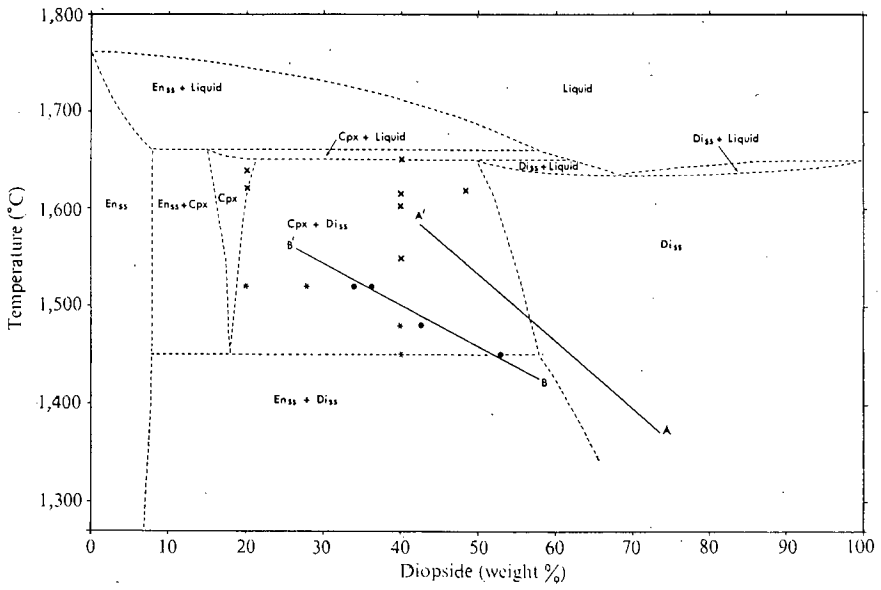

Fig. 3 Results obtained in this work at 20 kbar from compositions lying along the diopside–enstatite join, shown in relation to the interpretation by Kushiro[4]. B–B′= Approximate position of the diopside limb of the diopside–enstatite solvus obtained from experiments on gel starting materials. A–A′, and all symbols as in Fig. Cpx, clinopyroxene.

added to the mixed gel of bulk composition $Di_{20}En_{80}$ at 1,520 °C. The clinopyroxene which crystallised in equilibrium with enstatite and forsterite had the composition $Di_{37.5}En_{62.5}$. When the temperature of the forsterite bearing assemblage at 30 kbar is raised by 30 °C the clinopyroxene becomes 4 weight % richer in diopside. The effect of pressure on the diopside solvus (20–30 kbar) at 1,535±15 °C is to increase the amount of apparent diopside by 0.8 weight % per kbar in forsterite saturated assemblages. The effect in the stoichiometric join $CaMgSi_2O_6$–$Mg_2Si_2O_6$ is not necessarily the same as this. Translated into temperatures this would represent an error of +7 °C per kbar for assemblages equilibrated at a higher pressure than that of the experimental determinations.

Material of composition $Di_{20}En_{80}$ yielded a homogeneous clinopyroxene at 1,620 °C and diopside and enstatite at 1,520 °C. Kushiro[4] predicted an assemblage of pigeonite plus minor diopside for the 1,520 °C run. Material of composition $Di_{40}En_{60}$ yielded diopside plus enstatite at 1,450 °C and 1,480 °C and a single homogeneous clinopyroxene of composition $Di_{40}En_{60}$ at 1,550 °C. The two higher temperature runs lie within the reported[4] field of diopside plus pigeonite stability but fail to verify its existence. Runs on bulk composition $Di_{40}En_{60}$ at 1,620 °C using homogeneous gel and glass starting materials, and at 1,614 °C using the mixture of diopside and enstatite gels, all yielded a homogeneous clinopyroxene. There was again no evidence for the coexistence of two clinopyroxenes as required by Kushiro[4]. He reported[4] that he was not able consistently to generate the pigeonite plus diopside assemblage. It is possible that the two clinopyroxene field is a quenching phenomenon. Deliberately slow quenching of the $Di_{40}En_{60}$ gel, run at 1,620 °C failed, however, to produce two clinopyroxenes, nor were they obtained from glass or homogeneous ge starting materials of the $Di_{40}En_{60}$ composition when run at 1,620 °C in the same equipment used[4] by Kushiro. We conclude that there is no stable field of pigeonite separate from a diopside field on this join at 20 kbar.

In the light of these results the temperatures on the geotherm estimated by Boyd[2] may require some revision, and the method should only be applied to olivine saturated assemblages when compared with a diopside solvus determined in the presence of excess forsterite.

S. HOWELLS
M. J. O'HARA

Grant Institute of Geology,
University of Edinburgh,
Edinburgh EH9 3JW, UK

Received January 23; revised February 14, 1975.

1 Nixon, P. H., and Boyd, F. R., in *Lesotho Kimberlites* (edit. by Nixon, P. H.), 48–56 (Lesotho National Development Corporation, Maseru, 1973).
2 Boyd, F. R., *Geochim. cosmochim. Acta*, 37, 2533–2546 (1973).
3 Davis, B. T. C., and Boyd, F. R., *J. geophys. Res.*, **71**, 3567–3576 (1966).
4 Kushiro, I., *Yb. Carnegie Instn Wash.*, **67**, 80–83 (1968).
5 O'Hara, M. J., Richardson, S. W., and Wilson, G., *Contr. Miner. Petrol.*, **32**, 48–68 (1971).
6 Davis, B. T. C., *Yb. Carnegie Instn Wash.*, **63**, 165–171 (1964).
7 Kushiro, I., *ibid.*, **63**, 101–108 (1964).

Printed in Great Britain by Henry Ling Ltd., at the Dorset Press, Dorchester, Dorset

ABSTRACT OF THESIS

Name of Candidate Susan Howells

Address 51 Havers Lane, Bishop's Stortford, Herts.

Degree Doctor of Philosophy *Date* March, 1976

Title of Thesis Experiments on eclogites and peridotites relevant to magma generation and temperature distribution in the upper mantle

Pyroxene solid solutions crystallized experimentally at high pressure (20-35 kb) and high temperature (> 1400°C) have been analysed using optical and x-ray diffraction techniques. Enstatite solid solution in $CaO-MgO-SiO_2$ clinopyroxenes at high temperatures is less extensive than previously accepted, is greatly reduced by pressure increase between 20 and 30 kb, and is dependent on the extent of forsterite saturation. No evidence was found for an inflection in the clinopyroxene(orthopyroxene) solvus or for a field of two clinopyroxenes in the system $CaO-MgO-SiO_2$ at either 20 or 30 kb, or in the system $CaO-MgO-Al_2O_3-SiO_2$ or a natural system at 30 kb. Previous evidence for a reaction from a calcic clinopyroxene-bearing garnet-lherzolite to a subcalcic clinopyroxene-bearing garnet-lherzolite is inconclusive.

Much lower solubilities of Al_2O_3 in orthopyroxenes than hitherto predicted were obtained for orthopyroxenes crystallized in equilibrium with garnet from compositions in the system $MgO-Al_2O_3-SiO_2$, and for orthopyroxenes crystallized in the equilibria clinopyroxene + orthopyroxene + garnet ± olivine from compositions in both the $CaO-MgO-Al_2O_3-SiO_2$ system and a natural system.

Discrepancies between these and previous results reflect the use of different starting materials. The probable errors in the previous determinations may explain the "kink" in deduced pyroxene geotherms.

Stable equilibrium was not achieved at high temperature in experiments on anhydrous $CaO-MgO-Al_2O_3-SiO_2$ glass charges with the period of reliability of Pt/Pt13Rh thermocouples.

Experiments carried out in the systems $CaO-MgO-Al_2O_3-SiO_2-Na_2O$ and $CaO-MgO-Al_2O_3-SiO_2-Na_2O-H_2O$ at 25 kb showed that nepheline-normative magmas may be generated by partially melting certain anhydrous clinopyroxene-orthopyroxene-garnet assemblages. Orthopyroxene is in reaction with this liquid. Both nepheline- and quartz-normative liquids may be generated by partially melting H_2O-saturated garnet-lherzolite at 1080°C, 25 kb.

The presence of glass spherules, glass coatings and vapour bubbles in H_2O-bearing experimental run products is not evidence of the presence of a vapour phase at high temperature.

Use other side if necessary.